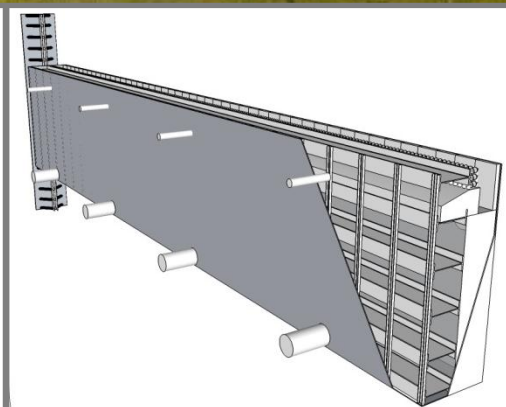
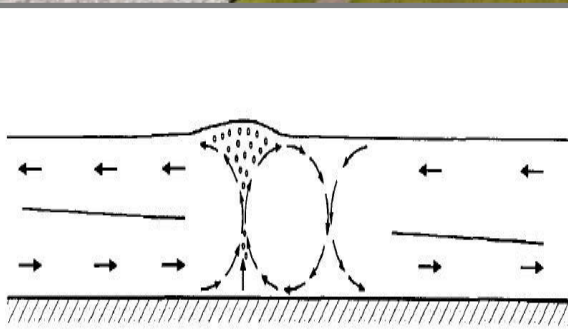


Master's thesis:

SALT INTRUSION PREVENTION IN LOCKS;

DESIGNING A MOVABLE SILL IN THE EXISTING KRAMMER COMMERCIAL NAVIGATION LOCK



Author

Bram van Tongeren, BSc
(TU Delft reg. nr. 1304291)

Graduation Committee

Prof. *dr. ir.* S.N. Jonkman
ir. A.J. van de Kerk
ir. W.F. Molenaar
Prof. *dr. ir.* W.S.J. Uijttewaal

Starting date

3-sep-2012

Finishing date

26-4-2013

Version

Final
-22-4-2013-

This Master's thesis is written as finalisation of the Master's degree programme
Hydraulic Engineering at Delft, University of Technology.

The research is performed from September 2012 to April 2013
at engineering company Royal HaskoningDHV, Amersfoort.



Graduation Committee

Prof. <i>dr. ir.</i> S.N. Jonkman	<i>Chairman</i>	Delft, University of Technology
<i>ir.</i> A.J. van de Kerk	<i>Member</i>	Royal HaskoningDHV
<i>ir.</i> W.F. Molenaar	<i>Member</i>	Delft, University of Technology
Prof. <i>dr. ir.</i> W.S.J. Uijttewaal	<i>Member</i>	Delft, University of Technology

No part of this publication may be reproduced, stored in a retrieval system, or transmitted, in any form or by any means, electronic, mechanical, photocopying, recording, or otherwise, without prior permission of the writer.

Preface

The idea for this graduation project finds its origin in the spring of 2012. Various engineering companies were contacted with the question whether it was possible for me to do research to an innovative technique alongside a project in execution. Desired was to make a design of a new innovative solution from the perspective of structural hydraulic engineering.

Royal HaskoningDHV (called DHV at that time) reacted positively and gave the opportunity to start working within the "*Pilot Krammer Jachten Sluis*" project in September 2012. I want to thank my mentor from Royal HaskoningDHV – Arend Jan van de Kerk – for his support. Meetings with him always resulted in new insights or exciting ideas and confirmed the fun of engineering.

Working on this project has been exciting since the current phase of the project serves as base for the decision of what system will be applied in the Krammer locks. The findings of this study may affect the way certain choices on this design will be made.

Salt intrusion has been prevented for decades. Since the last few years, extensive research resulted in significantly improved systems to reduce salt intrusion through locks. Improvements are never unwelcome, which also holds in this case. Knowledge on the effects of countermeasures to salt intrusion continues to be elaborated and is expected to be in development for a long time from now.

I want to thank specifically Mr. Jonkman, Mr. Uijttewaai, Mr. Molenaar and Mr. Van de Kerk – the members of the exam committee – for their support, time and advice throughout the process.

I enjoyed the project and hope you'll find it interesting.

Amsterdam, March 2013
Bram van Tongeren

Table of contents

Preface	v
Summary	viii
List of symbols	x
List of figures	xii
List of tables	xv
1. Introduction	2
2. Salt intrusion in locks	4
2.1. Salt intrusion in general	5
2.1.1. Problems regarding salt intrusion	5
2.1.2. Physical description of the salt intrusion process	6
2.1.3. Current counter measures to salt intrusion	11
2.2. Description of the Krammer locks	14
2.2.1. Outline	14
2.2.2. Commercial locks	19
2.2.3. Recreational locks	24
2.3. Description of pilot project: Krammer recreational lock	26
2.3.1. Effects of pilot in Krammer recreational lock	26
2.3.2. Air bubble screens	26
2.3.3. Water screen	28
2.3.4. Flushing system	30
2.4. Exploration of possibilities: Krammer commercial lock	31
3. Problem, objective & approach	40
3.1. Problem	40
3.2. Objective & approach	41
4. Alternatives of movable sill	42
4.1. Description of alternatives	43
4.2. Comparison of alternatives	44
4.3. Best alternative	45
5. Detailing of vertical sliding movable sill	46
5.1. Location and construction	47
5.1.1. Elements of the structure	47
5.1.2. Movement of the structure	48
5.1.3. Water tight connections	50
5.1.4. Construction of the structure	51
5.2. Air bubble- and water screen layout	54
5.2.1. Water screen	54
5.2.2. Air bubble screen	57
5.2.3. Fitting of screens in sill	59
5.3. Driving mechanism	61
5.3.1. Requirements to driving mechanism	61
5.3.2. Description of different driving mechanisms	61
5.3.3. Best alternative	63

5.3.4.	Vertical connection to lock chamber	63
5.4.	Loads	64
5.4.1.	Basic information	64
5.4.2.	Loads	64
5.4.3.	Load combinations	69
5.5.	Structural design of the sill	71
5.5.1.	Materials	71
5.5.2.	Plates	71
5.5.3.	Studs	72
5.5.4.	Main beams	72
5.5.5.	Force distribution to lock chamber	72
6.	Verification	74
6.1.	Description of system	75
6.1.1.	Water levelling	75
6.1.2.	Comparison of configurations	75
6.2.	Effectiveness	76
6.2.1.	Basic information	76
6.2.2.	Salt intrusion reduction	76
6.2.3.	Fresh water loss	77
6.2.4.	Improvements	78
6.3.	Energy consumption	79
6.3.1.	Water levelling	79
6.3.2.	Movement of sill	79
6.3.3.	Air bubble- and water screen	79
6.4.	Costs	81
6.4.1.	Construction costs	81
6.4.2.	Operational and maintenance costs	82
6.5.	Capacity of lock chamber	84
6.6.	Future perspective	85
	Conclusion	86
	Recommendations	88
	References	90
	Literature	90
	Websites	92
	Terms, translations & abbreviations	94
	Terms & abbreviations	94
	Translations	96
	Appendices	Appendices - 2
	Colophon	Appendices - 100

This document contains 212 pages
Framework 16 :: Main report 96 :: Appendices 100

Summary

Salt intrusion is undesired because it has negative effects for drinking water and agricultural water intakes. At the Krammer locks (Zeeland, the Netherlands) a complex system is integrated in the design of the lock which prevents salt intrusion very accurate. This effective reduction of salt intrusion is regrettably accompanied with high energy consumption, high operational costs and high maintenance costs. On top of that, the entire system needs big maintenance in 2 years (20 M€) and an extensive expansion in 10 years (300 M€).

Retaining the current system is not expected to be the best option. Other options have been elaborated, which resulted in the execution of a pilot project in the smallest lock of the complex – the recreational lock. The pilot has as main objective to get insight in possibilities for a design in the much larger commercial locks.

The objective of this study is to present a feasible design for a salt intrusion prevention system in the commercial locks. The design should be comparably effective as the current system, while having lower energy consumption, lower construction costs, lower maintenance costs, lower operational costs and a higher lock capacity. After an analysis it became clear that this is possible by including a movable sill in the structure. A comparison with the design of the pilot and the current system must prove the abilities of the new design.

The reduction in height of the air bubble- and water screen in the new design is accompanied by the presence of an impermeable sill. This increases the overall efficiency of the configuration, since exchange of salt and fresh water is decreased more effective.

Figure 1 shows the design in the commercial lock chamber. The air bubble- and water screens are integrated in the movable sill. In operation, the sill moves vertically up and down once every tidal cycle of 12 hours. It allows ships to sail over it, while being positioned as high as possible. Above the top level of the sill, integrated air bubble- and water screens reduce the negative effects. In this way, the optimum reduction of water exchange is obtained.

The design of the screens is partly based on the design of the pilot. It's optimised by using other dimensions and reducing the required air pressure for the air bubble screens.

The governing loads on the structure occur when a ship sails over the sill, inducing a return flow of water alongside the ship. In the governing situation, the ideally maximum possible water density difference induces a force on the sill in the same direction. A dimensioning has led to the final design, which could withstand these loads. The driving mechanism is located above water and controls the height of the sill via vertical steel tubes to the sill. The structure is integrated in the existing lock chamber, to which no big adaptations have to be done. A guiding rail distributes the forces of the sill to the lock chamber.

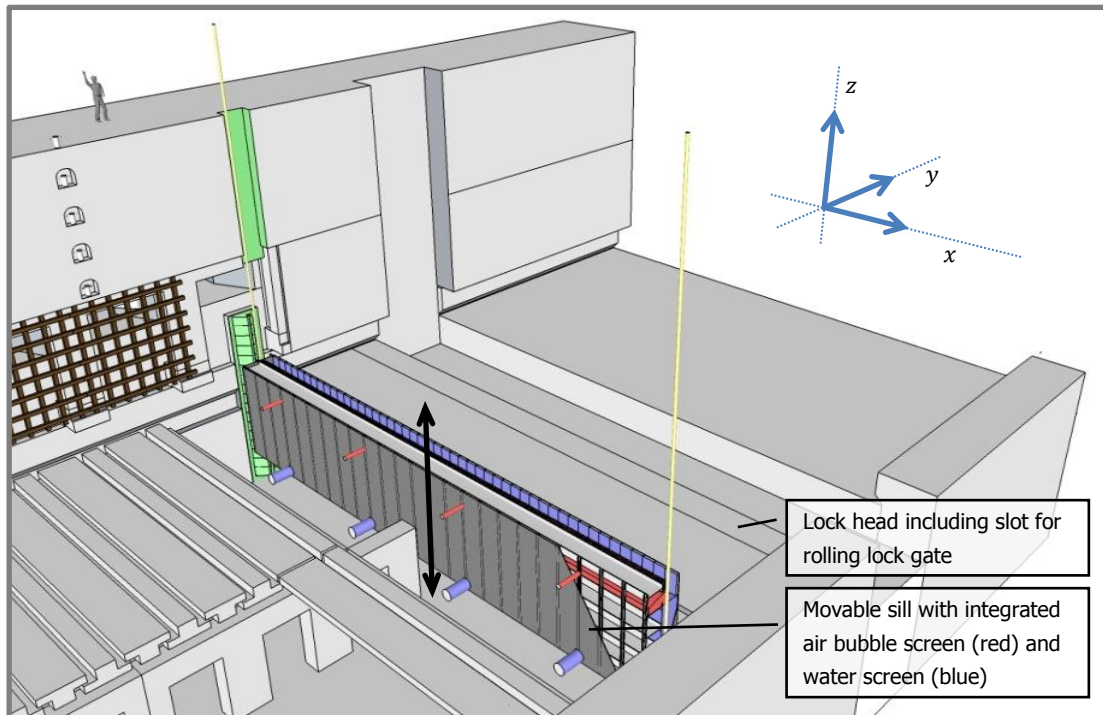


Figure 1: A 3D sketch of the design, placed at the commercial lock head at the Eastern Scheldt side. The most important detailed elements in this study are printed in colours.

The design is first compared to the current situation. In this comparison it becomes clear that salt intrusion prevention of the current system can be matched closely. The reduction of fresh water loss by the system improves considerably and the capacity of the lock increases by a third. A comparison of the design with the design of the pilot is at the end of this thesis summarised as follows:

Final conclusion

A new design has been made for salt intrusion prevention in the Krammer commercial locks. It combines air bubble- and water screens with an innovative movable sill.

It's expected that this design is approximately 20% more effective, consumes 50% less energy and is 30% cheaper than a configuration with air bubble- and water screens only.

The expected improvements of the design in this study show that it is an interesting design. The quantification are obtained by calculations based on various assumptions. Before the design can be realised, there are quite a few important recommendations which need to be elaborated. The assumptions in the used calculation methods need attention especially.

Nevertheless, the presented design shows that a movable sill is an interesting option, to which further studies seem worthwhile.

Apart from a realisation in the Krammer locks, the design has a broader potential; the benefits hold for all locks with salt intrusion countermeasures installed. It's especially interesting in deep locks or locks with an increasing average water level. In that case the effectiveness may increase even more.

List of symbols

Numerous units are used throughout the report. This chapter can be used as reference when unknown quantities or units are presented in formulas.

Table 1 presents the used base units in the report. All other used units can be expressed in terms of these units and are presented in Table 2. Some specific units are used which need a description, which can be seen in Table 3. Table 4 shows useful conversions between some important units in the report.

Table 1: SI units in this report.

Quantity	Symbol	Unit	Symbol
Length	L	Metre	m
Mass	m	Kilogram	kg
Time	t	Second	s

Table 2: Derived units in this report; including SI notation.

Quantity	Symbol	Unit symbol	SI Symbol
Acceleration	a	$m \cdot s^{-2}$	$m \cdot s^{-2}$
Angle	α	rad	1
Area	A	m^2	m^2
Area moment of inertia	I	m^4	m^4
Bending stiffness	EI	$N \cdot m^{-2}$	$kg \cdot m^{-1} \cdot s^{-2}$
Density	ρ	$kg \cdot m^{-3}$	$kg \cdot m^{-3}$
Energy	E	J $1 kWh$	$kg \cdot m^2 \cdot s^{-2}$ $3.6 \cdot 10^6 J$
Force	F	N	$kg \cdot m \cdot s^{-2}$
Impulse	p	$N \cdot s$	$kg \cdot m \cdot s^{-1}$
Mass	m	kg $1 ton(nes)$	kg $10^3 kg$
Moment of force	M	$N \cdot m$	$kg \cdot m^2 \cdot s^{-2}$
Moment of resistance	W	m^3	m^3
Power	P	W	$kg \cdot m^2 \cdot s^{-3}$
Pressure	p	Pa $1 bar$	$kg \cdot m^{-1} \cdot s^{-2}$ $10^5 Pa$
Specific weight	γ	$N \cdot m^{-3}$	$kg \cdot m^{-2} \cdot s^{-2}$
Stress	σ	$N \cdot m^{-2}$	$kg \cdot m^{-1} \cdot s^{-2}$
Velocity	v	$m \cdot s^{-1}$ $1 knot$	$m \cdot s^{-1}$ $0.514 m \cdot s^{-1}$
Volume	V	m^3 $1 l$	m^3 $1 \cdot 10^{-3} m^3$
Young's modulus	E	$N \cdot m^{-2}$	$kg \cdot m^{-1} \cdot s^{-2}$

Table 3: Specific (less common) units in this report.

Unit	SI symbol	Description
Cl	$kg \cdot m^{-3}$	Chlorine content in water. When salt dissolves in water, it separates in Cl^- and Na^+ -ions. The Cl^- -ions (atomic weight of 35.5) are responsible for 60.7 % of the weight of the initial $NaCl$ -molecule (molecular weight of 58.5). Other salts are dissolved in seawater as well, which results in a chlorine content within the salts of

		seawater of approximately 56%. 1 mg/l Cl corresponds with 56% of the total weight of salt in seawater, which means for the salts in seawater $\frac{1}{56\%} = 1.8 \text{ mg/l} = 1.8 \text{ ppt}$. So, a chlorine content of 1 mg/l corresponds to 1.8 ppt (= 1,001.8 kg/m ³). Other sources (Fischer, 1979) determine salinity as follows: $S \approx 0.03 + 1.805 \cdot Cl$
<i>mwc</i>	<i>m</i>	Metre water column.
<i>Nl/s</i>	$m^3 \cdot s^{-1}$	Normal litre per second. 1 Nl/s = 0.001 Nm ³ /s Unit of air discharge, used in air bubble screens. The amount of air used in an air bubble screen cannot be simply defined as the volume of air. Air will be compressed when under (water-) pressure. Since the air bubbles originate at strings a few metres under water, the volume of air at that location is less than at the water surface. So, a unit is needed which is not depending on the height of the air bubble screen. This 'specific air discharge' is only dependant of the length of the bubble screen. For that purpose the volumetric amount of air, which is sucked in by a compressor under normal atmospheric pressure and temperature is used. This is described by the symbol 'N', and can be complemented with litre per second or cubic metre per second. It is usually clear from the context that the unit of force (Newton) is not meant with the letter 'N'.
<i>Nm³/s</i>	$m^3 \cdot s^{-1}$	Normal cubic metre per second. 1 Nm ³ /s = 1000 Nl/s See description of Nl/s.
<i>ppm</i>	1	Parts per million. See description of ppt.
<i>ppt</i>	1	Parts per thousand. This unit is used to quantify the amount of salt in water. Parts per thousand (ppt) or parts per million (ppm) describe the weight dependent relative amount of salt in water. In this way 20 ppt means that 20 kg of salt is present in 1,000 kg of salt water. (Often, 'ppt' is displayed instead of 'ppt of salt'.) Formerly used psu (practical salinity unit) has the same meaning. Note: The North Sea contains 32 ppt. Average seas worldwide contain 34.7 ppt.
<i>S</i>	‰	Salinity. Is used equally as ppt. See description of ppt.

Table 4: Conversion of units.

Unit	Conversion of units		
Chlorine content	1 mg/l	=	1.8 ppt
Energy	1 kWh	=	$3.6 \cdot 10^6 \text{ J}$
Mass	1 ton(nes)	=	10^3 kg
Normal cubic metre per second	1 Nm ³ /s	=	10^3 Nl/s
Normal litre per second	1 Nl/s	=	$10^{-3} \text{ Nm}^3/\text{s}$
Parts per million	1 ppm	=	10^{-3} ppt
Parts per thousand	1 ppt	=	10^3 ppm
Pressure	1 bar	=	10^5 Pa
Velocity	1 knot	=	$0.514 \text{ m} \cdot \text{s}^{-1}$
Volume	1 l	=	10^{-3} m^3

List of figures

Figures in the main text

Figure 1: A 3D sketch of the design, placed at the commercial lock head at the ES side. The most important detailed elements in this study are printed in colours.	ix
Figure 2: Salt and fresh water movements in a lock chamber during levelling. Adapted from (Rijkswaterstaat Bouwdienst, 2000b).	5
Figure 3: Movement of initially separated salt and fresh water after removal of separation. Adapted from (Kranenburg, 1998).	7
Figure 4: Localisation of locks in the Netherlands. For more information, see Table 6 below.	13
Figure 5: Aerial view of Zeeland.	14
Figure 6: Overview of waters around the Krammer locks. The blue arrows indicate fresh water and red salt water flows. Black indicates a scouring lock.	15
Figure 7: Aerial view of the Philipsdam.	16
Figure 8: Overview of Krammer lock complex. (The viewing angle is visible in Figure 7.)	16
Figure 9: Overview of the perforated bottom floor in the Krammer commercial lock. Adapted from (Rijkswaterstaat Bouwdienst, 2000b).	20
Figure 10: Cross section of lock chamber, indicating how levelling of the salt-fresh interface is disturbed by a ship. Adapted from (Rijkswaterstaat Bouwdienst, 2000b).	21
Figure 11: Schematic cross sectional view of the flow through the perforated bottom. (Rijkswaterstaat Bouwdienst, 2000b).	21
Figure 12: Cross section of Krammer commercial lock with salt and fresh water flows. Adapted from (Rijkswaterstaat Bouwdienst, 2000b).	22
Figure 13: Top view of the culvert system of the Krammer locks. Adapted from (Rijkswaterstaat Bouwdienst, 2000b).	23
Figure 14: Schematic difference in orthogonal cross sections of a lock chamber between the system of the commercial (1) and the recreational (2) locks. Adapted from (Rijkswaterstaat Bouwdienst, 2000b).	24
Figure 15: Air bubble screen with two strands in test mode. (Deltares, 2011d)	27
Figure 16: Sketch of air bubble screen with two strands in Krammer pilot at VZM side.	27
Figure 17: Sketch of air bubble screen with six strands in Krammer pilot at ES side.	27
Figure 18: Layout of water screen in Krammer pilot at Eastern Scheldt side. (Rijkswaterstaat Zeeland, 2013).	28
Figure 19: Cross section of air bubble- and water screen. All dimensions in <i>mm</i> ; water level in <i>m</i> . Adapted from (Rijkswaterstaat Zeeland, 2013).	29
Figure 20: Sketch of lock paddles situated in lock gate at Volkerak Zoommeer side.	30
Figure 21: Configuration 0 – Longitudinal cross section of lock chamber with no active salt intrusion prevention.	32
Figure 22: Configuration 1.1 – Longitudinal cross section of lock chamber with <i>Duinkerken system</i> as salt intrusion prevention.	33
Figure 23: Configuration 1.2 – Longitudinal cross section of lock chamber with air bubble- and water screen as salt intrusion prevention.	34
Figure 24: Configuration 2.1 – Longitudinal cross section of lock chamber with fixed sill as salt intrusion prevention.	35
Figure 25: Configuration 2.2 – Longitudinal cross section of lock chamber with movable sill as salt intrusion prevention.	36
Figure 26: Configuration 2.3 – Longitudinal cross section of lock chamber with movable sill in combination with air bubble- and water screen as salt intrusion prevention.	37
Figure 27: A 3D sketch of the design, placed at the commercial lock head at the ES side. Several detailed elements are printed in colours and are described on the previous page.	48

Figure 28: Zoomed in on the sill to visualise some main structural elements.	48
Figure 29: Range of vertical moving sill in cross section of Krammer commercial lock chamber. Adapted from (Rijkswaterstaat, 1981). Dimensions are presented in metres.	49
Figure 30: Range of vertical movement of sill in Krammer commercial lock. Adapted from (Rijkswaterstaat, 1981). Dimensions are presented in metres.	49
Figure 31: Rail at lock wall; in the figure partly closed to block water past the sill.	50
Figure 32: Solid slab replaces bottom slabs on the right in the figure.	51
Figure 33: Photograph of bottom slabs in lock chamber. Adapted from (Rijkswaterstaat Bouwdienst, 2000b).	51
Figure 34: Details of connections of different steel construction elements. Welds are printed red; further, the same colours are used as in Figure 27.	52
Figure 35: Sketch of 1 of 8 sections of a water screen with small reservoir.	55
Figure 36: Sketch of 1 of 4 sections of a water screen with large reservoir.	56
Figure 37: Sketch of possible layout of air bubble screen with small reservoir, formed by 24m long strands. (six strands and numerous diffusers visible)	58
Figure 38: Sketch of possible layout of air bubble screen with large reservoir.	58
Figure 39: Cross section of movable sill. Integration of air (red) and water (blue) reservoirs.	60
Figure 40: Vertical sliding sill controlled by cables in a winch system.	62
Figure 41: Vertical sliding sill controlled by hydraulic jacks.	62
Figure 42: Vertical sliding sill controlled mechanically by cogwheels along vertical bars.	63
Figure 43: Ship-induced water movements. (CIRIA; CUR; CETMEF, 2007).	66
Figure 44: Specification of flow velocities by propeller jet. Adapted from (CIRIA; CUR; CETMEF, 2007).	67
Figure 45: Theoretical maximum water density difference over sill.	68
Figure 46: Overview of sliding movable sill in rail connected to lock wall.	73
Figure 47: Overview of parameters used for calculating salt leakage in Krammer commercial lock.	77
Figure 48: A 3D sketch of the design, placed at the commercial lock head at the ES side. The most important detailed elements in this study are printed in colours.	86
Figure 49: Pictures of pivot-inspection chamber.	96

Figures in the appendices

Figure 50: Flow pattern of water without density difference with air bubble screen.	5
Figure 51: Flow pattern of water with density difference with air bubble screen.	5
Figure 52: visualisation of air bubble and water screen in a lock chamber.	6
Figure 53: Artist impression of top view of liquid gel lock in the Netherlands. Adopted from http://www.architectenweb.nl/aweb/redactie/Photo.asp?iNID=27668&PhotoID=218673	9
Figure 54: Movable sill as salt intrusion prevention.	9
Figure 55: Salt water pit as salt intrusion prevention.	10
Figure 56: Schematic overview of the <i>Trapjeslijn</i>	14
Figure 57: Schematisation of a locking cycle at the Krammer recreational locks. Adapted from (Rijkswaterstaat, 1981). ('zout'=salt, 'zoet'=fresh).	19
Figure 58: Schematisation of a locking cycle at the Krammer commercial locks. Adapted from (Rijkswaterstaat, 1981). ('zout'=salt, 'zoet'=fresh).	20
Figure 59: Tide (red), represented as two discrete water levels (blue).	22
Figure 60: Intermezzo which explains why the minimum water height must be used for the air pipe flow velocity calculations.	25
Figure 61: Concept 1 – Rotating flap.	29
Figure 62: Concept 2 – Rotating segment.	30
Figure 63: Concept 3 – Rotating split gates.	31
Figure 64: Concept 4 – Translating vertical slider.	32
Figure 65: Concept 5 – Translating horizontal slider.	33
Figure 66: Concept 6 – Translating split rolling gate.	34

Figure 67: Concept 7 – Translating inflatable sill.	35
Figure 68: Connector consists of stiff box-shape. In light blue the air bubble- and water screen.	40
Figure 69: Connector consists of flexible sheet. In light blue the air bubble- and water screen.	41
Figure 70: Fragment of cross section of lock with movable sill. Units are displayed in feet.	47
Figure 71: Movable sill. Driving mechanism: Rubber bellow.	48
Figure 72: Visualisation of locations for return flow calculation.	52
Figure 73: Clarification of used locations and symbols in calculation of return force on sill.	55
Figure 74: Specification of flow velocities by propeller jet. Adapted from (CIRIA; CUR; CETMEF, 2007).	56
Figure 75: Situation 1 – Location of propeller in respect to sill.	57
Figure 76: Detailing of influence area of propeller at distance of 0 m after lowering of propeller in respect to sill's level.	58
Figure 77: Calculation of influence area of the sill.	58
Figure 78: Situation 2 – Location of propeller in respect to sill.	59
Figure 79: Propeller's velocity distribution along axis perpendicular to propeller jet axis at different distances from the sill.	60
Figure 80: Detailing of influence area of propeller at distance of 5 m after lowering of propeller in respect to sill's level.	60
Figure 81: Situation 3 – Location of propeller in respect to sill.	61
Figure 82: Ship impact force for 6.3 km/h and 12k DWT -line. Adapted from (Svensson, 2009, p. 23).	62
Figure 83: Schematic layout of force distribution of plates (grey) via studs (pink) and main beams (orange) in movable sill.	73
Figure 84: Comparison of deflection and bending moment of discontinuous and continuous beam.	73
Figure 85: Dimensions of UPE -profile.	75
Figure 86: Dimensions of rectangular profile.	75
Figure 87: Loads and bending moment on main beam.	76
Figure 88: Dimensions of HE -profile.	76
Figure 89: Dimensions of CHS -profile.	78
Figure 90: Cross-section of lock chamber. Blue area must remain unharmed for navigational purposes. Yellow area is available for the movable sill. Ranges on the left side indicate different locations of the sill. Adapted from (Rijkswaterstaat Bouwdienst, 2000b).	79
Figure 91: Top view of the recess. F indicates location of exerted force from sill on concrete.	80
Figure 92: Ratio between compressive force F and tensile force T in the concrete.	81
Figure 93: Cross section of recess in top view with reinforcing steel indicated. Adapted from unpublished technical drawings of the lock complex.	81
Figure 94: Dimensions of sill in respect to the rail are presented left (range 3 in Figure 90) and in respect to the recess on the right (range 2 in Figure 90).	82

List of tables

Tables in the main text

Table 1: SI units in this report.....	x
Table 2: Derived units in this report; including SI notation.	x
Table 3: Specific (less common) units in this report.....	x
Table 4: Conversion of units.....	xi
Table 5: Overview of several salt intrusion countermeasures in locks. Composed with values from chapter 4.4 of (Deltares, 2011a). Values depend on regarded configuration.....	12
Table 6: Information about the locks of Figure 4.....	13
Table 7: Characteristic information of each of the two Krammer recreational locks.....	17
Table 8: Characteristic information of each of the two Krammer commercial locks.	17
Table 9: Tidal range Eastern Scheldt at Krammer locks.....	18
Table 10: Extreme water levels Eastern Scheldt at Krammer locks.	18
Table 11: Water levels Volkerak Zoommeer.	18
Table 12: Locking time of Krammer recreational lock (time in minutes).....	18
Table 13: Locking time of Krammer commercial lock (time in minutes)	19
Table 14: Overview of treated salt intrusion prevention configurations in this section in the Krammer commercial locks.	31
Table 15: Comparison of countermeasure configurations in Krammer commercial lock (*NA: not applicable)	38
Table 16: MCA of concepts on basic movements.	45
Table 17: Governing load combinations.....	70
Table 18: Systems compared for the verification.	75
Table 19: Basic information for the calculations.	76
Table 20: Effectiveness of different configurations in Krammer commercial lock.....	77
Table 21: Yearly averaged fresh water loss of Krammer locks.	78
Table 22: Consumed power for the air bubble screen in the Krammer commercial lock per locking cycle.	79
Table 23: Consumed power for the water screen in the Krammer commercial lock per locking cycle. ...	80
Table 24: Construction costs of the screens for a design in the Krammer commercial lock.	81
Table 25: Construction costs of the screens for a design in the Krammer commercial lock with sill.	82
Table 26: Energy consumption and costs per year for different systems.....	83
Table 27: Comparison of most important features for configurations in one commercial lock.....	87

Tables in the appendices

Table 28: MCA of connector.	42
Table 29: Descriptions of box.	42
Table 30: Descriptions of sheet.	43
Table 31: Weight factors.....	44
Table 32: Costs and effectiveness of several countermeasures of salt intrusion in the Volkerak locks. Adopted from (Rijkswaterstaat Bouwdienst, 2008).....	49
Table 33: Costs and effectiveness of several countermeasures of salt intrusion in the Dintelsas locks. Adopted from (Rijkswaterstaat Bouwdienst, 2008).....	49
Table 34: Costs and effectiveness of countermeasure of salt intrusion in the Benedensas locks. Adopted from (Rijkswaterstaat Bouwdienst, 2008).....	49
Table 35: Results of return current calculations for governing location.	54
Table 36: Overview of load cases.	70
Table 37: Governing load combinations.....	71

Table 38: Calculated salt intrusion through one Krammer commercial lock.	91
Table 39: Effectiveness of different configurations in Krammer commercial lock.	92
Table 40: Calculated fresh water loss in one Krammer commercial lock.	92
Table 41: Calculation of consumed energy per year.	93
Table 42: Calculation of consumed energy for water levelling per locking cycle.....	94
Table 43: Check on installed power at Volkerak locks.	94
Table 44: Calculated required air flow in Volkerak commercial lock.	94
Table 45: Calculated capacity.....	95
Table 46: Determined air flow rates for air bubble screens in various lock configurations.....	95
Table 47: Consumed power per locking cycle of Krammer commercial lock.	95
Table 48: Origin of working pressures for different configurations.	95
Table 49: Determined pump capacity of installed pumps.	96
Table 50: Determined capacity of pumps.	96
Table 51: Determined discharge in Krammer commercial lock. Bold values are calculated.....	96
Table 52: Consumed power per locking cycle.	97

1. Introduction

Salt intrusion in the Netherlands is undesired, because the affected water is often used for drinking water and agricultural purposes. The phenomenon is prevented at numerous locations by implementing systems to reduce the intrusion of salt. This is done in the Netherlands since the 1970's. In the last decade, much more investigations have been done to improve salt intrusion reduction techniques.

Royal HaskoningDHV (RHDHV) is engineering an improved design for the Krammer lock complex in Zeeland, the Netherlands. The design can be improved further; especially when it comes to energy consumption of the system.

The overall task is to make a design of a movable sill, which will reduce the energy consumption in comparison to air bubble screens alone and improve the effectiveness of the salt intrusion prevention. The main challenge is to make a design for the Krammer locks, which is acceptable in terms of its technical design, nautical preconditions, operational abilities and financial aspects. A broader view of an implementation at other locations must give insight in the possibilities of the improvement, shown in this study.

Designing such a solution is very challenging, since it has never been done before.¹ That is also where the advantages for *RHDHV* lie; they will be able to develop the technique further. The use of a sill can be interesting and profitable if implemented on a large scale.

An application may be very economic. Theoretically, a movable impermeable sill will block the salt water intrusion completely. It consumes a lot less power, compared to a continuously air blowing bubble screen. There are quite a few challenges to deal with. Ships with a certain draught have to sail in and out, which means the sill will not be able to block the entire hydraulic perimeter. Also, there are movable parts located in the water, which is not favourable in terms of maintenance and repairs. These are just a few of the questions which have to be answered before a realistic design is possible.

Structure of the report

On the next page, a schematic overview of this report is presented. It can be seen as a floor plan of the structure of this report. From a broad description of salt intrusion through locks in CHAPTER 2, the problem of this study is described in CHAPTER 3. To tackle this problem, various rough concepts are presented in CHAPTER 4. These concepts are detailed on their most important elements. This results in an outline of the final design, which is elaborated in CHAPTER 5. It's described and illustrated how this design fits in the Krammer commercial lock; construction aspects are mentioned and the design is dimensioned by calculations.

In the verification in CHAPTER 6, the design of this report is tested to the main components of the problem description. It answers the questions of the problem description and shows in what degree further improvement is possible. The results are discussed in the chapter CONCLUSION. Finally, RECOMMENDATIONS are made which have to be regarded before further research is done.

The appendices are separated from the main text by a blue thickened sheet of paper.

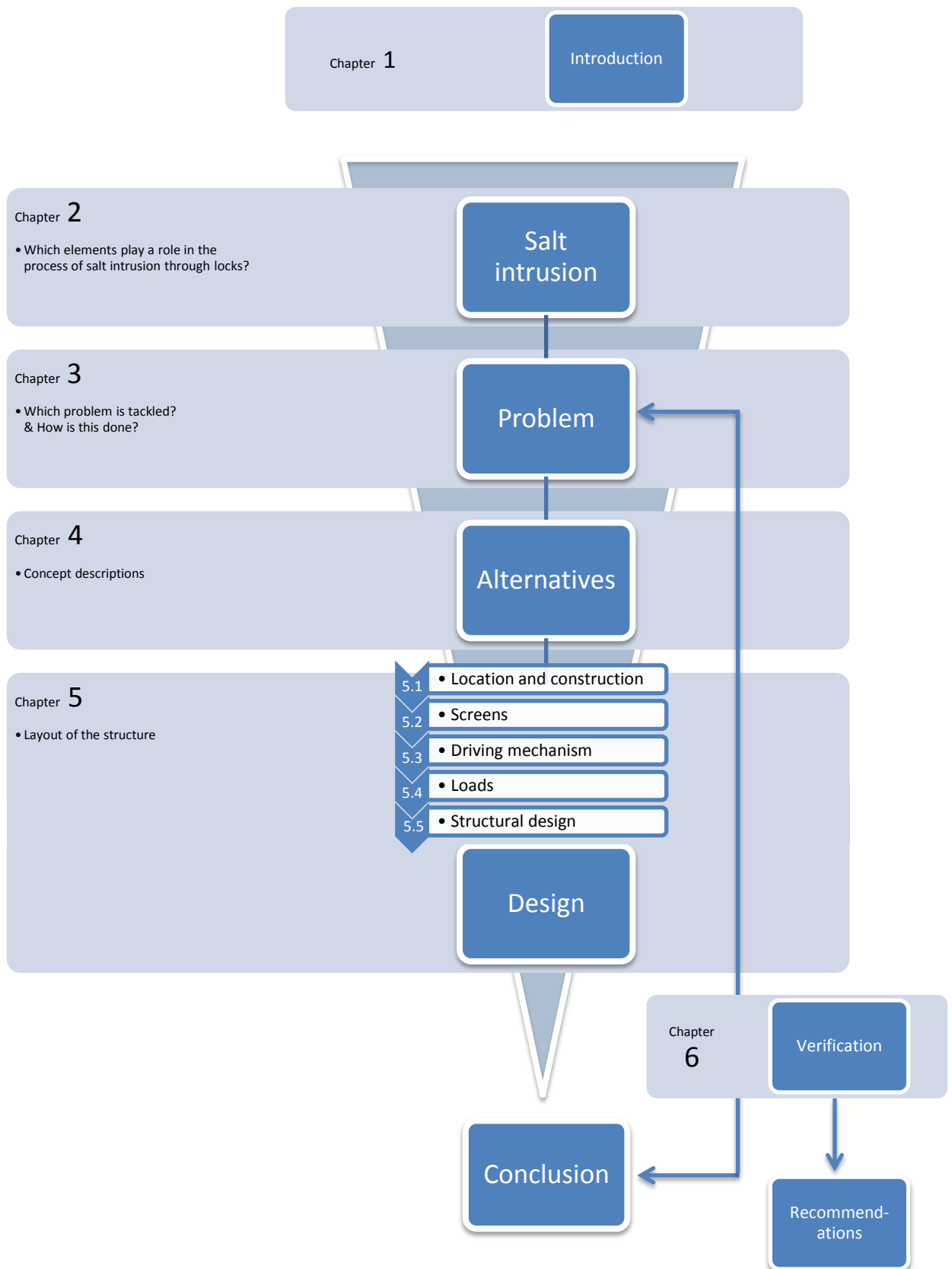
List of symbols

Uncommon and frequently used symbols in this report are explained in the list of symbols.

Terms, translations & abbreviations

Throughout this document, several terms and abbreviations need an explanatory note. This list gives an overview.

¹ One known application exists of which no documentation is available. It dates back to 1966.

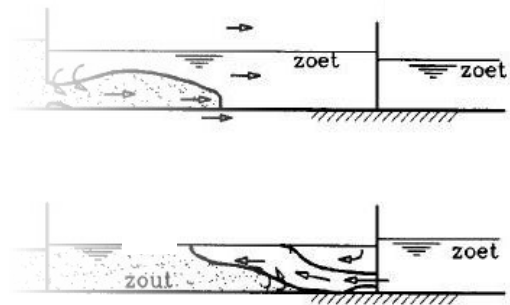


Chapter

2. Salt intrusion in locks

Before describing the problem which will be addressed in this study, a few subjects are highlighted. These subjects contribute to the basic understanding of the problem as described in chapter 3.

Salt intrusion occurs at locations where salt and fresh water are present. The two water types can be in open connection, or separated from each other by a structure. This chapter focuses on salt intrusion through locks. It also gives a description of the Krammer locks.



- 2.1 Salt intrusion in general
- 2.2 Description of the Krammer locks
- 2.3 Description of pilot project:
Krammer recreational lock
- 2.4 Exploration of possibilities:
Krammer commercial lock

2.1. Salt intrusion in general

To give insight in the present knowledge on salt intrusion, a description of its occurrence and prevention is presented in this section.

First, it is outlined in what perspective salt intrusion is problematic. Then, a description is given about which formulas are used to describe its physical processes. Finally, an overview is presented of what countermeasures to salt intrusion exist.

2.1.1. Problems regarding salt intrusion

In different scenarios it's desired to prevent salt water intruding a certain fresh water system. Environmental issues can play a role, but critical situations especially occur when it concerns water intake locations for agricultural use or drinking water supply.

Salt water intrusion in a fresh water system occurs for instance when a river discharges into sea. The tide causes the salt water to enter into the fresh water environment. In the Netherlands, this scenario is especially causing problems during the summertime, when the river discharges are relatively low. In times of extreme drought in Europe, the problems are at their maximum level. This results in silted fresh water intake locations. Even when the tide is blocked in a certain way (for instance by a lock, barrier or weir), it can sometimes still be possible for salt water to cause unwanted situations.

If for instance a lock disrupts the tide, salt water enters the location behind it when the lock is in use. This process is illustrated in Figure 2 for both high and low water levels at the outer side of the lock. To be clear, this is a situation for a lock without any salt intrusion preventive measures. If levelling takes place under free decay to the lock chamber, a salt water wedge will enter the lock (see upper figure). After opening the gates, the total lock chamber will be salt. When passage to the inner side is made, levelling under free decay will result in losing salt water from the lock chamber to the inner side. After opening the gates, all salt water will exchange with fresh (or brackish) water. If there is low water at the outer side of the lock, fresh water is lost by levelling under free decay. After opening of the gates, the entire lock chamber will become salt. Levelling to the inner side, results in an inflow of fresh water (see lower figure). After opening the gates, salt water will intrude in the fresh water regime at the inner side of the lock.

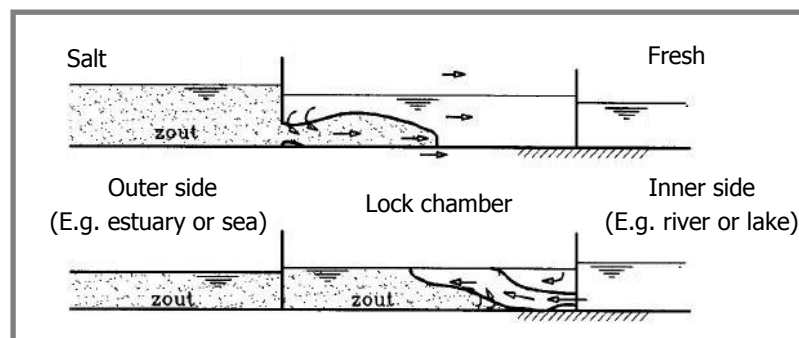


Figure 2: Salt and fresh water movements in a lock chamber during levelling. Adapted from (Rijkswaterstaat Bouwdienst, 2000b).

In different cases (blocked tide as in a lock; free entering tide as in the Nieuwe Waterweg) preventive measures to control water salinity exist. Salt water has a higher specific density than fresh water. This fact is used in the prevention of salt water intrusion by implementing a threshold or a salt catchment. These are not the best solutions², but they do work and have the benefit of being implemented quite easily in the design of the structure. To equip an existing structure with these features will be a lot harder. There are more innovative solutions, but these are rather new and have not yet been developed

² More effective solutions exist as well. See section A.2 and (Rijkswaterstaat Bouwdienst, 2000b).

to a high level of detail. Use is made of the principle that water mixes less easily if the different water types are separated in terms of state (flow velocity, flow direction) from each other. Air bubble- and water screens are able to provide such difference. The salt water wedge will be mixed with layers at the top of the water column. Apart from that, a vertical flow arises, reducing horizontal exchange flows. Appendix A elaborates on this subject.

Why prevent salt intrusion?

If salt intrudes in a fresh water regime, it turns rather quick in brackish or even salt conditions. In this intermezzo a quick quantification of the effects is provided for the Volkerak Zoommeer.

The Volkerak Zoommeer is a fresh lake. Fresh water enters the lake via the Volkerak locks in the north and via two small rivers in the east. Salt water intrudes this fresh water regime via the Krammer locks in the south, which separates the salt Eastern Scheldt from the fresh Volkerak Zoommeer.

A total salt leakage through the entire Krammer lock complex of maximal 60 kg/s is accepted by the Dutch Department of Public Works. This equals approximately $5.2 \cdot 10^6 \text{ kg/day}$ for the lock complex and $0.15 \cdot 10^6 \text{ kg/cycle}$ for one lock chamber.

The worst case scenario can be defined as the maximum possible salt intrusion through the locks. This occurs when the volume of a salt lock chamber exchanges completely with fresh water from the Volkerak Zoommeer, with a maximum water density difference present. In that case $280 \cdot 24 \cdot 6.25 = 42,000 \text{ m}^3$ of water, adds 25 kg of salt to the VZM for every exchanged cubic metre of water (when $\rho_{\text{salt water}} = 1,025 \text{ kg/m}^3$). In this way $1.1 \cdot 10^6 \text{ kg}$ of salt enters the Volkerak Zoommeer every locking cycle for every lock chamber. This equals a quantity of 35 big trucks – fully loaded with salt – every locking cycle for both lock chambers.

Without countermeasures, the most extreme salt leakage exceeds the maximum allowed salt leakage by more than 700%.

Conclusion

The above is not a detailed calculation, but even if the exchange per locking cycle is only half or a quarter of the most extreme salt leakage, it is significant and exceeds the maximum allowed leakage. Salt water will also flow out of the system, which is not taken in account here. The described processes continue day after day and will nevertheless lead to big environmental impacts if no countermeasures are taken.

Intermezzo 1: Salt load through Krammer lock complex on the fresh lake Volkerak Zoommeer.

2.1.2. Physical description of the salt intrusion process

To describe either salt intrusion effects or its prevention, it must be clear how this salt water acts or what it basically is. First the underlying theory is explained, followed by a more practical description of the occurring processes. Finally, it's described how salt intrusion is calculated in this report.

Theory

The main difference between salt and fresh water is that salt is dissolved in salt water. It settles between the water molecules, increasing its volumetric weight but hardly changing the volume of the water. When salt intrusion is expressed in numbers, the unit kg/s is used. The volume of salt which leaks through a lock in a year's time, is averaged over a year expressed in seconds. This depends mainly on the salt content of the water, the discharge or exchange flow of the water and the duration of the discharge.

The content of salt in water can be quantified in several ways. Parts per thousand (ppt) or parts per million (ppm) describe the weight dependent relative amount of salt in water. In this way 20 ppt means that 20 kg of salt is present in $1,000 \text{ kg}$ of salt water. Also salinity (with sign S) is used in this same way. In that case the sign for promille (‰) is used instead of ppt .

Another way to describe the amount of salt in water is based on its chlorine content expressed in mg/l . A chlorine content of $1 mg/l$ corresponds roughly to $1.8 ppt$. A more thorough description can be found in the *List of symbols* on page x.

A layer of salt water can be present at the same time as a layer of fresh water. Because of the difference in density, flows arise between the different layers. The situation of an initially closed lock gate is examined, as visualised in Figure 3. Fresh and salt water are separated by the lock gate. At the bottom of the gate, the hydrostatic pressure of the salt water is higher than that of fresh water, because of its higher density. This causes the salt water to push slightly to the fresh water.

As can be seen in the figure, the fresh water at the right side is levelled higher than the salt water. In this way, the forces on the gate are in equilibrium. By this induced equilibrium of forces on the gate, it's possible to take into account the internal effects of stratified flows only. When no equilibrium is present, an external wave will arise, which results in a net flow in one direction. That is not desired in an analysis of internal stratified flows.

The salt leakage S from the salt to the fresh water side of a certain lock can be derived by using expressions for different stages and locations. When the lock gates are closed, salt intrudes due to levelling of water. After that, salt water enters the lock chamber by moving past the opened outer lock gates. At the end of the locking cycle, it enters the fresh water side by leaving the lock chamber via the opened inner lock gate.

It may be clear that the (fluctuating) water level at the salt water side of the lock and the timespan the gates are open are of great influence on the salt leakage through the system.

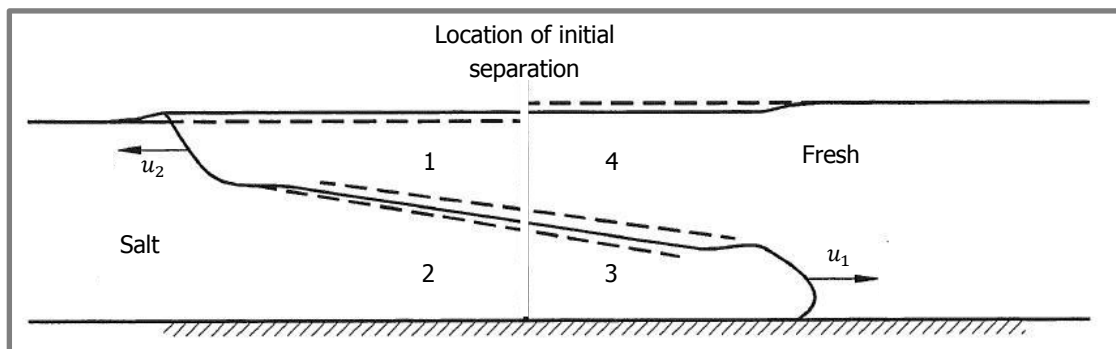


Figure 3: Movement of initially separated salt and fresh water after removal of separation.
Adapted from (Kranenburg, 1998).

When the gates are opened at one side, an exchange flow arises. Figure 3 shows the situation just after a gate is opened. The salt water which was initially standing still at location 1, has moved via location 2 to location 3. When the friction losses are neglected, all potential energy from the salt water at location 1, is converted to kinetic energy of the moving salt water wedge in location 3. Potential energy of the density difference $\Delta\rho$ (Eq. 2.1) is the driving force. The kinetic energy on the other hand (Eq. 2.2), is described for the energy needed to move both water wedges with the total water density in opposing directions.³ Eq. 2.3 shows the formula which describes the theoretical velocity of the two opposing water wedges – illustrated in Figure 3 as u_1 and u_2 . The formula for salt leakage in an infinitely long⁴ lock chamber during a time interval Δt is shown in Eq. 2.4.

³ Theoretically, the velocity of a salt water wedge must be calculated by using $\rho + \Delta\rho$; the velocity of the fresh water wedge by using ρ . In the presented calculation for kinetic energy, an initial water density difference of 0 is assumed.

⁴ Formula is only valid when an infinitely long lock chamber is assumed, since in that case reflection of water at an opposing lock gate does not occur. That effect is not inserted in the formula.

$$E_{p,\Delta} = m \cdot g \cdot h = \frac{1}{4} \cdot u \cdot h^2 \cdot \Delta\rho \cdot g \cdot \Delta t$$

Eq. 2.1

With:	$E_{p,\Delta}$	Potential energy of water density difference [J]
	m	Mass of considered volume of water [kg]
		$m = \Delta\rho \cdot u \cdot \frac{1}{2} h \cdot \Delta t$
	$\Delta\rho$	Water density difference between fresh and salt [kg/m ³]
	u	Velocity of salt wedge [$\frac{m}{s}$]
	h	Height of water column, subjected to exchange flow [m]
	Δt	Duration of opened gates [s]

$$E_k = 2 \left(\frac{1}{2} \cdot m \cdot u^2 \right) = \frac{1}{2} \cdot u^3 \cdot h \cdot \rho \cdot \Delta t$$

Eq. 2.2

With:	E_k	Kinetic energy [J]
	m	Mass of considered volume of water [kg]
		$m = \rho \cdot u \cdot \frac{1}{2} h \cdot \Delta t$
	ρ	Water density [kg/m ³]

$$E_{p,\Delta} = E_k, \quad u = \frac{1}{2} \sqrt{g \cdot h \cdot \epsilon}$$

Eq. 2.3

With:	ϵ	Relative water density difference [–]
		$\epsilon = \frac{\Delta\rho}{\rho}$

$$S_{\Delta t} = q_{salt}^0 \cdot \Delta t \cdot w_{lock} \cdot \frac{\Delta Cl}{0.56} = \frac{1}{4} \sqrt{g \cdot h \cdot \epsilon} \cdot h \cdot \Delta t \cdot w_{lock} \cdot \frac{\Delta Cl}{0.56}$$

Eq. 2.4

With:	$S_{\Delta t}$	Salt leakage during Δt [kg]
	q_{salt}^0	Initial discharge of salt water wedge [m ² /s]
		$q_{salt}^0 = u \cdot \frac{1}{2} h = \frac{1}{4} \sqrt{g \cdot h \cdot \epsilon} \cdot h$
	w_{lock}	Width of the lock chamber [m]
	ΔCl	Difference of chlorine content between both sides of the lock [kg/m ³]

Salt intrusion occurs in reality by passing the outer gate and the inner gate of the lock chamber subsequently. At high water, more water exchanges at the outer gate than in the same time at the inner gate after downward levelling of water. The actual possible intrusion is restricted by the minimum water column.

Another restriction is the maximum intrusion. When the lock gates are opened long enough, the entire lock's volume is exchanged. The maximum intruding amount of salt able to pass the lock in one cycle is described in Eq. 2.5.

Finally, Eq. 2.6 describes salt intrusion through a lock chamber. Both restrictions are inserted in the form of the minimum water height $\min\{h_{salt}, h_{fresh}\}$ and the maximum salt leakage S_{max} .

The presented theoretical formulas only hold for a situation immediately after opening of the gates with an initial water density difference of ΔCl .

$$S_{max} = A_{lock} \cdot \min\{h_{salt}, h_{fresh}\} \cdot \frac{\Delta Cl}{0.56} = 1.2 \cdot 10^6 \text{ kg}$$

Eq. 2.5

With:	S_{max}	Maximum salt leakage [kg]
	A_{lock}	Surface of the lock chamber [m ²]
	ΔCl	Maximum difference in chlorine content between both sides of the lock [$\frac{kg}{m^3}$]

$$S_{total \text{ per cycle}} = \frac{1}{4} \sqrt{g \cdot \min\{h_{salt}, h_{fresh}\} \cdot \epsilon \cdot \min\{h_{salt}, h_{fresh}\} \cdot \Delta t \cdot w_{lock} \cdot \frac{\Delta Cl}{0.56} < S_{max}}$$

Eq. 2.6

With:	$S_{total \text{ per cycle}}$	Total salt leakage during one locking cycle [kg]
	h_{salt}	Height of water column at salt side, outside of the lock chamber [m]
	h_{fresh}	Height of water column at fresh side, outside of the lock chamber [m]

Practice

The theoretical salt leakage through a lock is influenced in many ways. Bottom friction, turbulence, mixing and ship movements disturb the stratified flows. Also not included in the theoretical description is the reflection of a salt wedge in a lock chamber when it encounters the opposing closed gate.

Since these features are too complex to fit in formulas, a description of a more realistic behaviour of the water wedges follows in this section.

Salt and fresh water do not behave as homophobic as oil in water, but it still intends to remain separated in different layers. For this reason the interface in Figure 3 is presented as double dashed lines instead of a solid line. Mixing of layers and a vaguer interface between them are stimulated by two effects. If the velocities of both layers are in the opposite direction and exceed a certain value, there will be short instable internal waves – caused by internal friction. These short waves induce turbulence and mixture. Secondly, mixing can be caused by some external force; for instance the turbulence from a ship's propeller.

If the opposing velocities of the two layers are small enough, this will prevent short instable internal waves, which cause mixing. To quantify the actual flow velocities, measurements have shown an actual difference in magnitude of opposing flow velocities. Especially bottom shear forces (not present in fresh water wedge) cause the lower wedge to move slower. Eq. 2.7 shows the velocities of water wedges in a lock, by use of empirical coefficients.

In an ideal situation without friction, flow is exactly critic for both wedges ($Fr = 1$). Due to friction, all flows are subcritical. A velocity inequality is stimulated by either a density difference, or layer thickness or channel width⁵ and by suction behind the lock gates. When both velocities are added, Eq. 2.8 and Eq. 2.9 show that flows are indeed subcritical ($Fr < 1$). (Kranenburg, 1998, p. 6.9)

⁵ At the outer side of the lock gate, the width of the channel will increase compared with the lock chamber width in most cases.

$$u_1 = C_1 \sqrt{\epsilon g a} = 0.69 \text{ m/s}, \quad u_2 = C_2 \sqrt{\epsilon g a} = 0.84 \text{ m/s}$$

Eq. 2.7

With:	C_1, C_2	Coefficients which take into account the effects of friction on the opposing exchange flow velocities. Values are obtained from (Barr, 1963) [-]
	h_{max}	Maximum height of water column in operational Krammer lock (See section 2.2) [m]
	a	Thickness of water layer at location of initial separation [m]
	C_1	0.44 [-]
	C_2	0.53 [-]
	ϵ	$\frac{\rho_{salt} - \rho_{fresh}}{\rho_{salt}} = 2.9126 \cdot 10^{-2} \text{ kg/m}^3$
	h_{max}	8.75 m
	a	$\frac{h_{max}}{2} = 4.375 \text{ m}$

$$\Delta u = u_1 - u_2 = 0.97 \cdot u = 0.97 \cdot \sqrt{\epsilon \cdot g \cdot a}$$

Eq. 2.8

$$Fr = \frac{\Delta u^2}{\epsilon g a} < 1$$

Eq. 2.9

When a salt water wedge enters a lock through an opened gate, it reaches a closed gate at the other side of the lock chamber. In this case, the salt water wedge will deflect on the closed gate and climbs to the water surface. Theoretically, it will climb up to the water surface completely, but due to friction losses the top of the water column will not be reached and remains fresh. Experiments (Deltares, 2011b, p. 24) show that approximately 10% of the (fresh) water volume does not exchange and remains in the lock chamber, even when the gates are kept open for a long time.

The exchange flow is set in motion by a density difference. When the water in a lock chamber is not very salty and only a small density difference is present, the exchange flow reduces. Also the amount of salt is lower in that case. The internal flow maintains itself as long as salt and fresh water are available. The exchanged volume is equal for both layers.

The exchange flow stops completely when approximately 90% of the lock chamber volume is exchanged or when the lock gates are closed. By the flow velocity of the salt wedge (0.69 m/s, see Eq. 2.7) in combination with the time the gates are open (28 minutes see Table 13), it is clear that exchange has stopped before the gates close. So 90% of the lock chamber volume exchanges when no countermeasures are taken.

Countermeasures to salt intrusion reduce the exchanging volume of water. A countermeasure is expressed as an (empirically obtained) percentage ($f_{reduction}$) of its reduction of the exchanging water volumes. In that way it can be easily inserted in an analysis of salt intrusion through a lock.

Intermezzo 2 shows how salt leakage is calculated in this report.

Theoretical calculation of salt intrusion

A calculation for 1 Krammer commercial lock (gates open 28 minutes and averaged water level of ES assumed equal to VZM) results in the following salt intrusions:

- Theoretical formula Eq. 2.6 $2.2 \cdot 10^6 \text{ kg}$
- Restricted by S_{max} Eq. 2.5 $1.2 \cdot 10^6 \text{ kg}$

The theoretical formula calculates a value approximately twice as large as the maximum possible salt intrusion. This can be understood by taking in mind that the salt wedge (0.69 m/s) travels the length of the lock chamber (280 m) more than 4 times. When the thickness of the layer remains half of the initial water depth, the lock chamber is filled two times.

In reality, the exchange flow stops after 90% of the lock chamber is filled with salt water.

Calculation method of this report

This leads to a more simple way of calculating salt intrusion. It's based on an analysis of exchanging water volumes. Reduction factors for countermeasures are inserted as a complement of its intrusion reduction (100% reduction means 0% intrusion and vice versa).

$$(90\% \cdot A_{lock}) \cdot h \cdot \Delta\rho \cdot 100\% = 1.1 \cdot 10^6 \text{ kg}$$

As an example, a salt intrusion countermeasure with an effectiveness of 70% would result in:

$$(90\% \cdot A_{lock}) \cdot h \cdot \Delta\rho \cdot 30\% = 0.33 \cdot 10^6 \text{ kg}$$

Conclusion

The used calculation method for salt intrusion in this report is:

$$(90\% \cdot A_{lock}) \cdot h_{min} \cdot \Delta\rho \cdot f_{reduction}$$

Intermezzo 2: Calculation of salt intrusion through Krammer locks using different formulas.

2.1.3. Current counter measures to salt intrusion

There are various options to decrease or even eliminate the effects of salt water intrusion in fresh water systems. In the past, most research on this subject was focusing on air bubble screens. This doesn't mean it is the only good and effective option, though. A thorough analysis on several counter measures to salt intrusion is given in appendix A, including a description of how they prevent salt from intruding.

In this section, several technical solutions which are implemented in the Netherlands are presented. These are listed in Table 5, including information of costs and effectiveness. These are very hard to quantify in exact numbers, because they depend on many variables and are location specific. All numbers are explained in the corresponding sections in appendix A. The costs are presented relative to each other; the effectiveness in terms of percentages compared to a doing nothing scenario.

In Table 6, the most important fresh and salt water separating locks in the Netherlands are specified.

Table 5: Overview of several salt intrusion countermeasures in locks. Composed with values from chapter 4.4 of (Deltares, 2011a). Values depend on regarded configuration.

Type of measure	Applications worldwide	First application	Last application	Construction methods	Costs (+ high & - low)			Effectiveness	
					Construction	Maintenance	Operation	Reduction salt intrusion	Fresh water loss
Air bubble screen	± 10 in Netherlands ± 50 worldwide	± 1960	Still being applied	Prefabricated parts are placed under water Embedding in existing structure possible	-	+	++	40%	20%
Liquid gel	Not yet built	-	-	Unknown	++	+	-	(100%)	(0%)
Movable sill	1 known application in the USA	1966	1966	In dry lock chamber or under water Embedding in existing structure possible	+	+	-	50%	10%
Salt water pit	2 in Netherlands ± 10 worldwide	1968	Still being applied	Construction during construction of lock in drydock or on (temporary) artificial island	++	--	++	80%	200%
Flushing of lock chamber	± 6 in Netherlands ± 20 worldwide	?	Still being applied	Paddles can be placed in the doors after construction of the lock	+	-	+	95%	80%



Figure 4: Localisation of locks in the Netherlands. For more information, see Table 6 below.

Table 6: Information about the locks of Figure 4.

	Name	Location	Type of lock	Salt intrusion prevention	Length [m]	Width [m]	Sill depth [m]	Lift height [m]
1	Nieuwe Statenzijl Spuisluis	Nieuwe Statenzijl	Stop lock	none	-	-	-	-
2	Munsterzijl Sluis	Termunterzijl	Navigation lock	none				
3	Zeesluizen	Delfzijl	Navigation lock	Flushing of lock chamber				
4	Robbengatsluis	Lauwersoog	Navigation lock	none				
5	Tjerk Hiddessluizen	Harlingen	Navigation lock	Flushing of lock chamber & Air bubble screen				
6	Lorentzsluis	Kornwederzand	Navigation & Stop lock	Air bubble screen	120	13	4	
7	Stevinsluis	Den Oever	Navigation & Stop lock	Air bubble screen	120	13	4	
8	Koopvaardersschutsluis	Den Helder	Navigation lock	Flushing of lock chamber & Air bubble screen	90	16	5.5	2.5
9	Zuider-, Midden-, Noordersluis	IJmuiden (NL)	Navigation lock	Air bubble screen	400	50	15	2.9
10	Schiedam	Schiedam	Navigation lock	Flushing of lock chamber	71	9	3	2.9
11	Rozenburgsesluis	Spijkenisse	Navigation lock	Air bubble screen	330	24	6	3.3
12	Goereese Sluizen	Stellendam	Navigation lock	Air bubble screen	145	16	5	3.75
13	Krammer recreational lock	Krammer	Navigation lock	Air bubble screen	90	9	2.7/3.7	2.5
14	Krammer commercial lock	Krammer	Navigation lock	Flushing of lock chamber	280	24	6.25	2.5
15	Volkeraksluizen	Volkerak	Navigation lock & Stop lock	Air bubble screen	345	24	11.25	2.6
16	Bergse Diepsluis	Bergse Diep	Navigation lock	Flushing of lock chamber				
17	Kreekraksluizen	Kreekrak	Navigation lock	Flushing of lock chamber	340	24	5.45	2.8
18	Zandkreekdam	Katse Heule	Stop lock	none	-	-	-	-
19	Terneuzen 1	Terneuzen (NL)	Navigation lock	Salt water pit	290	40	6.85	6
20	Terneuzen 2	Terneuzen (NL)	Navigation lock	Salt water pit & Air bubble screen	305	24	3.7	5.1

2.2. Description of the Krammer locks

This report describes a solution to a problem related to the Krammer locks. For this reason more detailed information of these locks are given in this section. First, the outline and localisation is displayed, after which a description of its complex salt intrusion measure is given.

2.2.1. Outline

After a storm surge and the severe flooding⁶ in the Netherlands in 1953, it was agreed that a barrier had to be built. In the original plan this was designed as an impermeable dam. This dam would have no tidal influence behind it, and as a result, the lakes behind it would become fresh. In the early 70's, the public opinion changed towards a more environmental friendly idea. The dam in the Eastern Scheldt⁷ had to be permeable for the tide, and the ES itself should remain salt.

It was decided to install a barrier instead of a dam. A dam would cancel out the tide completely, and that was not desired. The proposed Eastern Scheldt storm surge barrier would allow tide to enter into the ES. This would decrease the tidal influence by more than 25%. To restore the tidal influence, it was decided to decrease the area of the ES. This was done by dividing the basin in several compartments. The Philipsdam is one of these compartmentalisation works – in which the Krammer locks are located. Due to this change, the compartmented waters became fresh instead of salt. Only the ES remained salt. The exact localisation of the locks in the Philipsdam is shown on satellite pictures; see Figure 5 to Figure 8.

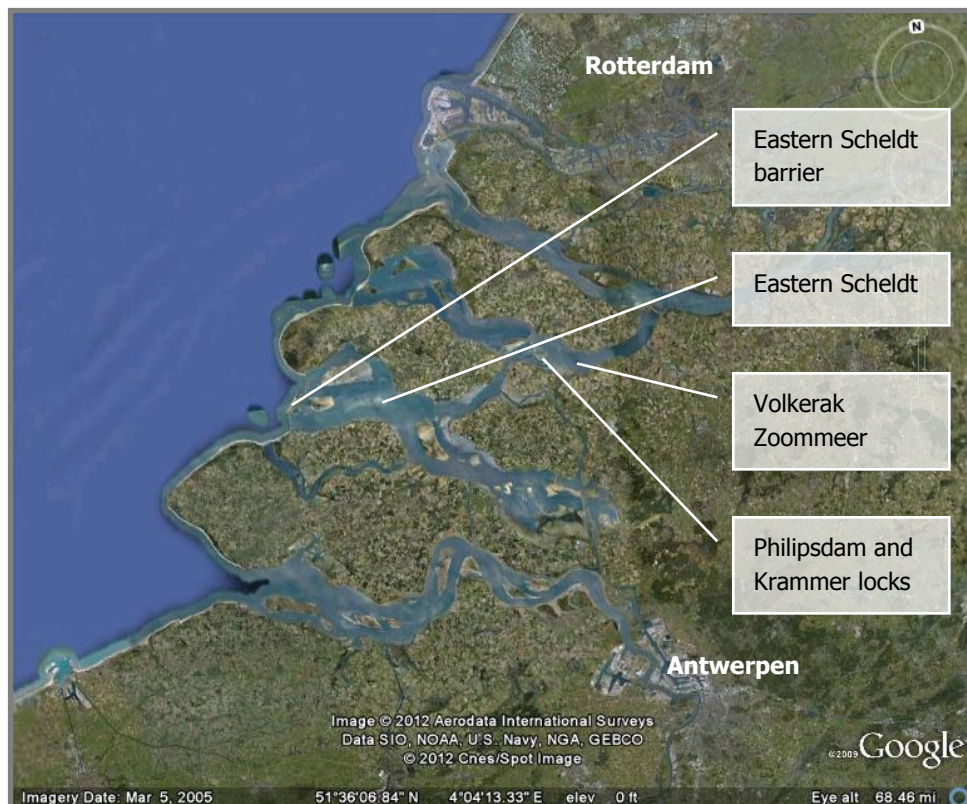


Figure 5: Aerial view of Zeeland.

⁶ For more information: http://nl.wikipedia.org/wiki/Watersnoodramp_van_1953

⁷ 'Eastern Scheldt' is from now referred to as 'ES'.



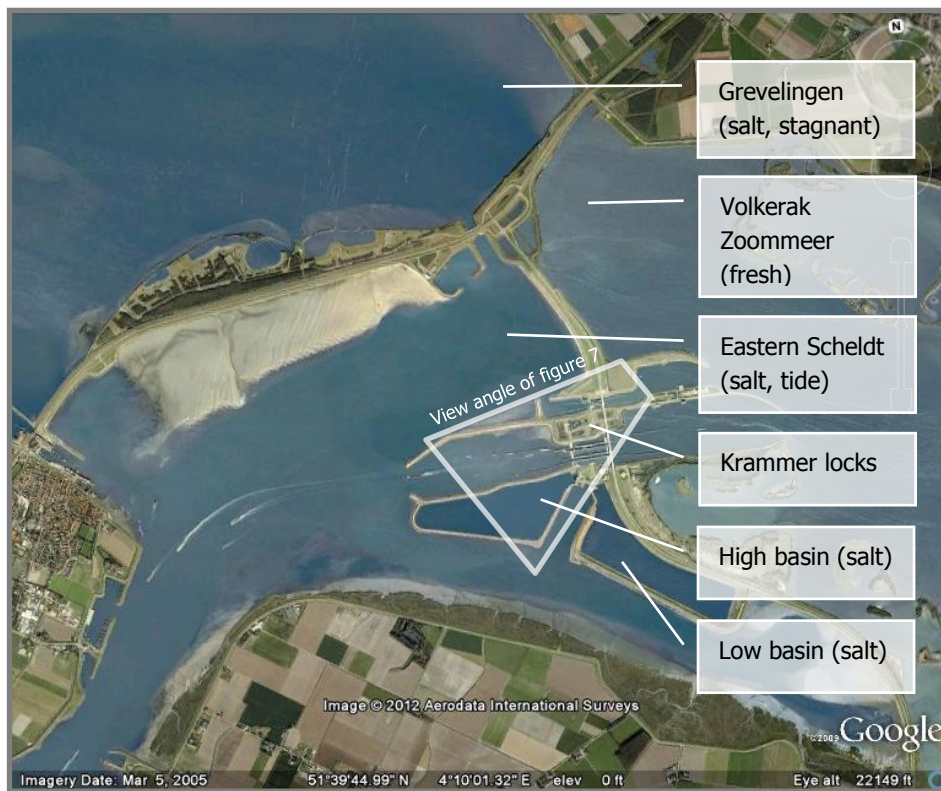


Figure 7: Aerial view of the Philipsdam.

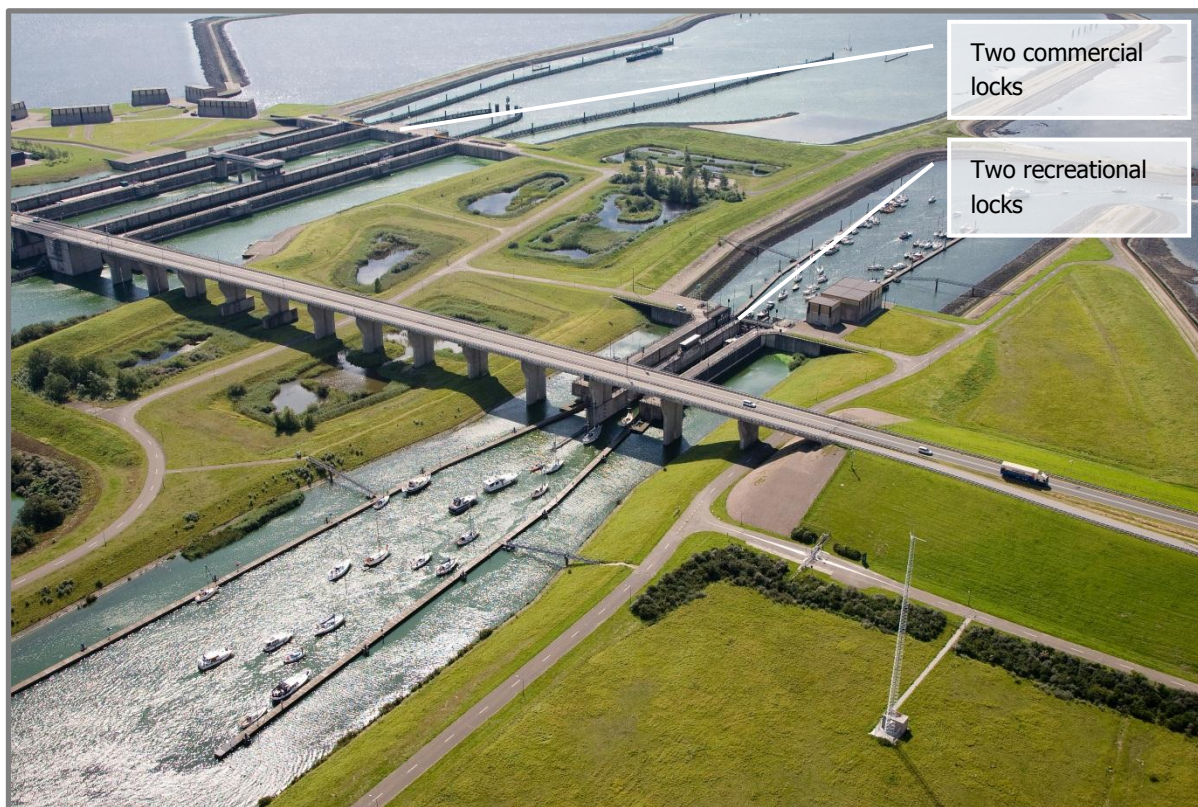


Figure 8: Overview of Krammer lock complex. (The viewing angle is visible in Figure 7.)

The Krammer locks were built between 1977 and 1984. However, they were not operational before 1987, as the locks were finished approximately three years ahead of finishing of the compartmentalisation dam. The lock complex consists of two recreational and two commercial navigation locks. Figure 8 in combination with Table 7 and Table 8 show the most important characteristic information of them. Every year, nearly 100,000 vessels make use of the Krammer locks. This is approximately equally divided over two types of ships – commercial vessels and the much smaller recreational boats – and over the two types of locks. It should be kept in mind that the commercial locks are always operational and the recreational locks at daytime only. The general idea behind the salt intrusion counter measure used in both types of locks, is that the content of the lock chamber is being exchanged with salt or fresh water, before the lock gates are opened.

Table 7: Characteristic information of each of the two Krammer recreational locks.

Length	90 m
Width	9.1 m
Sill height	Eastern Scheldt: -3.7 m NAP Volkerak: -2.7 m NAP
Bottom	-6.9 m NAP
Gate system	2 (vertical) revolving gates
Salt intrusion measures	In-/Outlet at bottom of inner gate Wall valves
Vessel class	AZM ($< 2.1\text{ m depth}$)
Shipping passages per year (both directions)	48,000 in 2005 63,000 in 2006 50,000 in 2007
Average number of locking cycles per day per lock	14.97 cycles/day in 2008
Energy consumption	$2.8 \cdot 10^5\text{ kWh/year}$

Table 8: Characteristic information of each of the two Krammer commercial locks.

Length	280 m
Width	24 m
Sill height	-6.25 m NAP (both sides)
Bottom	-11.0 m NAP
Gate system	2 (horizontal) rolling gates
Salt intrusion measures	Fixed sill Perforated bottom Wall valves
Vessel class	VIb ($< 4.7\text{ m draught}$)
Shipping passages per year (both directions)	42,000 in 2005 43,000 in 2006 43,000 in 2007
Average number of locking cycles per day per lock	14.26 cycles/day in 2011
Energy consumption	$5.0 \cdot 10^6\text{ kWh/year}$

The tidal influence on the ES at the west side of the Krammer locks is measured rather precise. Based on historical data from the last decade, future water levels can be estimated. Table 9 and Table 10 display estimated water levels at average and at extreme events.

The water level of the Volkerak Zoommeer⁸ is tended to be fixed around 0 *m NAP*. The possible variation range is provided in Table 11. The mentioned boundaries were opted in the original design, dating back to 1987. However, wind effects are not taken into account in these values. In the current situation, more extreme values are found for water levels of the VZM. This is shown in (Deltares, 2013, p. 13). Particularly, the wind effects increase the extremes to approximately +0.5 *m NAP* and –0.5 *m NAP*. Since the water level is tried to be kept fixed at 0 *m NAP*, that value is used in the calculations in this report.

The locking cycles of both lock types differ. The locking cycle of the recreational lock is 65 minutes, while the larger commercial lock needs 90 minutes for one locking cycle. Details of the *averaged* times of the different processes in the locking cycle are presented in Table 12 and Table 13. It should be noted that in the last column, the processes 'water exchange' and 'levelling' are changed. The reason for that change is explained in section 2.2.2.

It should also be noted that the average time for '*in- and out sailing*' is fluctuating very strongly. Also the overall time is depending on the way the locks are (manually) operated.

Table 9: Tidal range Eastern Scheldt at Krammer locks.

	Mean tide	Spring tide	Neap tide
High water (HW)	+1.63 <i>m NAP</i>	+1.84 <i>m NAP</i>	+1.35 <i>m NAP</i>
Low water (LW)	–1.45 <i>m NAP</i>	–1.51 <i>m NAP</i>	–1.29 <i>m NAP</i>
Tidal range	3.08 <i>m</i>	3.35 <i>m</i>	2.64 <i>m</i>

Table 10: Extreme water levels Eastern Scheldt at Krammer locks.

Highest water 2012	+2.06 <i>m NAP</i>
1/10 year high water	+3.50 <i>m NAP</i>
1/100 year high water	+4.65 <i>m NAP</i>
Lowest water 2012	–1.84 <i>m NAP</i>
1/10 year low water	–2.50 <i>m NAP</i>
1/100 year low water	–3.30 <i>m NAP</i>
Mean water level	+0.10 <i>m NAP</i>

Table 11: Water levels Volkerak Zoommeer.

Mean water level	0 <i>m NAP</i>
Upper boundary	+0.15 <i>m NAP</i>
Lower boundary	–0.10 <i>m NAP</i>

Table 12: Locking time of Krammer recreational lock (time in minutes)

	To VZM		To ES
Levelling	4	Water exchange	2
Water exchange	8	Levelling	5
Opening of gates	4	Opening of gates	4
In- and out sailing	15	In- and out sailing	15
Closing of gates	4	Closing of gates	4
<i>Total</i>	<i>35</i>	<i>Total</i>	<i>30</i>
		Locking cycle total	65

⁸ 'Volkerak Zoommeer' is from now referred to as 'VZM'.

Table 13: Locking time of Krammer commercial lock (time in minutes)

To VZM		To ES	
Levelling	5	Water exchange	8
Water exchange	15	Levelling	6
Opening of gates	4	Opening of gates	4
In- and out sailing	20	In- and out sailing	20
Closing of gates	4	Closing of gates	4
<i>Total</i>	<i>48</i>	<i>Total</i>	<i>45</i>
Locking cycle total		93	

In the year 2015 a major maintenance programme is planned for the Krammer lock complex; the salt intrusion system will be maintained for some 20 M€. Apart from that, the capacity of the locks should be increased in 10 to 15 years. A possible third commercial lock will cost approximately 300 M€.

The question is, whether this locking time can be brought down, while keeping the salt intrusion at the same (or a better) level. The current salt intrusion counter system takes relatively long locking time for trespassing ships. It should also be investigated whether maintenance and operational costs could be lowered. The pilot project at the Krammer recreational lock is initiated to give answers to these matters and is described in section 2.3.

2.2.2. Commercial locks

The most important figures of the commercial locks are displayed in Table 8. Figure 8 can be used to get a feeling of the dimensions. There are significant differences between the two types of locks, that's why they are described separately.

Description of system

The intermezzo on page 6 shows why counter measures against salt intrusion are needed in the Krammer locks. A rather complex system is included in the current locks design. This system is called the *Duinkerken system* (Kerstma, Kolkman, Regeling, & Venis, 1991).

Use is made of a perforated bottom floor in the lock with a chamber underneath it. Salt water enters and leaves the lock chamber via this floor. Adjustable valves at the side walls allow fresh water to flow in and out of the lock chamber. These valves are located perched along the long sides of the whole lock chamber and are in connection with fresh water, surrounding the lock. This surrounding fresh water is the same water as the VZM and has a fixed level (approximately 0 m NAP). A picture of the inner side of the commercial lock chamber during construction is visible in Figure 9.

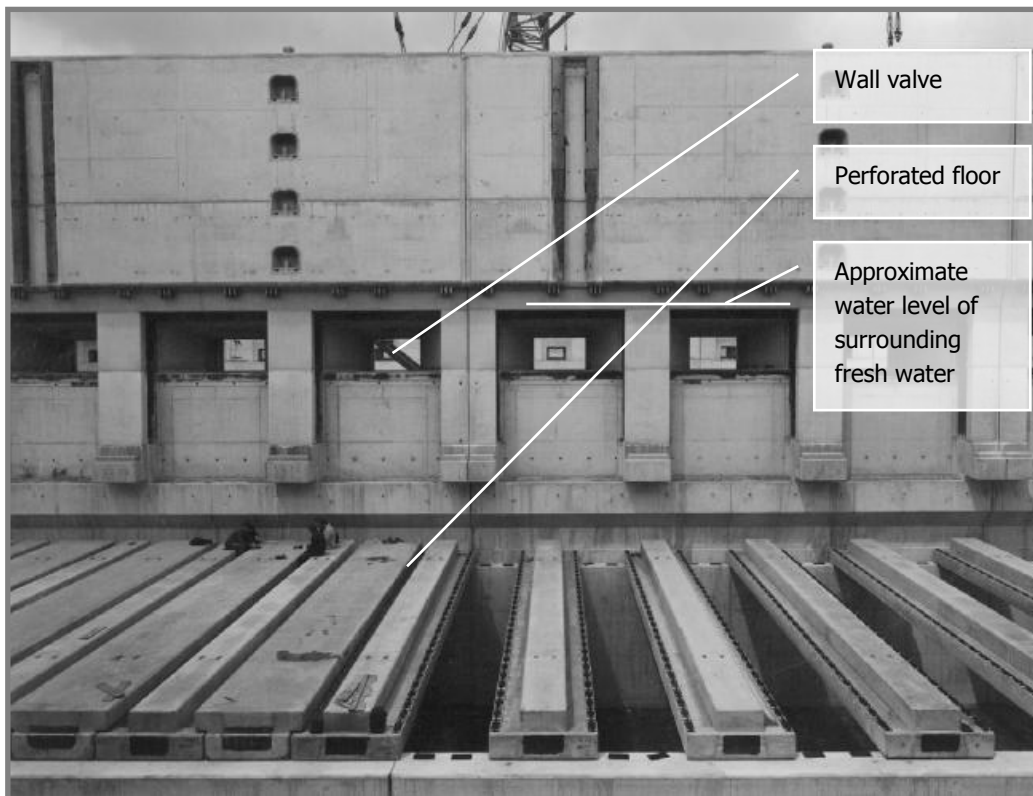


Figure 9: Overview of the perforated bottom floor in the Krammer commercial lock. Adapted from (Rijkswaterstaat Bouwdienst, 2000b).

To describe the system, a visualisation of this description can be found in appendix B. Before a ship leaves the lock to the salt ES side, the fresh water inside the lock chamber is exchanged with salt water. The intention is to lose as little fresh water as possible. Salt water is flowing in at the bottom; fresh water is flowing out via the wall valves. After the exchange, the water is levelled with the level of the ES, affected by the tide. This is done by letting water in or out of the chamber via the perforated floor of the lock.

The other way around, when a ship leaves the lock to the VZM, the water is levelled with the (fixed) water level of the VZM first. This means that salt water is flowing in or out of the lock chamber via the perforated floor. After the correct level is reached, fresh water is flowing in via the wall valves, while salt water flows out of the floor. When the lock chamber is completely filled with fresh water, the gates open so that the ship can sail onto the VZM.

This system takes more time than a conventional lock for passing ships. Apart from only levelling the water, salt and fresh water is being exchanged as a separate process. Because of the perforated floor, levelling itself is actually faster in this system than in a conventional lock. The exchange of the water is causing the delay. During this exchange of water, ships are moored in the lock chamber. The fresh water in- and outflow is processed through valves in the side wall. The discharge through these valves can't be too high, since this would impose high shear forces on the ships. Another important issue is that the mixture of the interface between salt and fresh water has to be counteracted. This is achieved by keeping the flow velocities through the wall valves rather small.

Interface between salt and fresh water

The effectiveness of this fresh water 'preserving' method depends on a horizontal flat interface between salt and fresh water inside the lock chamber. Also mixture must be counteracted. If any of these two aspects fail, fresh water will flow to the ES, or salt water will enter the VZM needless.

The valves in the walls and the perforations in the floor are both equally divided along the length of the lock chamber. In this way longitudinal⁹ differences are minimised. They tend to cancel out any longitudinal flows. The lateral¹⁰ flows are harder to minimise. The inflow at the bottom is divided over the total width, and is therefore as equally distributed over the length as possible. As it is not possible to extract or add water equally divided over the total width from the top, since this is done by the valves at both sides. Additional to this inadequacy, ships inside the lock cause disturbances in the interface between salt and fresh when fresh water flows in or out. See Figure 10.

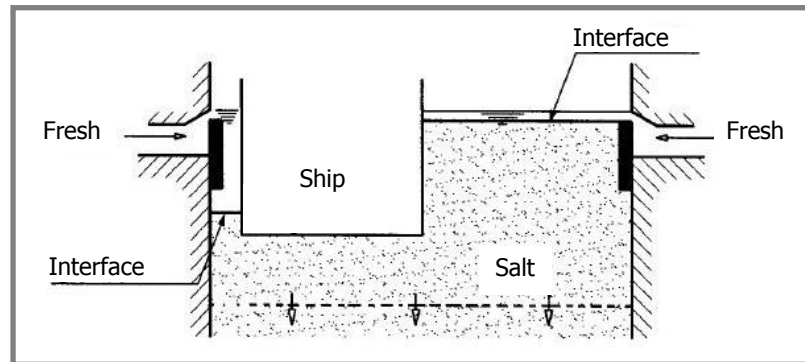


Figure 10: Cross section of lock chamber, indicating how levelling of the salt-fresh interface is disturbed by a ship. Adapted from (Rijkswaterstaat Bouwdienst, 2000b).

A schematisation of the perforated floor is given in Figure 11. It fulfils three main functions. Numerous small pores provide a more or less homogeneous vertical in- and outflow of water. Pores come together in underlying slits, which has the effect that water flows in and out with low velocities and does not cause much turbulence above the floor. Sailing ships do not disturb the area underneath the floor. When ships sail in from the VZM, the interface between salt and fresh is located beneath that floor. This means that no mixing is being imposed by the ships.¹¹

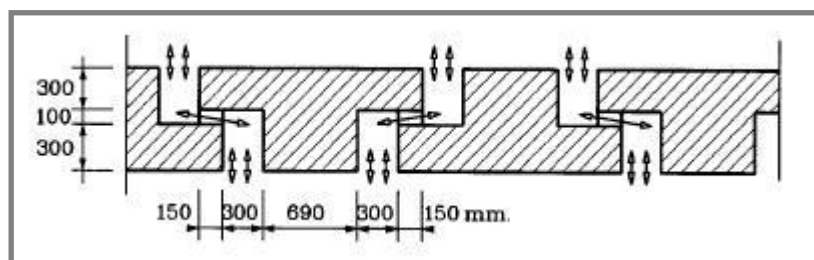


Figure 11: Schematic cross sectional view of the flow through the perforated bottom. (Rijkswaterstaat Bouwdienst, 2000b)

The valves in the wall can be seen in a schematisation in Figure 12. The valves are positioned as high as possible, but just underneath the water level of the VZM. If they are placed higher, there is no free decay of fresh water into the lock chamber possible anymore. When fresh water flows into the lock chamber, its discharge is controlled with adjustable valves. The velocity of inflowing water is kept as low as possible to diminish mixing with salt water in the lock, but kept high enough to prevent salt water flowing into the wall valve as back flow.¹² The valve openings are of relatively small height and large

⁹ In direction of the length of the lock chamber.

¹⁰ In direction of the width of the lock chamber.

¹¹ To be complete: It should be noted that ships are not allowed to use their propellers during exchange of salt and fresh water. In this way they don't disturb the interface between salt and fresh water when it is lowered or heightened.

¹² This is achieved by an internal Froude number of approximately 1. With a Froude number above 1, an internal hydraulic jump occurs, which induces much turbulence.

width. In this way the upper water layer flows out first. The top layer is the layer with the lowest density, and so to say 'the freshest'.¹³

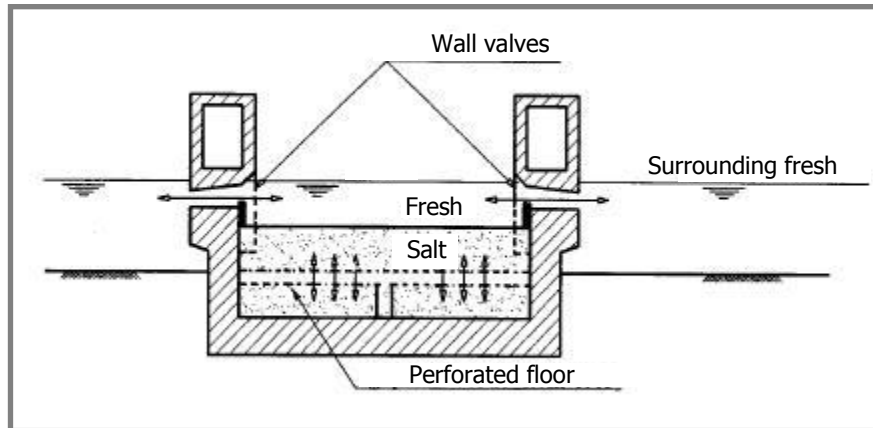


Figure 12: Cross section of Krammer commercial lock with salt and fresh water flows. Adapted from (Rijkswaterstaat Bouwdienst, 2000b).

The rolling gates of the lock have their own compartment to roll in and out of. If the gate is in closed position, the gate compartment is filled with water. During exchange of salt and fresh water, this compartment would bring the interface between the different densities out of balance. Also, the extra amount of water in the compartments needs to be exchanged. To prevent this, the gate is pushed firmly towards the lock chamber. The compartment is not in connection with the lock chamber any more, but with the water surrounding the lock. When the water outside of the lock is higher than in the lock chamber, the gate is pushed against the lock chamber by the (pressure-)head difference.

Water flows in system

The flow of salt water is controlled actively in this system. Fresh water follows in a passive way. Two basins of salt water are located next to the lock. A high basin provides water to the perforated floor when the interface between salt and fresh in the lock chamber is heightened. When that interface is lowered, the salt water is flowing through the perforated bottom to a lower lying basin. A pumping station provides for a connection between the two basins and the ES. It also takes care of enough water in the high basin. All these water movements take place in an extensive culvert system, which is displayed in Figure 13. The water flows are (actively) controlled by valves in the culvert system.

Main reason for the use of basins instead of pumps is the capacity of the pumping system. This capacity can be relatively low. The basins are a buffer and are able to provide or store a large volume of water in a short time. During the time between two locking cycles¹⁴, a pumping station can maintain the water levels in the basins. If the basins are not used, a pumping station would have to move the same volume of water in only ten minutes.

The fresh water is said to be 'passive' in this system, as all fresh water flows are under free decay. The water level in the high basin of salt water is maintained by a pumping station. So this water flow is not under free decay.

The Slaak is in direct connection with the ES and has therefore the same water level.

¹³ The valves are positioned at a fixed height in the lock. This configuration works because the water is levelled to the water level of the Volkerak Zoommeer first, before exchange of water between both sides of the lock occurs.

¹⁴ One locking involves all processes from the opening of a gate at one side, to the opening of a gate at the opposing side. This takes nearly one hour.

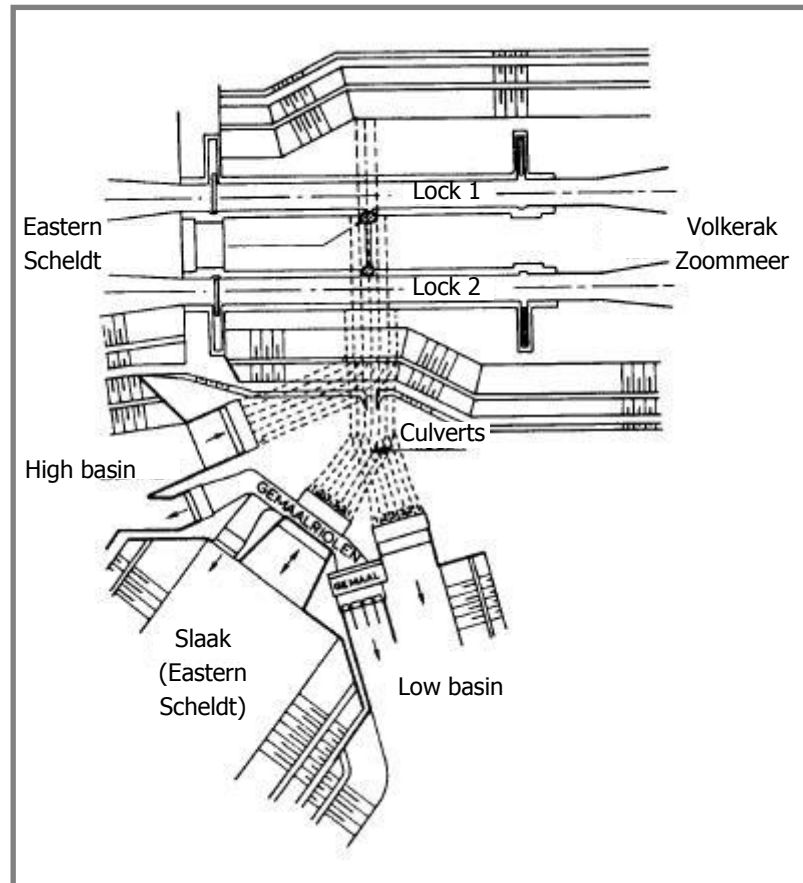


Figure 13: Top view of the culvert system of the Krammer locks.
Adapted from (Rijkswaterstaat Bouwdienst, 2000b).

Results/efficiency of system

During every locking to the ES there is a loss of fresh water. It is called a 'loss' when it flows into the salt ES and is therefore out of the fresh water regime. This loss is diminished by heightening of the interface between salt and fresh during locking. When this occurs, the interface is only heightened up to the level of the bottom of the ships. If the interface reaches higher than the bottom of a ship, it's likely for the valves in the wall close to the ship to let salt water through instead of only fresh. In Figure 10, which was earlier referred to, the occurring situation is visible in the other way around. Salt water in the VZM is considered worse than a fresh water loss to the ES, so a heightening of the interface up until the bottom of ships is accepted.

The loss of fresh water is quantified as a percentage of the lock volume. It's mainly depending on whether the interface is heightened or not. This takes more time and is not needed in all scenarios. If enough fresh water is available by discharges north of the Krammer locks from the rivers and Volkerak locks, it is more economical to provide for a shorter locking time. The fresh water loss isn't the most important decisive argument any more. The fresh water loss can vary roughly between 30 and 80%.

There are quite some disadvantages to the explained system. Building costs are high, just as the maintaining and operational costs. The locking time is higher than in a conventional lock and the control is more complex. Nevertheless, it is a really effective system as the salt leakage to the fresh water regime is decreased in the order of 90 to 98%. (Rijkswaterstaat Bouwdienst, 2000b, pp. 21-18)

2.2.3. Recreational locks

For the most important figures concerning the recreational locks, a reference is made to Table 7. The recreational locks are designed differently than the commercial locks. The general idea is still the same, but there is a significant difference. This difference is explained in this section.

Description of system

The *Duinkerken system* – applied at the commercial locks – only stimulates flows in the lock chamber in vertical and lateral direction. (1A and 1B in Figure 14) The difference in the recreational locks is that salt water flows in the longitudinal direction. (2A and 2B in Figure 14) The perforated floor is not present in the design. Salt water flows in and out at the bottom of the outer¹⁵ side of the lock. Fresh water is controlled the same as in the previous described system and flows in and out of the lock chamber via valves along both side walls. A schematisation of the difference of the two systems is provided in Figure 14.

(In sketches 1B and 2B fresh water flows in from one side, at the Krammer locks this happens at both sides of the lock chamber. The outflow of salt water at the bottom of sketch 1B is shown as low wall valves, at the Krammer locks this happens via the culvert system and the perforated floor. The outflow of salt water in sketch 2A is drawn as in reality at the Krammer locks.)

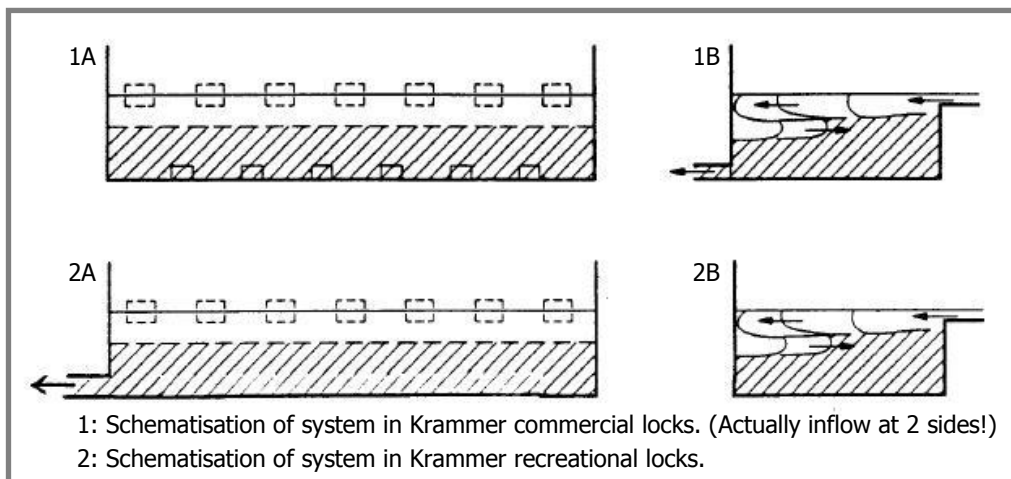


Figure 14: Schematic difference in orthogonal cross sections of a lock chamber between the system of the commercial (1) and the recreational (2) locks. Adapted from (Rijkswaterstaat Bouwdienst, 2000b).

The main reason for this different layout is due to the costs. A system as the *Duinkerken system* is able to diminish salt leakage and fresh water loss at the same time, but is very expensive. The recreational locks are much smaller and have as main objective to reduce salt leakage. This resulted in a simpler system, which accepted the fresh water loss, but maintained a good salt leakage reduction. Without the perforated floor and extensive culvert system, the structure is much cheaper than the one for the commercial locks.

It seems harder to maintain a horizontal interface between the salt and fresh water, without the perforated floor. This function is adopted by low flow velocities and a deeper lock chamber. The interface does never come below 0.5 m under the sill at the VZM side.

¹⁵ By 'outer' side, the salt side is meant, while the 'inner' side refers to the fresh side of the lock complex.

A consequence of this system is that a lock chamber filled with fresh water is not exchanged with salt water before the gates to the ES open. The other way around, a lock chamber filled with salt water is exchanged with fresh water before the gates to the VZM open. The system is actually a 'salt preventive' system, not a 'salt/fresh water separating' system.

This system takes a little more time than a conventional lock. The time consuming fresh and salt water exchange is only performed in one locking direction (to the VZM). The additional time relative to conventional locks is less than for the commercial locks.

Water flows in system

Just as in the *Duinkerken system*, the flow of salt water is actively controlled. Fresh water follows in a passive way. The low culvert mouth (located lowest at the bottom at the outer side of the lock chamber) is connected with the ES via a pumping station. The pumps are able to pump in two directions. The chamber can be levelled up- or downwards. When the chamber is exchanged with fresh water, salt water is pumped out. In some situations it is possible to let the water flow under free decay. Then, the pump is not used.

Results/efficiency of system

In this system, no fresh water is saved. This results in a loss of 100%, meaning that the volume of an entire lock chamber of fresh water is lost per locking to the ES. Besides the fact that the system is less complex, the efficiency is still considerable. The salt leak to the fresh water regime can be decreased with approximately 80%. (Rijkswaterstaat Bouwdienst, 2000b, pp. 21-18) So it can be concluded that the complex extra measures taken at the commercial locks, primarily contribute to fresh water preserving, rather than introducing solid salt intrusion prevention.

A restriction to the system is that the lock chamber cannot be too long. This is due to the flow patterns in different directions. The outflow of water at the bottom during water exchange (locking to VZM) could easily include fresh water – with salt water still present, if the chamber is too long. This effect can only be prevented by using really low flow velocities. Since this would increase locking times significantly, the lock chamber length is limited. There is no exact 'maximum length'; this should be examined case by case-dependent.

When it comes to salt intrusion prevention, this system has an efficiency in the same order of magnitude than the *Duinkerken system*. Much fresh water is lost, though. Building and operating costs are significantly lower, which makes it an attractive system especially for smaller locks.

2.3. Description of pilot project: Krammer recreational lock

The description of the pilot in the Krammer recreational lock is displayed rather detailed, since it forms the starting point of the design made in this study.

The pilot serves two main objectives. Firstly, physical measurements of the effect of the new salt intrusion prevention system will help deciding what system to apply in the much larger commercial locks. Model calculations of the expected salt leakage in the pilot project are already made, but need to be validated with the results of the physical measurements. In this way, uncertainties can be cancelled out. With the adapted calculation model, more certain predictions can be made for the commercial locks.

Secondly, experience with the innovative technique should give insight in future possibilities of implementations of the technique elsewhere and on a larger scale.

The current configuration of the recreational lock is described in section 2.2.3. The layout of the new salt intrusion prevention was obtained after thorough modelling studies as can be read in (Deltares, 2011b, p. 32). It includes air bubble screens at both sides of the lock chamber, a water screen at the salt side of the lock and a flushing system. The three different parts of the system will be described and visualised in the following sections. First, the expected effects of the pilot are presented.

The applied dimensions and calculations are based on requirements in (Rijkswaterstaat Zeeland, 2012) and specifications in (Rijkswaterstaat Zeeland, 2013).

All main elements of the salt intrusion prevention are elaborated. Levelling of water is also part of that, but is not detailed. It takes place via a pump between the ES and the lock chamber. When the tidal levels allow it, levelling under free decay with the VZM occurs via the lock paddles of the flushing system.

2.3.1. Effects of pilot in Krammer recreational lock

This pilot's design is cheaper than the current system (exchange of water, section 2.2) and results in shorter locking cycles. Because the process of exchanging water disappears, the duration of a locking cycle reduces for the recreational lock from 65 to 55 minutes (–15%). This means that the locking capacity increases significantly.

The pilot will be operational in April 2014. In September that same year, the decision will be made on what system to apply in the Krammer commercial locks. In the few months in between, extensive measurements will be performed regarding functionality of the pilot in the recreational lock.

Model calculations indicate that salt intrusion prevention of this system is at least as effective as the current system (Deltares, 2012). Salt intrusion is reduced by the following percentages, compared to a situation without a countermeasure:

- | | |
|--------------------------------|-----|
| ▪ Air bubble screen | 70% |
| ▪ Water screen | 60% |
| ▪ Air bubble- and water screen | 85% |
| ▪ Configuration of pilot | 85% |

2.3.2. Air bubble screens

Air bubble screens were originally created by blowing air into perforated tubes. An elaborate description of the development of air bubble screens is described in appendix A.1.1. A revised version with reservoirs and internal pressure built-up proved to be much more efficient. Based on this principle, different designs are possible.

Two fundamentally different designs are described in section 0. In this section, the air bubble screens as configured in the pilot for the Krammer recreational lock are being described.

Figure 15 shows a test set-up equal to the design of the air bubble screen in the pilot of the recreational lock. The air bubble screens consist of supply pipes attached to a few horizontal reservoirs at the bottom of the lock chamber. The reservoirs are rounded bars with a diameter of $\varnothing 10\text{ cm}$. Every 15 cm along its length a regulator and a diffuser are present. The regulators can't be seen in the figure, since they are located inside the connection of the diffuser to the reservoir. Without the use of reservoirs, air

isn't able to spread along the numerous openings. Air is highly compressible and doesn't need much space to spread evenly in space. Therefore, the reservoirs are relatively small. One horizontal bar with reservoir, openings, regulators and diffusers is called a strand.

The diffusers can be compared with showerheads, and make the air release as tiny bubbles. In the test layout of Figure 15 they can be seen in operation. Two strands are visible in that figure.

Regulators are used to obtain an evenly distributed screen. They regulate the amount of air flowing through the pipe in which they are installed by having exact pressure-characteristics; it opens only when a pressure difference of at least 1 *bar* is present between both sides of the regulator. When it's opened, a higher pressure difference does not increase the size of the opening. In all other cases, the regulator closes off the opening completely. In this way, pressure can be built up in the strand and air leaves at all openings with an equal discharge when the pressure *difference* exceeds 1 *bar*.

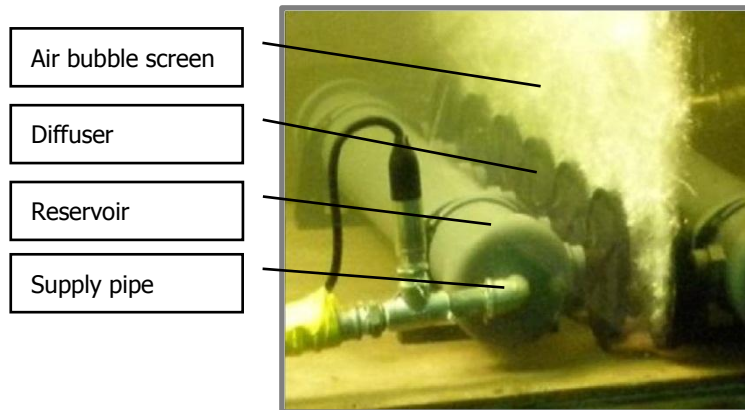


Figure 15: Air bubble screen with two strands in test mode. (Deltares, 2011d)

Both sides of the lock chamber are equipped with air bubble screens at the inner side of the lock gates. Figure 17 shows the layout at the ES side. Six strands are connected to steel plating, which is integrated in the design of the water screen (see Figure 18). Figure 16 shows two strands at the VZM side in a steel HEA 400-profile.

With this configuration it's possible to vary the air supply discharge. A range from zero to eight strands can be activated to create an effective bubble screen at different water levels at both sides of the lock.

Both configurations are equipped with eyebolts at both ends for lifting purposes. Since the air screen at the ES side is integrated in the water screen, they cannot be lifted out separately.

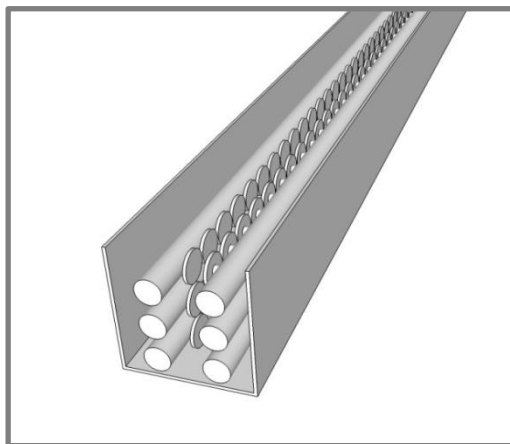


Figure 17: Sketch of air bubble screen with six strands in Krammer pilot at ES side.

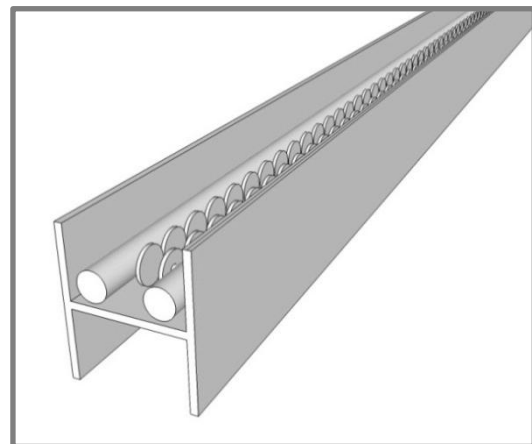


Figure 16: Sketch of air bubble screen with two strands in Krammer pilot at VZM side.

The maximum discharges of the screens are needed when the water levels are highest (largest compression of air). Those discharges¹⁶ are at the ES side 575 *Nl/s* and at the VZM side 125 *Nl/s*. A configuration of strands with a maximum capacity of 88.5 *Nl/s* was accepted by *Rijkswaterstaat* and *Deltares*. The demanded requirements are not met completely. Namely, six strands at the ES side and two at the VZM side result in $(6 \cdot 88.5 =) 531$ *Nl/s* and $(2 \cdot 88.5 =) 177$ *Nl/s*.

Calculations of the required pipe diameters are made in appendix D. The result is that each strand of 9 m long needs a supply pipe with a diameter of 80 mm.

The same calculations as presented in appendix D can be used in other situations. When the dimensions of the reservoir or the water height above the reservoir alter, a few aspects should be acknowledged.

First, when the strands increase in length, the amount of required air increases linearly. Further, the water height above the outflow openings influences the amount of air needed. It's assumed that when the same flow velocity is present at the outflow openings of the air screen, the screen is comparably effective.¹⁷ To gain an equal volumetric outflow at a larger water depth, the amount of air must increase. For every 10 metre increased water depth, the required amount of air increases with 1 bar.

Non-return valves at the outflow openings prevent the reservoir to be filled with water when there is no air pressure. Without these valves, the pipes must be constantly over pressured or the water must be pumped out of the reservoir before it can be used as an air bubble screen. At the Krammer recreational pilot it's chosen to keep the pipes constantly under pressure. It's expected that energy consumption for pressurised pipes is low. In this way an additional pressure loss over non-return valves can be prevented. Measurements must demonstrate and quantify the actual effects of this.

2.3.3. Water screen

A water screen can be visualised as a reservoir located under water. It is filled by an inflow pipe (or a few pipes), while wide openings at the top result in a desired laminar outflow. The water screen is most effective in terms of salt intrusion reduction when the water is evenly distributed over these outflow openings. There are different ways to control an even distribution of the water along the length axis of the screen. In favour of a refined choice of the best layout for the eventual design in this report, two fundamental different possibilities are lined out in section 0. But first, in this section a description follows of the design of the pilot in the Krammer recreational lock.

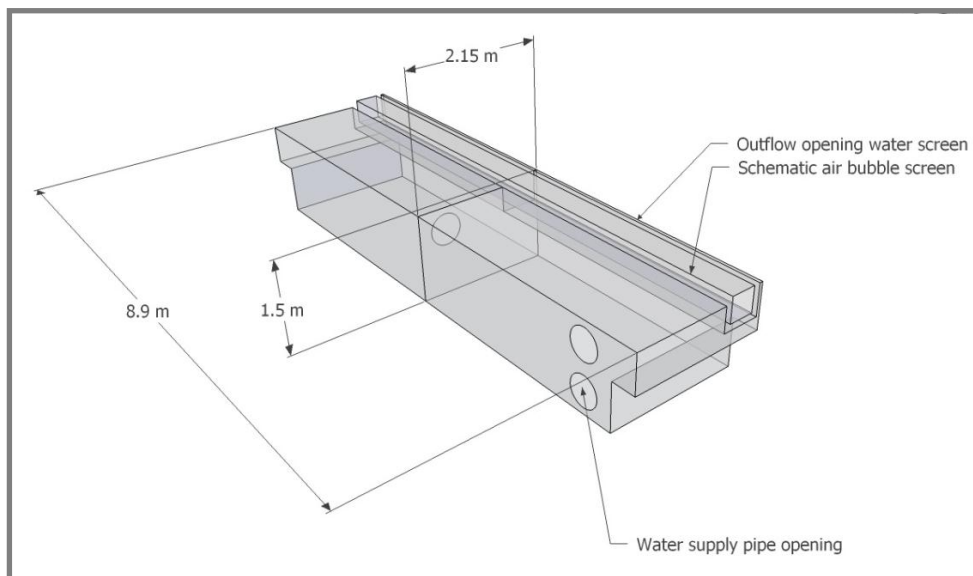


Figure 18: Layout of water screen in Krammer pilot at Eastern Scheldt side. (Rijkswaterstaat Zeeland, 2013)

¹⁶ *Nl/s* means *normal*/litre per second and has nothing to do with the symbol for the force unit Newton (*N*). See description in the *List of symbols* on page x.

¹⁷ This is a conservative assumption, since this probably affects the effectiveness of the screen positively. As the compressed volume of air increases at outflow, the volume of the air at the water surface increases as well.

In the pilot's design, the water screen (only one is present) is located in the lock chamber at the ES side, between the air bubble screen and the lock gate. In Figure 18 the design is made visible. The reservoir has the dimensions of $2.15\text{ m} \cdot 1.5\text{ m} \cdot 8.9\text{ m}$ made by 8 mm thick steel plates. The reservoir length¹⁸ is split up into two sections, each fed by its own water supply pipe. The pipe as visible in the figure has openings at all sides to result in a spreading in the reservoir. The sections are designed in this configuration for two main reasons.

The screen must be effective against salt intrusion, which strongly depends on the spreading of water along the outflow openings. If a section is too large, an even spreading is harder to maintain.

The other reason has to do with future implementations. The pilot has to give insight in possibilities of the technique when applied on a larger scale. Initially, 3 sections of 3 m length were chosen. By making longer sections in the order of 4.5 m , knowledge can be acquired of the effects of larger sections. This knowledge must help in the translation to the larger dimensions of the commercial locks.

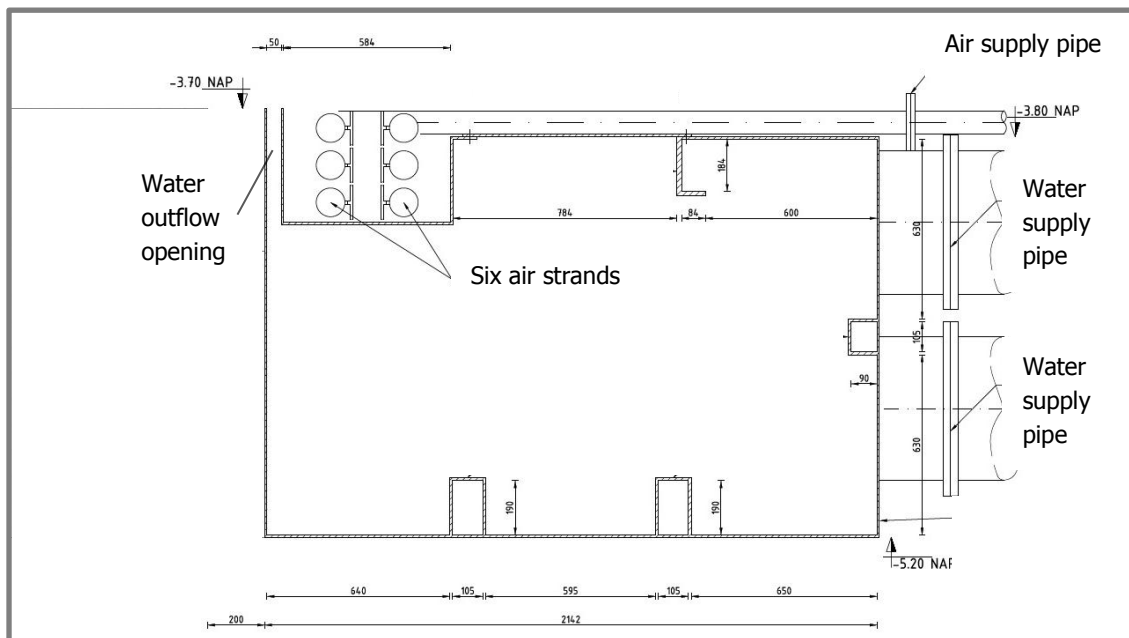


Figure 19: Cross section of air bubble- and water screen. All dimensions in mm; water level in m. Adapted from (Rijkswaterstaat Zeeland, 2013).

Just as for the air requirements for the air bubble screen, the amount of water required for the water screen depends strongly on the water height. At the ES, the water screen must be effective for a water level variation between -1.7 m NAP to $+2.5\text{ m NAP}$. This means that the water height above the outflow opening varies from 2 to 6.2 metres. The corresponding discharge needed to feed the screen at these water levels varies from 0.6 to $1.4\text{ m}^3/\text{s}$ for the 9 m long screen.

Calculations of the required supply pipe diameters are elaborated in appendix D. The result is a supply pipe with a 500 mm diameter for every section of 4.5 m long.

In other situations – with other reservoir layout or other hydraulic boundary conditions – calculations can be made in the same way as presented in appendix D. In that case a linear dependency holds for the amount of water needed for the screen and the length of the reservoir.

In the calculations made for the Krammer recreational pilot, a linear dependency is assumed for the amount of water needed for the screen and the height of water above the outflow opening. This linear dependency is a conservative assumption.

¹⁸ In favour of the orientation: attention should be paid to the equal direction of the length of the screen compared to the width of the lock chamber.

2.3.4. Flushing system

The flushing system allows fresh water from the VZM to enter the lock chamber when the gates are closed. By maintaining a constant inflow of fresh water, it is tended to reduce salt intrusion further. Especially when levelling, the amount of salt inside the lock chamber reduces. The area in front of the lock at the ES side becomes less salty as well. Three lock paddles¹⁹ – closing off seven round holes with a 600 mm diameter – are installed at the bottom of the lock gate at the VZM side.

No thorough description of this system is inserted, because the system is and will not be present in this phase in the commercial locks.

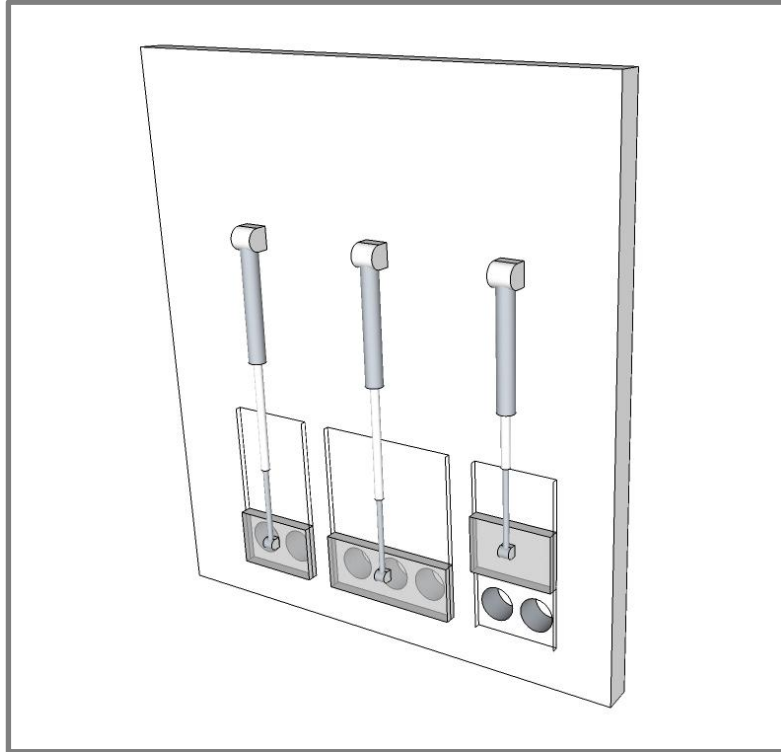


Figure 20: Sketch of lock paddles situated in lock gate at Volkerak Zoommeer side.

¹⁹ In Dutch: *Rinketschuiven*.

2.4. Exploration of possibilities: Krammer commercial lock

In this section, the layout is compared of several possible salt intrusion preventive systems in the Krammer commercial locks. An overview of options will be presented, including their possible benefits. After reading this section it will be clear what configuration is best and why others are less interesting options for future elaboration.

To prevent ambiguities, the different configurations of salt intrusion preventive measures are given a name. Table 14 gives an overview of the treated configurations in this section. All systems are located *inside* the lock chamber. In this way it's possible to make a comparison with the pilot (also located inside the lock chamber), there is space for the structure and a construction in dry conditions is possible. For each system, three aspects are described.

First, a description is presented of its elements and the way salt intrusion is reduced. Then, the maximum possible salt intrusion reduction is calculated with the dimensions of the reducing elements. The general salt intrusion reduction from (Rijkswaterstaat Bouwdienst, 2000b) is displayed. Also the value obtained by *Deltares* is given (Deltares, 2011d). These three values give good insight in the actual possible salt intrusion reduction. Finally, the energy consumption of the system is described.

The first number of the configuration name tells something about the place in time of the system. The zero-alternative has number 0. Configurations 1.*x* are the present situations or designs, while configurations 2.*x* describe possible future improvements.

The section is completed with final conclusions. It shows what configuration has the best possibilities to result in a realistic design, fulfilling the same requirements as given for the pilot, but at lower energy consumption.

Table 14: Overview of treated salt intrusion prevention configurations in this section in the Krammer commercial locks.

Configuration	When?	Description of system
0: No system	<i>none</i>	No salt intrusion prevention is active in the lock.
1.1: Water exchange	Present	Current <i>Duinkerken system</i> of the Krammer locks: Exchanging salt and fresh water via an extensive culvert system. This system is described in section 2.2.
1.2: Air bubble screen & Water screen	Present	Design of salt intrusion prevention in the pilot for the Krammer <i>recreational</i> locks, applied in the <i>commercial</i> locks: 2 air bubble screens in combination with 1 water screen. This system is described in section 2.3.
2.1: Fixed sill	Future	A fixed sill at the bottom blocks the salt water partly.
2.2: Movable sill	Future	A movable sill at the bottom blocks salt water more effective by moving up and down with the tide.
2.3: Movable sill & Air bubble screen & Water screen	Future	Movable sill in combination with air bubble- and water screen. This system is described in chapter 5.

Configuration 0: No active system

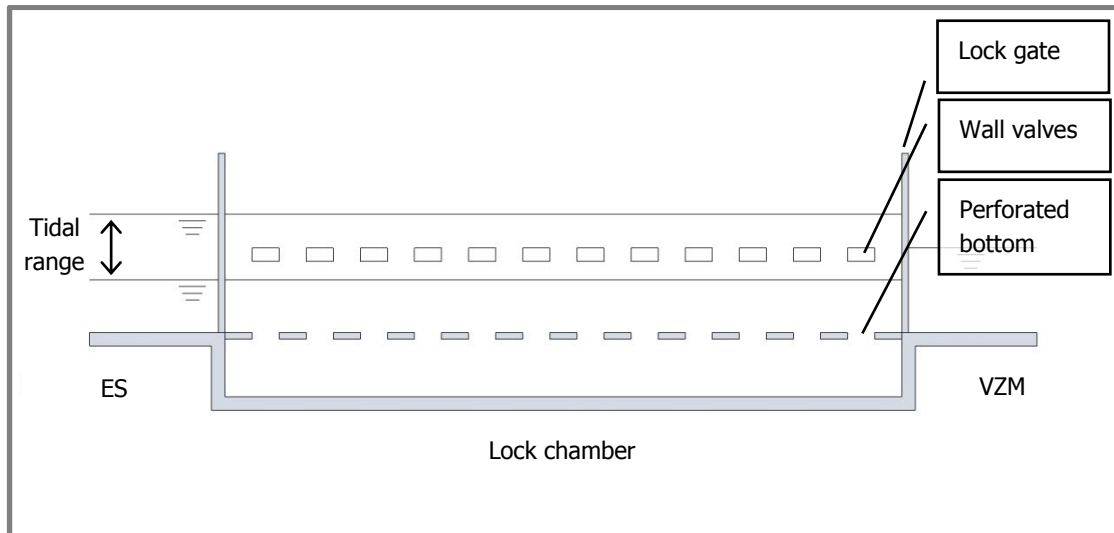


Figure 21: Configuration 0 – Longitudinal cross section of lock chamber with no active salt intrusion prevention.

Figure 21 represents configuration 0. It also names several parts of the lock chamber. These names apply to all configurations in Figure 21 until Figure 26.

Description

No salt intrusion reduction is active in the lock. The perforated bottom floor, culvert system and wall valves are inactive. By levelling of water in the lock chamber under free decay, salt or fresh water flows freely in or out of the lock chamber.

Effectiveness

Without any countermeasure to salt intrusion, the intrusion through the gates is maximal. This means that if the gates are open long enough, the entire lock chamber will be filled with salt water, before the gates close at the ES side. When the gates open at the VZM side, the entire volume of the lock chamber will be subject to exchange with water from the VZM.

Energy

No energy is needed for this configuration, since there is no salt intrusion prevention present.

Configuration 1.1: Water exchange

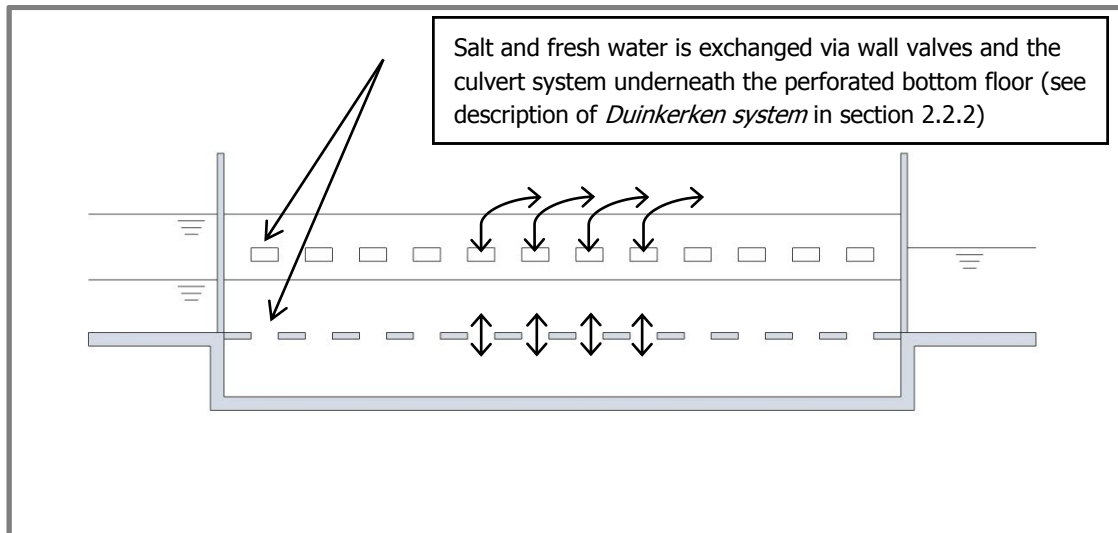


Figure 22: Configuration 1.1 – Longitudinal cross section of lock chamber with *Duinkerken system* as salt intrusion prevention.

Description

This configuration represents the current situation of the Krammer commercial locks. A thorough description is described in section 2.2.2.

Effectiveness

Ideally, the system reduces salt intrusion completely – by 100%. During every locking cycle, salt and fresh water is exchanged inside the lock chamber. In this way, the salt intrusion reduction is theoretically 100%, since no salt water enters the VZM.

According to (Rijkswaterstaat Bouwdienst, 2000b), salt intrusion reduction by this system is in reality 90 to 98% instead of a full reduction.

Energy

The energy consumption of this system is very high. For every locking cycle 481 *kWh* is needed.²⁰

Since water levelling is part of the system (see section 2.2.2), the expression of energy consumption for this system automatically integrates levelling of water. To be able to make a fair comparison between the different configurations, ideally water levelling should be cancelled out of the equation. The actual water levelling happens under free decay, for instance by using the high and low basins. After levelling of water inside the lock chamber, the exchange of water and controlling the water levels of the basins consumes all the energy. As it is hard to quantify which part of the consumed energy is exactly used for water levelling, for the comparison of the various configurations in this chapter, the total amount of energy consumption is used. It is hereby assumed that the required energy for levelling is much less than the required energy for the salt intrusion prevention.

²⁰ Based on: 5,007,000 *kWh/year* and 28.52 *locking cycles/day* (see Table 8).

Configuration 1.2: Air bubble- and water screen

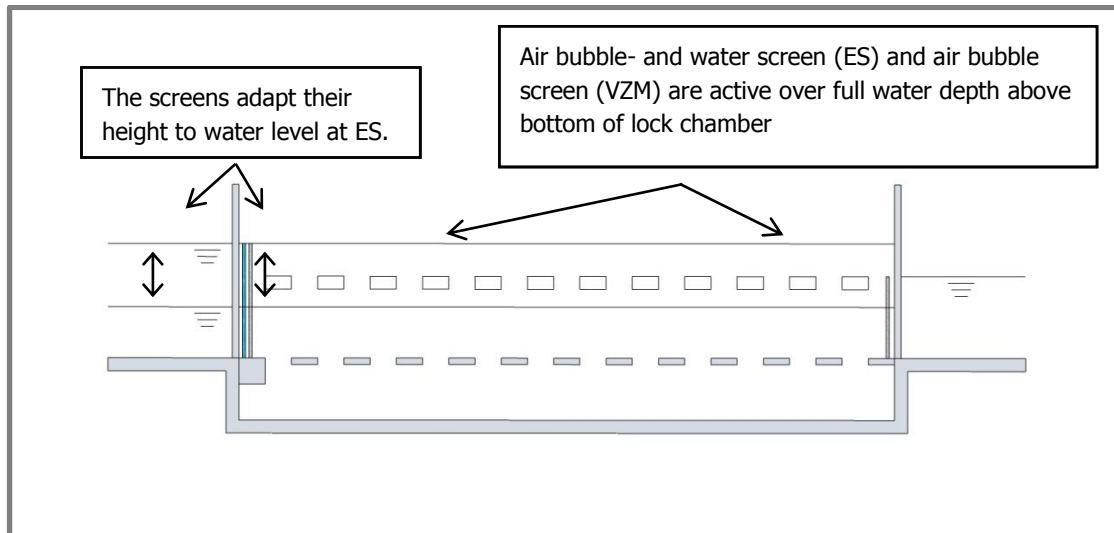


Figure 23: Configuration 1.2 – Longitudinal cross section of lock chamber with air bubble- and water screen as salt intrusion prevention.

Description

In this configuration, a water- and air bubble screen is present at the ES side and another air bubble screen at the VZM side. Both are active over the full water depths when the corresponding gates are opened. In contrast to the fluctuating water depth (and screen height) at the ES side, the air bubble screen at the VZM side has a fixed height, equal to the fixed water depth at that side.

This same configuration is used in the design for the pilot project in the Krammer *recreational* lock.

Effectiveness

According to (Rijkswaterstaat Bouwdienst, 2000b), intrusion can be reduced by approximately 85% by implementing this system. Experiments (Deltares, 2011d) also show a possible reduction of 85%. The theoretical calculations for other situations with air bubble- and water screens give the same value. Hence, the theoretical reduction for this configuration is assumed to be 85%.

Energy

The screens consume a lot of energy. For every locking cycle, 216 *kWh* is needed.²¹

The amount of power needed to feed the screens at the ES side is dependent on the water heights; this is related to the difference in water pressure at the bottom of the screen.

²¹ Based on 2,250,000 *kWh/year* and 28.52 *locking cycles/day* for two lock chambers (see Table 8).

Configuration 2.1: Fixed sill

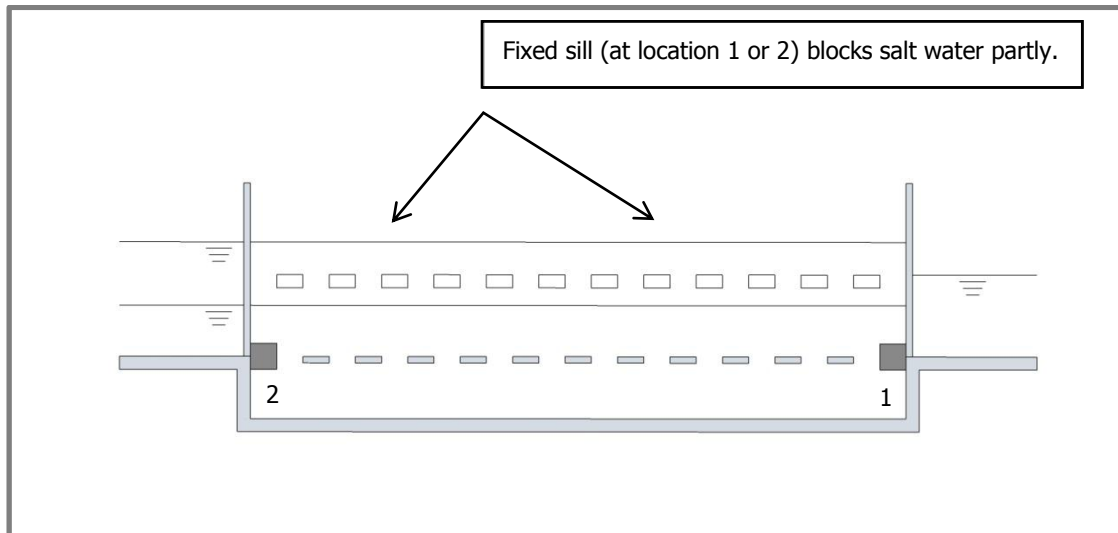


Figure 24: Configuration 2.1 – Longitudinal cross section of lock chamber with fixed sill as salt intrusion prevention.

Description

In this configuration a fixed sill is present. This solid structure has an elevated level compared to the lock bottom, which prevents exchange of water from the bottom of the lock to the top of the sill. The height of the initial salt wedge decreases after opening the lock gate.

Salt leakage is decreased by reducing the water depth over which exchange of water takes place. Also the thickness of both the fresh- and the salt water wedge decreases. As a result, the wedge's propagating velocity which is dependent of the height, decreases.

A sill located at the VZM side (number 1 in Figure 24) will give a higher reduction of salt intrusion than a sill located at the ES side (number 2 in Figure 24). This is caused by the tidal influence of the ES.

The lock is operational for water levels at the ES from -2.35 m NAP minimum to $+2.5 \text{ m NAP}$ maximum. A navigational depth of 4.7 metres must be maintained for shipping. (See section 2.2) A fixed sill should not decrease the navigational depth at the lowest operational water level. Since 4.7 m lower than this lowest level of -2.35 m NAP is lower than the lock bottom (located at -6.25 m NAP), it is not possible to implement a fixed sill at the ES side.

Effectiveness

At the VZM side this is different. The lower water level boundary of the VZM is -0.10 m NAP . Taking in mind a 4.7 m depth for ships and a lock bottom level of -6.25 m NAP , this leaves space for a fixed sill. Calculations show that a reduction of salt water intrusion could reach a maximum value of 24%.

$$h_{sill} = 6.25 - 0.1 - 4.7 = 1.45 \text{ m}$$

$$reduction = \left(\frac{1.45}{6.15} \right) \cdot 100\% = 23.6\% \approx 24\%$$

According to (Deltares, 2011d) a value of up to 30% can be reached by a fixed sill. Though, it must be noted that this value is strongly dependant on the configuration (water depth in relation to sill height).

Energy

A benefit of this configuration is that after installing the sill, no energy is needed for the sill to partly block intruding salt water.

Configuration 2.2: Movable sill

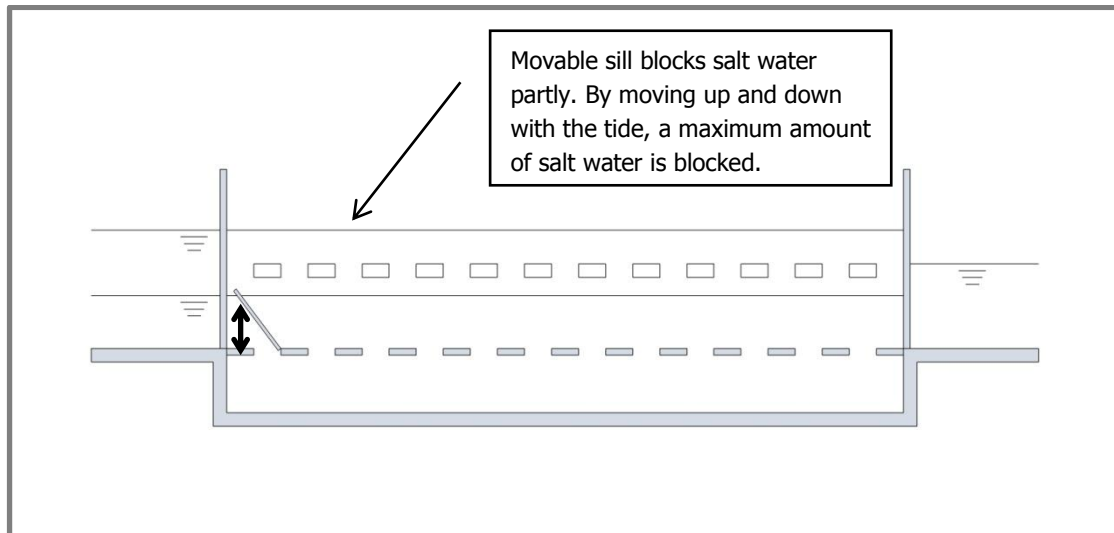


Figure 25: Configuration 2.2 – Longitudinal cross section of lock chamber with movable sill as salt intrusion prevention.

(The movable sill is displayed as some sort of hinged rotating flap, but several sorts of structures are possible)

Description

A movable sill is able to adapt its height to the tidal influence on the ES. In this way, the maximum possible height is blocking water exchange between the ES and the lock chamber. For navigational purposes, the upper 4.7 metres of water may not be blocked by anything. The top of the sill is always located minimum 4.7 metres under water.

At low water, the sill is in its lowered position and does not block anything. Salt water can enter the lock chamber freely.

At the VZM side, a movable sill has no use, since the water level at that side does not fluctuate regularly and is tried to be kept at a fixed water level. A fixed sill does make sense, which is included in configuration 2.1.

Effectiveness

To calculate roughly its effectiveness, an assumption is made for the tidal water levels. The tide is represented as two discrete water levels, both present half of the time. The salt intrusion reduction is calculated by the relative decrease in effective water depth by the movable sill during these two periods. An effectiveness of 100% is used for the blocked part.

Appendix C shows how the tide can be represented by two discrete water levels. With water levels of +1.1 m NAP and -0.9 m NAP, water columns of 7.35 m and 5.35 m are present half of the time. Respectively 2.65 m and 0.65 m of that depth are blocked by the sill.

$$reduction = \left(\frac{1}{2} \cdot \frac{2.65}{7.35} + \frac{1}{2} \cdot \frac{0.65}{5.35} \right) \cdot 100\% = 24.1\% \approx 24\%$$

According to (Rijkswaterstaat Bouwdienst, 2000b) a value of up to 25% can be reached for salt intrusion reduction by the use of a movable sill. It must be noted that the presented values are maximum values and depend strongly on the aerial configuration. Movement of ships, propeller disturbances and 'overtopping' of salt water over the sill are other aspects which reduce the percentage of reduction as presented here.

Energy

Energy needed for the movement of the sill itself is neglected, since it is expected to be in the order of a factor 100 smaller than the energy needed for an air bubble screen (see appendix N.4).

Configuration 2.3: Movable sill & Air bubble- and water screen

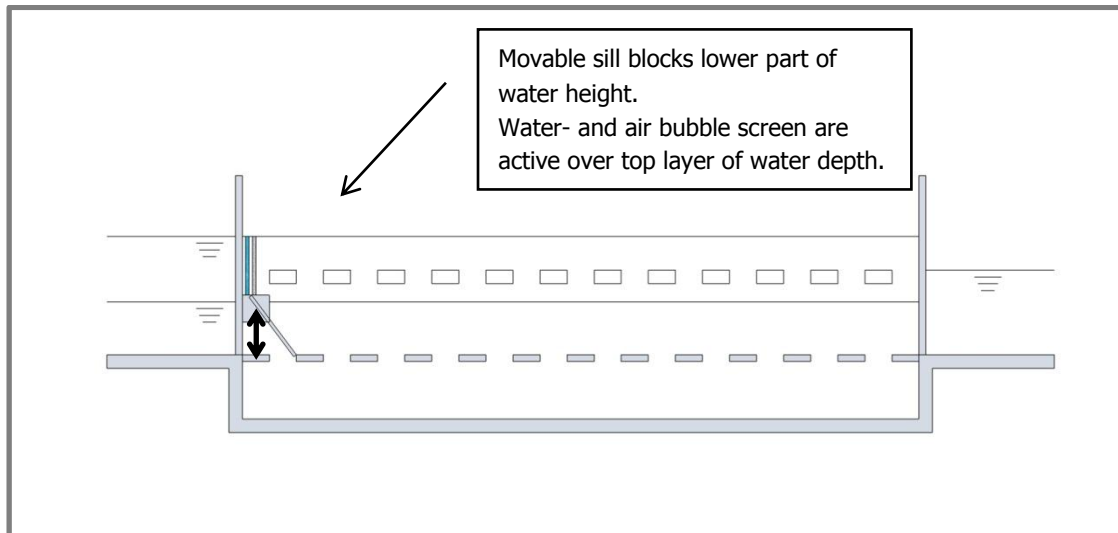


Figure 26: Configuration 2.3 – Longitudinal cross section of lock chamber with movable sill in combination with air bubble- and water screen as salt intrusion prevention.

(The movable sill is displayed as some sort of hinged rotating flap, but several sorts of structures are possible)

Description

The lower part is blocked by a movable sill. Connected on top of the sill are an air bubble- and a water screen, which reduce the salt intrusion through the upper 4.7 metres of the water column only. In this way, energy consumption by the screens is lowered compared with screens over the entire depth, while effectiveness in terms of salt intrusion increases.

At high water, both parts of the system are active since the water column is higher than 4.7 metres. When water is equal or lower than 4.7 metres at the ES, only the air bubble- and water screen are active. The sill is in its lowest position.

Effectiveness

No references are available for this configuration, since it isn't applied anywhere yet. A rough calculation gives the maximum expected effectiveness.

The calculated reduction of the lower part is added to the reduction of the upper part. They are both calculated separately, as if they have no interaction. In reality, both parts will probably strengthen the overall effect of salt intrusion reduction, but that has to be proved by experiments.

For the lower part, the same numbers as for configuration 2.2 hold.

The upper part is calculated by multiplying its relative water depth by a reduction of 85% for air bubble- and water screens.

$$reduction = \frac{1}{2} \cdot \frac{(2.65 \cdot 100\% + 4.7 \cdot 85\%)}{7.35} + \frac{1}{2} \cdot \frac{(0.65 \cdot 100\% + 4.7 \cdot 85\%)}{5.35} \approx 89\%$$

The effectiveness increases for an increasing water depth. With a larger water depth, a larger relative part of the water column is covered by the sill. In that case the first term in the formula gets larger, relative to the second.

An increase of effectiveness can also be achieved when ships with a smaller draught pass the lock. In that case the sill can be positioned higher; this results in a larger relative first term in the formula.

Energy

For the same reason as for configuration 2.2, the energy needed for the movement of the sill is neglected. The required energy for the air bubble- and water screen depends on the height of the screens. The water level of the ES fluctuates around +0.10 m NAP, which means for the screens to have an average height of 6.35 m, if no sill were present. In this configuration a sill is present, which makes the screens only 4.70 m high. It's assumed that 74% (4.7/6.35) of the amount of energy is needed, which results in a value of 162 kWh per cycle.

Most promising configuration: 2.3

Table 15 gives an overview of the most important factors for the different configurations. All values are obtained by quick calculations and references; as discussed on the previous pages. To draw a conclusion regarding the most promising design, the columns will be discussed from left to right.

Configuration 0 reduces no salt intrusion and doesn't consume energy. The current situation in the lock (configuration 1.1) has a high reduction, but also high energy consumption. With the design of the pilot (configuration 1.2), energy consumption is lowered considerably for a comparable salt intrusion reduction.

A fixed sill (configuration 2.1) is not possible at the ES side of the Krammer commercial locks. A movable sill (configuration 2.2) is an interesting option, since it consumes almost no energy while reaching a considerable salt intrusion reduction. When this option is combined with air bubble- and water screens (configuration 2.3), the expected salt intrusion reduction becomes comparable with the current situation. Since the energy consumption is expected to be even lower than for configuration 1.2, this seems the most interesting option.

The analysis in this chapter only focuses on the energy consumption and potential effectiveness in terms of salt leakage. Other important features as fresh water loss, lock capacity and costs are not yet regarded; a complete and more detailed analysis of the most promising design is detailed in chapter 6.

Table 15: Comparison of countermeasure configurations in Krammer commercial lock

(*NA: not applicable)

Source	Configuration	No system	Water exchange	Air bubble- and water screen	Fixed sill	Movable sill	Movable sill & Air bubble- and water screen
		0:	1.1:	1.2:	2.1:	2.2:	2.3:
Effectiveness [%] - This study - (Rijkswaterstaat Bouwdienst, 2000b) - Deltares		0	100	85	$\pm 0 - 24^{22}$	± 24	89
		0	90 – 98	± 85	NA*	25	NA*
		0	NA*	85	30	NA*	> 85
Estimated energy consumption [kWh/locking cycle]		0	481	216	0	2	162

When the different configurations are regarded, it may seem strange that a movable sill is not inserted in the pilot's design. Main reason is that there is nearly no experience yet of the technique for this purpose. A movable sill was until now accepted to be too complex, new and risky. It was thought to exceed the main purpose of the pilot.

A big advantage of configuration 2.3, though, is that a water column with a constant height is present above the outflow openings of the air bubble- and water screens. This means that the required discharge is constant as well. At the Krammer recreational pilot, a difference in discharge was needed (see section 2.3). This caused complex operational efforts.

It should be noted, that perhaps configuration 2.3 can be combined with a fixed sill at VZM side. A fixed sill at the ES side would not be possible due to the available depth, but at the opposite side, that's not the case. The actual effectiveness of this solution is hard to predict with calculations or even models, but it seems only logic that the overall effectiveness will improve.

This study does not focus on combinations of several salt intrusion reduction systems for both sides of the lock chamber. Since the highest energy savings and the highest salt intrusion reduction both can be achieved at the ES side, only the ES side is being examined.

²² At the ES side, a fixed sill has no use, which is why the reduction is 0%. At the VZM side a reduction of approximately 24% is possible.

Chapter

3. Problem, objective & approach

First, the outline of the problem is described shortly. After the problem definition, it's described how the stated objectives are tried to be fulfilled.



3.1. Problem

Salt intrusion in a fresh water system is in some cases a problem. Salt intrusion occurs at waterways in open connection with the sea or at locks, in which salt water passes the lock every locking cycle. It affects intakes for both drinking water and agricultural use. Especially densely populated areas in coastal deltas are subject to the problem. The phenomenon has been counteracted for decades. How this has been done until now is not very accurate or it exchanges its accuracy for power inefficiency, high fresh water loss or a big environmental impact.

Until now, salt intrusion has been prevented in locks in several ways. Different techniques have been researched quite thoroughly. Especially many studies have been performed to the application of air bubble screens. From this, it has become clear that air bubble screens in combination with a water screen can effectively reduce salt intrusion. Energy consumption of this system is relatively high, though.

The Krammer locks in Zeeland, the Netherlands consist of two locks for recreational use and two locks for commercial use. Their dimensions are $2 \cdot (90 \cdot 9) m^2$ and $2 \cdot (280 \cdot 24) m^2$ respectively. They are located in the Philipsdam and are part of a very busy sailing route; approximately 100,000 ships pass the locks yearly. The sailing route can be seen as one of the largest water 'highways' for commercial shipping in the Netherlands.

In this lock complex, a rather complex system is present to counteract salt intrusion. It has a high efficiency, reducing salt intrusion in the order of 95%. This high efficiency is obtained by high energy consumption and high operational and maintenance costs.

In the near future, the current capacity will be too low. The existing system in the lock is planned for big maintenance within two years. By increasing the capacity of the current locks, plans for a third commercial lock can be avoided or postponed.

Problem The current salt intrusion preventive system in the Krammer commercial locks is highly effective, but:

- *The energy consumption is high (equivalent to high operational costs)*
- *The costs for maintenance are high*
- *The lock's capacity will be too low in the near future*

3.2. Objective & approach

The ultimate solution to the problem is to eliminate salt intrusion in the Krammer locks completely and at the same time eliminate all negativities of the current situation. To move in the direction of this desired situation, the objective is simple:

Objective Design a salt intrusion preventive system in the Krammer commercial locks which is comparably effective in terms of salt intrusion and fresh water loss as the current system, but at lower energy consumption, lower costs and resulting in a higher lock capacity.

The current system has yearly maintenance costs of 3.6 M€, while estimated cost of the big maintenance required in 2015, is more than 20 M€. The capacity of the lock needs to be increased in 10 to 15 years at the expense of 300 M€.

Since other systems exist and tend to be very effective, a pilot will be operational in one of the recreational locks in April 2014. Main objective of this pilot is to gain insight in possible designs for the larger commercial locks. A water screen and two air bubble screens are part of the design, which was accepted after thorough modelling studies of various alternatives. It's expected that the combination of air bubble- and water screens will be able to reduce salt intrusion in the same order of magnitude as the current system.

The first calculations show a large potential for this design, since high salt intrusion reductions can be achieved with lower energy and maintenance costs than the current system. The decision of which system to apply in the larger commercial locks will be made in September 2014.

Approach Fulfil the objective by an innovative design with an integrated movable sill in the Krammer commercial locks to improve salt intrusion reduction.

The design should score equal or better when compared to:

- 1. Current system in Krammer lock complex*
- 2. Pilot's system – when installed in Krammer commercial locks*

Several basic alternatives for a possible improvement of the pilot's design are compared in section 2.4. Here, it is explained that an integration of a physical barrier is most promising for the design of the commercial locks. The barrier should move up and down with the tide, working as a movable sill. This leads to a significant reduction of the height of the air bubble- and water screen (averagely ~25%). A screen of less height consumes less energy. The sill blocks salt water at a higher rate than the screens, which results in an increased effectiveness of the system.

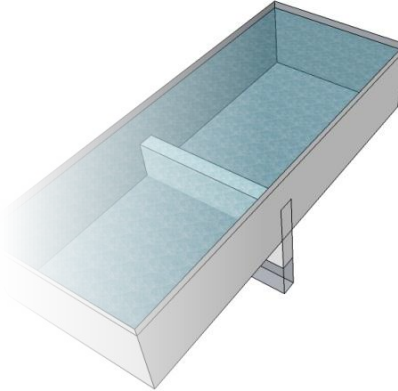
For the exact layout of the improved system, different alternatives are compared. The most promising option is evaluated in more detail. A structural analysis is followed by a dimensioning of key elements of the structure. In this way it is proved that a realistic detailed design is feasible.

The elaborated design is tested and compared in terms of salt intrusion reduction, fresh water loss, energy consumption, construction-, operational- and maintenance costs and capacity of the lock.

Chapter

4. Alternatives of movable sill

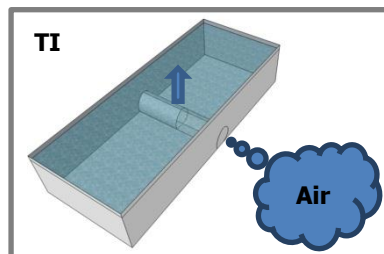
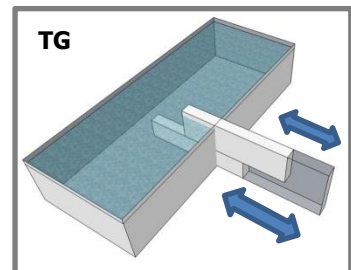
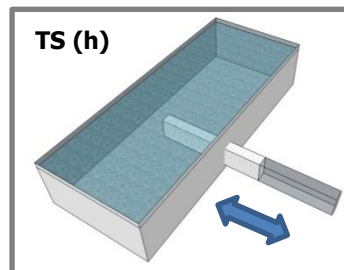
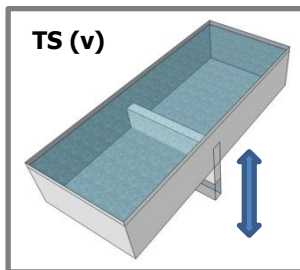
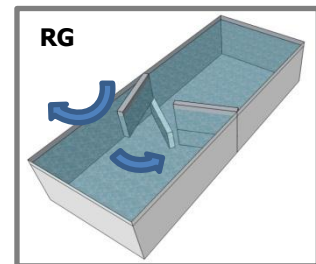
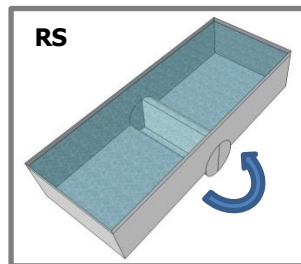
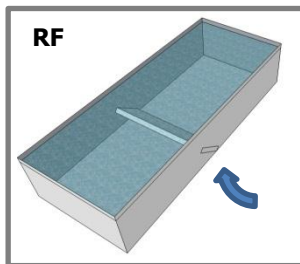
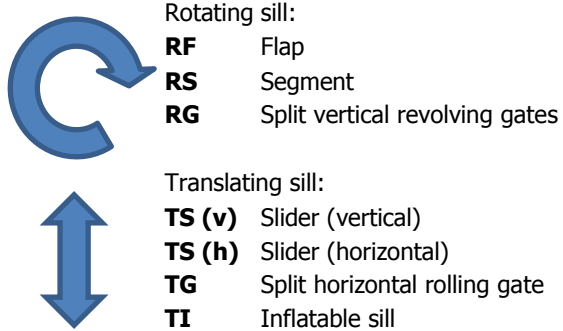
This chapter describes rough concepts, based on movements of the sill. It gives insight in a few promising options, and shows clearly why some are not. In the next chapter, a more detailed design will be described.



- 4.1 Description of alternatives
- 4.2 Comparison of alternatives
- 4.3 Best alternative

4.1. Description of alternatives

A few concepts are worked out in appendix E and compared here. These concepts differ on basic movements and are divided in two categories: rotating and translating. The concepts are shown in sketches below. They are very basic and show only a rough outline of the main structural element, which will act as salt prevention in the lock.



4.2. Comparison of alternatives

Appendix E.1 contains a larger version of the sketches, accompanied by a description of their properties. The seven concepts are described in terms of the twelve features below. The conclusion of section 2.4 explained that a sill must be adjustable in height, when situated at the ES side in the Krammer commercial lock. Three of the seven concepts are hard to adjust in height (*RS*, *RD*, *TS(h)* and *TG*) and will not be taken into account in a further analysis.

- Constructability
- Investment costs
- Operational costs *(Equivalent to energy consumption)*
- Operation time
- Wall connection *(Water tight connection at the sides)*
- Height adjustability
- Maintenance
- Parts under water *(Corrosive conditions affect under water parts)*
- Collision effects
- Hydraulic circumstances *(Resistance to hydraulic loads)*
- Sediment *(Settlement on top of the structure)*
- Experience

4.3. Best alternative

A multi criteria analysis (MCA) is worked out. All remaining concepts are ranked to the twelve features mentioned before. The features are ranked for the purpose of a weighted rating. The ratings are linearly proportioned from 1 (unimportant or negative) to 10 (important or positive). In this way the most promising and best applicable solution becomes clear.

The reasoning behind all ratings is outlined in appendix E.2.

Table 16: MCA of concepts on basic movements.

	Feature	Rating of feature	Weight factor	Rating of concepts			
				RF	RS	TS (v)	TI
1	Constructability	7	11%	10	4	7	10
2	Investment costs	8	12%	8	4	7	1
3	Operational costs	10	15%	10	10	10	1
4	Operation time	2	3%	9	10	10	1
5	Wall connection	8	12%	6	10	9	3
6	Height adjustability	10	15%	3	10	8	1
7	Maintenance	5	8%	8	3	3	6
8	Parts under water	8	12%	4	1	8	10
9	Collision effects	4	6%	1	1	1	8
10	Hydraulic circumstances	1	2%	5	10	9	1
11	Sediment	1	2%	6	5	5	10
12	Experience	2	3%	5	8	10	10
Total:			100%				
Unweighted rating:				6.3	6.3	7.3	5.2
Weighted rating:				6.5	6.3	7.5	4.5

The outcome of the MCA in Table 16 shows that the vertical translating slider ($TS(v)$) is the best solution to elaborate. It also shows clearly that there is a large difference between the bellow (TI) and the three other solutions.

Most important is to take notice of the fact that the features where the bellow scores high, are mostly ranked low at all other concepts. Therefore, it may be interesting to implement these features in the other three concepts. An example is for instance the use of rubber or plastic as material to prevent corrosive effects.

Differences between the three concepts are mainly based on differing ease of height adjustability and the initial costs. Weighing of the features does not alter the results very much, which tells us that especially at the bellow the more important features (high weight factor) are ranked low.

Reasons to accept this conclusion can be supported by taking in mind that a vertical option needs less adjustments in the existing lock chamber. The driving mechanism is installed above water easily with a vertical connection to the slider. Easy height adjustability is supplemented with the fact that an easy height indication of the sill under water is possible above water.

Above all, the structure can be compared in terms of dimensions and (watertight) wall connections with a rolling gate of a lock. This makes it acceptable that a realistic design is possible.

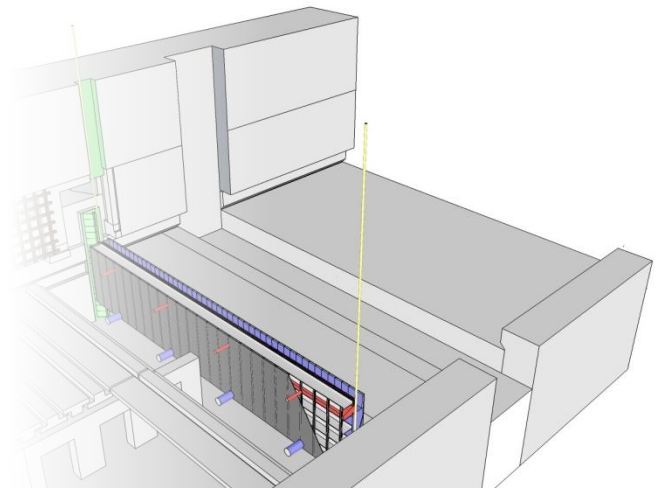
Chapter

5. Detailing of vertical sliding movable sill

In the previous chapter, an elaboration is made on basic movements of the structure. It was concluded that a vertical sliding sill was the best option.

In this chapter, a distinction is made on how these movements can be realised, how the structure is controlled mechanically and which dimensions are required.

The result is a conceptual design, which proves that a realisation of the structure is possible. It does not result in a tested design which is ready to be built; it does result in a helpful tool to quantify its expected effects, costs and future perspective in the next chapter.



5.1 Location and construction

5.2 Air bubble- and water screen layout

5.3 Driving mechanism

5.4 Loads

5.5 Structural design of the sill

5.1. Location and construction

Before the design of the sill is elaborated, a few important features of the design are presented. Its exact location is described by defining the main elements of the structure. Their location in the existing lock determines how certain elements are detailed. The movement of the structure is also important for the detailing of the structure. When the elements of the structure are described, construction aspects show that a realisation of the structure is possible.

5.1.1. Elements of the structure

Figure 27 gives a three dimensional sketch of the situation in the lock chamber. After zooming in, more detailed elements of the structure are visible in Figure 28.

The same orientation of the axes is used in other – two dimensional – sketches from now on.

- x Along width axis of the lock chamber; (equal to *length* axis of movable sill)
- y Along length axis of the lock chamber;
- z Along height axis.

The colours represent different parts of the structure. They are treated separately in this chapter.

<i>Colour</i>	<i>Section</i>	<i>Description</i>
▪ Red	5.2	Elements of the air bubble screen;
▪ Blue	5.2	Elements of the water screen;
▪ Yellow	5.3	Vertical force distribution and driving mechanism;
▪ Dark grey	5.5.2	Enclosing of the structural elements and air bubble- and water screen by plates;
▪ Pink	5.5.3	Studs;
▪ Orange	5.5.4	Main beams;
▪ Green	5.5.5	Horizontal force distribution, fitting in lock chamber and water tight connection.

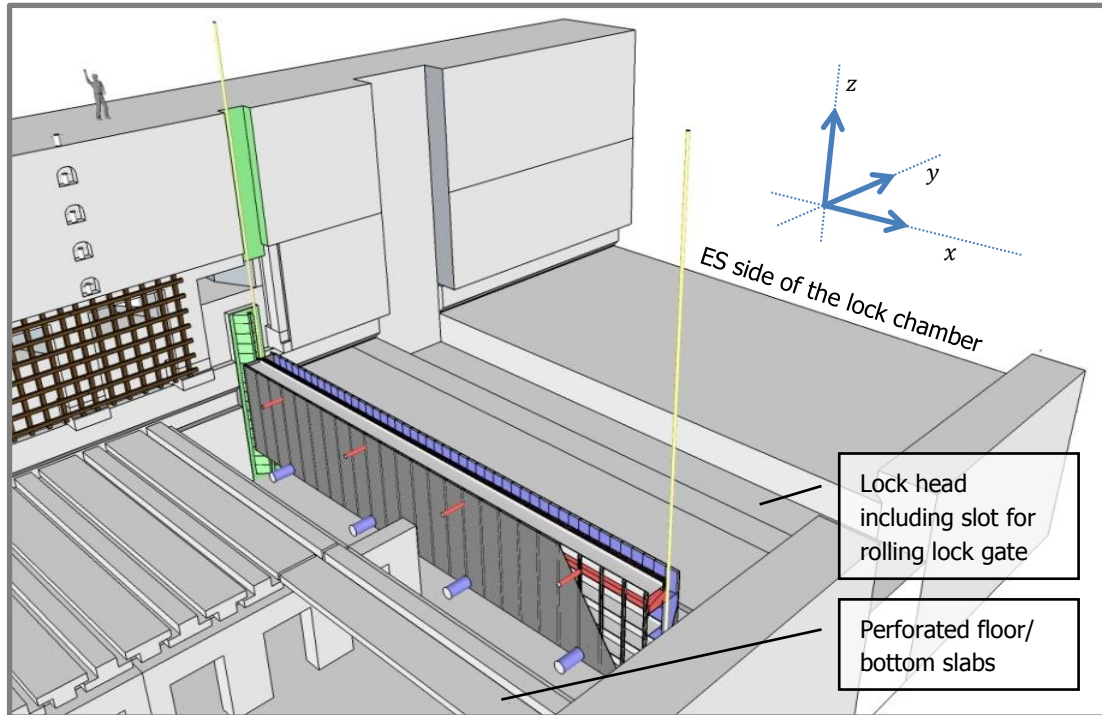


Figure 27: A 3D sketch of the design, placed at the commercial lock head at the ES side. Several detailed elements are printed in colours and are described on the previous page.

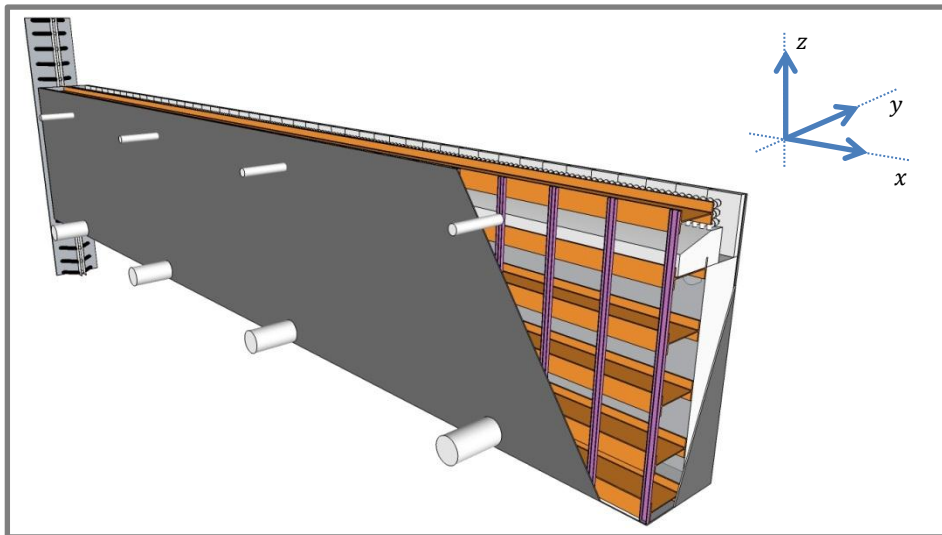


Figure 28: Zoomed in on the sill to visualise some main structural elements.

5.1.2. Movement of the structure

The range in which the sill in operation moves up and down is indicated in two figures. Figure 29 shows a cross section parallel to the sill; Figure 30 shows a side view of the lock wall. The range of the sill and the dimensions of the sill are presented to scale in both figures.

The sill itself has a height of 4.5 m (see section 0). The range in which the sill moves when in operation has its boundaries as specified below. It stretches for 8.8 m along the z-axis.

- Upper boundary –2.2 m NAP: The highest water level at ES (+2.5 m NAP), minus the navigational depth (4.7 m).
- Lower boundary –11.0 m NAP: At the bottom of the lock chamber.

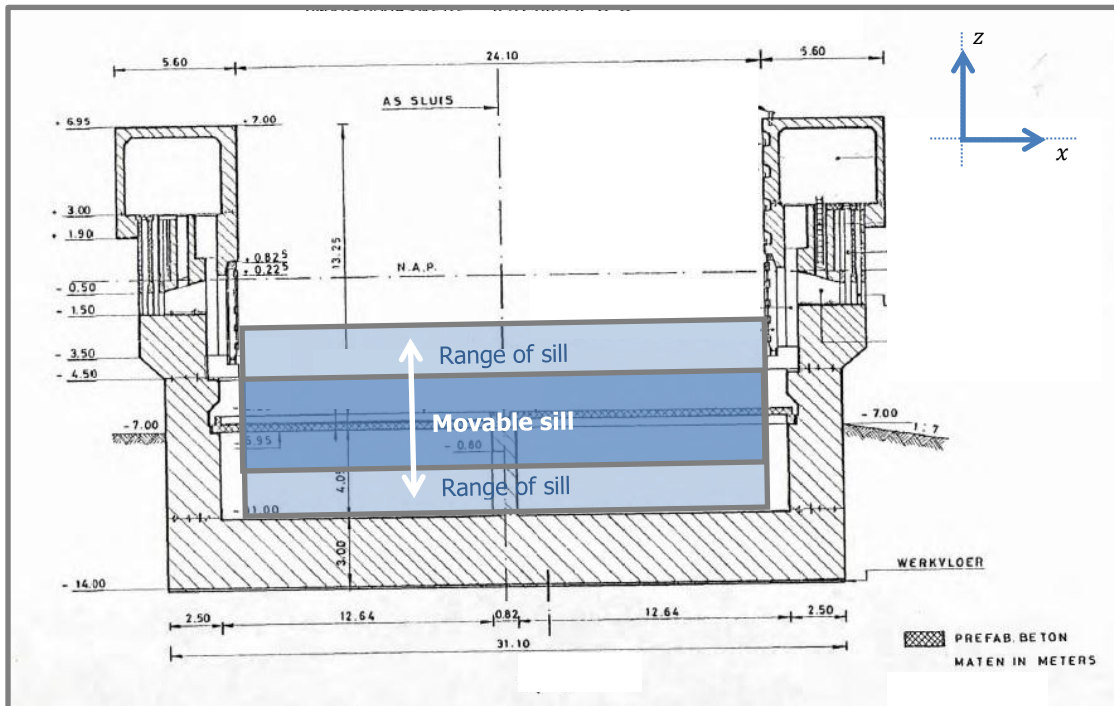


Figure 29: Range of vertical moving sill in cross section of Krammer commercial lock chamber. Adapted from (Rijkswaterstaat, 1981). Dimensions are presented in metres.

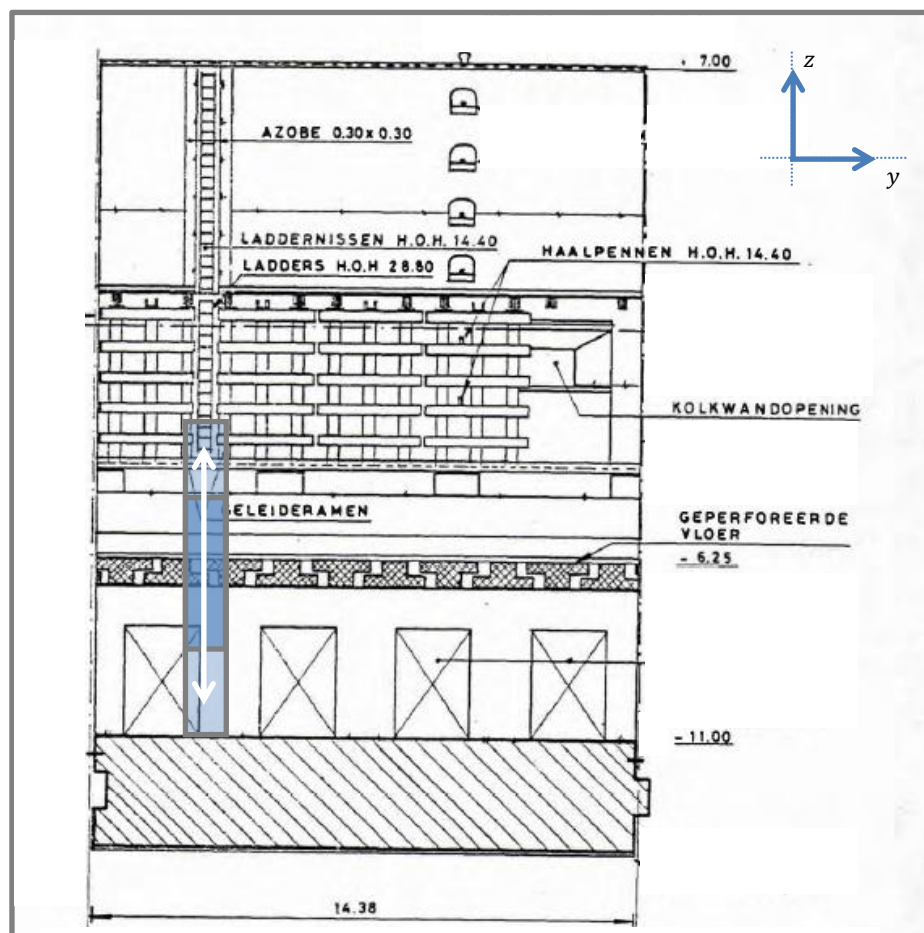


Figure 30: Range of vertical movement of sill in Krammer commercial lock. Adapted from (Rijkswaterstaat, 1981). Dimensions are presented in metres.

To be able to move freely in the location as visualised in Figure 29 and Figure 30, some concrete has to be removed from the current lock configuration. Figure 30 shows that the range in which the structure moves, crosses a few bottom slabs and the arch-structure supporting the slabs in the middle of the lock.

The concrete slabs and arch-structure don't have any other use than being part of the *Duinkerken system*. Since this system becomes obsolete in the new configuration, a removal is assumed not to be problematic.

This design of a movable sill of which no reference is known and very little knowledge is present, can be compared to a well-known and – above all – well-documented design. Namely, the vertical movement of a solid body, used to retain water is very much like a lift gate.

5.1.3. Water tight connections

Figure 31 shows an overview of how the vertical movable sill slides through the rail at one of the side walls. The supports of the rail are able to distribute the forces exerted on the sill in both directions to the concrete wall.

If the structure had been lifted out of the water and is going to be placed back in position, at a certain moment the sill must slide into the rail. A tolerance of only 5 cm to all sides is assumed, so attention must be paid to prevent the rail to be damaged in that situation.

The sill can only be effective against salt intrusion when it blocks water. Connections at the bottom and sides of the sill must be water tight. Small gaps are assumed to be no problem; in respect to the total dimensions of the sill, a gap in the order of centimetres is still as if it's water tight.

Side connection

A water tight connection at the side walls is easily obtained since the sill is pressed to one side in the rail by the pressure of a density difference. Figure 31 shows how the steel structure at the side walls is adapted to become impermeable. Plates can be installed against the supports of the rail.

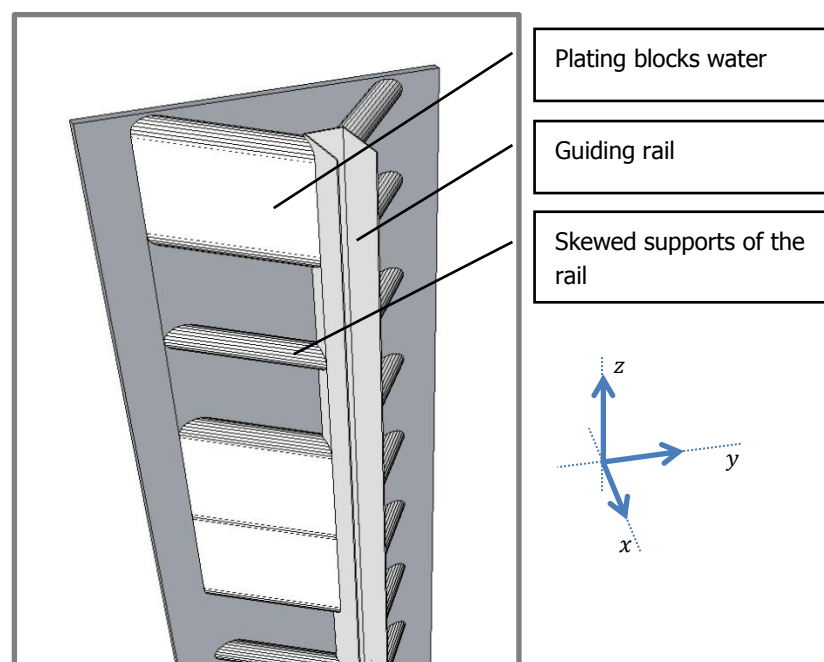


Figure 31: Rail at lock wall; in the figure partly closed to block water past the sill.

Bottom connection

Bottom slabs are removed to make the movement of the sill possible. This is earlier explained and illustrated in section 5.1. An easy way to prevent water from flowing underneath the sill, is by replacing the bottom slabs between the sill and the lock gate by a solid concrete plate. Figure 32 shows that water flows through the lock bottom are completely prevented in this way. The location of the sill is highlighted blue, the solid bottom slab red. A photograph of the same view as Figure 32 shows the location of the solid bottom slab in Figure 33.

Eq. 0.38 in appendix J.3 shows that the deflection of the main beams in the sill is maximum 422.6 mm . The entire structure is probably stiffer than the main beams only, which is why this is a conservative value of the maximum deflection. The approximate last 0.5 m of the solid slab must be made of rubber to allow deflection of the sill without damaging any element. This is not detailed in this study.

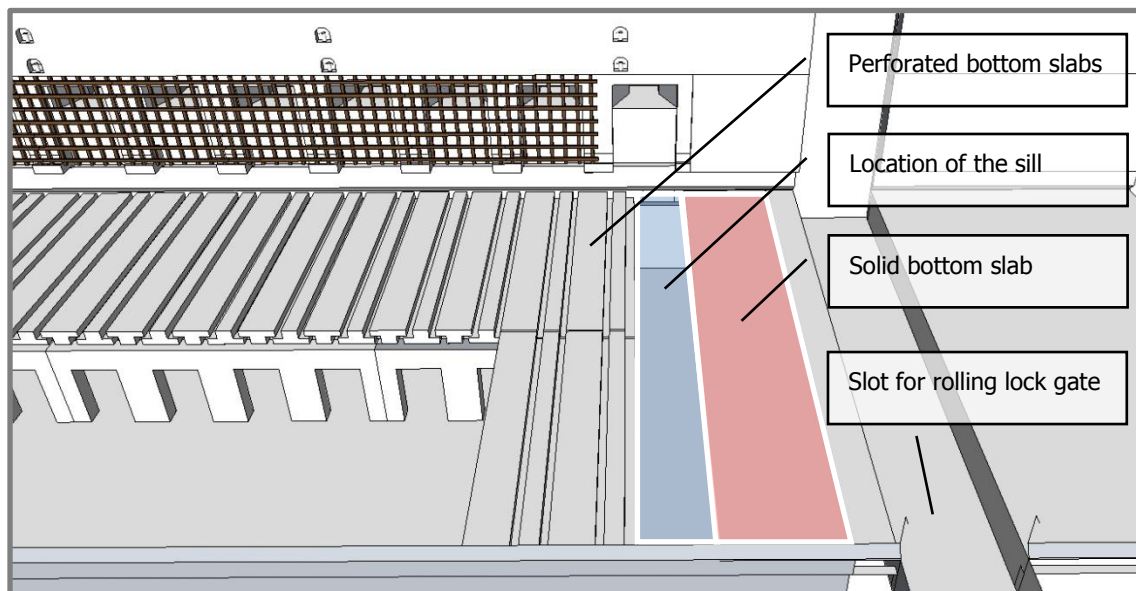


Figure 32: Solid slab replaces bottom slabs on the right in the figure.



Figure 33: Photograph of bottom slabs in lock chamber. Adapted from (Rijkswaterstaat Bouwdienst, 2000b).

5.1.4. Construction of the structure

The designed structure is located in an existing lock. This makes construction of the design more complicated. To result in a complete construction of the design the required actions are divided in two

stages of construction: preparation and execution. Some important features of the lock throughout the process of construction are described in terms of the expected costs and accessibility.

However some structural elements are detailed quite thorough, the design as presented in this study is still a conceptual design. Typical solutions suffice as proof of a possible realisation of the structure. Hence, a brief description of the construction shows in what way a realisation is possible.

Preparation

In the preparatory phase the lock is still operational. Prefabricated elements are made and transported to the lock. An overview of the features in this phase is presented; a description follows afterwards.

- Transport main construction elements to assembly site;
- Prefabricate the steel structure and the solid bottom slab(s);
- Transport all elements to the lock;
- Prepare all works that do not interfere with the lock's operation.

The steel structure will most probably be assembled in a workplace near a steel factory or in a maritime construction environment. The largest elements are the main beams of the sill. The 24 m long beams can be transported to the construction area over water if a transport via road is problematic.

The steel structure can be assembled by welding it together. The structure consists of relative large main elements, combined with an air bubble- and water screen. Welding should be possible without enclosing areas that need to be accessible to make the required connections. Figure 34 shows a possibility of how welds in this complex configuration are possible. Connections with bolts are also possible.

The solid bottom slabs are made of concrete. They can be prefabricated in a factory.

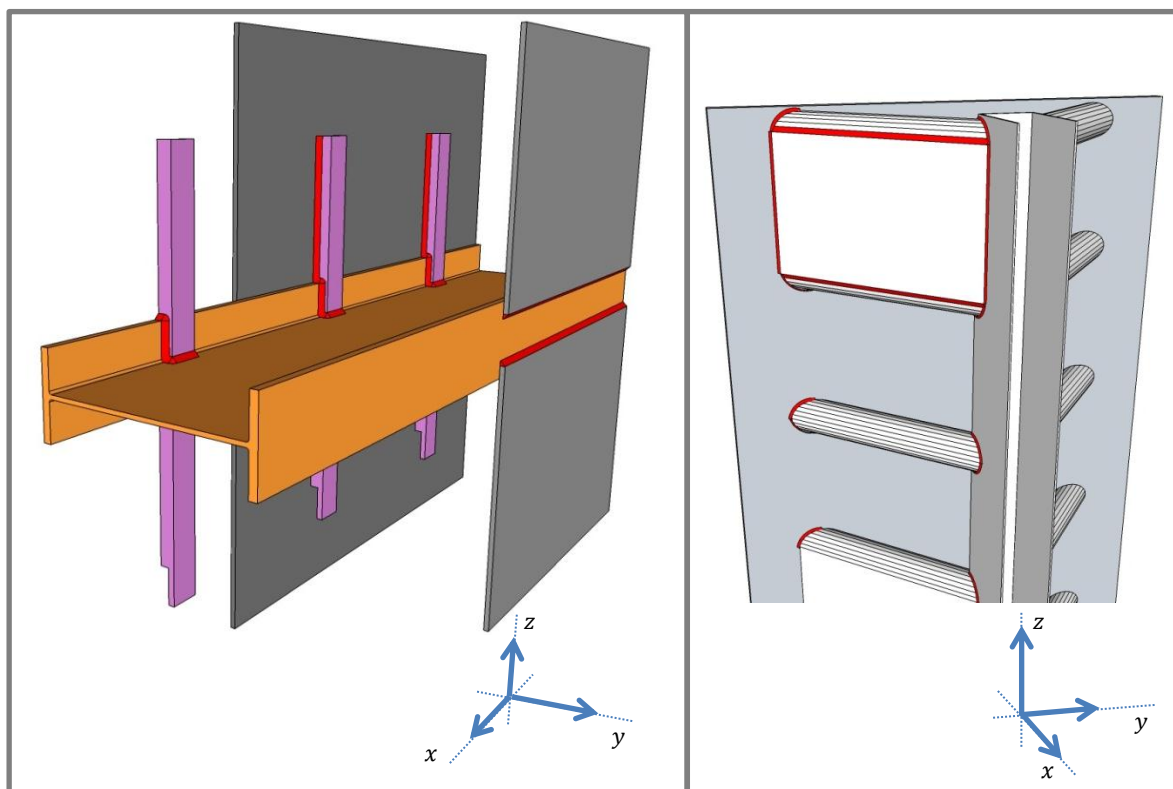


Figure 34: Details of connections of different steel construction elements. Welds are printed red; further, the same colours are used as in Figure 27.

The steel structure has large dimensions and must be transported over water. A ship could transport the structure to the lock complex. The solid bottom slabs are approximately 12 metres long and can be transported by road.

The driving mechanism of the structure is situated above and aside the lock. It doesn't affect shipping directly. It's possible to install the engines for propulsion of the movable sill before the lock is closed for shipping.

Other works can be carried out in the preparatory phase as well; as for instance altering the technical controlling system of the lock complex.

Execution

The execution works are characterised by a dysfunctional lock. Main actions can be carried out in the wet, but some require a dry lock chamber. The lock is able to withstand the hydraulic loads on the closed gates when the lock chamber is set dry.

A brief summation of the required actions in this phase is presented.

- Remove bottom slabs;
- Remove concrete arch structure;
- Place solid bottom slab(s);
- Install guiding rail at lock chamber walls;
- Connect fixed point of supply pipes at lock bottom;
- Hang sill-structure in its position by crane;
- Connect sill to the driving mechanism;
- Connect flexible supply pipes for the screens to the sill.

Costs & accessibility

The required large machinery which is expected to be required throughout the construction process remains probably limited to a lifting crane and transport ship. The highest costs will be formed by the time during which the lock is not operational. There is no obvious redirecting sailing route to prevent passage of the Krammer locks. It's not possible to reduce the effects of a closed lock by closing it for shipping in a period when the lock is used less often; the commercial locks are used by commercial vessels, so a significant difference in busyness throughout the day or throughout the year is not present.

Since the lock complex has two commercial locks, construction works must be limited to one lock chamber at a time. The available capacity reduces by half. After the construction in one lock chamber is finished, its capacity has been upgraded approximately by a third (see section 6.5). When the second lock is closed for construction works, this results in a capacity decrease of the entire complex of a third.

The duration of a dysfunctional lock chamber may be reduced by adapting the lock without setting it dry. For construction works at the walls of the lock, this can for instance be achieved by use of a pivot-inspection chamber²³.

²³ In Dutch: *Taatskuip*.

See Figure 49 in *Terms, translations & abbreviations* on page 97.

5.2. Air bubble- and water screen layout

Different configurations of air bubble- and water screens are thinkable. In this chapter, the most important differences and possibilities are lined out and compared. The result is a founded choice for the most promising option.

The description of air bubble- and water screens in section 2.3 is required knowledge for this section. Aspects and calculations on screen capacity, reservoir pressures and pipe flow velocities are explained there.

Size

To result in an effective screen, it is desired to have an evenly spread thickness or even dense distribution of water or air particles along its length axis. Without an even distribution, salt leakage is reduced less effective. This undesired situation can be compared with a fluid, conserved in a membrane with weak points or holes in it.

To let the pressure be distributed evenly along the outflow openings, a certain pressure built-up is required. This can be achieved in two fundamental different designs; one which needs a lot of space (*large reservoir*), or one that is relatively slender (*small reservoir*).

Fixation

To reduce energy consumption of the screens, section 1.4 shows that the outflow of the screens must adapt their height to the sill's height. This leaves two options for the configuration of the sill, consisting of a reservoir and an outflow opening. All elements move up and down, (*movable reservoir*) or only the outflow opening moves up and down (*fixed reservoir*).

A fixed reservoir will be located lower than the level of the concrete slabs in the lock chamber. (see Figure 27) It doesn't disturb the wetted cross-sectional area of the fairway.

These two features (*reservoir large or small* and *reservoir movable or fixed*) are described for both the air bubble- and the water screen. After a description and illustration, it's explained what the best configuration is.

The different layouts are accompanied by Figure 35 until Figure 38. Those are sketches which intend to clarify the order of magnitude and do not visualise a proofed layout. Blue arrows in the figures indicate the flow of water or air through the particular structure.

All dimensions in the considerations of this chapter are based on rough calculations and assumptions. A qualitative choice is made based on these considerations. Further calculations in the next chapter result in a quantitative design.

5.2.1. Water screen

Small reservoir

One way to achieve an even distribution of water along the screen, is to control water flows physically. Figure 35 shows how the water is diverted from the inlet to the small outflow opening. Energy is dissipated because of the small outflow opening. The opening must be engineered correctly, to result in an even distributed outflow of water. The thickness of the screen reduces towards the outflow opening.²⁴

A structure like this does not exist yet for this purpose. It needs more calculations and perhaps physical modelling studies, before an implementation is possible.

²⁴ When the internal cross-sectional area decreases from inflow to outflow, pressure drops, which is undesired.

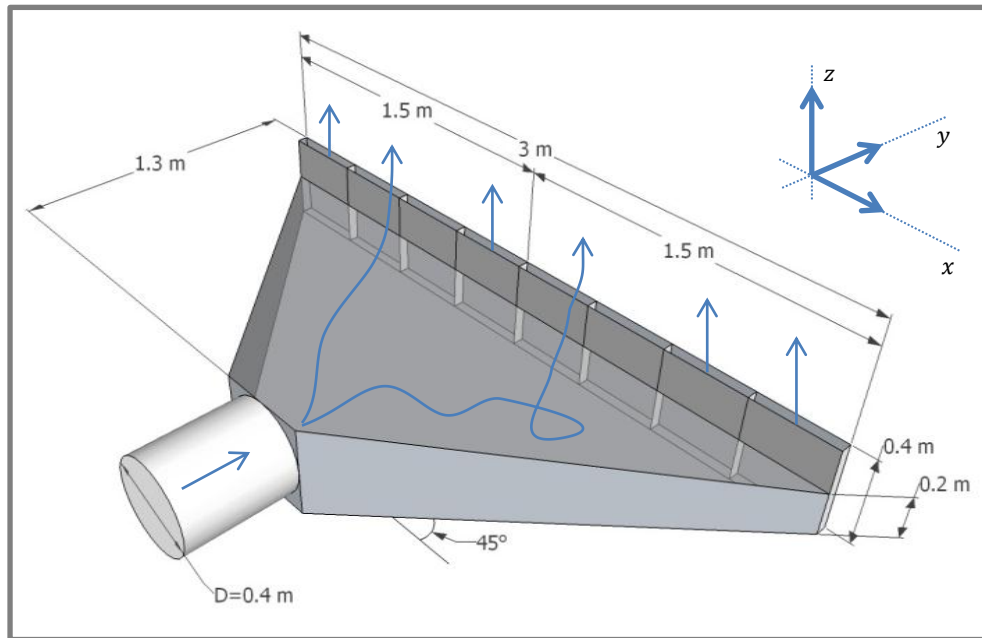


Figure 35: Sketch of 1 of 8 sections of a water screen with small reservoir.

The dimensions in Figure 35 are based on the following assumptions:

- To remain the 'small' option, the reservoir's width must not exceed 1.5 metres.
- The angle at which the reservoir broadens from inlet to outlet is assumed to be 45 degrees. This results directly in a maximum length of the screen of 3 metres. The 24 m wide screen is divided in 8 sections total.
- According to section 2.3, a water screen of 3.0 m long and 4.7 m high needs a discharge of $0.35 \text{ m}^3/\text{s}$. The required diameter becomes in the order of 350 mm, by using the same formulas as in section 2.3. A rounded value of 400 mm is chosen.

Large reservoir

Another way to achieve an even water distribution along the openings, is to increase the dimensions of the reservoir as visualised in Figure 36. If the reservoir is large enough, an unsymmetrical inflow doesn't necessarily lead to an unsymmetrical outflow, because the pressure at outflow has become equal. The current design of the water screen in the pilot of the Krammer recreational locks is based on this principle. A design is made; a realisation does not exist though. The comparable pilot's design is described in section 2.3.

Additional benefit of this design is a possible integration of the retaining function of the movable sill. Appendix F describes different options for the layout of the possible gap underneath the reservoirs. By integrating these designs, one element of the design becomes obsolete.²⁵

²⁵ The layout as presented in Figure 36 is vertically orientated. A horizontal orientation is also possible, but not taken into account here. A benefit of a horizontal layout is the possibility of installing vertical connections at a larger spacing. This improves the stability of the entire movable sill.

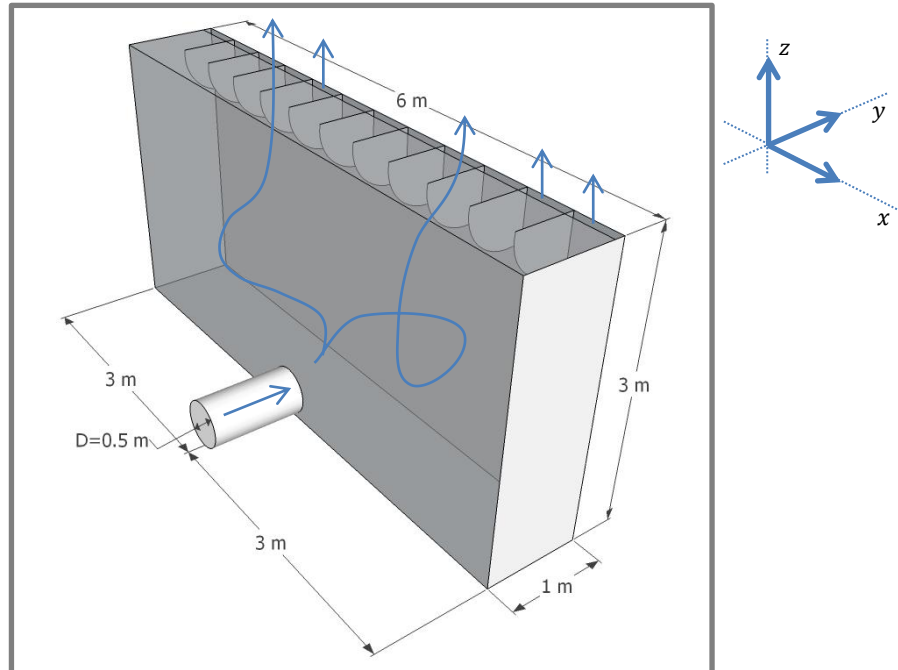


Figure 36: Sketch of 1 of 4 sections of a water screen with large reservoir.

The dimensions in Figure 36 are based on the following assumptions:

- A cross-section of the reservoir has dimensions in the order of 3 m^2 . (See the description of the pilot's design in section 2.3 as a reference.)
- An even spread outflow will be obtained by an equal water pressure at the top of the 3 m high reservoir.
- With a length of approximately two times its height ($\sim 6 \text{ m}$), and inflow pipe at the middle along the longest axis, an even spread screen is expected to be acquired.²⁶
- According to section 2.3, a water screen of 6.0 m long and 4.7 m high needs a discharge of $0.71 \text{ m}^3/\text{s}$. The required diameter becomes in the order of 500 mm , by using the same formulas as in section 2.3.

Choice – large air reservoir

A slender design with a small reservoir is in this case not needed, because enough space is available in the lock chamber of the Krammer commercial lock underneath the bottom slabs. A small reservoir results in an even spread outflow because of energy dissipation; when such a reservoir is long, it will induce high energy losses; a short reservoir results in many sections. A screen built up from many sections is disadvantageous, because of more supply pipes, higher construction costs and relatively more energy dissipation.

Because a more robust design has less energy dissipation, a larger width per section is possible. This results in less sections and supply pipes. Stiffness can be easily inserted in the heavier structure, which is less vulnerable and better resistant to vibrations than a slender design. The retaining function of the sill as described in appendix F can be integrated in the design of the reservoir, which is an additional benefit.

²⁶ In the reasoning of the design of the pilot – screen sections 4.5 m wide – it's mentioned that wider sections are possible, but need further investigation. The internal distribution of water is acquired by an internal horizontal pipe with holes in it. (Rijkswaterstaat Zeeland, 2013, p. 6)

The exact layout of the inside of the large reservoir is not elaborated in this report.

Movable or fixed reservoir

The outflow opening of the reservoir moves up and down with the top of the movable sill. This doesn't necessarily mean that the entire reservoir moves up and down as well. The connection from the reservoir to the outflow opening or of the water supply pipe to the reservoir must be flexible to achieve this. Both options result in the use of a telescopic or flexible element.

When the reservoir is fixed at the bottom, a flexible connection between the reservoir and the outflow is needed. An idea could be to use small tubes, but this will result in an uneven spread screen. A better option is some sort of sheet which can be compared with a waterbed. It is flexible and contains water. Major difference is that the dimensions are scaled up and there are openings at the top- and bottom-ends. Water flows through the sheet and is flexible at the same time. A realised work based on this idea cannot be found, so the possible design must be examined and tested thoroughly before an implementation.

When the reservoir is movable, the connection of the supply pipe to the reservoir moves as well. The supply pipe should be flexible from the reservoir to a certain fixed point. Since the pipe has a large diameter, it should be quite long to possess the needed flexibility. Beneath the concrete slabs of the lock chamber, an area of 4.75 metres deep is available with the same width- and length-dimensions of the lock chamber.²⁷ This space can be used without interfering in processes of the lock in any way. The fixed point of the pipe can be located underneath the concrete slabs.

Choice – movable water reservoir

A reason to fixate the reservoir at the lock bottom is its protection by the layout of the lock chamber. For the connection with the outflow openings, a 'waterbed-sheet' is required. This must be engineered from scratch without any experience or existing reference. Because the reservoir is not attached to the outflow openings, it's a less stiff structure and will be more vulnerable to vibrations.

By making a movable reservoir, a flexible water supply pipe is required for every section of the screen. The pipes are approximately 500 mm in diameter. To make such pipes flexible, they must be relatively long which requires space. Space for these long pipes (for example installed as a helix), is available underneath the bottom slabs of the lock chamber. A detailing of these pipes is not inserted in this report.

Beneficial is that the entire screen (including reservoir) can be lifted out of the water for maintenance or replacement. The flexible pipes need to be uncoupled.

5.2.2. Air bubble screen

Small reservoir

The screen remains relatively slender, because of the presence of regulators. A visualisation can be found in Figure 37. A more thorough description is presented in section 2.3, where the most important feature is the working air pressure of $\sim 2.3 \text{ bar}$. Air only escapes at the outflow openings when a pressure difference of at least 1 bar is present. The regulators aren't visible in the sketch, since they are located inside the pipes. This design is based on the actual design at the Stevin locks, which is described in (Deltares, 2011a).

²⁷ See Figure 30. The bottom level of the lock chamber underneath the slabs is -11.0 m NAP ; the top level of the slabs is -6.25 m NAP .

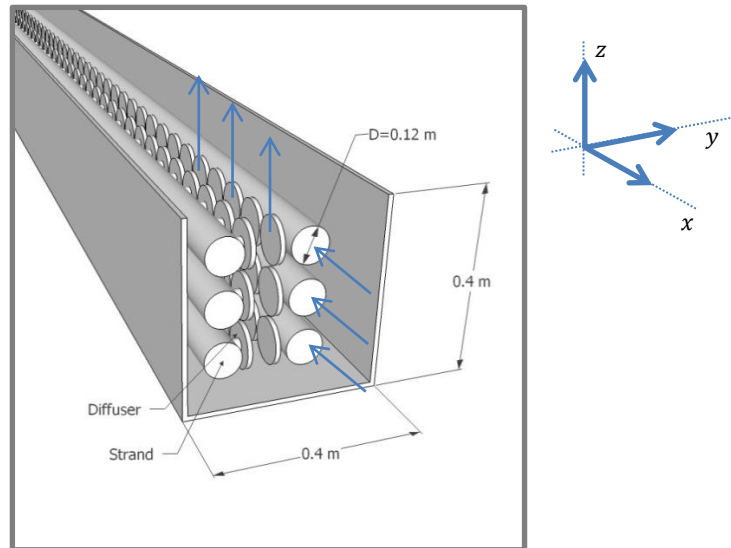


Figure 37: Sketch of possible layout of air bubble screen with small reservoir, formed by 24m long strands. (six strands and numerous diffusers visible)

The dimensions in Figure 37 are based on the following assumptions:

- The same number of pipes is used as in the pilot, but a larger screen is fed. For that reason the diameter increases. By using more than 6 pipes, this diameter can be decreased.
- According to section 2.3, an air bubble screen of 24.0 m long and 4.7 m high needs a discharge of 1,333 m^3/s . The required diameter becomes in the order of 110 mm, by using the same formulas as in section 2.3. A rounded value of 120 mm is chosen.

Large reservoir

Regulators are responsible for a high energy consumption of the screen. Figure 38 gives an overview of a possible layout without them. An implementation of this technique does not exist yet.

In a design without regulators and without the corresponding pressure loss of 1 bar, a working air pressure of ~ 1.5 bar suffices (see section 2.3). An effective screen with an even spreading of air bubbles along the openings is obtained when the air pressure at all openings is approximately the same.

The layout of the diffusers is directly copied from the layout of the proofed 'small reservoir'- option.

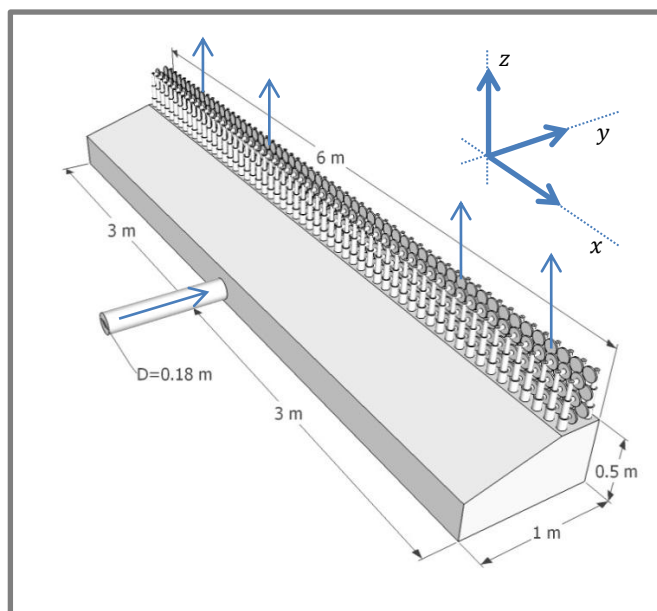


Figure 38: Sketch of possible layout of air bubble screen with large reservoir.

The dimensions in Figure 38 are based on the following assumptions:

- According to section 2.3, an air bubble screen of 6.0 m long and 4.7 m high needs a discharge of 333 Nl/s . The required diameter becomes in the order of 170 mm, by using the same formulas as in section 2.3. A rounded value of 180 mm is chosen.
- The screen is 6 m wide. It is assumed that an even spreading of air pressure can be achieved at the diffusers.
- With a cross-section in the order of 0.5 m^2 , it is assumed that an equal air pressure along the length axis can be built up.

Choice – large air reservoir

An advantage of the small option with strands is that if one strand gets damaged, the loss in effectiveness is spread over the lock chamber width. When a section fails, there is a 'hole' in the salt intrusion prevention.

A huge and decisive advantage of the large option is the absence of the pressure loss of 1 bar over the regulators. With a total air pressure of ~ 2.3 bar, a major amount of energy can be saved.²⁸ The effective weight decreases, which reduces the required energy for movement of the screen further. Also, the large option gives the entire structure more stiffness. A disadvantage is that this technique has never been used before and probably needs more modelling before an actual implementation is possible. Nevertheless, the option with large reservoir is the most promising.

Movable or fixed air reservoir

Main reason to look into the option of a fixed water reservoir at the bottom of the lock, is the large size and weight of the structure. The air reservoir is not as large and heavy as the water reservoir. But the main reason to disregard a fixed air reservoir at the bottom of the lock is the benefit of a lower water column above the outflow openings of the screen (see section 6.3.3).

Choice – movable air reservoir

Supply pipes to the movable reservoir need to be flexible. The supply pipes for the air screen (for large reservoir $\sim \varnothing 17$ cm) are much smaller than the pipes for the water screen (for large reservoir $\sim \varnothing 50$ cm), and can be installed as flexible pipes easily. The same possibilities as described for a flexible connection with water pipes are possible and can be found on page 57.

The entire structure (including reservoir) can be lifted out of the water for maintenance operations. The effective weight of the movable part of the sill decreases by inserting a tank filled with air. In this way less energy is needed to move the screen.

5.2.3. Fitting of screens in sill

The reservoirs of both the air bubble- and the water screen are integrated in the structural design of the sill. Figure 39 presents a cross section of the sill with the reservoirs as well as the main structural elements on scale. The air reservoir is highlighted red. The water reservoir is highlighted blue and has changed its dimensions to fit in the design of the sill. The width of the sill has been increased from 1 to 1.7 m. The blue area is in the order of 3.5 m^2 . In section 5.2.1 an internal cross section of the reservoir of 3 m^2 was assumed to be sufficient to result in an even spread outflow.

As described in section 5.2.1, the supply pipes of both screens must be flexible. Only the fixed connection point of these supply pipes is presented in the figure. The flexible supply pipes have large space available underneath the perforated bottom of the lock as can be seen in several figures in this chapter, and especially in Figure 27.

²⁸ The non-return valves also have a pressure-loss, but that's assumed to be in the order of 0.3 bar at maximum.

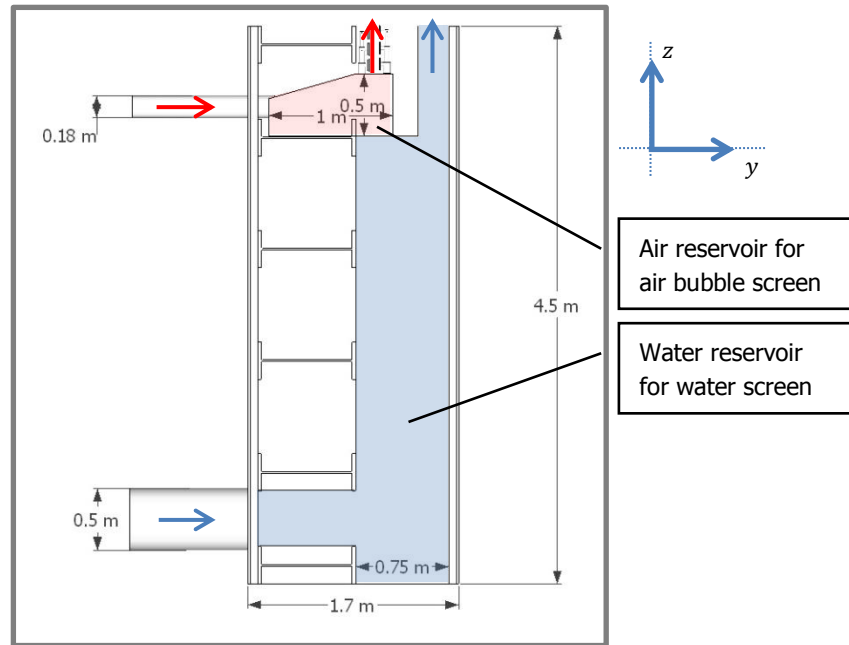


Figure 39: Cross section of movable sill. Integration of air (red) and water (blue) reservoirs.

The figure indicates the rough relation of dimensions, not a final design. The white areas could be filled with air, but need water tight connections in that case. They can also be filled with fresh or salt water. In that case openings are required to allow water out when the structure is lifted out of the water. The visualised main beams are used to show that a realistic design is possible. They could also be executed as a truss, allowing water for the water screen to flow through it.

In either case, the structure might have a slight horizontal eccentricity between the centre of mass and the connection to the driving mechanism at the top. In that case the structure wants to tilt. The effects and consequences of a possible tilting movement are described in section 5.5.5.

5.3. Driving mechanism

In most cases, a vertical moving gate is controlled by cables and winches. When for instance a lift gate is lifted out of the water, a large stroke must be made (order of 15 m). In case of a movable sill under water, the stroke is only in the order of 4 m since the sill doesn't have to be lifted entirely out of the water.²⁹ Therefore, other solutions are feasible as well.

The driving mechanism of the movable sill can be designed in different ways. After a description of certain requirements to this design, three different options are described. The differences between them, their rough dimensions and estimated energy consumption are used to choose the best option.

A mechanical design of the driving mechanism is not carried out in this study. Further, it's assumed that the vertical forces by the sill on the driving mechanism can be distributed to the concrete of the lock chamber. This is not detailed in this study.

5.3.1. Requirements to driving mechanism

The effectiveness of the system depends on the height of the movable sill. In order to save as much as possible on energy consumption, the sill must be situated as high as possible. When the water at the ES side rises due to tidal influence, the sill must follow the level of the water. This means for the driving mechanism that it should be possible to change the height in the order of centimetres. The sill should be fixed at the desired height.

The mechanism needs maintenance, which should be carried out easily. The lock may be out of order only as short as possible. It is favourable to diminish the need for maintenance; for instance by installing the mechanism above water, or use maintenance-poor materials.

In terms of energy consumption of the different mechanisms, the significance should be regarded. It is expected that energy consumption of the mechanisms is marginal in respect to consumption of the air bubble- and water screens.

It is desired to leave the option open to set the sill height higher than 4 metres. When in future plans less deep ships pass the lock, more energy can be saved by increasing the sill height. The lock is designed for ships which need a 4.7 m draught. If this type of ship only passes the lock once in a year, it is good to have the option of heightening the sill more than 4 metres. It is also possible to take into account potential water level changes at the VZM or ES.

In favour of the management of the lock complex, a physical indication of the height of the sill is rather useful. This will help in decreasing the chance on a potential collision.

5.3.2. Description of different driving mechanisms

A short description of three different systems follows. It's presented in what way they fulfil the requirements. To quantify the main dimensions and estimate energy consumption, general dimensions of the sill are assumed in appendix K.

Winch system

A winch system controls cables, which are connected to the structure. Due to loads on the structure, it may vibrate unwantedly. To prevent this, the sill must be very heavy or fixed between cables in opposing directions. Figure 40 shows an example of two winches and a vertical sliding sill. Since the winches are installed above water, maintenance is relatively easy.

The system consumes roughly 8.44 kWh/day. A height increase above 4 metres is well possible by installing longer cables.

²⁹ Operationally, it only has to move in the order of 4 m. Only for maintenance operations the option is left open to lift the entire structure out. It's probably more efficient to rent a crane, instead of over-dimensioning the driving mechanism for that occasional purpose.

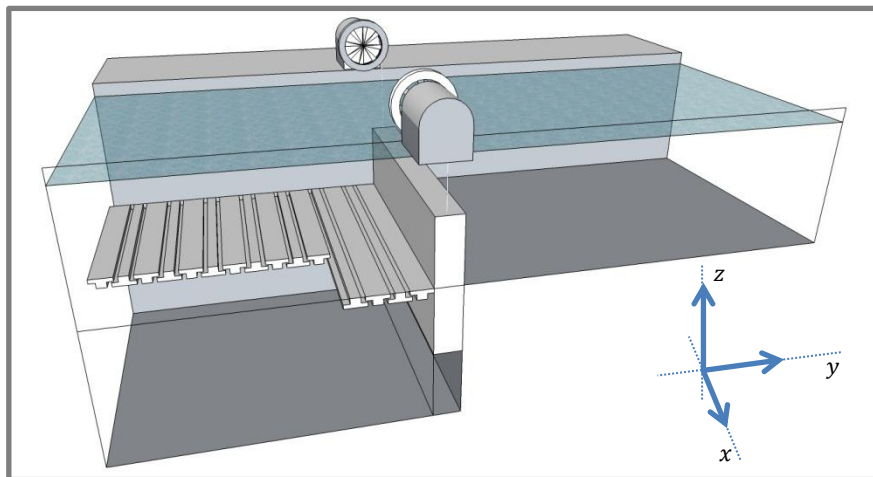


Figure 40: Vertical sliding sill controlled by cables in a winch system.

Hydraulic jacks

Hydraulic jacks heighten and lower the structure. An advantage is that jacks can be steered rather precise and are able to maintain the height of the sill when loads are exerted on it.

Figure 41 shows a vertical sliding sill, connected with jacks installed underneath it. It's also possible to install the jacks above water via a vertical connection just as with the mechanical option. Especially for maintenance actions that's favourable. The jacks consume roughly 15.33 kWh/day . It's not easy to increase the maximum level of the sill, since the jacks have a maximum elongation.

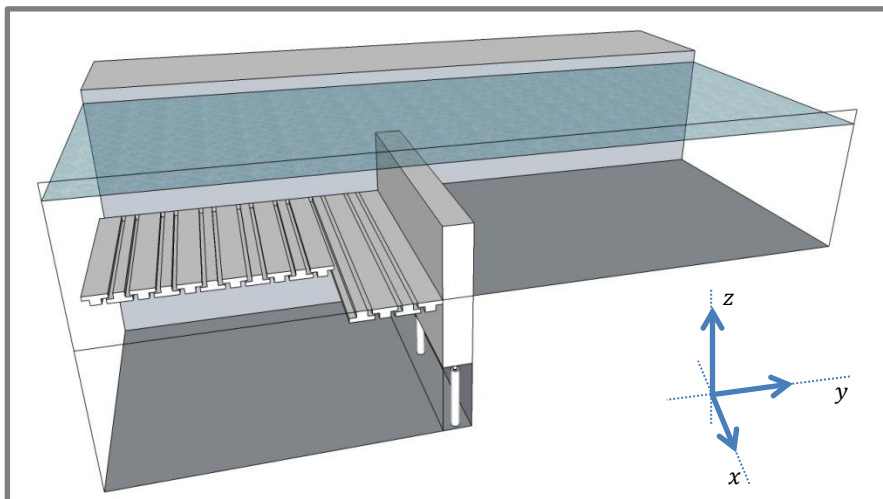


Figure 41: Vertical sliding sill controlled by hydraulic jacks.

Mechanical

An engine is connected to cogwheels, which propel the structure via a vertical connection to the sliding sill. A precise steering of the sill height is possible. Also loads can be resisted by the system when the engine is not active.

Figure 42 illustrates the option. The engines are positioned above water, which is favourable for maintenance. By elongating the vertical connection to the sill, it's very well possible to increase the sills height without high extra costs. The engines consume approximately 8.44 kWh/day .

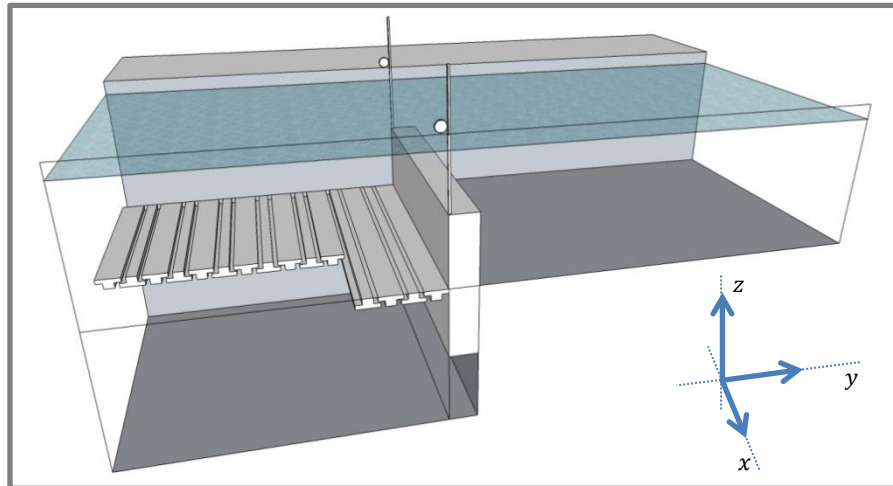


Figure 42: Vertical sliding sill controlled mechanically by cogwheels along vertical bars.

5.3.3. Best alternative

Altogether, the mechanical option above water seems best. With all presented options a detailed control of the sill's height is possible. Additional advantage of the mechanical- and the hydraulic jack-system is the fixture of the sill. By using cables, additional measures are probably needed to counteract or decrease undesired vibrations of the sill.

Maintenance actions are a result of failure of the system, negative outcome of inspections or planned operations. Maintenance actions and the inspections itself mustn't affect the operation of the lock too much. Driving mechanisms positioned out of the water are preferred above mechanisms installed in the water. Under water parts have negative influence on the operational time of the lock. Replacing crucial under water parts with more expensive maintenance-poor materials will decrease this. The best option is to prevent this completely by avoiding under water parts, though.

Energy consumption of the different mechanisms is not of significant importance. There are differences, but these are marginal compared with the energy savings of a less high air bubble- and water screen. The energy consumption of the air bubble- and water screens in the commercial locks is approximately 6,200,000 kWh/year. After introducing a sill – and decreasing the height of the screens – that value is reduced to approximately 2,800,000 kWh/year. 10 kWh/day matches roughly 3,650 kWh/year. This proves the difference in energy consumption of the driving mechanisms being only of marginal importance (order of 1/1000).³⁰

Additional benefit for the mechanical option is the possibility of controlling the exact height. A vertical sliding sill mustn't get stuck between its side supports by askew vertical movements. When at both sides of the sill cogwheels control its height rather precise, this undesired situation can be prevented.

5.3.4. Vertical connection to lock chamber

Vertical piles connect the structure to the driving mechanism. In this way it's always visible at which height the sill is levelled. Cables are not possible in combination with a mechanical driving mechanism. The piles are only subjected to tensile forces by the weight of the structure of 531 kN. To prevent large moments to occur in the tensile member, a hinged connection to the structure is advisable.

The length of the piles is chosen to be 15 m. The top of the sill is levelled lowest at -6.5 m NAP ($-11 \text{ m NAP} + 4.5 \text{ m}$). The highest level of the top of the piles is at the driving mechanism, located above the top level of the lock at $+7 \text{ m NAP}$.

The piles consist of CHS 114.3/4 profiles. This profile is obtained after calculations in appendix J.4. They are slightly over dimensioned to cope with possible frictions between the structure and the rail.

³⁰ Figures obtained from calculations on energy consumption of the Krammer commercial locks in section 6.3.

5.4. Loads

To be able to quantify the dimensions of the structure, different load cases are regarded. The load cases are based on governing loads, occurring situations and several life cycle stages.

But firstly, basic information is given by assumptions and descriptions to understand this chapter.

5.4.1. Basic information

Assumptions and a description of the movement of the sill are used as starting point for determining the loads which lead to the dimensioning of the structure.

Water densities

- Water densities for salt and fresh water of respectively $1,030 \text{ kg/m}^3$ and $1,000 \text{ kg/m}^3$ are used.

Ships

- Vessel class *V1b* is the governing passing vessel in the lock.
- Inside the lock chamber, ships are not allowed to lay berth within a 5 m range of the location of the sill.
- Only one ship may sail at a time. For sailing in, a maximum velocity is conservatively assumed of two times the ships' limit speed.
- The governing situation occurs when a ship sails in the middle of the lock; the sill is only supported at its sides.
- It's assumed that only the main thrusters are active when ships sail over the sill. The highest forces occur when a ship sails with full power, not when it is manoeuvring in the lock chamber. Bow thrusters are not taken into account.
- Total power of the governing ship is $4,000 \text{ kW}$. (Rijkswaterstaat, 2011, p. 20) It's assumed that this maximum amount of power is generated by two main thrusters, both having a maximum power of $2,000 \text{ kW}$.
- It's assumed that the ship's propellers are not mounted in a nozzle.
- Ships sail at full power. In reality this isn't allowed by the restrictions of the locks management, but since it occurs now and then, the sill should be able to resist the corresponding forces.
- The main thruster is assumed to have its lowest part at the same level than the bottom of the ship. In reality the thruster is located a little bit higher, but to calculate the extreme forces on the sill, the most conservative position is chosen.

Levels

- The top of the sill is in its highest operational position located at -2.2 m NAP .
- The governing situation occurs when the water level at ES is highest; $+2.5 \text{ m NAP}$.

The sill moves up and down with the movement of the tide at the ES. The tide changes from highest to lowest water level in approximately 6 hours, while a locking cycle takes approximately 70 minutes.

The movement of the sill is a separate process and takes place independent of the locking cycle processes. The sill can be controlled by adapting its height when the water level change at the ES exceeds a certain number, or by altering its height every fixed time step depending on the water level of the ES at that moment.

5.4.2. Loads

Numerous loads affect the structure during its life time. Not all of them are equally important for its structural design. In this design stage, the most important loads are examined. Many extreme events are not taken into account, since they do not affect the structure when the outer lock gates are closed. The calculated loads are used in load combinations in section 5.4.3.

Loads which are taken into account:

- Water flows, induced by a ship
- Ship collision
- Dead weight
- Hydrostatic water pressure
- Wind (*occurs when structure is lifted out of the water*)

Loads which are not taken into account:

- Water flows, induced by tide
Regular water levels are examined. When more extreme water levels are present (storm surge, wind set-up, etc.) the outer gates are closed and the sill is not affected by the different water levels.
- Water flows, induced by currents
(For instance: gates open before levelling has completed, seeping through narrow openings along sides of the sill, etc.)
These loads are assumed to be of marginal importance in respect to other loads. For a dynamic analysis they may be important, though.
- Water waves
The structure is never under attack by waves at the water surface, since the top level is in operation maximum levelled at -2.2 m NAP . Only when lifted out of the water, the sill is affected by waves for a short period.
- Drag force when sill is in operation
Appendix K shows that this force ($\pm 0.1\text{ kN}$) is marginal compared to other loads, which is why it's not inserted in the analysis of this report.
- Accidental operational loads
An anchor could accidentally get stuck behind the sill or something heavy could fall off a ship. This has been left out of the analysis in this report.
- Ice
The structure is accepted to be located under water at all times during regular operation. Ice loads are exerted at the top layer of the water column mainly. The connection of the sill to the driving mechanism could be affected, but because of the combination of salt water and the water being in movement nearly all the time, no ice loads are taken into account in this design stage.
(Possible ice loads: Thermal expansion/Ice accumulation/Collision of ice floes/Ice attachment)
- Earthquake
In the Netherlands it's not likely for an earthquake to occur. In a later design stage, attention could be paid to the phenomenon, but for now earthquakes are not inserted in the load combinations.

Water flows by ship

When a ship sails through a narrow canal, strong flows arise around the ship, inducing forces on the surrounding area. To gain insight in which forces are caused by a moving ship nearby a sill, an overview is provided of water movements caused by a sailing ship.

The most important water movements, induced by a sailing ship are (see Figure 43):

- | | |
|--------------------------|--|
| ▪ Front wave | ▪ Return flow |
| ▪ Water level depression | ▪ Secondary waves (also: interference waves) |
| ▪ Transversal stern wave | ▪ Propeller jet (also: propeller wash) |

These water velocities or water displacements cause forces to act on their surroundings. The most important ones are the ship's return current and the propeller jet. The return current is larger than the front wave in narrow fairways. The effects of a return current affect a relatively small area. Furthermore, the front wave can never act on the same location at the same time as the return current. For this reason the return current is governing in respect to the front wave. The force induced by the propeller may act directly above or against the sill and is therefore very powerful. It is directly driven by the main thruster(s) of the ship.

Considering the stability and dimensioning calculations for the movable sill, these two water movements are taken into account. The front-, transversal- and secondary waves have their effects mainly near the water surface and are not assumed governing for that reason.

Appendix H elaborates on the exact calculation of these two water flows. In this section, the results of the calculations are presented in the form of a force acting on the sill.

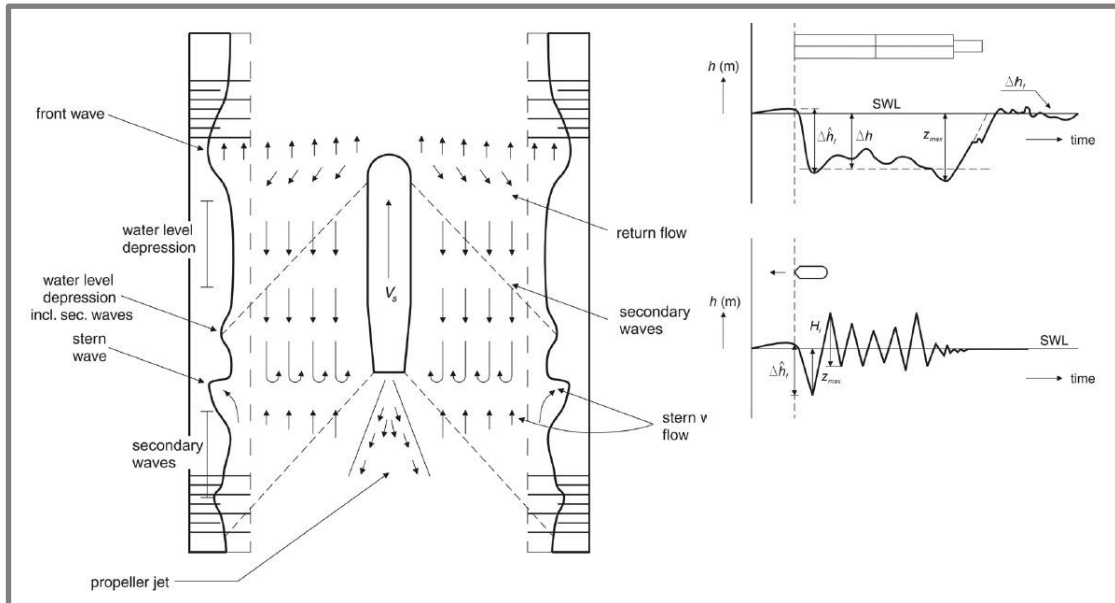


Figure 43: Ship-induced water movements. (CIRIA; CUR; CETMEF, 2007)

Return flow force

The return flow force is calculated and elaborated in appendix H by determining the return current. The governing return current is calculated using the limit speed of the governing vessel while sailing over the sill. This leads to a uniform spread load on the sill, possible in both directions with a rounded value of $q = 35 \text{ kN/m}$.

Propeller jet force

The forces on the sill by the propellers are calculated and described in detail in appendix H. Figure 74 shows the parameters used in this calculation. Since it's assumed that ships are not allowed within a 5 m distance of the sill, the governing situation is calculated as when all power from the thrusters is exerted to the sill orthogonally at a distance of 5 m .

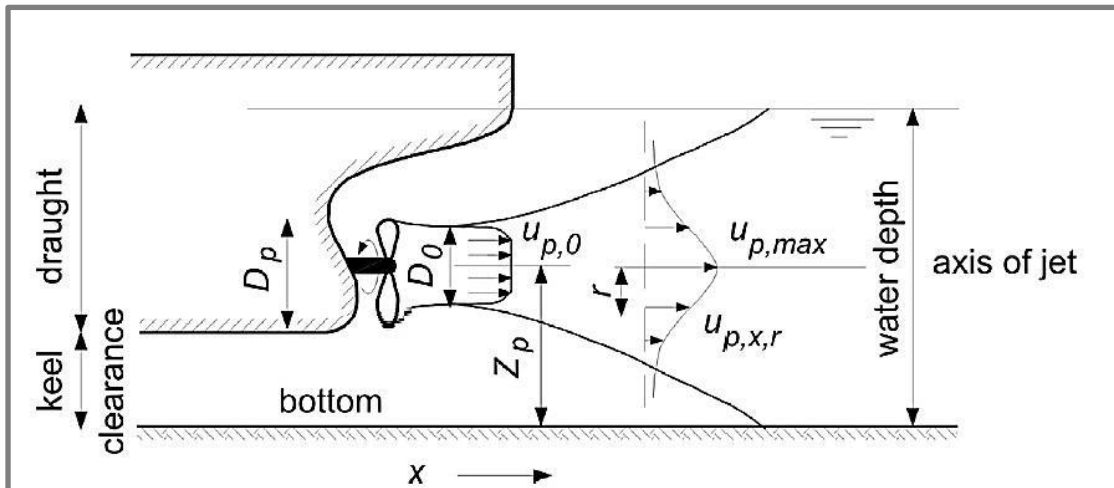


Figure 44: Specification of flow velocities by propeller jet. Adapted from (CIRIA; CUR; CETMEF, 2007).

The influence area of the force is approximated by a circle with a 4 m diameter. 90% of the largest velocities are present in that area. The calculated force is obtained by assuming conservatively that the entire maximum possible force spreads out within this circle.

The propeller jet as calculated is assumed to be acting like a concentrated force in the middle of the sill with a value of $F_{propeller} = 989.0 \text{ kN}$.

Ship collision

The collision force is a complex phenomenon, depending on many different variables. It's hard to calculate exact. In appendix H a calculation of the ship impact force uses the governing impact velocity and maximum weight of the ship. The result is the following collision force on the structure:

$$F_{collision} \approx 27.4 \text{ MN} = 27,400 \text{ kN}$$

The design of the sill will not take into account a possible ship collision, because it's probably not economically sound to do so. Apart from that, the structure is relatively small and easily lifted out of the water. It's possible to replace the structure by a new one when a collision took place.

Normally, in a situation like this guiding works and breaking structures can be used to protect the structure for collision. Since the structure is located inside a lock chamber and displaces in height, an implementation of guiding works is not realistic.

Dead weight

The entire structure has a dead weight. The weight of the structure is transferred to the driving mechanism above water via vertical piles; their dimensions depend strongly on the weight of the structure.

Appendix K shows that in a first estimate in calculations for the driving mechanisms, a weight of 1,900 kN is used.

The largest forces on the structure occur in horizontal plane. The weight of the structure does not directly affect the dimensions of the plates or the main beams. These are elaborated in section 5.5. At the end of that section, it became clear that the total dry weight of the steel of the main elements of the structure is approximately 531 kN.

Hydrostatic water pressure

A force by water density is only exerted on the sill when a water density difference is present between both sides of the sill. The water level is always the same at both sides, since the sill does not retain a certain water level.

The maximum force by a water density difference is theoretically present when water at the ES side of the sill is completely salt and water at the VZM side of the sill is completely fresh. In reality, such harsh separation of both water densities will not be present over the sill. Eq. 5.1 and Eq. 5.2 calculate the theoretical maximum force on the sill by use of Figure 45. This force can only occur directed from the ES to the VZM.

$$\begin{cases} p_1 = (\rho_{\text{salt}} - \rho_{\text{fresh}}) \cdot g \cdot d_{\text{top sill}} = 1383.21 \text{ N/m}^2 \\ p_2 = (\rho_{\text{salt}} - \rho_{\text{fresh}}) \cdot g \cdot d_{\text{bottom sill}} = 2575.125 \text{ N/m}^2 \end{cases}$$

Eq. 5.1

With:

ρ_{salt}	$1,030 \text{ kg/m}^3$
ρ_{fresh}	$1,000 \text{ kg/m}^3$
$d_{\text{top sill}}$	4.7 m
$d_{\text{bottom sill}}$	8.75 m

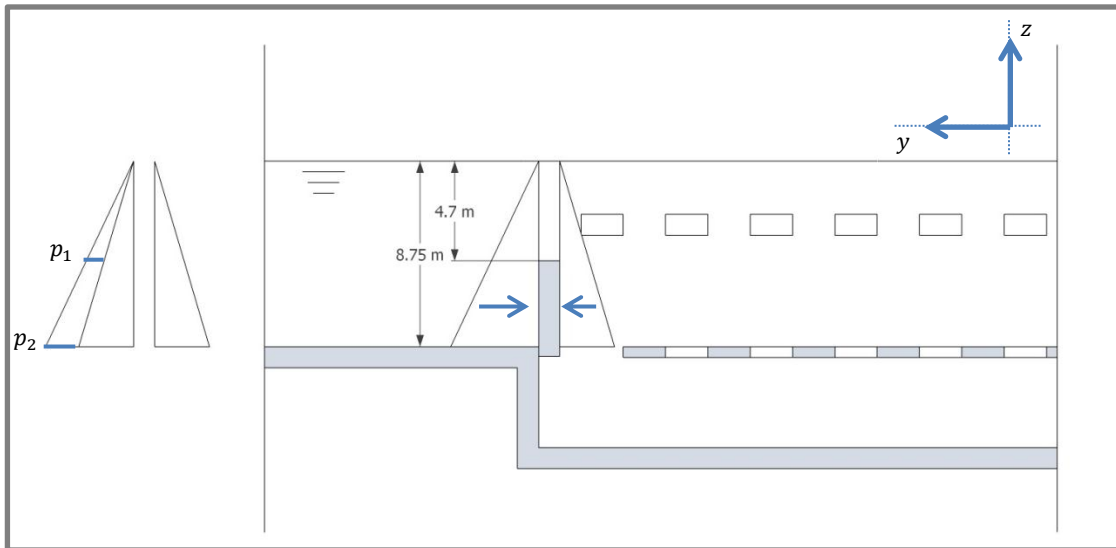


Figure 45: Theoretical maximum water density difference over sill.

$$F_{\text{density max}} = \frac{p_1 + p_2}{2} \cdot h_{\text{sill}} \cdot w_{\text{sill}} = 192,375.081 \text{ N} \approx 195 \text{ kN}$$

Eq. 5.2

With:

h_{sill}	4.05 m
w_{sill}	24 m

The minimum force occurs when no water density difference is present. Eq. 5.3 shows that the force exerted on the sill is 0. This minimum force can occur in both directions.

$$F_{\text{density min}} = 0 \text{ kN}$$

Eq. 5.3

Wind

Wind acts only as a load on the structure when the structure is located out of the water. This occurs only during construction when the lock chamber is set dry, or when the structure is lifted out of the water for maintenance operations.

A way to calculate wind loads is described in (Molenaar, Van Baars, & Kuijper, Manual hydraulic structures, 2008). When $h < 50 \text{ m}$ and $h/b < 5$ the wind load may be calculated by use of the simplified formula Eq. 5.4. The exerted force on the sill is calculated with Eq. 5.5.

The location of the Krammer locks specifies values for the following parameters:

$$u_* = 2.30, \quad z_0 = 0.2, \quad d = 0.0, \quad k = 1.0$$

$z = 5 \text{ m}$ Height above the surrounding plane. In this case the movable sill is assumed to be located highest when lifted out of the water. In that case the highest point is located approximately 5 metres above the top level of the lock.

$$p_{rep} = C_{dim} \cdot C_{index} \cdot p_w = 0.632 \text{ kN/m}^2$$

Eq. 5.4

With:

$$p_w = (1 + 7 \cdot l(z)) \cdot \frac{1}{2} \cdot \rho_{air} \cdot v_w^2(z)$$

$$l(z) = \frac{k}{\ln\left(\frac{z-d}{z_0}\right)}$$

$$v_w(z) = 2.5 \cdot u_* \cdot \ln\left(\frac{z-d}{z_0}\right)$$

$$p_w = 679.706 \text{ N/m}^2$$

$$l(z) = 0.31067$$

$$v_w(z) = 18.5085$$

$$z = 5 \text{ m}$$

$$\rho_{air} = 1.25 \text{ kg/m}^3$$

$$C_{dim} = 0.93$$

$$C_{index} = 1$$

$$F_{wind} = p_{rep} \cdot h_{sill} \cdot w_{sill} \approx 61.5 \text{ kN}$$

Eq. 5.5

With:

$$h_{sill} = 4.05 \text{ m}$$

$$w_{sill} = 24 \text{ m}$$

5.4.3. Load combinations

To regard the governing load combinations, all possible combinations are analysed. Appendix I shows the complete elaboration, which leads to 4 governing load combinations.

All possible load combinations are formed by combining 3 life cycle stages, 3 limit states, 2 sailing directions of ships and 4 extreme water levels. In this way, a complete analysis leads to 72 possible load combinations.

The 4 governing load combinations of Table 17 are obtained after removing 68 load combinations for the following reasons:

- During a life cycle stage, a certain water level never occurs;
- During a life cycle stage, no shipping occurs;
- A limit state is not regarded in this study;
- Another load combination has exactly the same resulting loads;
- Another load combination has a larger load in the same direction.

Table 17: Governing load combinations.

Load combination	Permanent load(s)	Safety factor	Variable load	Safety factor	Total loads
C1	q_{weight}	1.2			531 kN ↓
			F_{wind}	1.5	92.25 kN →
M1	q_{weight}	1.2			531 kN ↓
	$F_{density\ max}$	1.2			234 kN →
O3	q_{weight}	1.2			531 kN ↓
	$F_{density\ max}$	1.2			234 kN →
			q_{return}	1.5	52.5 kN/m →
O9	q_{weight}	1.2			531 kN ↓
			$F_{propeller}$	1.5	1,485.5 kN ←

5.5. Structural design of the sill

Several elements are regarded in terms of strength and stiffness. Effects like fatigue, wear and tear are not taken into account in this design stage. The relative short lifetime of the structure (in the order of 5 to 10 years) doesn't require an extensive analysis of those phenomena in a first design.

For the dimensioning of the sill, a design made out of S235 construction steel is assumed. In this way a first estimation on the dimensions of the sill and the corresponding costs can be made. It's recommended to evaluate a design in other material than steel, since highly corrosive conditions doesn't make steel the most favoured material to use in this case.

At the end of this study, it became clear that the costs of the required steel and its construction are not significant compared to the total costs. That's another reason to support the presented rough calculations to give a first insight in dimensions and costs.

The considered elements in the structural dimensioning are:

Plates form bodywork around the structure. The load on these plates results in a certain plate thickness. The plates are supported by **studs** in vertical direction. The **main beams** distribute the load from the studs horizontally to both sides of the 24 m wide structure. The **force distribution to the lock chamber** occurs in different ways, depending on the vertical location of the movable sill. The vertical **piles** which connect the structure to the driving mechanism, is elaborated previously in section 5.3.

5.5.1. Materials

Different materials can be used in the construction of the design. In most cases the easiest and cheapest option is chosen, which means a design made of steel. Almost all parts are positioned in salt water, which makes it interesting and worthwhile to take a look at the possibility of using other materials than steel.

The structure must be able to resist water pressures from the outside, and is filled with water or air in compression. The entire structure must be protected against extreme corrosive conditions. There are parts which are able to be lifted out of the water relatively easy, but there are also parts which are fixed under water.

The use of steel and synthetics (plastics) are compared by summing up their advantages, meaning that every named advantage is disadvantageous for the other material.

Advantages steel:

- Easy engineering
- Less expensive in terms of purchase and replacement
- Many references/Detailed knowledge on its behaviour

Advantages synthetics:

- Light-weighted
- Corrosive-resistant
- Less impact on potential colliding object (ship)

It can be concluded that the use of synthetics is a good option and has important advantages compared to the use of steel. A dimensioning in synthetics is not inserted in this study, since it requires a more complex design and is not within the scope of this study.

5.5.2. Plates

Plates are installed at all sides of the movable sill. They have a thickness of 20 mm and are connected water- and airtight. The weight of the plates is 426 kN.

These dimensions are able to cope with the largest load on the plates possible. This is the case when the reservoirs of the structure are empty, while the structure is located at its lowest level. This situation with a water pressure on empty reservoirs could be necessary for maintenance actions, but most probably the structure will in that case be lifted out of the water. After a further analysis, a smaller load can probably be used for the dimensioning.

Corrosion in extreme salt conditions is taken into account by a material loss of 0.55 mm/side every 5 year. (Table 4-2 of NEN-EN 1993-5) The inside of the reservoirs is ideally filled with fresh water only. In reality, brackish water will flow into the reservoirs as well, which is why extreme salt conditions are assumed for both sides of the plates. This adds 1.1 mm to the plate thickness for every 5 years of design life time.

To be on the safe side, the design accounts for 10 years of design life time. Other preventions against corrosion are also possible, but are very expensive (E.g. coating of the steel, or thermal galvanizing).

5.5.3. Studs

25 studs of 4.5 m long are present along both sides of the structure. Their total weight is 29.1 kN .

Since corrosion must be counteracted as much as possible, areas of steel in connection with water must be reduced maximum. For that reason, a tube is best as stud. When a U-profile is welded to the plates of the reservoirs, less steel is exposed to corrosive conditions than when an H-profile is used for instance. A *UPE – 120* profile is chosen to meet the requirements.

5.5.4. Main beams

The main beams will be formed by *HEA – 800* profiles. 6 beams of 24 m long result in a total weight by the main beams of 316 kN .

The main beams are calculated after assuming a centre to centre distance of 0.9 m . In this way, the total load is distributed over 6 main beams since the structure is 4.5 m high.

It's assumed that these beams with a length of 24 metres exist. Further it's assumed that the beams are integrated in the reservoirs and do not alter the outer dimensions of the sill.

5.5.5. Force distribution to lock chamber

Since the structure can be positioned at different height levels, different situations are regarded to detail the force distribution of the structure to its surrounding. When the sill is in operation, it exerts forces on another part of the lock than when it has been lifted out of the water. The largest loads are exerted on the structure when it is in operation. In that case, it is situated in a guiding rail, visible in Figure 46.

At both sides along the lock chamber walls, the same steel structure is applied. The structure consists of a steel profile, supported by diagonal round bars every half metre. The rail is present at the locations where the sill is able to move when its operational, meaning that it reaches 8.8 m high measured from the lock chamber bottom. The connection to the lock wall is not elaborated in this phase, since only rough calculations are made to proof the possibility of a certain structure.

The rail is present from -11 m NAP to -2.2 m NAP and is therefore 8.8 m high. The sill is able to induce forces in both directions, so the supports of the rail must be able to cope with tensile and compressive stresses. A *CHS – 114.3/5* profile is chosen and checked to be resistant to buckling.

The plate to which the supports are welded has to be 1.5 m wide. Assumed is that a plate thickness of 5 cm is sufficient. The plate is connected to the concrete by bolts or small anchors. This connection is not detailed in this report.

The two steel structures have a total weight of 113 kN .

The sill-structure is equipped with a steel cantilever which slides through the rail. This induces friction between both parts, which affects the required power for the driving mechanism. The friction in the rail increases, when the structure tilts along its length axis (x -axis in Figure 46). Appendix J.5 shows that a maximum additional force of 50 kN is required for the driving mechanism at each side of the structure to set it in motion.

It is possible to reduce this friction by implementing wheels in the rail for instance, but this doesn't seem necessary after a first estimation with rough calculations.

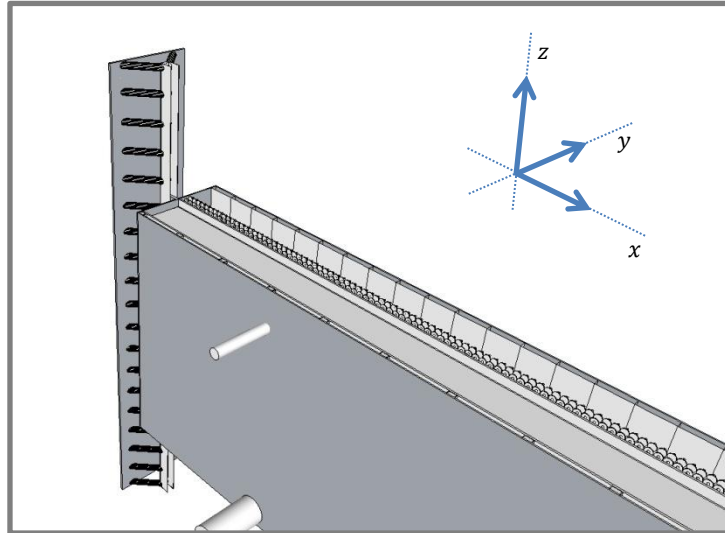


Figure 46: Overview of sliding movable sill in rail connected to lock wall.

Other configurations are possible as well. Especially a concrete alternative seems logical due to the occurrence of corrosion. Many connections and welds to the steel rail make the design relative expensive. Maintenance is hard since the steel is fixed to the lock wall and cannot be removed easily.

Chapter

6. Verification

The verification shows to which extent the problem is being solved by the solution of this report: a configuration with a movable sill and air bubble- and water screens. It quantifies the most important features of the design, and compares them with the current situation and a design without a movable sill. Before the verification starts, it is described which systems are used in the comparison. The features which are elaborated are described below.



- 6.1 Description of system
- 6.2 Effectiveness
- 6.3 Energy consumption
- 6.4 Costs
- 6.5 Capacity of lock chamber
- 6.6 Future perspective

6.1. Description of system

Before the design can be tested and compared with other options, a more thorough description will be given of its functionality. After that, a detailed description is presented of the configurations which are compared in this verification.

6.1.1. Water levelling

A sill reduces salt intrusion while the gates of the lock are opened. When the gates are closed, the degree of salt intrusion is influenced significantly by the way in which water is levelled.

In the *Duinkerken system*, levelling takes place via an extensive culvert system as described in section 2.2. Pumps control the water levelling during a locking cycle. The pilot in the recreational lock uses a pump to discharge salt water from the lock chamber to the ES at high water. In the new situation in the commercial locks, several options are possible. Most important in this selection is to prevent the salt water wedge to discharge on the fresh VZM when high water is present at ES.

It's chosen to use a comparable design as in the recreational lock. Appendix L shows the locking processes in a locking cycle at high and low water.

6.1.2. Comparison of configurations

Table 18 gives an overview of the compared configurations. The entire verification is based on a comparison of alternatives for the *commercial lock* only – not the entire lock complex.

The current system is called the zero-alternative, or *configuration 0*. The other three configurations are based on water levelling as described in appendix J. They differ in their salt intrusion prevention configuration only.

Table 18: Systems compared for the verification.

Config- uration*	Salt intrusion prevention	Description	Water levelling
0	<i>Duinkerken system</i>	Current situation	<i>Duinkerken system</i>
1.0	No system	No salt intrusion prevention	Pump at ES side; lock paddles at VZM side
1.1	Air bubble- and water screen	Design of pilot, installed in commercial lock	Pump at ES side; lock paddles at VZM side
1.2	Air bubble- and water screen in combination with sill	Design from this report	Pump at ES side; lock paddles at VZM side

**These configurations are not to be confused with the configurations used in section 2.4.*

6.2. Effectiveness

The effects of the design are twofold. Salt intrusion and fresh water loss are reduced by mixing of water and stagnating exchange flows. Both salt intrusion and fresh water loss are quantified separately in this section after required basic information is provided.

Salt intrusion and fresh water loss are dynamic processes which depend on many variables. It's hard to quantify them in exact numbers, but at the same time these numbers are very important. Without realistic numbers it's hard to know what to expect of certain countermeasures. Therefore, in this section it is first explained which numbers are already known. Then it's described in which way the values are calculated. To validate the calculations, known values are compared to the calculated values. Finally, the results of the calculation for the design are presented.

6.2.1. Basic information

Table 19 shows the basic information which is used in the calculations of salt intrusion reduction and fresh water loss for the different configurations. Appendix M elaborates on the origin of this presented information; the water levels are elaborated in appendix C.

Table 19: Basic information for the calculations.

Information		Used value
Maximum exchanging water volume		90% of lock volume
Maximum salt leakage through 1 commercial lock		196 kg/s
Averaged high water (HW) level		+1.1 m NAP
Averaged low water (LW) level		-0.9 m NAP
Degree of influence in respect to entire lock complex	1 recreational lock	3.5%
	1 commercial lock	46.5%
Water exchange through: (expressed as percentage of possible exchange without measure)	Air bubble screen	30%
	Air bubble screen	15%
	& Water screen	
	Sill	0%
Water density difference (ES-VZM)		29 kg/m ³

6.2.2. Salt intrusion reduction

The calculations in this section are based on salt intrusion from ES to VZM only. In reality salt leaves the VZM as well, but this 'extrusion' of salt is not included in the calculations. Results of the applied calculation method are compared with field measurements to judge if the final results are acceptable.

The applied calculation method for salt leakage can best be described as a static calculation model, ref. Figure 47. The exchanging water volume is calculated at both sides of the lock chamber. When the salinity difference between both sides of the lock is known, the increase of salt at VZM can be found per locking cycle. By dividing this value by the time of a locking cycle, salt leakage in terms of kg/s is obtained.

First the exchanging water volume between the ES and the lock chamber "Exchange volume I" is calculated. A reduction factor for the air bubble- and water screen at that location (Table 19) is multiplied by 90% of the lock chamber volume. This volume depends on the water level at ES. The water exchange between lock chamber and VZM "Exchange volume II" uses the first exchanged water volume. A reduction factor is added for the bubble screen at that side.

An extra reduction of the volume is added if the water height at VZM is smaller than at ES (HW). Appendix L shows that after an exchange at ES side, water is pumped back to the ES to get the level inside the lock chamber equal with VZM level. The fixed water height at that side (6.25 m) determines the exchange volume, not the mean high water level at ES (7.35 m). The extra height does not affect the salt intrusion towards the VZM, which is why in that case a reduction factor of 6.25/7.35 is added.

If the water level at VZM is higher than ES (LW), water from the VZM is added to the lock via lock paddles. This water has the same salinity as the VZM, so the salinity-increase of VZM only depends on the depth at ES.

The same holds when a sill is applied, except for the reduction factor. Namely, at HW only the top 4.7 m above the sill is subject to "Exchange volume I". After pumping water back the ES to level with the VZM level, the same volume of salt water is subject to "Exchange volume II". This makes the reduction factor obsolete in this case.

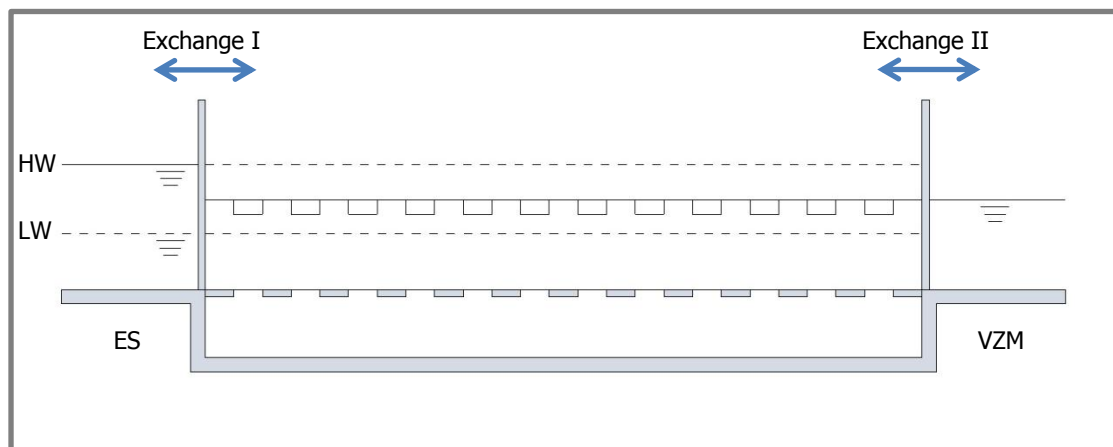


Figure 47: Overview of parameters used for calculating salt leakage in Krammer commercial lock.

The values for salt intrusion reduction in Table 20 are equal to 100% minus the salt intrusion of that configuration. Salt intrusion is obtained by dividing the passing amount of salt by the maximum possible passing amount of salt with no system present in the lock (hence 100% salt intrusion for configuration 1.0). These passing amounts of salt in *kg/s* are calculated in appendix M by the average amount of salt passing the lock chamber in one locking cycle, divided by the time of a locking cycle.

Table 20: Effectiveness of different configurations in Krammer commercial lock.

Configuration	Salt intrusion reduction	Salt intrusion
0 <i>Duinkerken system</i>	96.2%	3.8%
1.0 No system	0%	100%
1.1 Air bubble- & water screen	93.9%	6.1%
1.2 Air bubble- & water screen & sill	95.2%	4.8%

6.2.3. Fresh water loss

Fresh water loss is described in more detail, because the available fresh water has its limits. The same basic information as for effectiveness in section 6.2.2 applies for the presented method of calculating fresh water loss.

The calculated value for the fresh water loss is obtained by a comparable method as used for the effectiveness in section 6.2. The exchanging volumes are determined when the gates are open. This calculation is set-up in the opposite direction as the salt leakage calculation. Referring to Figure 47, first

"Exchange volume II" from VZM to lock chamber is calculated, then "Exchange volume I" from lock chamber to ES.

Finally, fresh water loss due to water levelling is added. This takes place at LW when fresh water flows under free decay to the ES.

In Table 21 the fresh water loss is shown for one commercial lock, as well as for the entire lock complex. Its calculation is elaborated in appendix M. The average loss of fresh water per locking cycle is divided by the duration of a locking cycle to obtain the presented values.

Table 21: Yearly averaged fresh water loss of Krammer locks.

Configuration	Fresh water loss [m^3/s]	
	1 commercial lock	Lock complex
0 <i>Duinkerken system</i>	4.8	10.3
1.0 No system	9.1	19.6
1.1 Air bubble- & water screen	1.10	2.37
1.2 Air bubble- & water screen & sill	1.02	2.19

The VZM doesn't have an infinite amount of fresh water available. Water agreements³¹ prescribe how much water is available for drinking water- and irrigation intakes, but also for water losses through a lock complex. At the Krammer lock the available fresh water is $20 m^3/s$ during dry season and $40 m^3/s$ during wet season. The water screen in *configuration 1.1* requires approximately $14 m^3/s$ for the entire lock complex. In combination with the total loss of $2.37 m^3/s$, the solution remains within the restricted boundary of $20 m^3/s$.

By use of a movable sill, it's possible to alter the operation of the lock. More fresh water can be preserved by increasing the sill's height and restricting the allowed draught of ships in the lock. In this way it remains possible to use the lock in extreme dry seasons, without exceeding restrictions of fresh water loss or salt intrusion.

6.2.4. Improvements

A few operational actions are possible to increase the effects of the design.

- When enough fresh water is available at the VZM, fresh water is allowed in the salt lock chamber via lock paddles in the VZM gate. This is possible when at HW levelling to VZM takes place. A surplus of water – not needed for levelling – is pumped back to the ES. The level in the lock chamber is increased by fresh water from VZM.
- Operationally it should be possible to let the sill adapt in front of and behind a ship, depending on the ship's draught. With a higher sill, salt reduction decreases further.
- A movable sill increases its effectiveness even more when either the mean water level rises, or ships with less draught pass the lock. If the draught of every ship is known detailed enough, the sill can be adapted to that.

The outcomes are in line with expectations and in the right order of magnitude compared to already known numbers. Even though, some important effects are not inserted in the calculation of the presented values.

- A lock chamber filled with ships reduces the exchanging volume of water, and thus affects the salt intrusion and fresh water loss.
- In direction from VZM to ES salt water leaves the VZM.

³¹ In Dutch: *Waterakkoorden*.

6.3. Energy consumption

The energy consumption of the design is presented in this section. All values of energy consumption are presented in *kWh* per locking cycle. Appendix N describes thoroughly how the presented values are obtained; only the results and brief descriptions are presented in this section.

6.3.1. Water levelling

In order to make a comparison with the current system which contains water levelling, water levelling must also be taken into account for the new configurations. Energy consumption by levelling of water is determined by the available pumps in the Krammer recreational lock. The ratio between consumed power and displaced water is used to estimate the consumed power for water levelling at the commercial lock. This means for the recreational and commercial lock for water levelling an energy consumption of respectively 7.09 and 58.8 *kWh/cycle*.

6.3.2. Movement of sill

The movable sill only moves up and down once in approximately 12 hours. During a tidal cycle the sill tends to follow the water level at the ES. The energy consumed by this movement depends on its driving mechanism.

Section 5.5 shows an energy consumption of roughly 15.3 *kWh* per day. With 28.5 locking cycles on an average day, this corresponds with 0.54 *kWh/locking cycle*.

6.3.3. Air bubble- and water screen

The energy consumption by the air bubble- and water screens is calculated by their configurations. The installed, required and used capacity of the water pumps and air compressors are used in combination with the time they are operational during a locking cycle.

To determine the amount of power required for the different configurations, reference is made to available figures in reports and earlier designs of comparable systems. The relationship is determined between the lock configuration and the required air flow. Knowing this number, estimations can be made of the required air flow in locks with other dimensions.

The required discharges depend on the maximum height in the configurations and the pressures. Both are at the configurations with sill significantly lower than at configurations without sill.

Table 22 shows the required power in the Krammer commercial lock with and without movable sill. The consumed power in the last column is calculated based on the fact that the screen is active 28 minutes during a locking cycle. (See Table 13 on page 19.)

Table 22: Consumed power for the air bubble screen in the Krammer commercial lock per locking cycle.

	Required air flow [Nm ³ /s]	Compressor capacity [kW/(Nm ³ /s)]	Required power [kW]	Consumed power [kWh/cycle]
Krammer commercial	2.02	250	506	236
Krammer commercial with sill	0.60	250	148	69.1

The power needed for an effective water screen in different configurations of locks is determined in a comparable way as with the air bubble screens. The required discharge is calculated after a dependency is made clear between lock configuration and discharges of known designs. Finally, the calculated discharge is translated to a power demand.

For the commercial lock without and with sill required discharges of respectively 5.3 and 2.8 m³/s are calculated. Table 23 shows the consumed power per locking cycle. In this calculation it's used that the screens are active for a period of 28 minutes per cycle.

Table 23: Consumed power for the water screen in the Krammer commercial lock per locking cycle.

	Max. required discharge [m ³ /s]	Pump capacity [kW/(m ³ /s)]	Required power [kW]	Consumed power [kWh/cycle]
Krammer commercial	5.3	78	351	164
Krammer commercial with sill	2.8	78	218	102

6.4. Costs

The costs of the entire structure can be presented in many ways. The most important costs for a comparison are categorised and will be treated separately for:

- Construction costs
- Operational costs
- Maintenance costs

6.4.1. Construction costs

The construction costs for the design of this report are compared to the cost of the same design without movable sill. The cost of the current situation is not available for comparison, since no such data is available of the 25 year old lock complex. Construction of the current salt intrusion prevention was carried out at the same time as the construction of the entire lock complex itself. The required adaptations to the current lock are also not included. They are less important for this comparison; above all, they are the same for both compared options.

To get insight in the construction costs, existing cost estimates are adapted. Cost estimations made for the construction of the pilot for the Krammer recreational lock are used for making a realistic cost estimation for the system in the Krammer commercial locks. The obtained value is compared with earlier expected costs of a design in the commercial lock. In that way the estimation method is supported. The same method is used to get insight in costs for a design including a movable sill in the commercial lock.

Only the highest costs of the cost estimation for the pilot are inserted in this analysis. Additional costs which are taken into account are determined by comparing the design with and without sill in the Krammer commercial lock. Elements which are expected to be significantly more expensive at one of the designs are evaluated as well. All presented costs are multiplied by 1.5 to include design costs (10%), tax (21%), profit (10%), risk (5%) and overhead (5%). The used values are rounded to five thousands and the totals to hundreds thousands.

The first four elements in Table 24 have to do with the air bubble- and water screen. Their price is assumed to be linear dependant on width and height of the screens, which results in an increase by 374% ($\left(\frac{8.7}{6.2}\right) \cdot \left(\frac{24}{9}\right) = 3.74$).

The existing technical controlling system is both extensive and expensive. It doesn't necessarily become more expensive when a larger pump or longer pipes are inserted in the controlling system.

A cost estimate of 6 M€ is found for a design in the commercial lock in a comparable but more extensive analysis; Table 24 shows a cost estimate of 6.0 M€, which confirms that the most important elements are present in this evaluation.

Table 24: Construction costs of the screens for a design in the Krammer commercial lock.

Feature	Price [10 ³ €]	Pilot Krammer recreational lock		Krammer commercial lock	
		[%]	Costs [10 ³ €]	[%]	Costs [10 ³ €]
Compressors	270	100	270	374	1,010
Water pumps	120	100	120	374	450
Pumping pit	30	100	30	374	115
Pipes and valves	795	100	795	374	2,975
Technical control	900	100	900	100	900
Phase power	150	100	150	374	560
		Total	2,300	Total	6,000

The determined construction costs are in Table 25 transposed to costs of a system in the same lock, but with movable sill installed. Costs for the compressors, water pumps, water pits, pipes and valves reduce, since the screens are smaller. A decrease of 45% is assumed ($\frac{8.75-4.7}{8.75} \approx 46\%$).

The technical controlling system becomes more complex and more expensive when the control of a movable sill is included, for instance sensors measuring water heights are connected to the driving mechanism of the sill.

Phase power cables are reduced since the total amount of required power drops approximately a third. Conservatively, a 25% decrease of required phase power installations is taken into account.

The last two elements are new in Table 25. The costs for the required steel are obtained by using a unit price per kilogram of €5.5 (€1.5 material and €4 labour and connections). The construction costs are calculated by using the weight of $54.1 \cdot 10^3 \text{ kg}$ from section 5.3.4 and the in this section explained factor 1.5. It's assumed that the movable sill requires twice the amount of steel compared with a fixed water reservoir. The sill needs a driving mechanism at both sides of the lock chamber.

The table shows that the largest cost reduction follows from the smaller screens. Beforehand it may have looked more logical to assume a higher price for this design, but since not much extra material is needed for the sill in respect to a fixed screen, the smaller screens are decisive in the price estimation.

Table 25: Construction costs of the screens for a design in the Krammer commercial lock with sill.

Feature	Price [10 ³ €]	Krammer commercial lock		Krammer commercial lock with movable sill	
		[%]	Costs [10 ³ €]	[%]	Costs [10 ³ €]
Compressors	1,010	100	1,010	55	555
Water pumps	450	100	450	55	245
Pumping pit	115	100	115	55	60
Pipes and valves	2,975	100	2,975	55	1,635
Technical control	900	100	900	120	1,080
Phase power	560	100	560	75	420
Steel	445	50	225	100	445
2 driving mechanisms	50	—	0	100	50
		Total	6,200	Total	4,500

Rent of machinery for construction can be inserted at an estimating percentage of 15% of the total construction costs (de Gijt & van der Toorn, 2012). In this case, it's chosen not to. When an actual realisation of the design takes place, adaptations to the current lock must be performed. This is not inserted in this analysis, but does affect the total picture regarding construction costs. Most important is to get insight in the order of magnitude of potential differences between the two designs.

6.4.2. Operational and maintenance costs

The operational costs are calculated by translating the energy consumption of the system from section 6.3 to energy consumption and costs per year. To do so, a few things are explained.

A ship sailing from one side to the other is called 1 locking.

A locking cycle is formed by 2 lockings.

During 365.25 days, on average 57.0 lockings take place in the Kramer commercial locks.

During a locking cycle, all screens are active for 28 minutes.

Water levelling occurs only at high water, which is assumed to be present half of the time with a fixed water level increase of 1 m.

It must be noted that calculated values of the required power are used for the pumps, where in reality the actual installed power of pumps determines the energy consumption. This depends on availability of pumps on the market.

Maintenance costs of the system are of significant importance and should definitely be taken into account when comparing different configurations of a salt intrusion prevention. It's hard to determine them beforehand, which is why a prediction is made.

Actual maintenance costs of different elements of the current *Duinkerken system* are obtained from unpublished internal reports from *RHDHV*. They are used to get a first insight in the expected difference in maintenance costs of the considered systems. The total yearly maintenance costs of the Krammer locks are 3.6 M€, but not all components should be inserted in the comparison with the maintenance costs of the other configurations.

Contributing to salt intrusion prevention in Krammer commercial lock: €500,000

Roughly 80% of the total maintenance costs relate to the commercial locks. If €1,880,000 corresponds with maintenance of elements like concrete of the lock, lock gates, gates driving mechanism, primary water defence, the remaining €1,000,000 corresponds with maintenance of the salt intrusion prevention system in both commercial locks. The maintenance costs for one commercial lock are therefore €500,000.

Contributing to water levelling: €54,000

15% of the pumps of the commercial locks. (58.8/426 kWh)

33% of the sewer system and corresponding valves. (Slaak remain operational, high and low basin become dysfunctional)

$$\rightarrow 0.15 \cdot 25,000 + 0.33 \cdot 150,000 = €54,000.$$

Cost estimations use percentages of the total construction costs to determine maintenance costs:

Civil	1%	Concrete, steel, etc.
Mechanical	7%	Pumps, compressors, motors (driving), pipes, valves
Electromechanical	7%	PLC's, Cables, technical controlling system

Since the steel in the design is situated in highly corrosive conditions, 7% is taken into account for maintenance costs instead of just 1%. That means that the maintenance costs are formed by 7% of the total construction costs: $7\% \cdot €6,200,000 = €434,000$, $7\% \cdot €4,500,000 = €315,000$

Table 26 combines the operational and maintenance costs for the compared configurations. It also shows that more than half of the energy consumption can be saved when a movable sill is combined with an air bubble screen in the Krammer commercial lock.

Table 26: Energy consumption and costs per year for different systems.

Configuration		Energy consumption [10 ⁶ kWh/year]	Operational costs [10 ³ €/year]	Maintenance costs [10 ³ €/year]
0	<i>Duinkerken system</i>	4.4	666	500
1.0	No system	0.3	46	54
1.1	Air bubble- & water screen	4.5	670	490
1.2	Air bubble- & water screen & sill	2.1	313	370

An energy price of €0.15/kWh is used in this calculation. This price is variable. Public consumers (i.e. households) in the Netherlands pay approximately €0.22/kWh. The rate for public works is often much lower. Prices of €0.08/kWh are known.

A variation in the unit price for energy results in a significant change of operational costs. The consumption in kWh shows a more fixed number to compare the different configurations.

€54,000 of maintenance costs for water levelling is added to the maintenance costs of the two last configurations to present a sound comparison.

6.5. Capacity of lock chamber

The absence of the process of water exchange in the *Duinkerken system* is the responsible cause of capacity increase. The duration of a locking cycle reduces for the commercial lock from 93 to 70 minutes. This means a decrease in locking time of 25.6% and at the same time a capacity increase of 32.9%.

The difference between these presented figures can be explained by the fact that in the new situation, 23 minutes time represents 23/70 locking cycle. So every 93 minutes, not 1 locking cycle, but $1 + 23/70 = 1.329$ locking cycle can be completed.

The need for a third commercial lock is expected to be present approximately 10 to 15 years from now. By a capacity increase of the current locks in the order of 33%, the planned expansion of the locking complex can be postponed a few years without doubt.

This benefit holds for both options, with and without a movable sill.

6.6. Future perspective

The presented design is possible in many other locks as well. It will have the same benefits as in the situation of the Krammer commercial locks. Energy consumption and costs will reduce when a sill is added to a design, instead of using air bubble- and water screens only. Dimensions of the specific location determine its exact efficiency.

The most extra added value occurs when the lock is relatively deep; this means that when the governing ship passes the lock at low water, there is still (large) free space present between the bottom of the ship and the bottom of the lock. A relative large percentage of the water column could in that case be blocked by the sill, which increases the effects of the salt intrusion prevention in a positive way.

Sea level rise will increase the average water level at the salt side of the lock. This makes it possible to position the top level of the sill higher, which increases the effects of the salt intrusion prevention even more.

To get a quick estimate of the increased salt intrusion reduction when a sill is used compared to a situation without sill, Eq. 6.1 can be used. It can be used as a rough general expression for the expected effectiveness increase. The salt side of the lock which is exposed to tide must be regarded. The average tidal water level must be used as water depth for a first estimation.

This is a rough first estimate. A more thorough analysis is required to quantify aspects as fresh water loss, energy consumption and costs. Although – following the results of this study – it may be expected that energy consumption will reduce when the determined effectiveness for a configuration increases according to Eq. 6.1.

The outcome of the equation presents the additional percentage of salt intrusion prevention, compared to a situation where $\eta_{air \& water}$ holds for the entire water depth.

The value of the effectiveness for the sill of 100% may seem unrealistic. But it should be noted that this value holds for a situation where the entire water column is blocked by the sill. In that case no shipping is possible and water of both sides of the lock is not in contact at all.

$$R = \eta_{air \& water} \left(\frac{d}{h} - 1 \right) + \eta_{sill} \left(\frac{h - d}{h} \right)$$

Eq. 6.1

With:	R d h $\eta_{air \& water}$ η_{sill}	<p>Expected increase of salt intrusion reduction by use of a sill [%]</p> <p>Draught of governing ship [m]</p> <p>Average tidal water depth [m]</p> <p>Effectiveness of air bubble and water screen (85%)</p> <p>Effectiveness of sill (100%)</p>
-------	---	---

Conclusion

Current systems which reduce salt intrusion through locks can be improved. They consume much power and are expensive in terms of maintenance and operation. A pilot project in the Krammer recreational locks is used to get insight in new possibilities. In a few years, a decision will be made on what system to apply in the larger Krammer commercial locks. Before this up-scaling of the pilot's design is done, this report shows that an optimisation is advisable.

After an analysis it became clear that a design with a movable sill could result in high improvements of the most important properties of a salt intrusion reduction system.

An innovative design of a salt intrusion prevention is made for the Krammer locks. Parts of the design are based on an existing design for a pilot project, but their features are optimised. Main parts of the design – including the movable sill itself – are newly designed to fulfil the requirements.

Main objective of the design is to score higher than the pilot's design on effectiveness (salt intrusion reduction and fresh water loss), energy consumption and costs. Different conclusions are treated subsequently in this chapter, leading to the following final conclusion:

Final conclusion

A new design has been made for salt intrusion prevention in the Krammer commercial locks. It combines air bubble- and water screens with an innovative movable sill.

It's expected that this design is approximately 20% more effective, consumes 50% less energy and is 30% cheaper than a configuration with air bubble- and water screens only.

The reduction in height of the air bubble- and water screen in the new design is accompanied by the presence of an impermeable sill. This increases the overall efficiency of the configuration, since exchange of salt and fresh water is decreased more effective.

Figure 48 shows a sketch of the design of the movable sill with integrated air bubble- and water screens. A connection to the driving mechanism above the lock is obtained via vertical steel tubes. Engines let the structure move up and down, following the tidal movement of the water on the Eastern Scheldt (ES). This movement is controlled in such a way that when the gates at the ES side open, the required water depth for shipping is exactly maintained and the maximum efficiency is obtained.

The governing loads are determined which lead to a dimensioning of the structure in steel. The integration in the lock is elaborated, since the design must fit in the existing lock chamber.

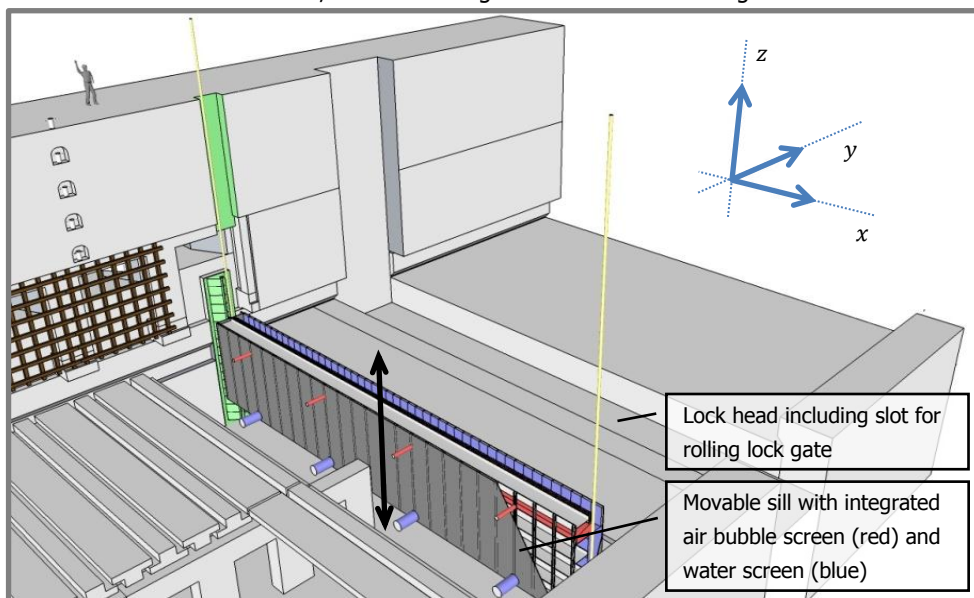


Figure 48: A 3D sketch of the design, placed at the commercial lock head at the ES side. The most important detailed elements in this study are printed in colours.

Table 27 shows a comparison of four configurations in the Krammer commercial lock. In the last row, rounded values are compared of the improvements of a design with to a design without a movable sill.

Table 27: Comparison of most important features for configurations in one commercial lock.

Configuration	Effectiveness		Energy consumption	Costs		Capacity increase
	Salt intrusion [%]	Fresh water loss [m^3/s]	[$10^6 kWh/year$]	Construction [$10^3 €$]	Operational and maintenance [$10^3 €/year$]	[%]
0: <i>Duinkerken system</i>	3.8%	4.8	4.4	–	1,160	0
1.0: No system	100%	9.1	0.3	–	100	+33
1.1: Air bubble- & water screen	6.1%	1.1	4.5	6,200	1,165	+33
1.2: Air bubble- & water screen & sill	4.8%	1.0	2.1	4,500	685	+33
Improvement of 1.2 to 1.1	+21%	+9%	+55%	+27%	+41%	0%

Effectiveness

Salt intrusion is effectively reduced in all configurations when compared to doing nothing. The design with movable sill shows compared to a design without sill an increase of salt intrusion reduction of approximately 21%.

Fresh water loss of both designs is significantly lower than for the current situation; the design with sill has a supplementary decrease of fresh water loss of 9% compared to the design of the pilot.

Energy consumption

Energy consumption of the configurations mainly depends on the height of the screens and the presence of a regulator in the air bubble screens. The design with sill requires for these reasons a much lower discharge, which results in a much lower energy consumption.

Costs

Construction costs are lower for a design with sill, because the most expensive main elements of the screens are smaller in that configuration. Operational costs are dependent on energy consumption, while maintenance costs depend on the construction costs in combination with pumps for water levelling. These show comparable improvements for a design with sill.

Capacity increase

The capacity for all configurations increases by the same number when compared to the current situation. This is the result of a time consuming process in the current situation which becomes obsolete in all other configurations.

The current *Duinkerken system* in the Krammer commercial locks has a low salt intrusion, but is very expensive to preserve. A pilot project in the recreational lock is used to get insight in possibilities for a design in the commercial locks. When the design of the pilot is used as base for the upgrade of the Krammer locks, this report showed that the implementation of a movable sill improves the design considerably on all important features. This is summarised in the lowest line of Table 27 above.

Construction costs, operational costs and maintenance costs decrease in comparison to the design of the pilot. The salt intrusion reduction is comparable with the current design, but fresh water loss decreases significantly. Both features score higher in a design with sill.

The numbers show that the design of this study scores high; these numbers are obtained after calculations based on assumptions. Before the design can be realised, there are quite a few important recommendations which need to be elaborated. The assumptions in the used calculation methods need attention especially.

Nevertheless, the presented design shows that a movable sill is an interesting option, to which further studies are required.

Apart from a realisation in the Krammer locks, the design has a broader potential; the benefits hold for all locks with salt intrusion countermeasures installed. It's especially interesting in deep locks or locks with an increasing average water level. In that case the effectiveness may increase even more.

Recommendations

This report shows that the insertion of a movable sill in the design of a salt intrusion prevention in combination with air bubble- and water screens is an interesting option. It scores high in terms of effectiveness and costs when compared to a design with only air bubble- and water screens. This conclusion is obtained after numerous assumptions, which should be verified or improved.

The following features are recommended to regard before the next step to a potential realisation of the design takes place.

1. A fixed sill at the Volkerak Zoommeer (VZM) side of the lock increases effectiveness of the salt intrusion prevention in the order of 25%. The option of a fixed sill at VZM side should be evaluated before a complex design as presented in this report is realised at the Eastern Scheldt (ES) side. The scope of this report didn't include preventions at the VZM side of the lock.
2. When a movable sill is applied, it should be verified that a water screen is still needed. The water screen is in the pilot primarily used to protect the toe/origin of the air bubble screen; a function which could be fulfilled by the sill as well. Experiments must prove the need for a water screen before it is used in a design.
3. When construction of the pilot in the recreational lock is finished, measurements will result in figures to be used in the validation of the calculations in this report. The methods can be altered to result in more realistic estimates of effectiveness. By use of that information, the design for the structure in the commercial locks can be optimised if needed.

The calculations in the report are created by a static analysis, validated by known figures in other locks. The results of the pilot must prove this method of calculation right or wrong.

4. The effectiveness of the structure increases when the navigational depth above the sill decreases to a value smaller than the 4.7 m of the current design. When detailed information on passing ships is known, the level of the movable sill can be adapted to the passing ship's draught.

Especially in extreme dry periods this is beneficial. A lot less fresh water is available in such periods, in which water is also shared with intakes for drinking water and agricultural purposes.

5. The hydraulic design of the water screen's inner side is not elaborated in this report. It's assumed that an even spread outflow is possible, which is based on references to existing designs. The design of the air bubble screens in this report does not possess regulators. There is no experience with this configuration of air bubble screens, which is why it should be tested first to prove its effectiveness.

Both designs should be tested by physical- or computer modelling.

6. This report presents a design made of steel. The use of synthetics instead of steel has big advantages and should be regarded in a next design phase.
7. In calculations of the required capacities for the air bubble- and water screens, the installed power is scaled up or down by the dimensions of the lock. This results in two sub-recommendations:
 - a. This means that the screens at the VZM side are also scaled, while they are not different for a design with or without a sill. This leads to a slight overestimation of energy reduction for a design with sill.
 - b. The assumed linear dependency between height of the screens and the required discharges for the screens must be elaborated or tested more detailed.

In a comparison with an existing configuration it was proved that the intended scaling is possible as first estimate, but should be detailed to obtain a more realistic insight.

8. Failure of the structure is not yet regarded. A risk assessment could assign which parts of the structure should be improved to reduce the chance of failing.

9. Large accidental loads as a ship's collision are not taken into account in the dimensioning of the design. In such a situation it's more efficient to replace the structure and leave the ship unharmed than the other way around. The structure must be able to resist smaller accidental loads, though. An accidental trailing anchor across the bottom of the lock is not uncommon. The structure must be protected against such loads.
10. Since the structure is positioned on a location where ideally a large water density difference is present, BlueEnergy could be interesting. Large space is needed for this; to generate 30 kW, a structure of approximately 8 m³ big is required. BlueEnergy generation is most efficient when the water density difference is largest, which is exactly what the design of this study tends to achieve.
11. Throughout the report, water densities for fresh and salt water of 1,000 kg/m³ and 1,030 kg/m³ are used, but in reality they are more in the order of 1,005 kg/m³ and 1,025 kg/m³ at the Krammer locks. The exact values must be determined before a further study is based on this report. See also (Deltares, 2010, p. 12).
12. A lock chamber filled with ships reduces the exchanging volume of water, and thus affects the salt intrusion and fresh water loss. It should be quantified what the effects are.
13. A few crucial assumptions have been made. These have to be checked before a realisation of the design is possible.
 - The use of flexible supply pipes for the air bubble- and water screen is assumed to be well possible.
 - The movement of the sill (following the tidal water levels at ES) is assumed to be operationally well possible.
 - The removal of the concrete perforated bottom slabs and arch construction underneath the slabs is assumed to be not problematic.
14. A few elements of the design are not detailed in the report, because it was not part of the focus of the presented study. It's thought that these elements are not complex and can be detailed relatively simple. The scope of the study was to make clear that a realistic design was well possible. Before the next design step is made, the following elements should be detailed further.
 - The mechanical design of the driving mechanism.
 - The connection of the supporting rail to the concrete wall of the lock chamber.
 - The solid slab(s) to prevent water from flowing below the initial level of the concrete bottom slabs.

References

The references are split up in **Literature** and **Websites**.

Literature

- AASHTO. (1991). *Guide specification and commentary for vessel collision design of highway bridges*. Washington D.C., The United States of America.
- Abraham, G. (1972). *Theoretische beschouwingen over zoutindringing bij schutsluizen door luchtbellengordijnen*. (Vol. 12, Year 84). Doetinchem, The Netherlands: De ingenieur.
- Abraham, G., & Van der Burgh, P. (1962). *Reduction of salt water intrusion through locks by pneumatic barriers*. Delft, The Netherlands: Delft hydraulics.
- Abraham, G., & Van der Burgh, P. (1964). *Pneumatic reduction of salt intrusion through locks. Proceedings American Society of Civil Engineers (ASCE). Journal of Hydraulics Division*. (Vol. 90).
- Abraham, G., Van der Burgh, P., & De Vos, P. (1973). *Pneumatic barriers to reduce salt intrusion through locks*. Den Haag, The Netherlands: Government Publishing Office.
- Barr, D. (1963). *Densimetric exchange flow in rectangular channels*.
- Battjes, J. A., & Labeur, R. J. (2009). *Collegehandleiding CT2140 Vloeistofmechanica 2*.
- Bresters, J. T., & Van der Velden, J. F. (1988). *Onderzoek naar het functioneren van een drempel in een zeesluis*. Delft, The Netherlands: Delft, University of Technology.
- Bruyn, J. (1963). *Waterschermen ter bestrijding van zoutbezwaar van schutsluizen aan zee (report M0799)*. Delft, The Netherlands: Waterloopkundig laboratorium.
- Chen, W. F., & Duan, L. (2000). *Bridge engineering handbook*. Boca Raton: CRC Press.
- CIRIA; CUR; CETMEF. (2007). *The rock manual. The use of rock in hydraulic engineering*. (2nd ed.). London, Great Britain: C683, CIRIA.
- de Gijt, J. G., & van der Toorn, A. (2012). *Structures in hydraulic engineering 2 - Barriers, weirs, quay walls and jetties*.
- Deltares. (2010). *Verkenning effectiviteit zoutlekbeperkende maatregelen op laboratoriumschaal (Project number 1201226-002)*.
- Deltares. (2011a). *Ontwerpstudie en praktijkproef zoutlekbeperving Volkeraksluizen - Beschrijving en resultaten praktijkproef Stevinsluis en evaluatie maatregelen Stevinsluis (Project number 1201226-005)*.
- Deltares. (2011b). *Ontwerpstudie en praktijkproef zoutlekbeperving Volkeraksluizen - Evaluatie maatregelen Volkeraksluizen (Project number 1201226-006)*.

- Deltares. (2011c). *Ontwerpstudie en praktijkproef zoutlekbepierking Volkeraksluizen - Implementatie en operationeel beheer zoutbepierkende maatregelen Volkeraksluizen; Mogelijke toepassingen andere sluizen (Project number 1201226-007).*
- Deltares. (2011d). *Ontwerpstudie en praktijkproef zoutlekbepierking Volkeraksluizen - Eindrapport van het onderzoek naar mogelijkheden voor de zoutlekbepierking door de Volkeraksluizen na verzilting van het Volkerak-Zoommeer (Project number 1201226-015).*
- Deltares. (2012). *Krammer-Jachtsluizen - Haalbaarheidsonderzoek beperking onderhoud, schuttijd en zoutlek. Simulaties met dynamisch zoutlekmiddel. (Project number 1205977-000).*
- Deltares. (2013). *Pilot Krammerjachtsluis - Functionele en hydraulische aspecten.* Delft.
- DHV B.V. (2012). *Concept besturingsplan PKJS* (2nd ed.). (J. W. Sandker, Red.)
- Dronkers, J. H. (2011, July 12). Letter SDG/NW2011/1367/112807: Droogte en trapjeslijn Nieuwe Waterweg. Den Haag, The Netherlands.
- Elling, R., Andeweg, B., De Jong, J., & Swankhuisen, C. (2005). *Rapportage techniek* (3rd ed.). Groningen, The Netherlands: Wolters-Noordhoff bv.
- Fischer, H. B. (1979). *Mixing in inland and coastal waters.*
- Gemeentewerken-Rotterdam. (1989). *Haalbaarheidsstudie naar de integratie van een luchtbellenscherm in de stormvloedkering in de Nieuwe Waterweg (report 69.30-R 8906).*
- Haralambidou, K. I., & Sylaios, G. K. (2003). *Testing alternatives for salt wedge management in an estuary with the use of monitoring and a mathematical model.* Lemnos, Greece.
- Hermans, M. A. (1996). *Optimalisatie sluis- en brugbediening Kornwederzand en Den Oever (Afsluitdijk) en bijbehorende remmingwerken.* Utrecht, The Netherlands.
- Kerstma, J., Kolkman, P. A., Regeling, H. J., & Venis, W. A. (1991). *Zout-zoetscheiding bij schutsluizen.* Delft, The Netherlands: Rijkswaterstaat and Waterloopkundig Laboratorium.
- Kranenburg, C. (1998). *Dichtheidsstromen.* Delft, The Netherlands.
- Ministerie van Verkeer en Waterstaat. (2008). *Scheepvaartinformatie hoofdvaarwegen* (2008 ed.). Den Haag, The Netherlands: Koninklijke De Swart.
- Molenaar, W. F. (2011). *Hydraulic structures - Locks.* Delft, The Netherlands.
- Molenaar, W. F., Van Baars, S., & Kuijper, H. K. (2008). *Manual hydraulic structures.*
- Nakai, M., & Arita, M. (2002). *An experimental study on the prevention of saline wedge intrusion by an air curtain in rivers (Journal of Hydraulic Research, 40(3), 333-339).* Saitama, Japan.
- Nguyen, A. D., & Savenije, H. G. (2006). *Salt intrusion in multi-channel estuaries: a case study in the Mekong Delta, Vietnam.*
- Parchure, T. M., Wilhelms, S. C., Sarruff, S., & McAnally, W. H. (2000). *Salinity intrusion in the Panama Canal.* Vicksburg, The United States of America.
- PIANC. (1986). *Final report of the international commission for the study of locks.* Brussels, Belgium.

- PIANC. (2009). *Report 106: Innovations in navigation lock design*. Brussels, Belgium.
- Rijkswaterstaat. (1981). *Compartimenteringswerken oosterschelde - Ontwerp sluizencomplex Philipsdam*. (J. C. Huis in 't Veld, & W. M. Polderman, Red.)
- Rijkswaterstaat. (1989). *Ontwerpnota compartimenteringswerken - Deelnota 6: Krammersluizen*.
- Rijkswaterstaat. (2011). *Richtlijnen vaarwegen 2011*. (J. U. Roelse, & K. Brolsma, Red.)
- Rijkswaterstaat Bouwdienst. (2000a). *Ontwerp van schutsluizen* (Vol. 1). (A. Glerum, & A. Vrijburcht, Red.) Emmeloord, The Netherlands: Drukkerij Feiko Stevens.
- Rijkswaterstaat Bouwdienst. (2000b). *Ontwerp van schutsluizen* (Vol. 2). (A. Glerum, & A. Vrijburcht, Red.) Emmeloord, The Netherlands: Drukkerij Feiko Stevens.
- Rijkswaterstaat Bouwdienst. (2008). *Maatregelen tegen zoutindringing bij schutsluizen* (3 ed.).
- Rijkswaterstaat Zeeland. (2001). *Waterakkoord Volkerak / Zoommeer*.
- Rijkswaterstaat Zeeland. (2007). *Het Krammersluizencomplex in de Philipsdam* (2nd ed.). (K. Steenepoorte, Red.)
- Rijkswaterstaat Zeeland. (2012). *Ontwerpnota DO en uitvoeringsplan, BO&E plan Volkerakschutsluizen*.
- Rijkswaterstaat Zeeland. (2012). *Vraagspecificatie eisen*. Middelburg, The Netherlands.
- Rijkswaterstaat Zeeland. (2013). *Ombouw zoet-zoutscheiding Krammerjachtensluis 2 - Definitief ontwerp (J09bis)*.
- Svensson, H. (2009). Protection of bridge piers against ship collision. *Steel construction 2, No. 1*, 32.
- Van Mazijk, A. (1971). *Reproductie zouttoestand getijrivieren (VIII): invloed luchtbellen-gordijn op zoutpenetratie (report M 0896-VIII)*. Waterloopkundig laboratorium.
- Vrijburcht, A. (1991). *Forces on ships in a navigation lock induced by stratified flows*. Delft, The Netherlands: Delft, University of Technology.
- Waterloopkundig laboratorium. (1975). *Invloed luchtbellenschermen op zoutindringing in de Rotterdamse Waterweg en op uitwisselingsdebiëten Botlek (report M1319)*.

Websites

- <http://nl.wikipedia.org/wiki/Bellenscherm> Consulted sep-2012.
- <http://www.waterforum.net/component/content/article/5-archief/2519-platform-zoetwater-west-nederland-wil-bellenscherm-nieuwe-waterweg> Consulted sep-2012.
- <http://www.royalhaskoningdhv.com> Consulted sep-2012.
- <http://www.bndestem.nl/regio/moerdijk/3555960/Gevolgen-afsluiting-smaken-zout-en-zoet-.ece> Consulted sep-2012.
- <http://www.deltares.nl/nl/actueel/nieuwsbericht/item/14403/uniiek-onderzoek-bellenscherm-nieuwe-waterweg> Consulted sep-2012.

<http://www.top-sectoren.nl/water> Consulted sep-2012.

http://www.rotterdam.nl/gelsluis_eeen_sluis_zonder_deuren Consulted sep-2012.

<http://www.vakbladvoordebloemisterij.nl/nieuws/9346/bellenscherm-tegen-verziltng> Consulted sep-2012.

<http://www.agentschapnl.nl/programmas-regelingen/projecten-sector-water> Consulted sep-2012.

<http://www.rijksoverheid.nl/documenten-en-publicaties/kamerstukken/2012/04/02/samenvatting-innovatiecontract-topsector-water.html> Consulted sep-2012.

<http://www.deltares.nl/nl/actueel/nieuwsbericht/item/14403/uniek-onderzoek-bellenscherm-nieuwe-waterweg?highlight=bellenscherm> Consulted sep-2012.

www.maps.google.com Consulted sep-2012.

<http://www.rijkswaterstaat.nl/kenniscentrum/innovatie/> Consulted sep-2012.

<http://www.dtic.mil/cgi-bin/GetTRDoc?Location=U2&doc=GetTRDoc.pdf&AD=ADA378475> Consulted sep-2012.

<http://www.patentgenius.com/patent/5211700.html> Consulted sep-2012.

http://books.google.nl/books?id=hpvqm4qVxIkC&pg=PA95&lpg=PA95&dq=movable+sill+lock&source=bl&ots=XbdPn_dqEP&sig=VIFjGie74QTbhd5IypUqaFimbvQ&hl=nl#v=onepage&q=movable%20sill%20lock&f=false Consulted sep-2012.

<http://publicwiki.deltares.nl/display/DV/Krammersluizen> Consulted sep-2012.

<http://www.deltawerken.com/Compartimenterings-werken/48.html> Consulted sep-2012.

http://www.rijkswaterstaat.nl/water/feiten_en_cijfers/vaarwegenoverzicht/oosterschelde/index.aspx Consulted sep-2012.

http://www.rijkswaterstaat.nl/water/feiten_en_cijfers/vaarwegenoverzicht/zijpe/index.aspx Consulted sep-2012.

<http://www.deltawerken.com/De-Philipsdam/52.html> Consulted sep-2012.

http://www.rijkswaterstaat.nl/water/feiten_en_cijfers/vaarwegenoverzicht/ Consulted sep-2012.

<http://www.volkerakzoommeer.nl/generator.php?id=28> Consulted sep-2012.

<http://www.watersport Almanak.nl/getijdentabellen-2012/krammersluizen-west> Consulted sep-2012.

http://www.rijkswaterstaat.nl/geotool/waterhoogte_tov_nap.aspx?cookieLoad=true Consulted sep-2012.

<http://www.bhic.nl/site/pagina.php?id=12261&zoek=marechaussee%20oss&helewoorden=0> Consulted sep-2012.

http://nl.wikipedia.org/wiki/Normaal_Amsterdams_Peil Consulted oct-2012.

http://live.getij.nl/getij_resultaat.cfm?location=KRAMMSZWT Consulted oct-2012.

<http://en.wikipedia.org/wiki/Salinity> Consulted oct-2012.

<http://swimright23.webs.com/dragandresistance.htm> Consulted oct-2012.

<http://en.wikipedia.org/wiki/Seawater> Consulted feb-2013.

http://www.windows2universe.org/earth/Water/dissolved_salts.html Consulted feb-2013.

<http://www.answersingenesis.org/articles/arj/v3/n1/sodium-chloride-abiogenesis> Consulted feb-2013.

<http://www.milieucentraal.nl/themas/energie-besparen/energieprijzen> Consulted feb-2013.

Terms, translations & abbreviations

Throughout this document, several terms and abbreviations need an explanatory note. The following list gives an overview.

Terms & abbreviations

Δ-bubble screen	New design of air bubble screen which makes use of a more complex lay out than the traditional bubble screens. It is invented by <i>Deltares</i> .
3D model Volkerak Zoommeer	A Delft3D model of the Volkerak Zoommeer, created by <i>Deltares</i> .
Afsluitdijk	32 km long dike in the Netherlands, which closes off the <i>IJsselmeer</i> from the Wadden Sea.
Botlek	An industrial area in the harbour of <i>Rotterdam</i> , the Netherlands.
Corporate innovatieprogramma Rijkswaterstaat	Programme which tries to create a connection between the topsectors, the Dutch Ministry of Infrastructure and Environment and the execution works of <i>Rijkswaterstaat</i> .
Deltares	Dutch research company.
DHV B.V.	Dutch engineering company, before it merged with <i>Royal Haskoning</i> on the 1 st of July 2012.
e.g.	Exempli gratia (Latin. English: for example).
Enschede	City in the East of the Netherlands.
Getijgoot	Test facility to perform physical model studies.
Getijmodel Rijnmond	Test facility to perform physical model studies. This model is more detailed than the <i>Getijgoot</i> .
i.e.	Id est (Latin. English: that is).
Krammer locks	Lock complex in the <i>Philipsdam</i> , <i>Zeeland</i> , the Netherlands.
MCA	Multi criteria analysis.
mwc	Metre water column.
NAP	Dutch for ' <i>Normaal Amsterdams Peil</i> ', meaning 'Regular Amsterdam Level'. It is a reference height, which is used in height measurements in the Netherlands. The level originates at the mean high water level of the <i>IJ</i> (Amsterdam) and doesn't differ much from the mean water level of the North Sea.

Nieuwe Waterweg	Artificially widened water way, connecting <i>Rotterdam</i> with the North Sea.
Ramspol barrier	Rubber bellow barrier in the Netherlands.
RHDHV	Abbreviation for company name <i>Royal HaskoningDHV</i> .
Rijkswaterstaat	<i>Rijkswaterstaat</i> is the Dutch executive agency of the Ministry of Infrastructure and Environment (in some countries known as Ministry of Public Works)
Rijnmaasmonding	Location where the merged rivers Rijn and Maas flow into the North Sea in the Port of Rotterdam. Located at the West end of the <i>Nieuwe Waterweg</i> .
Rozenburgse lock	Lock at <i>Rozenburg</i> , a town in the harbour of <i>Rotterdam</i> .
Royal Haskoning	Dutch engineering company, before it merged with <i>DHV B.V.</i> on the 1 st of July 2012.
Royal HaskoningDHV	Company name after merging of companies <i>DHV B.V.</i> and <i>Royal Haskoning</i> on the 1 st of July 2012.
s-bubble screen	Traditional air bubble screen. Consists of pipes with holes in it.
Stevin locks	Lock in the <i>Afsluitdijk</i> , the Netherlands.
Topsector Water	The Dutch government works together with professionals as well as scientists to write advices, describing which technologies should be analysed further or which techniques are important to develop further. It connects companies with each other and with the government.
Trapjeslijn	Measure to reduce salt intrusion in the Nieuwe Waterweg, Rotterdam.
Twentekanaal	Canal in the east of the Netherlands. In connection with Enschede.
Volkerak locks	Lock complex at the North side of the Volkerak Zoommeer.
Volkerak Zoommeer	Lake situated between Zeeland and Rotterdam.
Zeeland	Southern province in the Netherlands.
Zoutlekmodel	A model of salt leakage at any lock complex.

Translations

For Dutch readers, the following translations may help in the understanding of some terms used in the report.

Culvert	Riool in sluizencomplex
Cyanobacteria	Blauwalgen
Dewatering gate	Uitwateringssluis
Guard lock	Keersluis
Lock paddle	Rinketschuif
Navigation lock	Schutsluis
Paddle	Schuif in sluis (ook rinketschuif)
Pivot-inspection chamber	Taatskuip (see Figure 49; column is pumped dry to perform small operations)
Scouring lock	Spuisluis
Stop lock	Spuisluis
Water agreements	Water akkoorden



Figure 49: Pictures of pivot-inspection chamber.

Appendices

Appendices

A.	Literature study: Salt intrusion prevention.....	4
A.1.	Air bubble screens	5
A.1.1.	As salt intrusion counter measure.....	5
A.1.2.	Other applications of air bubble screens	7
A.2.	Other counter measures.....	8
A.2.1.	Liquid gel	8
A.2.2.	Movable sill	9
A.2.3.	Salt water pit.....	9
A.2.4.	Flushing of lock chamber	10
A.2.5.	River groins.....	10
A.2.6.	Increased river bottom roughness	11
A.2.7.	Navigable barrier	11
A.3.	Development of technique at <i>RHDHV</i>	11
A.3.1.	Why <i>RHDHV</i> interferes	12
A.3.2.	How <i>RHDHV</i> interferes	12
A.4.	Market demand of use of technique	13
A.5.	Gaps in knowledge	14
B.	Visualisation of <i>Duinkerken system</i>	18
C.	Mean high and low water	22
D.	Calculation of pipe capacity in the pilot	24
D.1.	Air bubble screen supply pipes.....	24
D.2.	Water screen supply pipes.....	27
E.	Concepts for movable sill.....	28
E.1.	Description of concepts.....	28
E.1.1.	<i>RF</i> Rotating flap	29
E.1.2.	<i>RS</i> Rotating segment	30
E.1.3.	<i>RG</i> Rotating split gates.....	31
E.1.4.	<i>TS (v)</i> Translating slider (vertical)	32
E.1.5.	<i>TS (h)</i> Translating slider (horizontal)	33
E.1.6.	<i>TG</i> Translating split rolling gate.....	34
E.1.7.	<i>TI</i> Translating inflatable sill.....	35
E.2.	Reasoning of concepts ratings	36
E.2.1.	<i>RF</i> Rotating flap	36
E.2.2.	<i>RS</i> Rotating segment	36
E.2.3.	<i>TS (v)</i> Translating slider (vertical)	37
E.2.4.	<i>TI</i> Translating inflatable sill.....	38
E.2.5.	Weight factors	39
F.	Solution for gap under sill's screens	40
F.1.	Alternatives.....	40
F.2.	MCA.....	41

G.	Various reference projects.....	46
G.1.	Reference projects of movable sill	46
G.2.	Reference projects of air bubble screens.....	48
G.3.	Reference of lift gate	49
H.	Calculation of loads by ships	52
H.1.	Return flow force.....	52
H.2.	Propeller jet force	55
H.3.	Ship collision force.....	62
H.4.	Maple calculations	63
H.4.1.	Force by return current.....	63
H.4.2.	Force by propellers.....	68
I.	Load combinations	69
J.	Dimensioning of sill.....	72
J.1.	Plates	72
J.2.	Studs.....	74
J.3.	Main beams	75
J.4.	Vertical connection	77
J.5.	Guiding rail	78
J.5.1.	Force distribution	78
J.5.2.	Friction in rail.....	83
K.	Details of driving mechanism alternatives.....	84
L.	New water levelling process in commercial lock	86
M.	Effectiveness calculation	90
M.1.	Basic information	90
M.2.	Salt intrusion.....	91
M.3.	Fresh water loss	92
N.	Energy consumption calculation.....	93
N.1.	Water levelling	93
N.2.	Air bubble screen.....	94
N.3.	Water screen.....	96
N.4.	Costs.....	97

Appendix

A. Literature study: Salt intrusion prevention

This appendix presents the most important parts of a literature study on salt intrusion preventions.

Air bubble screens are described more thorough, because this technique has been an important base for what the literature study was used for.

A.1. Air bubble screens

Air bubble screens are not only used to prevent salt water intrusion. Other applications do exist, and are mentioned after the most important use for hydraulic engineers is described in more detail.

A.1.1. As salt intrusion counter measure

In a situation where water densities at both sides of an air bubble screen are equal, water will flow as illustrated in Figure 50. Water is forced upwards by the air bubbles and spreads out at the water surface. The air bubbles are present in a line perpendicular to the drawings surface. As a consequence, the spreading out at the surface will occur in two directions. At the bottom water is supplied from both directions, leading to the forming of an eddy.

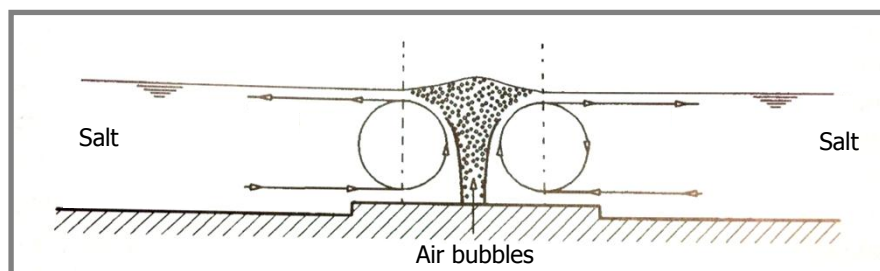


Figure 50: Flow pattern of water without density difference with air bubble screen.

In the situation when salt intrusion is an issue, a density difference is present. Figure 51 is used in the explanation. The heavier salt water wants to flow via the bottom to the right. The lighter fresh water wants to flow to the left via the water surface. This exchange flow results in the forming of an eddy at the fresh side of the air bubble screen. The salt water which ends up at the right side of the air bubble screen wants to sink down, which also feeds the presence of the formed eddy.

In the described system of water flows, salt water flows out via the eddy and passes the surface of the water at the fresh side. On the contrary, fresh water flows to the left in the figure via the eddy and passes the bottom of the lock. Meanwhile, the densities mix up with each other. This results in a lower density of the intruding water, than the water at the outside of the lock. The system works best, when the lock gates are opened as short as possible.

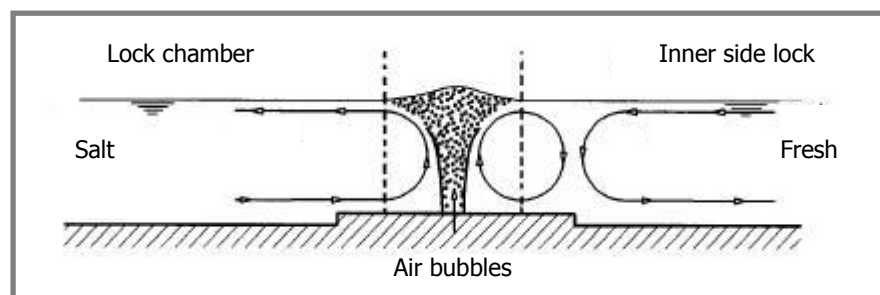


Figure 51: Flow pattern of water with density difference with air bubble screen.

The implementation of air bubble screens to prevent salt water intrusion is known, but the knowledge is not developed equally divided the last few decades. Experiments and applications go back from 1960's to 1980's. A few implementations of the technique are known in sluices in the Netherlands. Applications elsewhere are not plentiful and are concentrated in the UK.

The first known research on air bubble screens against salt intrusion was focussed on implementation in sluices. This dates back to 1962 (Abraham & Van der Burgh, Reduction of salt water intrusion through locks by pneumatic barriers, 1962) and was not before 1972 followed by experiments to validate the acquired theory. (Abraham, Theoretische beschouwingen over zoutindringing bij

schutsluizen door luchtbellengordijnen., 1972) In 1963 research resulted in the fact that water screens instead of air bubble screens also prove to be effective. The costs would be much higher, though. (Bruyn, 1963) A visualisation is presented in Figure 52.

To examine the possibility of an application of air bubble screens in the *Nieuwe Waterweg*, physical model studies were performed in 1971 at the *Getijgoot*³². It was concluded that salt water in deed intrudes less far into the fresh water system. This reduction was depending on the location of the screen, the possible usage of multiple screens and the amount of air used in the pipes of the screens. (Van Mazijk, 1971) The *Getijgoot*, used in these studies, was actually too much schematized to be realistic. For that reason, additional research was performed in the *Getijmodel Rijnmond*³³ in 1975. (Waterloopkundig laboratorium, 1975) Apart from more detailed data on the effectiveness of air bubble screens in different configurations, the model showed a reduction of the silting at the *Botlek*. In 1989, the municipality of Rotterdam decided not to apply air bubble screens. The cost reduction of less dredging at the Botlek was insufficient compared with the financially risky investments, needed to construct the air bubble screens. (Gemeentewerken-Rotterdam, 1989)

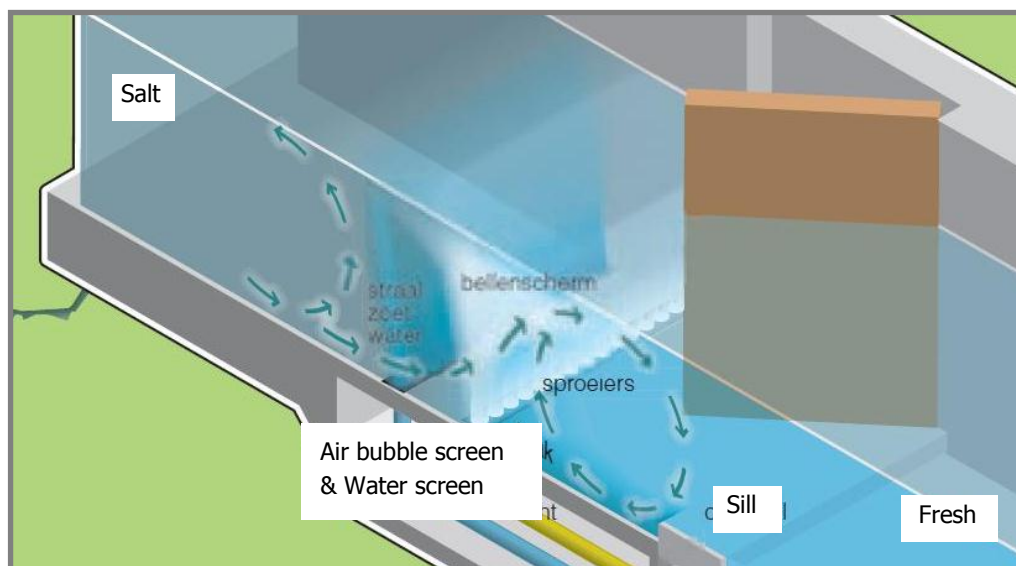


Figure 52: visualisation of air bubble and water screen in a lock chamber.

In the last decade, knowledge on optional implementations in estuaries (globally) is improved by the use of physical as well as numerical model studies. General conclusions of these studies can be summarized as three separate parameters, determining the effectiveness of an air bubble screen universally: The buoyancy of the bubble screen (controlled by the air flow), the strength of the salt wedge (characterised by the density difference and height of the wedge) and the inertial force of the freshwater flow (characterised by the river flow and -depth). (Haralambidou & Sylaios, 2003) (Nakai & Arita, 2002) (Nguyen & Savenije, 2006)

Practice experience in the Netherlands is limited to a few locks. In 1971 an air bubble screen was used at the *Rozenburgse lock*³⁴. Due to changes in the local system, the water is brackish at both sides nowadays, which makes the screen dysfunctional. A few years later bubble screens were built at the *Volkerak locks*. Also at that location, the water at both sides is nowadays of the same type. Both sides are fresh now, which makes the bubble screen unnecessary.

To prevent the acquired knowledge from the last century to be forgotten, *Deltares* performed research on this subject with higher detail. Old knowledge was used in the design of several laboratory tests, resulting in improved insights. An example is a new type of bubble screen, called *Δ -bubble screen*. The

³² <http://www.digibron.nl/search/share.jsp?uid=00000000012e967f17ea53c39feb1696&sourceid=1011>

³³ <http://www.digibron.nl/search/share.jsp?uid=00000000012e9d89497a0f9cd5a7c562&sourceid=1011>

³⁴ <http://nl.wikipedia.org/wiki/Bellenscherm>

traditional *s-bubble screen* was actually a pipe with holes in it, allowing the air bubbles to leave the pipe at the bottom of the lock. The newly developed Δ -bubble screen is equipped with some sort of valve, resulting in a fixed air discharge. This improvement proved to be a positive change when it comes to effectiveness. Locations where the old system wasn't good enough before, are now able to be equipped with bubble screens. During the process of modelling this technique, a full-scale model test was done. In contrast to numerous laboratory tests in the past, practical tests to this extent are quite unique. The *Stevin locks* in the *Afsluitdijk* were used to gain insight in the effects of bubble screens on salt intrusion and on the dynamic behaviour of trespassing ships. The results of these tests were used to validate computer models, improving their applicability and accuracy.

RHDHV is performing a pilot project at the Krammer locks in *Zeeland* to acquire more knowledge about the subject. Not only the technical background of the effects of a bubble screen is important (as is the case for *Deltares*), but also the way it is constructed and what problems are encountered there. Another important reason to improve the knowledge on this subject, is that in previous implementations very little data was acquired. This pilot is carried out in combination with *Deltares*. Main goal of the project is to gain experience on the subject and to see whether the technique can be implemented elsewhere and on a larger scale.

Air bubble screens don't make an impermeable barrier. Due to the reduced exchange flow, there is still fresh water loss in the system. The salt intrusion is reduced in the order of 40% with a Δ -bubble screen. With a traditional *s-bubble screen*, this value is even lower. If a combination of several bubble screens is implemented, combined with good management of the locking cycles, values of salt intrusion reduction up to 70% can be reached.

Construction costs are relatively low. The screen can often be prefabricated and sunken into its position. A benefit of this is that a bubble screen can be embedded in an existing lock. The lock has to be large enough to do this, because else the navigational perimeter will decrease. Maintenance costs are not very high because the structure can be lifted out of the water. Especially in comparison with the maintenance of river groins for instance. Operational costs are very high. The air pressure needs to be maintained when the bubble screen is 'inactive', to prevent the pipes to be filled with water. The energy consumption of the compressed air is very high.

A.1.2. Other applications of air bubble screens

Air bubble screens are not only used as a preventive measure against salt intrusion. In other fields, the technique has proven to be useful as well. In order to visualise other usage of the technique of bubble screens, a few of them are portrayed here.

The screen can be applied in case of a desired blockage of something. This something can vary from polluted water or oil spills to dead plants and other lightweight material. An example is provided by making reference to a fire at a tire factory in *Enschede* in 2003. The firewater, flushing away from the fire back into the nearby located *Twentekanaal*, caused serious pollution. In this case, the bubble screen was used to prevent polluted silt from moving downstream of the canal.

When plant remains or cyanobacteria³⁵ have to be blocked from entering into a marina or recreational lake, bubble screens can be applied.³⁶ Even when an oil spill has occurred, it is possible to use a bubble screen to reduce the possible damage.³⁷

In some cases, dredging works need to be performed with high accuracy. The efficacy greatly depends on the dredging equipment used, but is also controllable by the use of bubble screens. Particles from the bottom get in flow and move less easily through the bubble curtain due to the vertical water flow, induced by the air bubbles. In this way it is possible to dredge the level of a bottom rather precise. It is assumed, though, that all particles which are not dredged by the dredger stay in the area

³⁵ In Dutch: *Blauwalgen*.

³⁶ <http://www.oxydent.nl/toepassingen/bellenscherm/>

³⁷ <http://www.oxydent.nl/referenties/olie-lek-bestrijding/>

closed off by the bubble screen. Another application in this way can be the removal of a polluted layer of soil on the bottom of a river bed.³⁸

The disadvantage of these other applications is that not much data or experience is useful for the implementation as counter measure for salt intrusion. It gives a complete image of the different implementations of this type of screens, but it is not useful in the research which is described in this report.

A.2. Other counter measures

Apart from air bubble screens, other solutions are possible when it comes to the prevention of salt water intrusion. This section provides insight in the most important other options. Reason why they are presented separated from air bubble screens, is that the technique of air bubble screens is emphasised more; besides the fact that more detailed scientific knowledge is available. Knowledge on other techniques is an inferior subject of this study and is therefore described less detailed.

Salt water intrusion can be prevented in sluices, but also in regular waterways. To all the presented alternatives – in sluices, but also in waterways – different implementations are possible. They can be combined or applied at a slight different manner than displayed in this section. Often, model tests provide a decisive answer on what options are going to be used and in what combination or configuration.

A.2.1. Liquid gel

A total blockage of water seems impossible if navigation needs to be an option, but even that is a possibility. A new technique is invented, where a liquid gel allows ships to pass. A height difference can be bridged and the water at both sides is not in connection with each other.³⁹ In this way, salt water doesn't intrude in the fresh water system at all. The gel acts like a pudding and needs a long base as some sort of foundation. The Figure 53 shows a possible design of the new technique in the *Nieuwe Waterweg* near *Rotterdam*.

If the system works as it is thought of in studies, salt intrusion will be blocked completely. Fresh water loss will not be present. The values in the table are displayed between brackets, because they are theoretical values. The other values depend on realistic experience.

Since the technique is only tested in a laboratory, approximations on costs are hard to make. A very long structure is needed (± 4 km) and the gel needs to be created at a special facility. This makes it acceptable that costs will become very high. They cannot be quantified because a realistic design doesn't exist yet. In current plans, the technique seems only feasible in large waterways. This makes a dry construction dock unrealistic, since water ways can generally not be closed for long periods. It can be assumed that construction and maintenance of the gel will be relatively expensive; operational costs will be very low since no power or material is needed if the system works according plans.

³⁸ <http://www.neerslag-magazine.nl/magazine/artikel/375/>

³⁹ http://www.rotterdam.nl/gelsluis_eeen_sluis_zonder_deuren

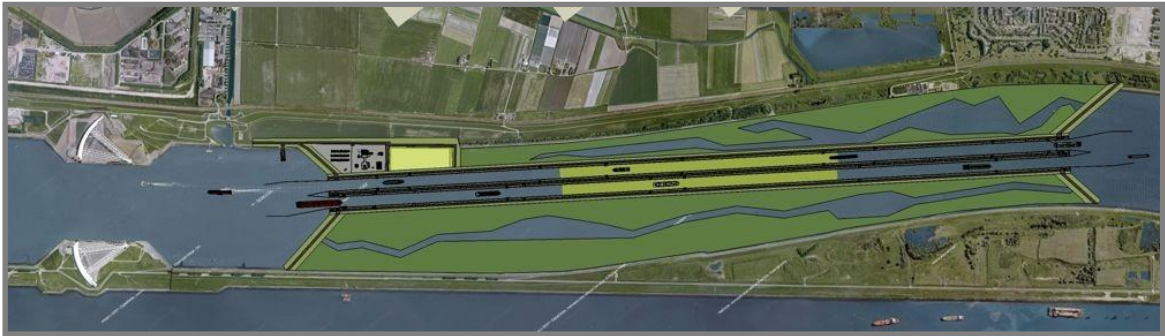


Figure 53: Artist impression of top view of liquid gel lock in the Netherlands. Adopted from <http://www.architectenweb.nl/aweb/redactie/Photo.asp?iNID=27668&PhotoID=218673>.

A.2.2. Movable sill

Another option is a threshold or sill at the bottom of the lock in front of the sluice gate. This barrier blocks the salt water from flowing out of the sluice as can be seen in Figure 54. The salt water has a higher density, which is why this technique will work theoretically. The level of the sill is adaptable. When a ship sails out, the threshold has to be lowered to a level depending on the draught of the ship. In this way less salt water will exchange with the fresh water at the other side. The technique is only applied once⁴⁰ until now. It is not applied in the Netherlands yet, because there is too less experience with it and there are reasons to doubt the effectiveness of the solution. For instance, people are shivery when it comes to moving parts in a ship-passing waterway, where unknown dynamic and turbulent loads appear.

A movable sill is able to block the salt intrusion up to 100%. It doesn't block the whole depth of the waterway, though. In deeper locks, effectiveness increases since only a relatively small part of the depth is kept open for shipping. In shallow locks, this isn't a good option for that reason. Fresh water loss is kept low because only the upper part of the waterway exchanges water. This can be further reduced by combining this method with a bubble screen for instance.

The costs of a structure like this are mainly focussed on construction works. If the lock cannot be emptied, it has to be constructed under water. This would also increase the difficulty of performing maintenance operations. If the lock chamber can be emptied, this would be beneficial for the construction in an existing lock. Operational costs are not high, since it only implies levelling of the sill with hydraulic jets or an air pump to fill a hollow sill.

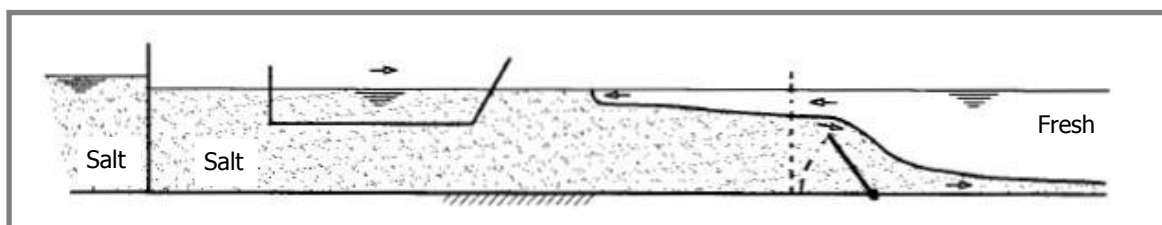


Figure 54: Movable sill as salt intrusion prevention.

A.2.3. Salt water pit

There is another technique which makes use of the fact that salt water has a higher density than fresh water. As soon as the gate opens and salt water is flowing out of the sluice, it stays at the lower section

⁴⁰ Only one application is found. A movable sill is constructed in 1966 in the Hiram M. Chittenden locks, located at Lake Washington, Seattle, USA.

of the water column. The exchange flow is only in the order of 1 m/s (Rijkswaterstaat Bouwdienst, 2000b, pp. 21-30), which results in a relatively slow moving salt water layer, shoving over the bed of the canal or river. By making a pit behind the inner sluice gates, this salt layer will move into that pit before it is able to intrude deep into the fresh water system. See Figure 55. For example underneath the gates, pumps can pump this salt water away to reduce the negative effects of salt water intrusion.

Salt intrusion reduction can be very effective in this way. This comes with a high loss of fresh water, since there will arise an extra demand of fresh water.

Construction costs are really high. The design of a lock will increase significantly when a system like this is inserted in the locks design. An extensive (often concrete) culvert system is needed. Pumps provide the backflush of salt water, which increase the operational costs. Maintaining the system is less expensive since the great deal of the system has a life expectancy comparable with that of the lock itself.

In the Netherlands, two implementations of this technique exist. Information on the existence of this type of salt intrusion is hard to find. Probably a few other locations will have a comparable system to prevent salt intrusion, but this will not exceed ten worldwide.

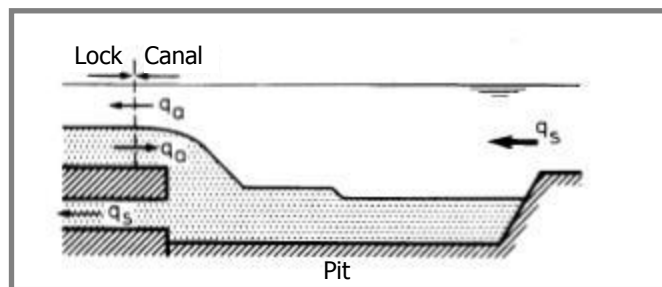


Figure 55: Salt water pit as salt intrusion prevention.

A.2.4. Flushing of lock chamber

The lock chamber can be flushed before opening the lock gates. In this way it can be prevented that salt water enters the fresh water system. Therefore, it is a very effective solution when it comes to salt intrusion. This effectiveness is compensated by a high fresh water loss. This has a negative effect on the locking time. Apart from that, a lot of fresh water is needed, which cannot be reused later, since it flows into a salt basin or sea. The earlier explained *Duinkerken system* is a variant of this, but differs in a way that fresh water loss is minimised.

A large reduction of salt intrusion is possible. This costs a lot of fresh water, which flows into the salt water regime. At the *Duinkerken system*, the fresh water is brought back into the fresh water regime. This increases the locking time, but is able to reduce the fresh water loss from 80% to approximately 30%.

The system is not a very expensive option, and can be implemented in various ways. A simple way is to supply the gates with paddles. This is even possible after the lock is constructed.

In the Netherlands, six locks are equipped with this type of system. Worldwide implementations will probably not exceed 20, but information to this matter is hard to retrieve.

A.2.5. River groins

Groins are able to reduce salt water intrusion in rivers. Due to the groins, more turbulence is added to the flow through the river. Behind them, eddies form, inducing mixture of the different water layers. Also water velocity gradients and exchange flows between river and groin sections induce mixing of water layers.

The reduction of salt intrusion is very low. Fresh water loss is comparable with the situation of not constructing river groins.

The costs of building numerous river groins are high. Also maintaining them has its price. All this together makes it unrealistic to construct these groins for the purpose of salt intrusion. If they are needed for another purpose, though, it can be very attractive to adapt the design to help the prevention of salt intrusion.

A.2.6. Increased river bottom roughness

Mixing of different water layers can be encouraged by a high bottom roughness. Moreover, the tidal wave is slowed down with a rougher bottom, resulting in a less far intruding salt water wedge. This higher roughness can be achieved by laying down rocks at the bottom of the river. There should also be enough depth to lay down the rocks, and let ships navigate through the river. Another option to achieve a higher bottom roughness is to vary in water depth along the course of a river. This is performed at the *Nieuwe Waterweg* for instance.⁴¹

The effects of an increased river bottom roughness are small. Salt intrudes in the system, but the length over which this happens reduces. This is very location specific. Fresh water is not blocked or preserved, so fresh water loss is accepted to be equal to doing nothing.

Construction and maintenance costs are very high. A benefit of the solution is that operational costs are zero. If the system can be combined with the regular programme which provides the maintenance of water depths in waterways (for instance in a harbour), it is a good option.

A.2.7. Navigable barrier

It is also possible to make a physical separation between fresh and salt water. Artificial reed or rubber flaps are able to provide this separating measure. The lamellae can be located next to each other closely, or at a distance from each other. In the first option it functions as a physical separation between salt and fresh water, in the second option focus lies on causing mixing of the water layers. Navigation through this obstruction is possible, given the fact that the lamellae are designed for it. This implies that it should be flexible enough to prevent damage to ships, but also that it should be solid enough to resist encounters with rudders and sharp edges. It must be noted that only really small ships are allowed to pass and the salt leak is only diminished compared with the situation without any measure. The mild effects cannot be compared with the other mentioned alternatives. The other options are possible at the scale of commercial navigation, this technique is not.

The effectiveness of a navigable barrier can be high. It blocks the water depth up to the water surface. In an ideal situation, there is only small leakage through the barrier. The values in the table are between brackets because no experience with the system is present.

Construction of this barrier will be possible in a dry dock, formed by the use of sheet piles. The depth in which this technique is possible is small namely. Operational costs are zero, which makes it attractive to research this option further.

A.3. Development of technique at *RHDHV*

This section is used to describe what the role of *Royal HaskoningDHV* is in this matter. Why is it interesting for them to involve in this development? It is also explained what actions they take, contributing to the development of the promising technique of salt water intrusion preventive measures.

⁴¹ In Dutch: *Trapjeslijn*, see Figure 56.

A.3.1. Why *RHDHV* interferes

There are numerous reasons why *RHDHV* should interfere with the technique of air bubble screens as separation of salt and fresh water, and salt intrusion preventive measures in general. At first there is the *Topsector Water*⁴². This initiative stimulates companies to work together with researchers and scientists to improve knowledge of certain subjects. Promising technologies as air bubble screens are a good example of a subject, worth investigating for several different parties.

Rijkswaterstaat launched their '*Corporate innovatieprogramma Rijkswaterstaat*'. Main goal of this innovation programme is creating a connection between the topsectors (e.g. topsector water, described in the footnote below), the Dutch Ministry of Infrastructure and Environment and the execution works of *Rijkswaterstaat*. This is done by a coupling of knowledge and innovations in studies of every stakeholder in connection with *Rijkswaterstaat*. Innovations are stimulated, since innovative ideas can now be realised in practice more easily.

The technology of air bubble screens is implemented before, but no accurate data was acquired during usage of the technique. This only happened at the Stevin locks, where data was acquired by *Deltares* in favour of the design of the bubble screens at the Volkerak locks. This design at the Volkerak locks is postponed to later than 2025, which is the reason that the knowledge is applied for the design of the Krammer locks pilot project now.

Salt intrusion preventive measures can be designed more accurate and effective these days. Especially when it's compared with implementations decades ago; implementations which are nowadays subject to big maintaining operations. By smart implementation, several benefits can be achieved. Locking times can be reduced, operational costs can be diminished or possible expanding plans can be postponed due to higher capacities in new systems.

There are numerous locations throughout the world, where problems with salt water can be avoided by this technique. Not only in sluices, but also on a larger scale in deltas bubble screens can be a solution. Due to climate change and continuous growth of fresh water demands throughout the world, problems with salt water will increase everywhere. Before governments can be persuaded to take measures to avoid these negative effects, there has to be a proper implementation of a working solution as example. Accurate data from a pilot project helps enormously in trying to expand the use of this technique.

In addition to that, it can be interesting for *RHDHV* to have experience and knowledge about the implementation and results of bubble screens for this purpose. Especially, knowledge about encountered difficulties and errors is valuable for the company.

A.3.2. How *RHDHV* interferes

Commissioned by *Rijkswaterstaat*, *RHDHV* is investigating the implementation of air bubble screens in the Krammer recreational lock. The project is realised as a pilot project. This does not mean that the intervention is temporary, but that it has an educative character for the technique of bubble screens. The obtained knowledge will be used for the final designs of applications in the Volkerak locks, when the VZM will be turned into a salt water basin.⁴³ The pilot is planned for the so called 'Krammer recreational lock 2', which doesn't embosom commercial sailing. Later, the commercial sailing sluices may be adapted as well.

⁴² *Topsector Water*: The Dutch government assigned 9 topsectors in the Netherlands: Horticulture and starting materials, water, agrofood, life sciences, chemistry, high tech systems and materials, energy, logistics and creative industries. Each sector corresponds to a profession or subject of which the Dutch are world leading regarding knowledge and implementation. In the different sectors, the government works together with professionals as well as scientists. Advices are written, which describe which technologies should be analysed further or which techniques are interesting and important to maintain an international competing status or position.

⁴³ The current fresh Volkerak Zoommeer is infested with cyanobacteria. The government thinks that the only way to get rid of it, is to turn the lake back into a salt lake. At the time that the decision was taken to turn the lake fresh (1970's), people didn't think of environmental consequences like this.

The innovative separation of salt and fresh water will be designed in compliance with earlier studies of *Deltares*. This implies that two air bubble screens will be constructed; one at each side of the sluice. At the salt side of the ES, a water screen will be placed. The gates at the side of the VZM will be applied with lock paddles⁴⁴, which are part of a flushing system. The bubble screens and water screen provide mixing of the layers, inducing less salt water intrusion. The flushing system can be described most easily as if the closed brackish content of the lock is replaced with fresh water. This fresh water enters through openings in the gate – the lock paddles – at the VZM. At the other side water is able to exit the lock under free decay or by the use of pumps.

The design for the pilot was accepted to be a final design at the end of august 2012. The realisation phase was planned to start right after that, which is why September 2012 would be the planned start of the tender phase. Due to several reasons, the call for tender was postponed a year to September 2013. Postponing for the period of a year is actually somewhat radical, but because of the recreational season, postponing construction to summer time isn't an option. Main reasons for pushing the date forward have a financial-, capacity- and time-based character. There is, however, an advantage to this issue. The original planning contains a decision about the entire Krammer lock complex at the end of 2013. Big maintenance is needed to the sluices; the pilot needs to assist in answering about what type of salt intrusion measures will be applied. Because this includes the commercial navigation, research has to be performed about what changes will be needed to the current pilot design in the much smaller recreational lock. This date is also pushed a year forward, which gives more time to elaborate on that question. If required, it is even possible to implement rough changes of the design in the pilot in the recreational lock.

A.4. Market demand of use of technique

Air bubble screens can be important and interesting for several groups and several locations. This holds especially when the technique becomes available on a larger scale, and will be available for use at the bottom of wide estuary openings like the *Rijnmaasmonding*.

It must be noted that implementation of all kinds of salt water intrusion countermeasures, is only favourable at specific locations. Dense populated areas close to the sea are often depending on fresh water supply from rivers nearby. Farmers in deltaic environments will be influenced negatively if salt water is able to intrude far into the delta system. If reasons like this are not present in a certain area, it is often wished for that the environment is as less influenced by human actions as possible. In this way a brackish or salt water area can house a habitat which is destroyed by taking salt intrusion preventive measures.

Rotterdam does comply with the requirement of a dense populated area, which has to have access to fresh water at their water intake points of water treatment plants. Since former applied measures don't work to well anymore (*Trapjeslijn*⁴⁵, see Figure 56), different actions have to be taken. In addition to that, fresh water discharges in the Dutch rivers are not sufficient to cope with the increasing average sea water level, resulting in a larger salt water intrusion. A higher fresh water discharge in rivers is hard to achieve. This would mean that the fresh water discharge has to be lowered at other locations or that the water discharge has to be controlled out of the boundaries of the specific country. If the technique of air bubble screens was available on a larger scale, this would be a good solution to the portrayed problems at the sea mouth in the Netherlands. Not only in the Netherlands will people be interested in this kind of measures.

⁴⁴ In Dutch: *Rinketschuiven*.

⁴⁵ The *trapjeslijn* is literally translated as 'stepping line'. This line starts at the end of the Nieuwe Waterweg at the North Sea and follows along the Nieuwe Waterweg into Rotterdam. The intruding salt water wedge from the North Sea is slowed down or controlled along that line by an altering bottom profile. The depth of the profile decreases in three steps from 22.5 to 8 metres. Recent readings of depth measures showed that the condition of the *trapjeslijn* is not satisfactory anymore.

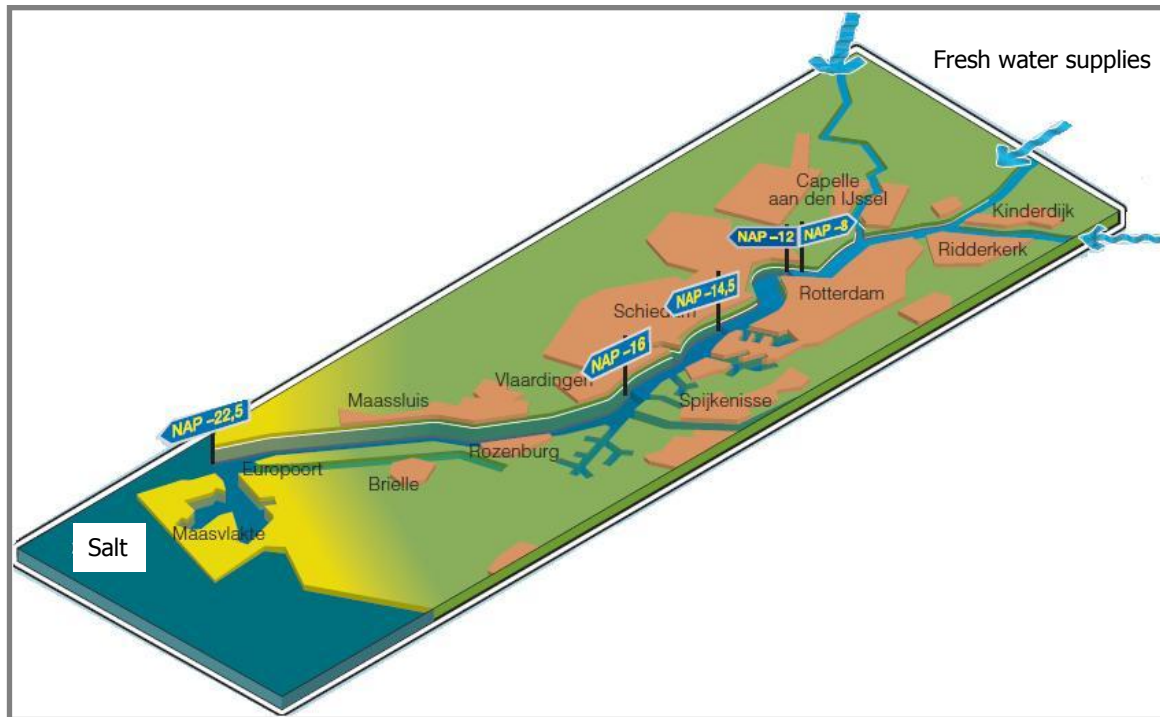


Figure 56: Schematic overview of the *Trapjeslijn*.

Current salt water intrusion preventive measures ask a lot of energy. Especially air bubble screens are large energy consumers. This can be reduced by improving the design of air bubble screens, or by using them in a smart way in combination with other measures. Since there is only little study performed to this matter, a further development is interesting for a wide range of people.

A.5. Gaps in knowledge

Since investigation of this subject is not carried out in great detail yet, there are numerous sub-subjects which can be elaborated further. Also the fact that there are aimed new applications (e.g. Rijnmaasmonding) and only a few agencies doing investigation on them, there is still a lot to be explored if it comes to valuable, reliable and useful information. Because the subjects are numerous, a summation follows. For some subjects, an explanatory text is provided after the summation.

- [1] Further development of computer model studies (e.g. *Zoutlekmodel* or *3D model Volkerak Zoommeer*)
- [2] Physical studies to the effects of air bubbles on salt and fresh water
- [3] Reliability of physical studies and coupling with developed computer models
- [4] Fundamental research on mixing of different water layers
- [5] Research on application of water screen in combination with air bubble screen(s)
- [6] Possibilities of less energy consumption in air bubble screens
- [7] Effect of air bubble screens on passing ships
- [8] Additional functionalities of air bubble screens
- [9] Implementation of air bubble screens on a larger scale
- [10] Implementation of air bubble screens in other environments
- [11] Implementation in tide affected areas; positioning of air bubble screens
- [12] Possibilities of 'floating' air bubble screens
- [13] Construction and maintenance of air bubble screen in a wide river (e.g. in Nieuwe Waterweg)
- [14] Possibility of (movable) sill as salt intrusion preventive measure

- [15] Investigate the effects of combinations of known salt intrusion counter measures
- [16] Protection of structures (e.g. piping and instrumentation) under water
- [17] Structural roadmap or handbook for constructing salt intrusion counter measures (or more specific: air bubble screens)

Clarifications:

- [1] The 'Zoutlekmodel' is a computer model that models the salt leakage through a lock complex in general. It is developed by *DHV B.V.* and *Deltares* and can be developed further. The '3D model Volkerak Zoommeer' is a Delft3D model, created by *Deltares*.
- [6] In current applications, energy consumption is very high. Therefore it is interesting to try to diminish that. Maybe it is possible to achieve this by combining air bubble screens with other salt intrusion preventive measures.
- [9] The current pilot project from *RHDHV* is situated in a relatively small lock for recreational use. It is attractive to look into the option of implementing air bubble screens in wider or deeper waters. This can for instance be in a river mouth (deltaic area) or a commercial navigation lock.
- [10] It will be enthralling to look at the implementation of bubble screens in environments which are not enclosed in pilots until now. For a wider implementation in the future, knowledge to this matter can become rather useful. A closer look to more rough standard conditions, higher water temperatures and extreme eroding/accreting areas are some possible interesting topics.
- [11] This is actually a sub-subject of [10]. Nevertheless it is a subject singly. Enough can be researched to the matter of tidal influences on preventive measures against salt intrusion. Not only the exact location of the screen needs attention; the arising problems regarding the screens capacity need attention as well. When the tidal range is large, water depths can fluctuate significantly, requiring several different air pressures.
- [12] It may be interesting to look at an option where the constructive elements are not fixed at the bottom, but afloat. This may be interesting because of the conditions of the bottom, but maybe even more because of the flexible possibilities of the screen. It is more easy to adapt the location of the screen or to maintain it at an other location. Moreover, the bubble screen will be less complex. When it is suspended from floaters, the bubble screen is always located at the exact same depth, relative to the water level. The tidal influence is cancelled out, so to say. This causes the instrumentation of the bubble screen to be designed less complex, since no water pressure differences exist at the spot where bubbles originate.
- [14] A sill – if high enough – is able to stop salt water intrusion completely. When ships pass, the sill height is restricted to the draught of the ship. When the sill is able to be adapted in height, salt water intrusion can be reduced significantly.
- [17] This results certainly in an interesting and wanted piece. Only thing is that more knowledge and experience is needed for such a descriptive handbook to be of practical use. In other techniques, a handbook (if written) is often composed after multiple pilots and field experience of more than 5 years.

A lot of the above mentioned subjects can be accommodated in different overall themes. The most important ones are computer modelling, physical modelling, smart/innovative designing and fundamental researching. *Deltares* is already performing (and has already performed in the past) a lot of computer studies and physical model studies. The other themes are quite unexplored until now.

The above mentioned topics are all interesting with a hydraulic engineering background. There are also quite a few interesting subjects concentrating more on water management issues. They are listed separate from the other topics, since they cannot be unmentioned. They are not of practical use for this Master's thesis, though.

- How can we live with salt intrusion? Allow salt water to intrude and take measures at the fresh water intake locations for example; or alter the geographical layout of the intake locations.
- With the implementation of an air bubble screen in the Nieuwe Waterweg, fresh water is saved (less outflow needed as 'counterflow' for incoming salt water). Who (municipalities, farmers, etc.) has the right to claim that water?
- Should the government be responsible for fresh water supply for farmers? If not, are they able to be independent?

Appendix

B. Visualisation of *Duinkerken* system

In this appendix, figures can be found which describe the consecutive processes of the Krammer locks during a locking cycle.

Figure 57 shows the processes in the recreational lock, Figure 58 the processes in the commercial lock. The differences between both locks are as follows:

- Commercial lock exchanges water via a perforated bottom. Bottom slabs are present in the figure as horizontal dashed lines.
- Commercial lock exchanges water before levelling to the ES side (process number 5 in Figure 58). This process does not occur at the recreational lock.

A normal lock differs from these figures on the following aspects:

- Exchange of water does not occur. (process 3 in Figure 57 and processes 3 and 5 in Figure 58)
- No culvert system is present (incl. perforated bottom, etc.)
- No wall valves are present. (visible as square block in visualisations of process 3 in Figure 57 and processes 3 and 5 in Figure 58)

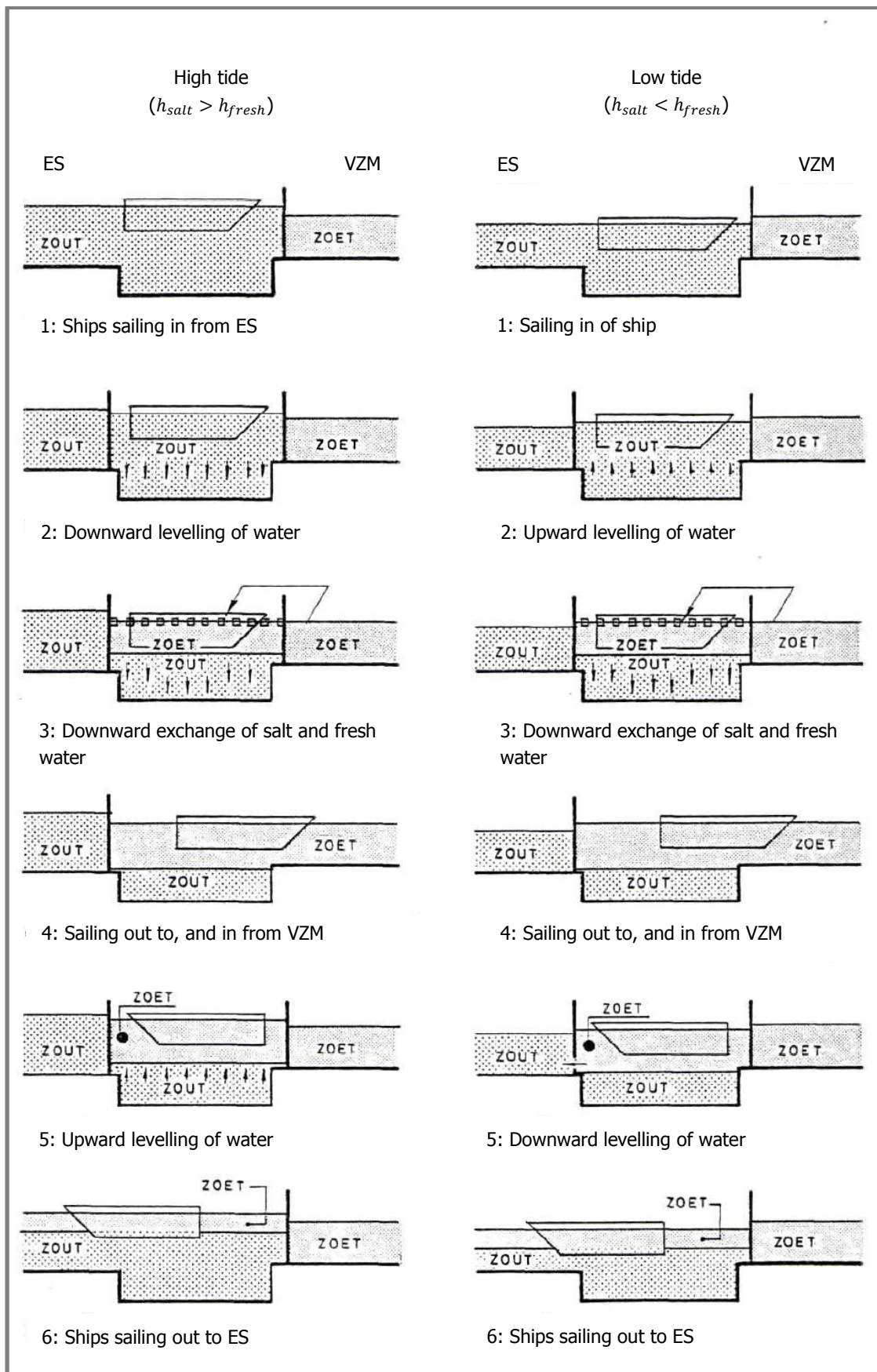


Figure 57: Schematisation of a locking cycle at the Krammer recreational locks. Adapted from (Rijkswaterstaat, 1981). ('zout'=salt, 'zoet'=fresh)

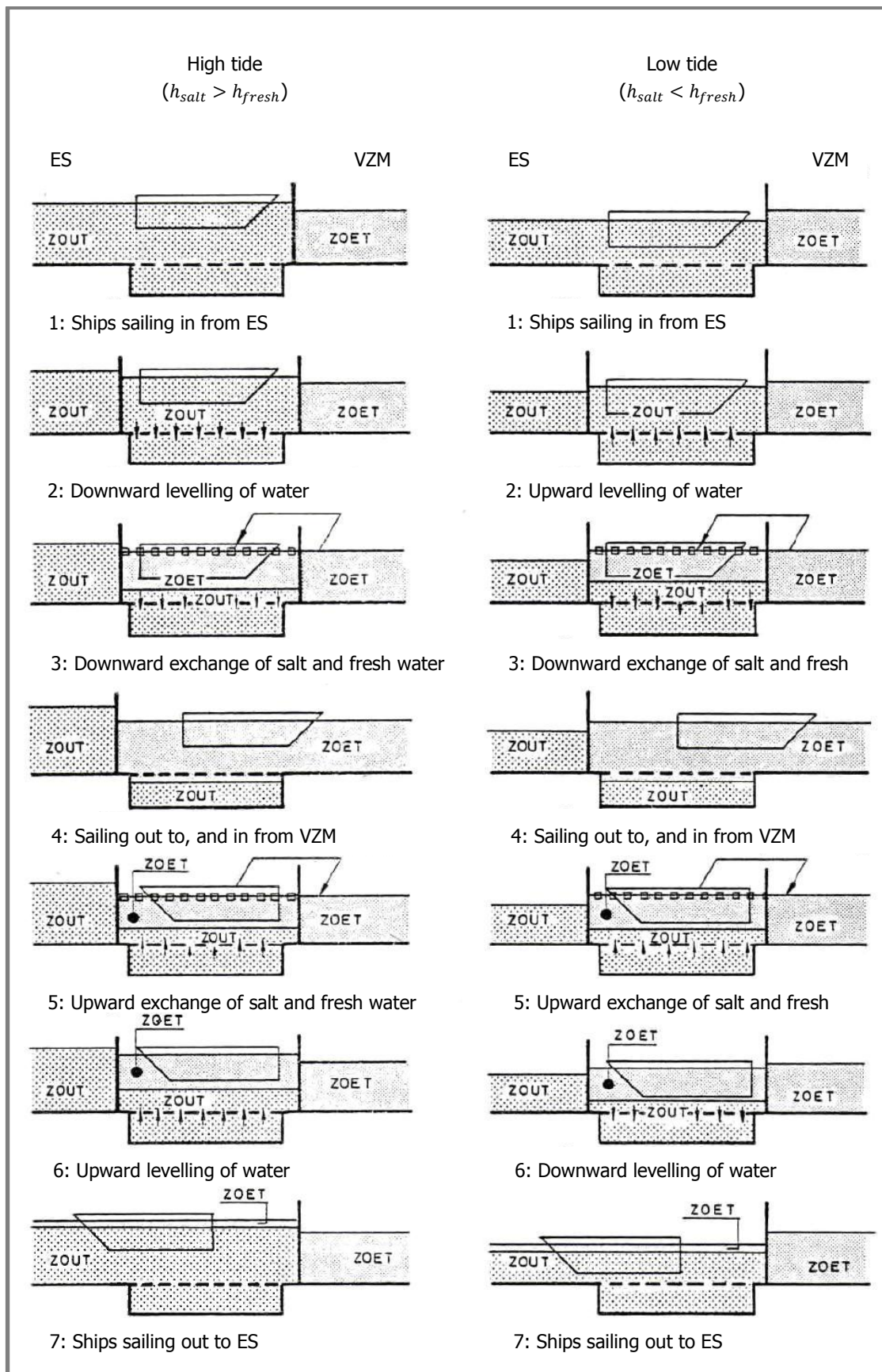


Figure 58: Schematisation of a locking cycle at the Krammer commercial locks. Adapted from (Rijkswaterstaat, 1981). ('zout'=salt, 'zoet'=fresh)

Appendix

C. Mean high and low water

The tide makes the water of the ES move up and down. This movement is very much like a sine-function. It is assumed exactly as a sine-function to calculate the mean water levels when the tide is approximated by two discrete water levels; one for high water and one for low water, both present half of the time. Figure 59 shows this in a graph. The water levels are calculated in Eq. 0.1.

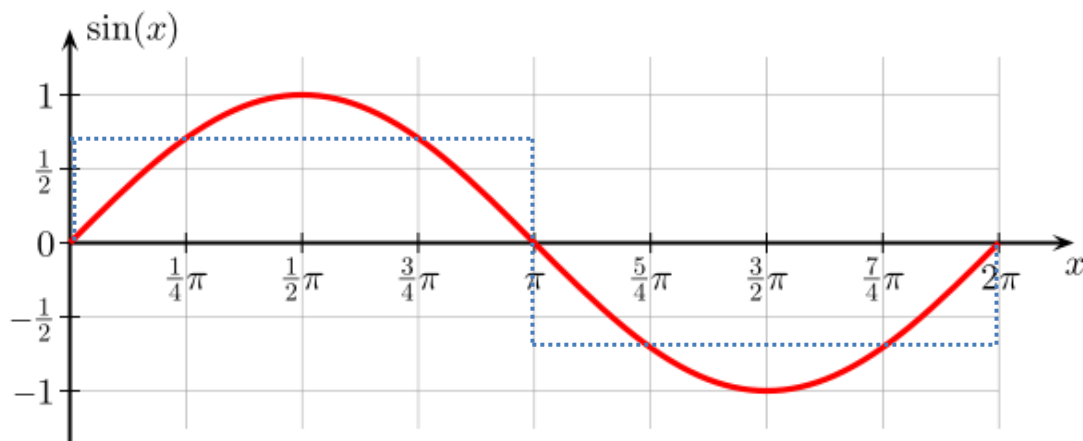


Figure 59: Tide (red), represented as two discrete water levels (blue).

$$\text{Mean tidal amplitude} = \frac{1}{2} \cdot x_{\text{tidal range}} \cdot y_{\text{mean}} = 0.98 \text{ m}$$

Eq. 0.1

With:

$x_{\text{tidal range}}$	3.08 m
y_{mean}	$\frac{1}{2} \cdot A_{\text{sine}} / \pi = \frac{2}{\pi} = 0.64$
$\frac{1}{2} \cdot A_{\text{sine}}$	$\int_0^\pi \sin x \, dx = [-\cos x]_0^\pi = 2$

Eq. 0.1 shows the mean tidal amplitude. Conservatively, a value of 1 m is assumed. The mean water level at ES is +0.1 m NAP, which results in the following mean extreme water levels:

- HW: +1.1 m NAP
- LW: -0.9 m NAP

Appendix

D. Calculation of pipe capacity in the pilot

In this appendix, calculations are made of the required diameters for the air and water supply pipes with the known required discharges of the pilot's design.

The calculation method can be used for other configurations as well.

D.1. Air bubble screen supply pipes

To calculate the dimensions of the supply pipes, the minimum water height above the outflow openings has to be used. Maybe the maximum water height seems more logical to apply, but Figure 60 explains why that is not correct in this case.

The maximum flow velocity is limited to 10 m/s . In this way friction is accepted to be relatively small for air flow in pipes. Each supply pipe feeds one strand, which has a maximum capacity of 88.5 NI/s .

The calculated minimum required diameter for a supply pipe per strand is displayed in Eq. 0.2. The actual diameter of the pipes to be installed will depend on available standard sizes of the pipes. Therefore, a rounded value of 8 cm is chosen for each supply pipe. The maximum occurring flow velocity becomes 7.9 m/s which is shown in Eq. 0.3.

Three compressors are installed with a total power of 120 kW . The pipes are able to resist a pressure of 3 bar .

Why minimum water height?

Why should the minimum water height over a pipe be used in air flow velocity calculations?

The fact that a difference is present is about air being in compression at outflow. Air discharge is expressed in Nl/s . When air is in compression, the same amount of air is present in a smaller volume.

For a constant discharge in Nl/s , gas has a lower flow velocity at higher compression. The other way around: the highest flow velocity occurs at the lowest air compression – which is present at the lowest water level.

Consider a constant discharge, expressed in Nl/s . Consider two pipes with equal diameter; one with compressed air and one with uncompressed air. When in both pipes an equal volume (expressed in Nl/s) passes, the actual passing volume of compressed air is smaller. For that reason the compressed air runs a smaller distance than the uncompressed air, when an equal amount of air (again, expressed in Nl/s) is displaced. This agrees with a smaller flow velocity for the compressed air.

Since the maximum flow velocity is governing, the lowest air compression must be used in calculations regarding maximum pipe flow velocity. The minimum water depth must be used.

(This does not hold for water pipe flow velocities, since water is much less compressible and the required energy is distracted from the manometric head instead of the water column above opening.)

Figure 60: Intermezzo which explains why the minimum water height must be used for the air pipe flow velocity calculations.

Krammer recreational lock:

At the ES side a *maximum* water column of 6.2 metres is present.

From the level of the sill: -3.7 m NAP

To the highest occurring water level when the lock is still operational: $+2.5 \text{ m NAP}$

At the ES side a *minimum* water column of 1.35 metres is present.

From the level of the sill: -3.7 m NAP

To the lowest occurring water level when the lock is still operational: -2.35 m NAP

At the VZM side a water column of 2.7 metres is present.

From the level of the sill: -2.7 m NAP

To the level of the maintained water level of the VZM: 0 m NAP

Krammer commercial lock:

At the ES side a *minimum* water column of 3.9 metres is present.

From the level of the perforated bottom: -6.25 m NAP

To the lowest occurring water level when the lock is still operational: -2.35 m NAP

In calculations, a total pressure loss Δp of $12.35 \text{ mwc} = 1.235 \text{ bar}$ is used. This value is obtained by:

- Regulator $1 \text{ bar} = 10 \text{ mwc}$
- Diffusor 0.5 mwc
- Pipes 0.5 mwc
- Minimum water depth 1.35 mwc

The working pressure p is 1 bar higher, since the atmospheric pressure must be added:

- Atmospheric pressure $1 \text{ bar} = 10 \text{ mwc}$

v_{actual}	Actual flow velocity in supply pipe $\left[\frac{\text{m}}{\text{s}}\right]$
Q_p	Air discharge of compressed air $\left[\frac{\text{m}^3}{\text{s}}\right]$
Q	Air discharge $\left[\frac{\text{m}^3}{\text{s}}\right]$
p	Working air pressure $[\text{bar}]$
p_{atm}	Atmospheric air pressure $[\text{bar}]$
Δp	Pressure loss $[\text{bar}]$

Δh_{total}	Total water head difference [m]
h_{min}	Minimum water head above air reservoir [m]
Σh_{losses}	Water head losses over components in system [m]
A	Area of cross-section of pipe [m ²]
r	Radius of pipe [m]
d_{actual}	Actual diameter of supply pipe [m]
d_{needed}	Needed diameter of supply pipe [m]
v_{max}	Determined maximum flow velocity in pipes $\left[\frac{m}{s}\right]$

$$d_{needed} = \sqrt{\frac{\frac{Q}{p}}{\frac{1}{4}\pi \cdot v_{max}}} = 7.1 \cdot 10^{-2} m$$

Eq. 0.2

With:	Q	$88.5 \text{ Nl/s} = 8.85 \cdot 10^{-2} \text{ Nm}^3/\text{s}$
	p	$p_{atm} + \Delta p = 2.235 \text{ bar}$
	p_{atm}	1 bar
	Δp	$\frac{1}{10} \cdot \Delta h_{total} = 1.235 \text{ bar}$
	Δh_{total}	$h_{min} + \Sigma h_{losses} = 1.35 + 10 + 0.5 + 0.5 = 1.235 \cdot 10^1 m$
	v_{max}	$1.0 \cdot 10^1 \text{ m/s}$

$$v_{actual} = \frac{Q_p}{A} = 7.878 \text{ m/s}$$

Eq. 0.3

With:	Q_p	$\frac{Q}{p} = 3.960 \cdot 10^{-2} \text{ m}^3/\text{s}$
	A	$\pi \cdot r^2 = 5.03 \cdot 10^{-3} \text{ m}^2$
	r	$\frac{d_{actual}}{2} = 4.0 \cdot 10^{-2} m$
	d_{actual}	$8.0 \cdot 10^{-2} m$

D.2. Water screen supply pipes

High flow velocities in pipes result in disproportionate high resistance, accompanied with high energy consumption. For this reason, a maximum velocity of 4 m/s is assumed. Because the 9 metre long reservoir is divided in two sections with their own supply pipe, each pipe has to be able to handle up to $0.7 \text{ m}^3/\text{s}$ at a maximum flow velocity of 4 m/s .

The exact diameter for which the pipe velocity doesn't exceed its maximum is displayed in Eq. 0.4. The actual diameter of pipes to be installed depends on the available standard pipe sizes. A rounded value is chosen, which results in a diameter of 500 mm for both supply pipes. With this chosen diameter, the actual maximum occurring flow velocity becomes 3.57 m/s and is displayed in Eq. 0.5.

Two water pumps are installed with a total power of 110 kW .

At the ES side a maximum water column of 6.2 metres is present.

From the level of the sill: -3.7 m NAP

To the highest occurring water level when the lock is still operational: $+2.5 \text{ m NAP}$

v_{actual}	Actual flow velocity in pipe $\left[\frac{\text{m}}{\text{s}}\right]$
Q	Water discharge $\left[\frac{\text{m}^3}{\text{s}}\right]$
A	Area of cross-section of pipe $[\text{m}^2]$
r	Radius of pipe $[\text{m}]$
d_{actual}	Actual diameter of pipe $[\text{m}]$
d_{needed}	Needed diameter of pipe $[\text{m}]$
v_{max}	Determined maximum flow velocity in pipes

$$d_{needed} = \sqrt{\frac{4 \cdot \left(\frac{Q}{v_{max}}\right)}{\pi}} = 0.472 \text{ m}$$

Eq. 0.4

With:	Q	$0.7 \text{ m}^3/\text{s}$
	v_{max}	4.0 m/s

$$v_{actual} = \frac{Q}{A} = 3.57 \text{ m/s}$$

Eq. 0.5

With:	Q	$0.7 \text{ m}^3/\text{s}$
	A	$\pi \cdot r^2 = 0.196 \text{ m}^2$
	r	$\frac{d_{actual}}{2} = 0.250 \text{ m}$
	d_{actual}	0.500 m

Appendix

E. Concepts for movable sill

Descriptions of different concepts on basic movement of the movable sill are presented in E.1. After that, E.2 contains explanations for the ratings of the concepts.

E.1. Description of concepts

A description of the concept is followed by a sketch of the basic movement. All seven concepts are evaluated in terms of the twelve features described below this paragraph. If beneficial, they are listed under 'advantages'; if unprofitable, they are listed under 'disadvantages'.

- Constructability
- Investment costs
- Operational costs *(Equivalent to energy consumption)*
- Operation time
- Wall connection *(Water tight connection at the sides)*
- Height adjustability
- Maintenance
- Parts under water *(Corrosive conditions affect under water parts)*
- Collision effects
- Hydraulic circumstances *(Resistance to hydraulic loads)*
- Sediment *(Settlement on top of the structure)*
- Experience

In visualisations in this appendix, the sill is shown as a movable box. It gives no information on how this box is filled in. It can be a steel hollow box, but also some sort of cloth or a structure built up from telescopic elements. This is elaborated in appendix F.

The presented features are not quantified, but serve the goal of informing about possibilities per concept.

E.1.1. RF Rotating flap

A simple flap provides a barrier for salt water. The flap can be rotated up- and downwards. The flap rotates from lying down to the 'upright' position, which means it makes an angle with the bottom in the order of 30° - 45° . The driving mechanism that rotates the flap can be realised in several ways, i.e.: Hydraulic cylinders, a hollow box filled with air/water, a bellow between bottom and flaps at the hinge or a cable connected to a winch.

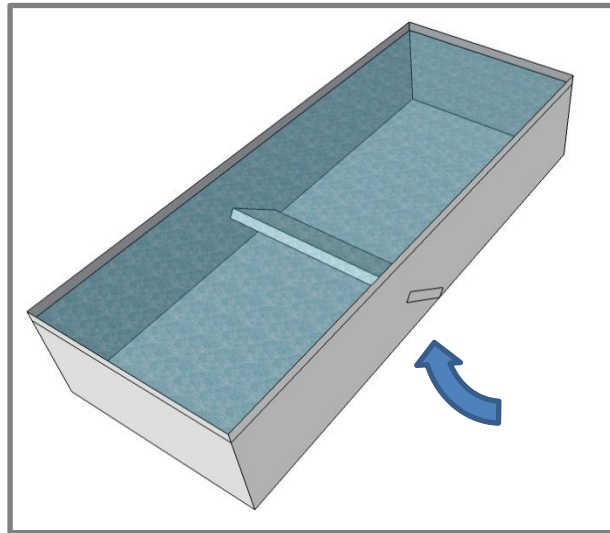


Figure 61: Concept 1 – Rotating flap.

Advantages:

- Construction of the flap is not hard. Construction in a dry lock chamber is easiest; else a structure on a concrete slab is possible. The slab can be placed in the wet lock chamber after construction.
- Energy consumption is low for the driving of the flap.
- The structure can be put in its upright position quite fast.
- The connection with the wall is relatively simple. Flaps with rubber sides can close tightly. Another option is a more complex structure which pushes itself stuck between the two lock chamber walls.
- The structure is adjustable in height.
- If the structure is placed on a concrete slab, it can be lifted out for maintenance. If not, a dry lock chamber still provides for easy maintaining actions.
- It is possible to create a driving mechanism above the water. In this way maintenance will be easier and less disturbing, since possible shutdowns can be prevented.

Disadvantages:

- If the driving mechanism of the flap is located under water, this would be a weak spot in the design.
- A collision will be bad for the ship as well as for the flap.
- Hydraulic forces can be a problem for this design. Forces exerted on the backside of the flaps have to be encountered by cables or metal strips. Else, the flaps could break from the hinges.
- If sediment deposits behind the flaps, the flaps will not be able to lie down on the bottom entirely. This will decrease the hydraulic perimeter. This effect is expected to be marginal, since sediment carrying flows are blocked by the sill itself.
- There is no experience with this technique for this purpose. Flaps as these do exist as barrier for small water depths.

E.1.2. RS Rotating segment

A segment can be rotated upwards. The segment can be visualised as a cylinder cut in half along the longitudinal axis. When rotated upwards, it blocks the lower part of the lock chamber. Rotated downwards, the structure doesn't reach higher than the locks bottom and does not affect the navigable depth.

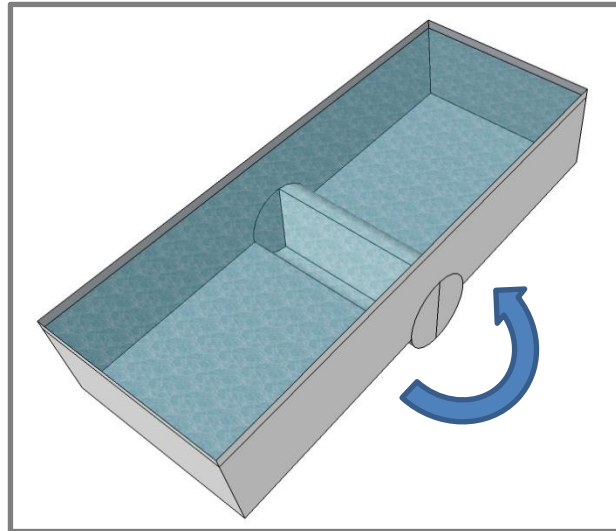


Figure 62: Concept 2 – Rotating segment.

Advantages:

- Energy consumption is not very high for the driving of the segment.
- The structure can be rotated in its upright position quite fast.
- The water tight connection with the wall is easy, since it will be in direct connection with the rest of the cylinder segment.
- The height of the sill can be easily controlled.
- Maintenance in a dry dock is relatively easy.
- The driving mechanism can be constructed out of the water. (Disadvantage is that this will probably result in a construction in already existing concrete.)
- The structure is able to cope with the hydraulic loads exerted on it quite easily. It should be made stiff enough, though.

Disadvantages:

- Construction will not be easy. The structure has to be secured in the lock walls. Maybe it is enough only to use milling cutters to create space for this purpose; else it will be an even more expensive option.
- A collision will result in high impact on ship and structure.
- Sediment can be a problem for the solution. If the cylinder rotates, a hole in the bottom remains. This hole has to be covered rather tight. If sediment comes into this area, the segment is not able to rotate back completely. In that case, the hydraulic perimeter decreases.
- There is experience with the technique as a barrier, not as a solution to salt intrusion problems.

E.1.3. RG Rotating split gates

Revolving gates can be split in two independent turning parts. The lower part can be left closed when the upper part of the gates open. In this way a barrier is formed.

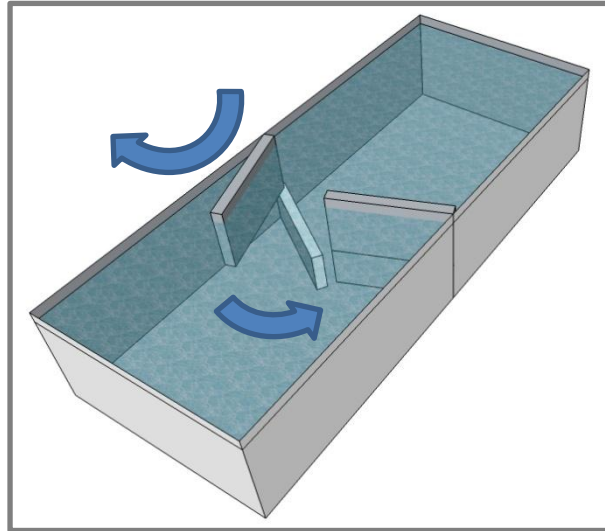


Figure 63: Concept 3 – Rotating split gates.

Advantages:

- A major advantage is that existing gates can be reused (if revolving gates are present in the lock). Also beneficial is the possibility of an adaption of the gates in dry conditions. The gates have to be lifted out of the water when the other gates are closed.
- Operation is energy economic.
- The sill is quickly in use.
- The connection with the wall is easy, since it shouldn't have to be adapted compared with the old situation.
- Maintenance is not hard, since the structure isn't sensitive to wear. If it is needed, the gate can be lifted out of the water for relatively easy repair actions.
- The structure will be able to withstand hydraulic forces rather good. The lower barrier is comparable strong as the gate itself.
- Sediment won't be a problem, since the propulsion of the gate will be strong enough to push possible deposits aside.

Disadvantages:

- The height of the sill can't be adapted.
- There has to be some sort of locking switch under water, which allows the lower part of the gate to be attached to the upper part of the gate or not. Also a (more expensive) own propulsion system can be an option. Both of these options will be located under water, and may be weak spots in the design.
- A possible collision will have large effects on the ship as well as on the gate structure.
- There is no experience with split revolving gates yet. A new hinge in an existing gate could therefore lead to problematic design.

E.1.4. *TS* (*v*) Translating slider (vertical)

A barrier is created by allowing a slider to move up and down. In its upright position it is still submerged and only forming a barrier to block salt water. Sunken down, the top of the barrier is levelled with the locks bottom and doesn't alter the hydraulic perimeter.

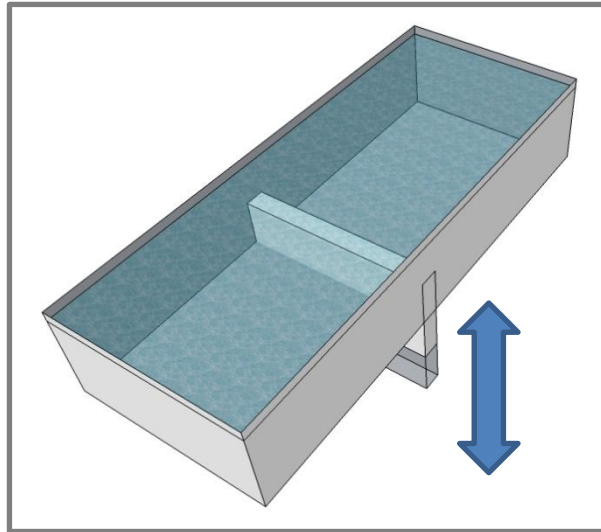


Figure 64: Concept 4 – Translating vertical slider.

Advantages:

- A major disadvantage is that the structure is located underneath the existing locks bottom. This makes construction very hard and very expensive. In the Krammer commercial lock, this doesn't play a role. The (perforated) bottom slabs can be easily lifted out and there is a roughly 5 m high area underneath that bottom. The dock can be set dry, so an implementation in this exact lock is not extra expensive, as this in regular locks would be.
(*So in case of the Krammer locks, this is an advantage.*)
- The control of the slider isn't expensive in terms of energy.
- If the slider is controlled comparable as a rolling gate, it can be closed and opened quite fast.
- The connection with the wall is relatively easy. For instance a slit along the wall of the lock in the concrete is possible.
- The height is adjustable. It is depending on the propulsion system whether this is an option, but if wished for, it is among the possibilities.
- The structure is located under water, but has as big advantage that a vertical driving mechanism can be located out of the water.
- Hydraulic forces are easily handled with. The slider can be made out of steel, allowing the forces to be directed to the concrete quite simple.
- There is experience with this type of sill; this is in favour of the reliability of the solution.

Disadvantages:

- A major disadvantage is that the structure is located underneath the existing locks bottom. This makes construction very hard and very expensive. (This does not hold for the Krammer commercial lock, due to the bottom slabs.)
- Maintenance of the structure is relatively hard. Especially when the driving mechanism for the slider is located under water as well.
- Effects after a possible collision are big for the ship, as well as for the structure.
- In its upright position, sediment can come into the slot of the slider. The slider won't be able to slide down completely.

E.1.5. $TS(h)$ Translating slider (horizontal)

A slider is located in a slot in the wall (instead of in the bottom as with the vertical slider). The slider is able to slide from the left to the right into the lock chamber, closing off the lower part of the chamber. When the slider is located in the slot in the wall, the hydraulic perimeter isn't decreased.

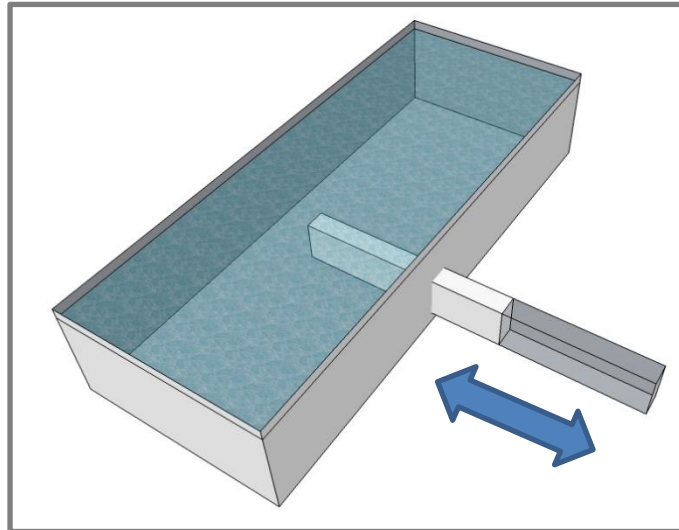


Figure 65: Concept 5 – Translating horizontal slider.

Advantages:

- The control of the slider isn't expensive in terms of energy.
- If the slider is controlled comparable as a rolling gate, it can be closed and opened quite fast.
- The connection with the wall is relatively easy. For instance a slit along the wall of the lock in the concrete is possible.
- Hydraulic forces are easily handled with. The slider can be made out of steel, allowing the forces to be directed to the concrete quite simple.
- There is experience with this type of sill; this is in favour of reliability of the solution.

Disadvantages:

- A major disadvantage is that the structure needs a slot for the slider alongside the lock chamber. This makes construction hard and very expensive.
- The height of the sill isn't adaptable.
- Maintenance of the structure is relatively hard. Especially when the driving mechanism for the slider is located under water as well.
- Effects after a possible collision are big for the ship, as well as for the structure.
- Sediment on the floor is not a bigger problem in this option than with regular rolling gates. (no disadvantage, nor an advantage)

E.1.6. TG Translating split rolling gate

Rolling (shifting, translating movement) gates can be split in two independent rolling parts. The lower part can be left closed when the upper part of the gate rolls open on top of the lower one. In this way a barrier is formed.

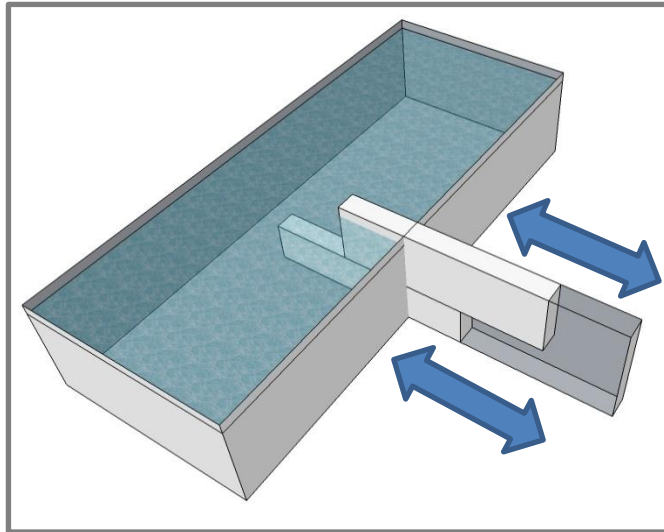


Figure 66: Concept 6 – Translating split rolling gate.

Advantages:

- Existing gates can be reused (if rolling gates are present in the lock). Also beneficial is the possibility of an adaption of the gates in dry conditions. The gates have to be lifted out of the water when the other gates are closed.
- Operation is energy economic.
- The sill is quickly in use.
- The connection with the wall is easy, since it shouldn't have to be adapted compared with the old situation.
- The structure will be able to withstand hydraulic forces rather good. The lower barrier is comparable strong as the gate itself.

Disadvantages:

- Reconstructing rolling gates will be a very expensive option.
- The height of the sill can't be adapted.
- Maintenance of the structure is not necessarily hard (gate can be lifted out of the water), but the rolling parts aren't insensitive to repairs either.
- Especially the rolling parts under water have to be inspected on a regular basis, to check whether they are subject to wear.
- A possible collision will have big effects on the ship as well as on the gate structure.
- Sediment on the floor is not a bigger problem in this option than with regular rolling gates. (no disadvantage, nor an advantage)
- There is no experience with split rolling gates yet.

E.1.7.7I Translating inflatable sill

A rubber flexible sill is inflated. A submerged barrier is formed by the elongated balloon at the bottom.

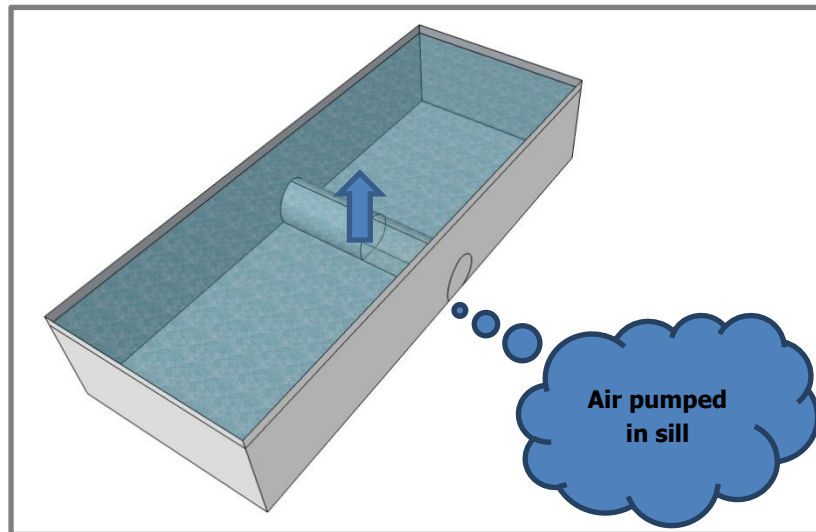


Figure 67: Concept 7 – Translating inflatable sill.

Advantages:

- Construction in wet conditions is not necessary.
- Maintenance is relatively easy due to the fact that the air pumps are situated out of the water.
- All parts that are located under water are not sensitive to repairs.
- Damage to ships after a possible collision is marginal.
- Possible sedimentation is no problem, since the sill is filled from the inside and causes the sediment to fall off of the elevated body.
- There is experience with the technique as a barrier or weir, not as salt intrusion countermeasure. The experience can be used in the design of this solution.

Disadvantages:

- Operation costs a lot of energy.
- It takes a lot of time before the sill is completely filled with air and is in its upright position.
- The connection with the wall is not easy. If a simple balloon is used, salt leaks past the structure. A solution can be the implementation of a flap, which is pushed upwards by the inflatable part.
- The structure is not adjustable in height. The sill only functions when it is fully filled with air and has some stiffness. A solution to allow height adjustability can be to roll a metal bar over the rubber at the bottom, but this seems like an unreliable option.
- Damage to the sill after a possible collision may be significant.
- The sill is flexible, which causes it to move when subjected to high (hydraulic) forces. This will decrease the effectiveness of the salt intrusion blockage.

E.2. Reasoning of concepts ratings

The rating of the concepts to the twelve features is explained here. Also the features are ranked in terms of importance to be able to make a weighted rating of the concepts.

Only four of the seven concepts are described here. A conclusion in section 2.4 stated that three concepts were not applicable, because they don't adjust in height easy.

E.2.1. RF Rotating flap

Feature	Ranking	Description
Constructability	10	Construction is possible in dry conditions and no adaptations have to be made to the current structure.
Investment costs	8	Costs needed for construction are relatively low.
Operational costs	10	Energy consumption is low.
Operation time	9	Depending on the driving mechanism. Only with compressed air it will take a lot of time to become operational, else it will be very fast.
Wall connection	6	A water tight wall connection needs some adaptations of the current wall, but is well makeable. This connection covers a relatively small length (two short sides) and can be water tight.
Height adjustability	3	The flap can be adjusted in height, but is hard to lock at a given depth securely.
Maintenance	8	Maintaining will be based on the driving mechanism mainly. If able to be lifted out of the water, it is quite easy to perform.
Parts under water	4	The driving mechanism of the flap can be located above water. Since this is not possible in vertical direction, it will result in a large adjustment to the concrete of the lock.
Collision effects	1	Collision will be harmful for both the ship as the flap.
Hydraulic circumstances	5	Extra measures need to be taken in order to protect failure of the structure due to hydraulic forces.
Sediment	6	Sediment is of bad influence to the navigable depth if it causes the flaps to be blocked at lying down on the lock bottom. Even though it is thought the effects are marginal, it has to be investigated or tested.
Experience	5	Only experience with the technique for other purposes and at a small scale is available.

E.2.2. RS Rotating segment

Feature	Ranking	Description
Constructability	4	Main parts of the structure can be made prefabricated, but the current walls of the lock chamber have to be adapted. This will probably be a costly engineering work. For the part of the structure that will be situated below the current lock floor, there will be enough space if some perforated bottom floor slabs will be removed.
Investment costs	4	The construction costs of the segment itself are probably slightly higher than the costs of the sill. The adaptations to the

		current lock walls will be expensive in engineering and execution.
Operational costs	10	Energy consumption is low, just as with the flap.
Operation time	10	The driving mechanism will be able to rotate the segment very fast.
Wall connection	10	The connection with the wall is provided by the prefabricated segment itself and does not need adaptations of other parts of any kind. The connection with the bottom is easily water tight when the segment is realised as a half cylinder.
Height adjustability	10	The segment can be adjusted in height in detail, and is fixed at its height by locking the driving mechanism. If this is for instance done with cogwheels, it is really easy.
Maintenance	3	Maintenance of the segment itself is easy if the segment can be lifted out of the water. The driving mechanism will be harder, since this will be situated under water.
Parts under water	1	The driving mechanism of the segment will most probably be located under water.
Collision effects	1	Collision will be harmful for both the ship as the segment.
Hydraulic circumstances	10	The stiff segment can easily cope with hydraulic loads.
Sediment	5	The open space underneath the segment if it is in its upright position can get filled with sediment. The navigable depth of the lock is in danger if this occurs.
Experience	8	There is experience with segment gates in barriers. This technique can be used in the design of this smaller sill.

E.2.3. *TS* (*v*) Translating slider (vertical)

Feature	Ranking	Description
Constructability	7	If some bottom slabs are removed from the lock chamber floor, there is enough space for a slider of approximately 5 metres high. Only small adaptations to current structure are probably necessary. The slider can be made prefabricated. The structure can be installed in dry conditions.
Investment costs	7	Costs will be comparable with the flap, but the driving mechanism is expected to be more expensive.
Operational costs	10	Energy consumption is low, just as with the flap and the segment.
Operation time	10	The driving mechanism will be able to pull up the slider very fast.
Wall connection	9	A water tight connection is formed not as easily as with the segment, but is still very well makeable by the use of a hard rubber for instance. Just as with the flap, this connection covers a relatively small length (two short sides) and can be water tight.
Height adjustability	8	The height is adjustable in detail and quite easily; the fixture at that height is less simple.
Maintenance	3	Maintenance of the segment itself is easy if the segment can be lifted out of the water. The driving mechanism will be harder, since this will most probably be situated under water.
Parts under water	8	A vertical driving mechanism can be located out of the water.
Collision effects	1	Collision will be harmful for both the ship as the slider.

Hydraulic circumstances	9	The slider is just as the segment able to cope with hydraulic loads easily. Beneficial to the segment compared with the slider is that it is fixed at both opposing ends. That is why the slider is ranked just below the segment.
Sediment	5	Just as with the segment, the open space underneath the slider if it is in its upright position can get filled with sediment. The navigable depth of the lock is in danger if this occurs.
Experience	10	There is experience with translating sliders at the same scale, not for this purpose though.

E.2.4. TI Translating inflatable sill

Feature	Ranking	Description
Constructability	10	The structure can be made in dry conditions if it is installed on a slab which is later placed in position.
Investment costs	1	The costs of the bellow will be the highest compared with the other three options. The rubber has to be prefabricated and the connection with the compressor units is not very easy.
Operational costs	1	Operational costs are high, since compressors fill the bellow with air. The compressors have to maintain the delivered pressure to prevent a collapse of the bellow under water pressure.
Operation time	1	Compared with the other options, this is the slowest to become operational. Compressed air will fill the bellow by the use of compressors.
Wall connection	3	A water tight connection with the wall is hard to make. It is possible by a complex wall-rubber connection as done at the Dutch <i>Ramspol barrier</i> . This is very expensive. ⁴⁶
Height adjustability	1	Height adjustability is hard to achieve. There are possibilities to do this, but these have to be worked out in great detail before their effectiveness is proved.
Maintenance	6	Maintaining will be quite easy if the entire structure is able to be lifted out of the water. Perhaps, the rubber bellow needs to be replaced every few years. This could be costly. The compressors can be maintained at their location next to the lock (dry).
Parts under water	10	The compressors which provide air for the bellow can be situated out of the water. Only the bellow and pipes leading to the bellow are under water.
Collision effects	8	Collision will not be harmful for the ship. The bellow may get affected by a collision, but is quite flexible.
Hydraulic circumstances	1	The flexible bellow is able to move under high loads. This decreases the effect of salt intrusion prevention.
Sediment	10	Settled sediment on top of the bellow does not interfere with its functionality.
Experience	10	There is experience with rubber bellows at a larger scale, not for this purpose though.

⁴⁶ This situation can be evaded by using the bellow as driving mechanism for a flap to move up and down. This is not taken into account here, because that will result in a significant other design

E.2.5. Weight factors

Feature	Ranking	Description
Constructability	7	How the structure is formed is very important, but engineering difficulties can be overcome.
Investment costs	8	The costs needed to build the structure are also very important, but not as much as operational costs. That's why it is ranked slightly lower.
Operational costs	10	Operational costs are for all alternatives low, except for the rubber bellow. For that reason either a 10, or a 1 is marked for the different alternatives. The importance is then expressed in the weight factor. Since operational costs will increase the total costs significantly, a high weight factor is given to this important feature.
Operation time	2	The operation time is quite determining for the amount of salt leakage. It is possible to activate the barrier (each type), before the gates open, though. In this way the effect of a slow operational time can be diminished.
Wall connection	8	The wall connection determines the effectiveness of the solution. Without a water tight connection, salt seeps alongside the barrier. It is important to create a good connection. That is why this feature is ranked high.
Height adjustability	10	Height adjustability is one of the most important features. Since the situation is subject to a large tidal range, height adjustability improves effectiveness significantly. (tidal range $\pm 3\text{ m}$; average depth $\pm 6\text{ m}$)
Maintenance	5	Maintenance is important, but not decisive for the choice of the best solution.
Parts under water	8	Especially in terms of corrosion, parts under water can make the design more complex. To prevent this, other materials can be used. But the driving mechanism is beneficial above water.
Collision effects	4	The rubber bellow may get affected by a collision, but it's expected that effects will be marginal. All other alternatives will have major impacts. It is important to take notice of possible effects of collision, but in the choice for this matter, it's taken to be less important than features as costs and effectiveness.
Hydraulic circumstances	1	The design can be adapted to withstand the expected hydraulic loads.
Sediment	1	The effects of the presence of sediment on the concept structures is expected to be marginal. If sediment settles in small spaces underneath parts of the structure, high water velocities will probably induce the sediment to relocate.
Experience	2	It is useful to have some experience with the technique, but if a design sounds promising when tested to more important features, a lack of experience isn't always a problem.

Appendix

F. Solution for gap under sill's screens

The layout of the water retaining part of the sill is elaborated in this appendix. After a description of the possibilities, an MCA is worked out to analyse different options.

F.1. Alternatives

Basically two possibilities can be pointed out. The connector can be made of stiff or flexible material. A stiff connector will be box-shaped, constructed from steel or concrete. A flexible connector has a fixed (stiff) top, but has a body fabricated from rubber or plastic.

Examples can be seen in Figure 68 and Figure 69.

A reasoning of the ratings per concepts is presented in Table 29 and Table 30. Some weight factors altered compared with the factors used previously in appendix E. These are explained in Table 28.

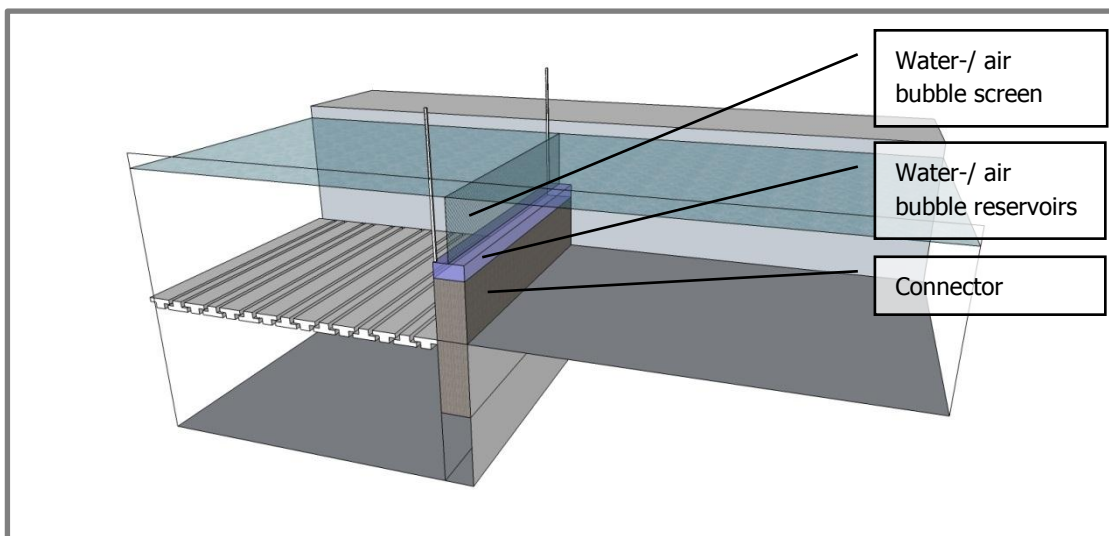


Figure 68: Connector consists of stiff box-shape. In light blue the air bubble- and water screen.

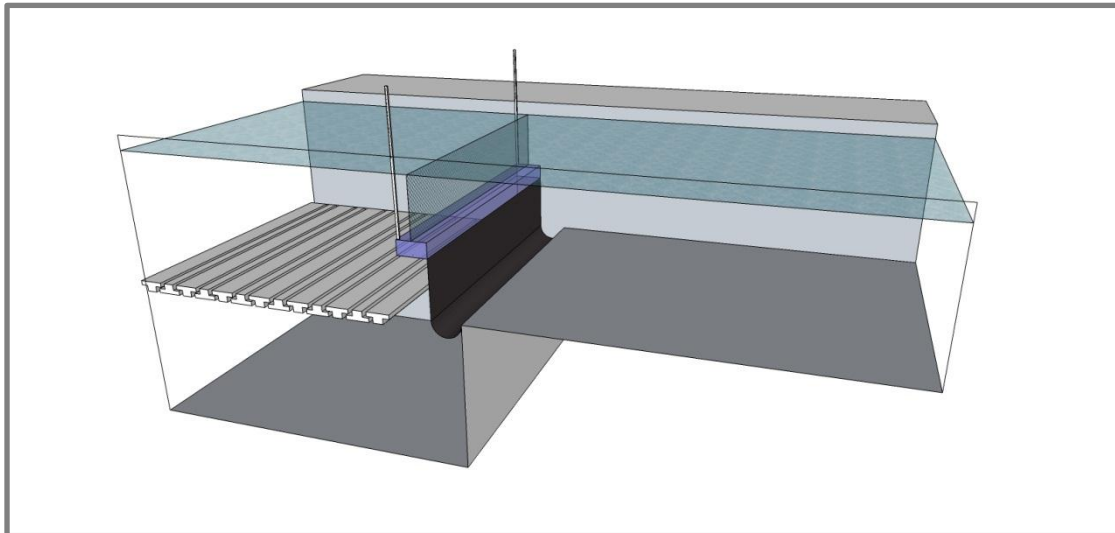


Figure 69: Connector consists of flexible sheet. In light blue the air bubble- and water screen.

F.2. MCA

An MCA is worked out to gain insight in the best possibility for the layout of the connector. The reasoning of all ratings is presented in the MCA in Table 28. The ranking of the features itself is visible in Table 31.

Both options are ranked to the same features as used before in the MCA in section 4.2, taking into account the following two changes and resulting in the list of eleven features below:

- 'Operation time' and 'height adjustability' are not included in this MCA. Those were features, which made a difference in the choice for basic movements of the sill. For the choice of the layout of the connector, they are of minor importance.
 - One feature is added: 'Sill heightening above four metres'. As pointed out earlier, it is wished for to be able to raise the sill higher than four metres.
-
- | | |
|--------------------------------------|--|
| ▪ Constructability | |
| ▪ Investment costs | |
| ▪ Operational costs | <i>(Equivalent to energy consumption)</i> |
| ▪ Wall connection | <i>(Water tight connection at the sides)</i> |
| ▪ Maintenance | |
| ▪ Parts under water | <i>(Corrosive conditions affect under water parts)</i> |
| ▪ Collision effects | |
| ▪ Hydraulic circumstances | <i>(Resistance to hydraulic loads)</i> |
| ▪ Sediment | <i>(Settlement on top of the structure)</i> |
| ▪ Experience | |
| ▪ Sill heightening above four metres | |

Table 28: MCA of connector.

	Feature	Rating of feature	Weight factor	Rating	
				Box	Sheet
1	Constructability	7	11%	10	10
2	Investment costs	8	12%	10	4
3	Operational costs	6	9%	6	10
4	Wall connection	10	15%	7	1
5	Maintenance	10	15%	5	8
6	Parts under water	6	9%	4	10
7	Collision effects	4	6%	4	6
8	Hydraulic circumstances	1	2%	6	7
9	Sediment	1	2%	5	10
10	Experience	2	3%	10	1
11	Height adjustable > 4 m	10	15%	5	9
Total:			100%		
			Unweighted rating:	6.5	6.9
			Weighted rating:	6.6	6.8

The MCA shows a minor difference between both options in advantage of the flexible connector. After weighing of the ratings the difference becomes even smaller.

Since the total outcome is approximately equal, individual features are observed to compare the different configurations. It then becomes clear that an almost equal total outcome doesn't come from an almost equal rating per feature. On the contrary; many features ranked high for an option, are ranked low for the other option – and the other way around.

This outcome is understandable, since in a comparison of both options, they have their own benefits and drawbacks.

Both options are relatively easy to construct. The sheet is a more expensive option in terms of initial costs, but is certainly more durable. Less maintenance is needed and no corrosion is able to occur. The sheet has fewer problems with sediment, since it has no openings where it's able to accumulate. In terms of a larger height than four metres, the sheet is preferred as well.

The box, on the other hand, is less expensive in terms of initial costs. It's much heavier than the sheet; a heavier design means also a heavier driving mechanism and more energy consumption for the movements of the structure. A water tight wall connection is relatively easy for the box. When the box is compared with a lift gate, much experience is available for the construction of this type of structure.

Table 29: Descriptions of box.

Feature	Ranking	Description
Constructability	10	Both types can be prefabricated, which is favourable for constructability. Both are ranked high for that.
Investment costs	10	A steel or concrete box is relatively easy to make. With casting or welding, a box can be adapted to the desired dimensions. It is assumed that investment costs are not high for that reason.
Operational costs	6	A box will be heavier than a sheet and consume more energy

		for sill operating.
Wall connection	7	The wall connection of a box is better than of a sheet, because of its stiffness. It is able to block the entire wetted cross-sectional area.
Maintenance	5	If the box is made of steel, stainless material should be used or it corrodes heavily in salty conditions.
Parts under water	4	A steel box will corrode.
Collision effects	4	Collision is at both types a problem. The box is probably heavier and leaves the colliding object with more damage than the light sheet.
Hydraulic circumstances	6	Both types are designed to withstand the loads which can possibly be exerted on them, and should be rated neutral for that reason.
Sediment	5	Sediment can enter between loose parts, which can be a problem.
Experience	10	A vertical sliding box for this purpose it not yet implemented anywhere. The concept has strong similarities with a lift gate, though.
Heightening > 4 m	5	There is a big difference whether the extra height above four metres is added to the design before or after placing of the structure in the lock complex. The box needs extra space and needs more adaptations to the lock.

Table 30: Descriptions of sheet.

Feature	Ranking	Description
Constructability	10	Both types can be prefabricated, which is favourable for constructability. Both are ranked high for that.
Investment costs	4	A sheet must be custom-made. This asks for more craftsmanship and is assumed to take more time.
Operational costs	10	Energy consumption for operating the sill will be much lower when a light sheet is applied instead of a heavy box.
Wall connection	1	A sheet has to be made stiff to prevent large gaps at the side walls to occur.
Maintenance	8	A sheet needs very low maintenance attention. Only the connections of the sheet need to be checked.
Parts under water	10	A sheet will be no problem in the water.
Collision effects	6	Even though a sheet is connected to some sort of horizontal bar, it will cause much less harm than a solid box.
Hydraulic circumstances	7	A sheet is ranked slightly higher than the box because it has less stiffness and more flexibility, which makes it better resistant/adjustable to high loads.
Sediment	10	Every time the sill moved up and down, settled sediment will fall of the sheet. A sheet has as advantage that no sediment can enter between loose parts.
Experience	1	This type of sheet as barrier is only known in total other configurations and dimensions. Therefore, the technique is accepted as inexperienced.
Heightening > 4 m	9	The sill only needs a longer sheet.

Almost the same weight factors are used as previously used for the same features in section E.2.5 of appendix E. All differing factors are presented below.

Table 31: Weight factors.

Feature	Ranking	Description
Operational costs	6	It is pointed out in 5.5 that the energy consumption of the driving mechanism is not significant compared with overall energy costs. For that reason the feature is ranked neutral.
Wall connection	10	The wall connection is very important in respect to the effectiveness of the solution. It is ranked high as a feature.
Maintenance	10	Maintenance is important, because the lock must be closed when big maintaining actions need to be taken. This is an expensive matter.
Parts under water	6	Much corrosion will increase the amount of required maintenance. The use of other materials decreases the occurrence of corrosion rather easy. Therefore the feature is less important.
Heightening > 4 m	10	The feature is ranked high because it may lead to a larger energy reduction of the air bubble- and water screens.

Appendix

G. Various reference projects

In this appendix, reference projects are inserted regarding the following subjects:

- Movable sill
- Air bubble screen
- Lift gate

G.1. Reference projects of movable sill

In this appendix, a short overview of projects or literature which encloses a movable sill as salt intrusion preventive measure is provided. Main goal is to inform on the current state of the technique. In the following summation, the successive subjects are mentioned.

- Quote stating that a realisation of the technique doesn't exist yet. (2000; Book *Sluisontwerp 2*)
- Realised movable sill in lock. (1966; Lake Washington, USA)
- Study to implementation of movable sill. (2010; Volkerak locks, The Netherlands)

Translated quote: (Rijkswaterstaat Bouwdienst, 2000b, pp. 21-27)

"That the system is not (yet) carried out, is because one is reluctant to a movable threshold underwater in a shipping route; also to the mechanical side, there are doubts."

The above quote is stated in a general handbook for lock design. This book is Dutch and originates from the year 2000. It says that a movable sill – in the book obtained as a sinking gate or as a hinged gate – does not exist yet. The movable sill in the Washington locks was built in 1966.

Given this fact, there is a reason to believe that there are more implementations of the technique, which are not generally known. Several handbooks and the internet are examined quite thoroughly, without success. Nevertheless, the Washington locks are used as reference project – in this case, solely.

Hiram M. Chittenden locks in Lake Washington⁴⁷

A salt water barrier is constructed in an existing lock in 1966. In this lock, vessels with a deep draught only pass the lock infrequently and not often. The original locks were built from 1911 to 1917.

The structure is hollow and made of welded steel. Five hinges connect the sill to the bottom of the lock chamber. 16 compartments, lined up in 2 horizontal lines are used for the buoyancy of the sill. The barrier is heightened by pumping air into the hollow structure. It is sunken down by letting water in. Figure 70 gives an overview.

⁴⁷ <http://oai.dtic.mil/oai/oai?verb=getRecord&metadataPrefix=html&identifier=ADA378475>

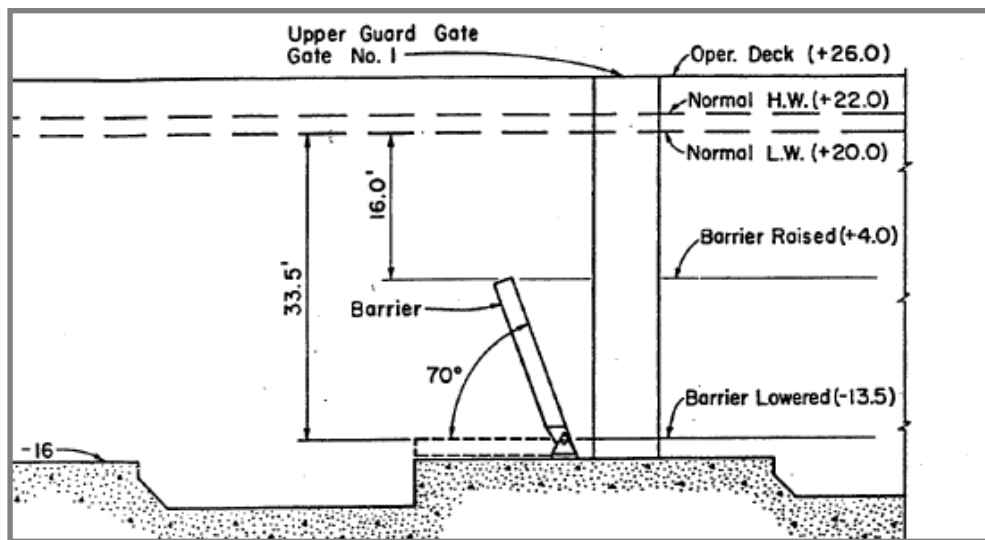


Figure 70: Fragment of cross section of lock with movable sill. Units are displayed in feet.

At its maximum upright position, more than half of the depth of the lock chamber can be blocked. So, if the sill is in its upright position, the salt water intrusion can theoretically be blocked from approximately 50 to 100%. Namely, if the salt water wedge doesn't reach the top of the sill, intrusion is fully reduced. When the salt wedge is as thick as the whole water depth, maximum half of the wedge thickness is able to flow over the sill. It must be said that in most cases the whole water column is salt, because of interchange of water and open lock gates at the salt water side. This means that the reduction of salt water intrusion is in most cases close to 50%.

Study to movable sill in Volkeraksluis

A study is performed to implement a salt intrusion preventive measure in the Volkerak locks. Air bubble screens, water screens and a movable sill are included in the study. It was concluded that the optimal design consisted of a movable sill in combination with one water screen and with one air bubble screen. The screens are situated behind the sill, all attached to the lock chamber floor.

The sill in the design is consisting of an inflatable air bellow and a 0.5 m thick metal flap. An example of this concept is visible in Figure 71. The sill in the design of the Volkerak locks is able to block the lower 1.3 m of the water column for salt intrusion. In its upright position, a navigational depth of 4.7 m is available above the sill. That is at a regular water level at both sides of the lock of approximately 0 m NAP and -0.2 m NAP.

The design is completed, but not realised yet. The reason for that is that a decision about the lake at one side of the lock made the design unnecessary. Both sides of the lock are fresh in the current situation namely. The lake would be turned into a salt water basin, but this is postponed to at least later than 2025.



Figure 71: Movable sill. Driving mechanism: Rubber bellow.

G.2. Reference projects of air bubble screens

In appendix A it is described what options are possible when it comes to salt intrusion prevention. In this section, some realisation of bubble screens are presented.

In A.1 the technique of air bubble screens is showed. Different types of screens are available, which differ mainly in effectiveness. The screens can be constructed out of one string, lying at the bottom. More often, a few of them are used to strengthen the effects of the air curtain. There is also a difference in effectiveness if the screens are applied at both sides of the lock chamber, instead of just one.

Current applications in the Netherlands are mainly s-bubble screens, applied at one side of the lock chamber. They are able to reduce the salt intrusion in the order of 35 to 40 %. An application at both sides of the lock chamber would increase this value to 45 or even 50 %.

Δ -Bubble screens are more effective. Research from *Deltares* resulted in a quantification of the different configurations. If applied at both sides of the lock chamber, a reduction of 70 % is possible. If two screens are combined with a fixed sill, salt intrusion can be reduced with approximately 80 %. If two screens are combined with a water screen, a reduction of approximately 85 % is possible.

When plans were laid down to turn the VZM salt again⁴⁸, studies were performed to the prevention of salt intrusion through the affected locks. Three lock complexes were taken a look at. The current salt leakage is provided. This value counts in the situation when no measures are taken. Per lock, a few countermeasures are quantified in terms of effectiveness and costs.

The mentioned air bubble screens in the following tables concern s-bubble screens⁴⁹.

⁴⁸ Currently postponed to at least 2025.

⁴⁹ The difference between s-bubble screens and Δ -bubble screens is explained in section A.1.1.

Table 32: Costs and effectiveness of several countermeasures of salt intrusion in the Volkerak locks. Adopted from (Rijkswaterstaat Bouwdienst, 2008).

Volkerak locks (Salt leakage ± 500 kg/s)	Approximate salt intrusion reduction [%]	Approximate costs [10^3€]
Air bubble screens at both gates of the lock	50	220
Fixed sill until deepest draught (1.3 m)	30	100
Movable sill which has to be lowered when deepest ships pass (2.6 m)	50	1,500
Combination of fixed sill (1.3 m) and bubble screen	70	330

Table 33: Costs and effectiveness of several countermeasures of salt intrusion in the Dintelsas locks. Adopted from (Rijkswaterstaat Bouwdienst, 2008).

Dintelsas locks (Salt leakage ± 40 kg/s)	Approximate salt intrusion reduction [%]	Approximate costs [10^3€]
Air bubble screens at both gates of the lock	50	80
Fixed sill until deepest draught (1.5 m)	35	50
Movable sill which has to be lowered when deepest ships pass (2 m)	50	450
Combination of movable sill (2 m) and bubble screen	85	150

Table 34: Costs and effectiveness of countermeasure of salt intrusion in the Benedensas locks. Adopted from (Rijkswaterstaat Bouwdienst, 2008).

Benedensas locks (Salt leakage ± 7 kg/s)	Approximate salt intrusion reduction [%]	Approximate costs [10^3€]
Air bubble screens at both gates of the lock	50	80

It can be seen that a fixed movable sill is the most economic efficient way to reduce salt intrusion through the different lock complexes. All other solutions are more expensive than they proportionally increase in reduction. It must be noted that the costs in the tables only display the initial construction costs. Especially with air bubble screens, the energy consumption is decisive if it's about total costs of a certain solution.

At the Krammer locks, a fixed sill is no option. The deepest draught at the lowest water level is already lower than the current sill at the ES side of the lock. Another solution has to be implemented there, which does not decrease the water level over the current lock's sill.

The relatively high costs of a movable sill in the presented tables can be compensated with much lower operational costs, when compared with air bubble screens.

G.3. Reference of lift gate

(Rijkswaterstaat Bouwdienst, 2000a)

Liftgates move vertically and are situated between two vertical slots or recesses. Normally, they're balanced, but still a large force is needed to lift the gates. Liftgates can be constructed as single- or as double retaining gates. The navigational height is restricted by the height over which the gates are lifted.

The gates close off at the bottom by plating and bottom supports. Horizontal beams transfer the loading from the plates to vertical baffles, one at each side of the gate. The baffles are supported inside the

slots on bottom and top support and/or wheels. Wheels are used to decrease the friction for moving the gates. Vertical studs reduce the magnitude of the plate fields.

The gates can slide or roll in their slots. Sliding gates are less complex to create than rollers, but induce more friction. The more expensive and maintenance-sensitive rolling gates are required when loads are high during movement of the gates. Sliding gates require a small slot in the order of decimetres; rolling gates have slots of over a metre to be able to contain rails and wheels.

The gates are pushed to one side of their slots by the pressure difference at both sides of the gate. With cam wheels, a push to close the gate neatly can be controlled mechanically.

Appendix

H. Calculation of loads by ships

This appendix elaborates on the presented values for return flow force, propeller jet force and ship impact force on the structure from chapter 5.4.2.

H.1. Return flow force

Figure 72 shows three locations which are used for calculating the force on the sill by the return current.

- 1 – Located at the ES side out of the lock chamber. The perimeter is assumed equal as inside the lock chamber.
- 2 – Located directly behind the sill. Water is only in movement when levelled higher than the top of the sill.
- 3 – Located inside the lock chamber.

The governing return current is calculated using the limit speed of the governing vessel at location 2. This location is used, because the return current is largest where the hydraulic perimeter is smallest. By use of the return current through the narrow opening between the top of the sill and the bottom of the ship, a discharge is calculated. With that discharge known, an impulse balance between the three locations is made to calculate the force on the sill.

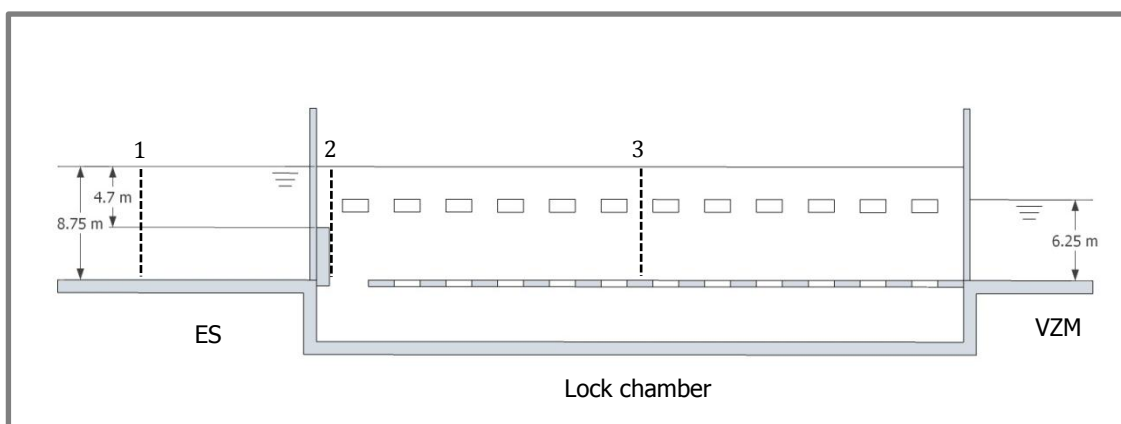


Figure 72: Visualisation of locations for return flow calculation.

Consecutive calculations show the values at location 2 of:

A_m	Vessel's submerged cross-section [m^2]
V_L	Limit speed of the vessel [m/s]
V_s	Actual speed of the vessel [m/s]

Δh	Mean water level depression [m]
U_r	Mean return flow velocity [m/s]
\hat{U}_r	Maximum return flow velocity [m/s]
$U_{r, below\ keel}$	Return flow velocity below keel [m/s]

In which the following terms are used:

C_m	Midship coefficient related to the cross-section of the ship [–]
B_s	Beam width of the ship [m]
T_s	Draught of the ship [m]
A_c	Cross-sectional area of the waterway [m ²]
b_b	Width of the waterway at the bottom [m]
b_w	Width of the waterway at the waterline [m]
f_v	Factor depending on load of ship [–]
α_s	Factor to express the effect of the sailing speed V_s relative to its maximum [–]
A_c^*	Cross-sectional area of the fairway next to the ship [m ²]
A_c	Cross-sectional area of the fairway in the undisturbed situation [m ²]
α	Slope angle of the bank [rad]

$$A_m = C_m \cdot B_s \cdot T_s = 91.2 \text{ m}^2$$

Eq. 0.6

With:	C_m	1.0 (0.9 to 1.0 for push units and inland vessels)
	B_s	22.8 m
	T_s	4.0 m

The value of C_m is chosen at its highest boundary to result in the most conservative answer – the most extreme value for the calculated return current.

$$V_L = \min \left\{ \begin{array}{l} F_L \cdot \sqrt{g \cdot A_c / b_w} \\ (g \cdot L_s / 2\pi)^{1/2} \\ g \cdot h^{1/2} \end{array} \right. = 0.312 \text{ m/s}$$

Eq. 0.7

With:	F_L	$\left[\frac{2}{3} \left(1 - \frac{A_m}{A_c} + 0.5 \cdot F_L^2 \right) \right]^{3/2}$
	A_c	$b_b \cdot h + h^2 \cdot \cot \alpha = 24 \cdot 4.7 = 112.8 \text{ m}^2$
	b_w	24 m
	L_s	195 m

$$V_s = f_v \cdot V_L = 0.234 \text{ m/s}$$

Eq. 0.8

With:	f_v	0.75 (0.9 for unloaded ship; 0.75 for loaded ship)
-------	-------	--

$$\Delta h = \frac{V_s^2}{2g} \cdot [\alpha_s \cdot (A_c / A_c^*)^2 - 1] = 0.105 \text{ m}$$

Eq. 0.9

With:	α_s	$1.4 - 0.4 \cdot V_s / V_L = 1.1$
	A_c^*	$b_b(h - \Delta h) + \cot \alpha (h - \Delta h)^2 - A_m = 19.090 \text{ m}^2$

$$U_r = V_s \cdot (A_c/A_c^* - 1) = 1.150 \text{ m/s}$$

Eq. 0.10

For $A_c/A_m < 5$ or $b_w/B_s < 10$ the flow field, induced by the ship, may be considered one-dimensional. In that case, Eq. 0.11 applies. The ship is accepted to be located in the middle of the fairway. The answer of Eq. 0.10 remains unchanged.

$$\hat{U}_r/U_r = \begin{cases} 1 + A_w^*, & \text{for } b_w/L_s < 1.5 \\ 1 + 3 \cdot A_w^*, & \text{for } b_w/L_s \geq 1.5 \end{cases}$$

Eq. 0.11

With: $A_w^* \quad y h/A_c$

Especially the return current underneath the keel is interesting in this matter. At the moment no formula exists to calculate this. For estimation purposes, the following formula can be used.

$$U_{r, \text{below keel}} = c \cdot U_r = 2.299 \text{ m/s}$$

Eq. 0.12

With: $c \quad 2.0 \text{ (1.5 to 2.0)}$

The value of c is chosen at its highest boundary to result in the most conservative answer: the most extreme values for the calculated water velocities below the keel.

Table 35: Results of return current calculations for governing location.

	Location 2
Water depth [m]	4.7
Maximum speed [m/s]	0.312
Actual speed [m/s]	0.234
Mean water level decrease [m]	0.105
Maximum return current [m/s]	1.150
Maximum return current under keel [m/s]	2.299

The maximum return current below the keel of the governing ship is 2.299 m/s . The opening through which this current flows is 0.7 m high, which leads to a discharge of $q = 1.609 \text{ m}^2/\text{s}$.

It's assumed that the ship has the same width as the lock chamber. In reality q will be larger since the ship is not exactly as wide as the lock chamber. A length of 0.6 m is present between lock wall and ship. The calculated value for the return current under the keel is a factor 2 times the actual return current. Since the actual cross-sectional area subject to the flow is smaller than a factor 2 times the 0.7 m high opening, the determination of q is conservative.

The following Eulerian balances⁵⁰ are used to calculate the actual force on the sill. The calculations are inserted in appendix H.4. Figure 73 clarifies the locations and forces used in the calculation.

The calculation is only acceptable after the assumption of no energy loss when widening or narrowing the cross-sectional area.

Mass balance: $\Sigma q_i = \text{constant}, q = h_i \cdot u_i$

⁵⁰ Eulerian specification of flow field: A fluid parcel is observed, moving through space and time.

Lagrangian specification of flow field: A specific location is observed, through which a fluid moves in time.

Energy balance: $\Sigma E_i = \text{constant}, E_i = h_i + \frac{u_i^2}{2g}$
Momentum balance: $\Sigma K_i = \text{constant}, K_i = \frac{1}{2} \cdot \rho_i \cdot g \cdot h_i^2 + \rho_i \cdot u_i^2 \cdot h_i$

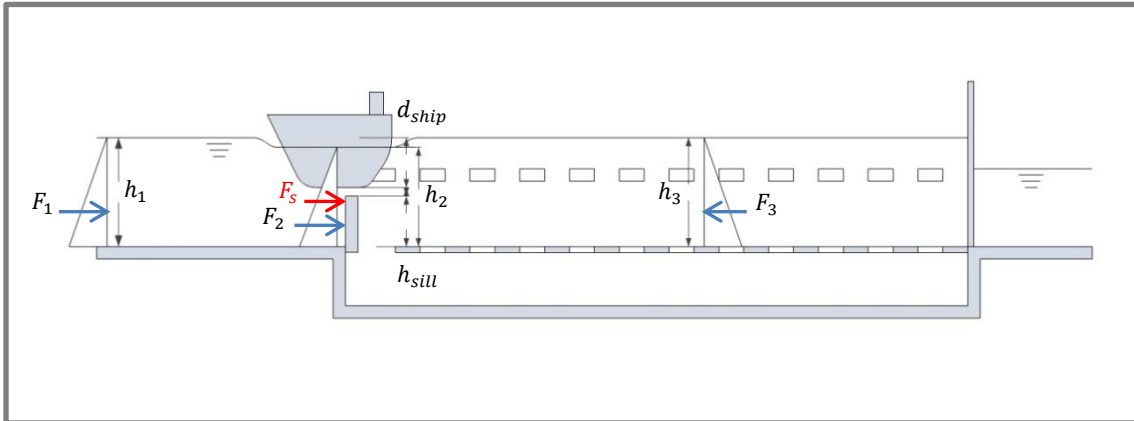


Figure 73: Clarification of used locations and symbols in calculation of return force on sill.

Part between ship and sill: $h_{2temp} = h_1 - d_{ship} - h_{sill} = 8.75 - 4 - 4.05 = 0.7 \text{ m}$.

This leads to a uniform spread load or concentrated force on the sill of:

$$q_{return} = 35.064 \text{ kN/m}$$

$$F_{return} = q_{return} \cdot w_{lock} = 841.526 \text{ kN}$$

The moment by load F is two times larger than the moment by load q , but assumes concentration of load in the middle of the sill. The return flow is present across the entire width of the lock chamber, so a force in the middle of the sill is not the way the force acts. For that reason the value of q is used.

When a ship sails in the other direction, the sign of both q and F_s changes. As a result, the sign of u_1 , u_2 and u_3 changes automatically. The impulse balance changes as well, but the solution for F_s remains the same.

Output

The force by the return current is assumed as an equal spread load on the sill, possible in both directions with a value of $q = 35 \text{ kN/m}$.

H.2. Propeller jet force

Governing is the situation of sailing at full speed, using the main thrusters only. Bow and stern thrusters have much less power than the main thrusters. Apart from that, the main thrusters are located close to each other and amplify its caused flow velocities.

The calculations that follow apply for situations with steady flow. In reality steady flow hardly applies for any situation. Also in this case, turbulence plays a major role. Simple calculations are therefore not sufficient. A thorough description of what calculations to apply in a case like this are not yet found.

Stability calculations are based on turbulent peak velocities. The equations in this chapter describe a time-averaged flow velocity. For these reasons, a factor of 3 is assumed to be a conservative factor to insert turbulence in the calculation of the maximum occurring force on the sill.

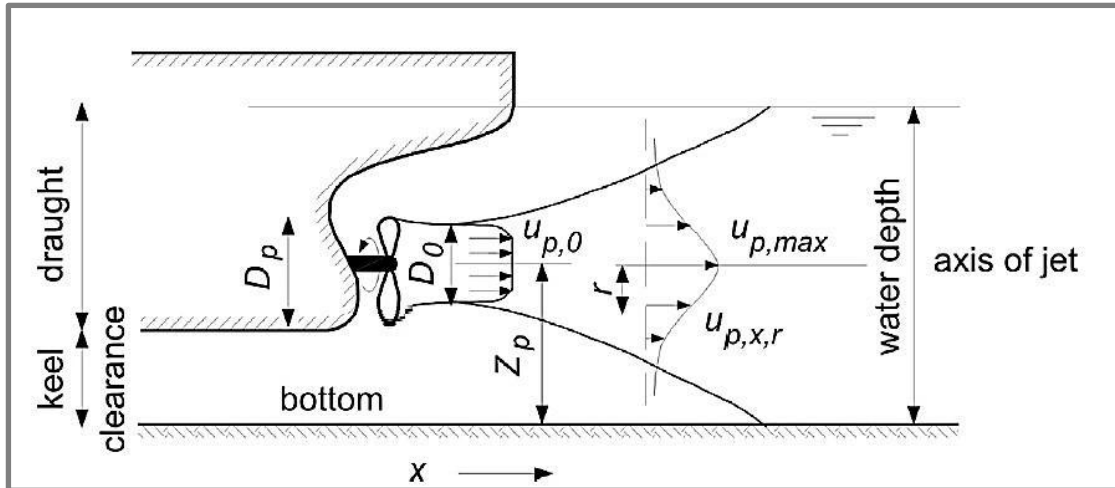


Figure 74: Specification of flow velocities by propeller jet. Adapted from (CIRIA; CUR; CETMEF, 2007).

Consecutive calculations show the values of:

$u_{p,0}$	Velocity behind propeller [m/s]
$u_{p,axis}(x)$	Velocity along jet axis
$u_p(x, r)$	Velocity distribution
$u_{p,max bed}$	Maximum bed velocity along horizontal bed

In which the following terms are used:

P	Applied power [W]
ρ_w	Water density [kg/m^3]
D_0	Effective diameter of propeller [m]
D_p	Real diameter of propeller [m]
x	Distance along axis of jet [m]
m	Empirical coefficient [–]
r	Distance from axis of jet [m]
a	Empirical coefficient [–]
b	Empirical coefficient [–]
c	Empirical coefficient [–]
z_p	Distance between jet axis and bottom [m]
h	Keel clearance [m]
n	Empirical coefficient [–]

The value for the factors a , b , c , m , n are obtained from The Rock Manual (CIRIA; CUR; CETMEF, 2007) and may be used for designs in the Netherlands.

$$u_{p,0} = 1.15 \cdot \left(\frac{P}{\rho_w \cdot D_0^2} \right)^{1/3} = 9.271 \text{ m/s}$$

Eq. 0.13

With:	P	2,000 kW
	ρ_w	1,030 kg/m^3
	D_0	$0.7 \cdot D_p$ (0.7 for free propeller without nozzle; 1.0 for propeller in a nozzle)
	D_p	2.75 m

$$u_{p,axis}(x) = a \cdot u_{p,0} \cdot (D_0/x)^m$$

Eq. 0.14

With: m 1
 a 2.8

$$u_p(x, r) = u_{p,axis}(x) \exp[-b \cdot r^2/x^2]$$

Eq. 0.15

With: b 15.4

$$u_{p,max bed} = c \cdot u_{p,0} \cdot (D_0/z_p)^n$$

Eq. 0.16

With: c 0.3
 z_p $h + 0.5 \cdot D_p$
 n 1

The forces on the sill by the propellers are calculated for three different situations. The first two situations occur in direction from lock chamber to ES only; the third situation is the only one able to act in two directions.

1. Maximum force possible – All power from the thrusters is exerted orthogonal and direct (distance of 0 m) to the sill.
2. Maximum allowed force – All power from the thrusters is exerted orthogonal at a distance of 5 m to the sill. Ships are not allowed closer than 5 m to the sill.
3. Force in both directions – A ship has sailed over the sill, inducing a force on the sill below it.

Situation 1

The largest force possible occurs after levelling of the water when high water is present at ES. This is visualised in Figure 75. The ship is maximum 2.5 m lower (levelled from +2.5 m NAP to 0 m NAP) and the thruster is in line with the sill. When all power of the thrusters is completely transferred orthogonal to the sill, the absolute maximum value is found.

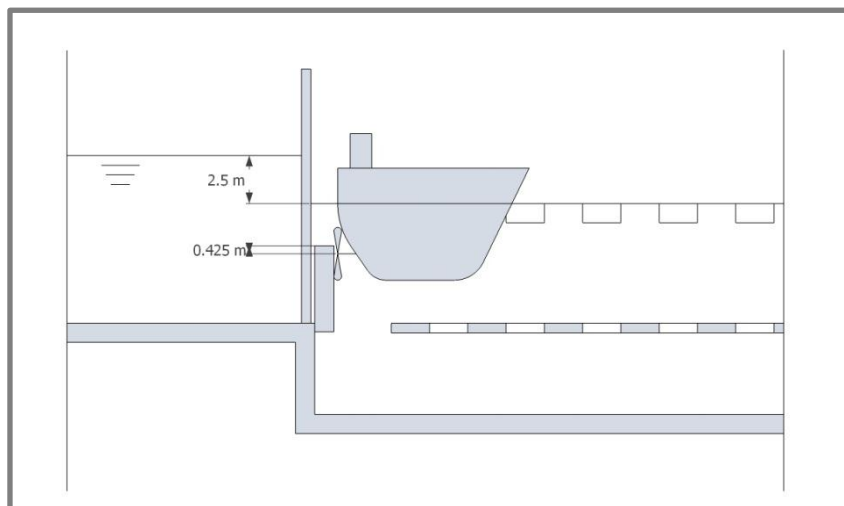


Figure 75: Situation 1 – Location of propeller in respect to sill.

The lowest part of the propeller is assumed to collide with the level of the bottom of the ship. Figure 76 shows the radius of the propeller. The horizontal line represents the top of the sill. The figure illustrates that after the ship has lowered 2.5 metres, only a part of the propeller force is exerted on the sill.

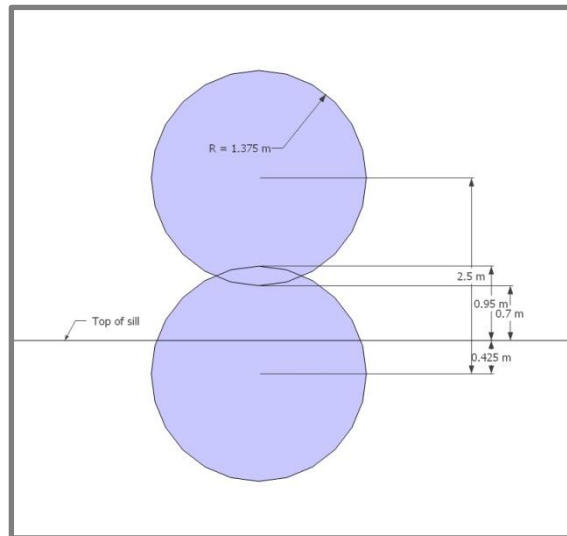


Figure 76: Detailing of influence area of propeller at distance of 0 m after lowering of propeller in respect to sill's level.

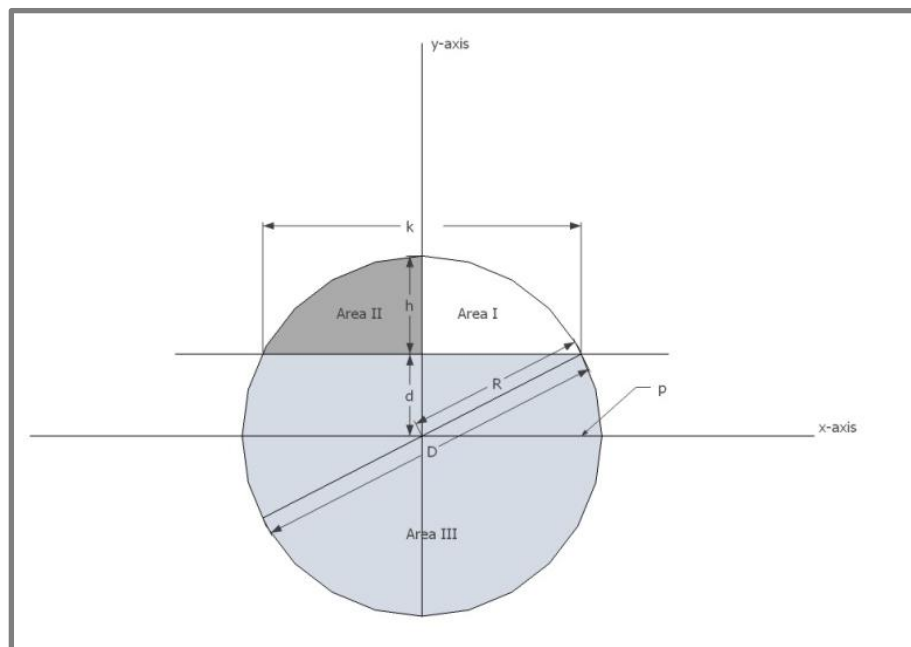


Figure 77: Calculation of influence area of the sill.

The part of the influence area that contributes to the force on the sill is calculated in Eq. 0.17 to Eq. 0.19 by use of the terms in Figure 77.

$$A_{total} = A_I + A_{II} + A_{III} = \pi \cdot R^2 = 5.9396 \text{ m}^2$$

Eq. 0.17

With: $R = 1.375 \text{ m}$

$$A_I = A_{II} = \int_0^p (\sqrt{R^2 - x^2} - d) dx = R^2 \arcsin \frac{k}{D} - \frac{1}{2} kd = 0.9099 \text{ m}^2$$

Eq. 0.18

With:

p	$\frac{k}{2}$
k	$2\sqrt{2Rh - h^2}$
h	$R - d$
d	0.425 m

$$f_{\text{reduction } 1} = \frac{A_{III}}{A_{\text{total}}} = 69.4\%$$

Eq. 0.19

$$F_s = \rho \cdot A \cdot v^2 = \rho \cdot \left(\frac{\pi \cdot D_0^2}{4} \right) \cdot v^2 \approx 260 \text{ kN}$$

Eq. 0.20

With: v 9.27 m/s

$$F_s \cdot f_{\text{reduction } 1} \cdot f_{\text{turbulence}} \cdot 2 = 1082.6 \text{ kN}$$

Eq. 0.21

With: $f_{\text{turbulence}}$ 3

Eq. 0.20 shows the force by one thruster. Eq. 0.21 takes two thrusters and the turbulence and reduction factor into account, resulting in a force on the sill of 1082.6 kN.

Situation 2

In reality the distance from the main thrusters to the sill is 5 m at minimum (Figure 78), which reduces the force on the sill. Figure 79 shows the velocity distribution along the axis perpendicular to the jet axis. At larger distances, the velocities decrease, while the influenced area increases significantly.

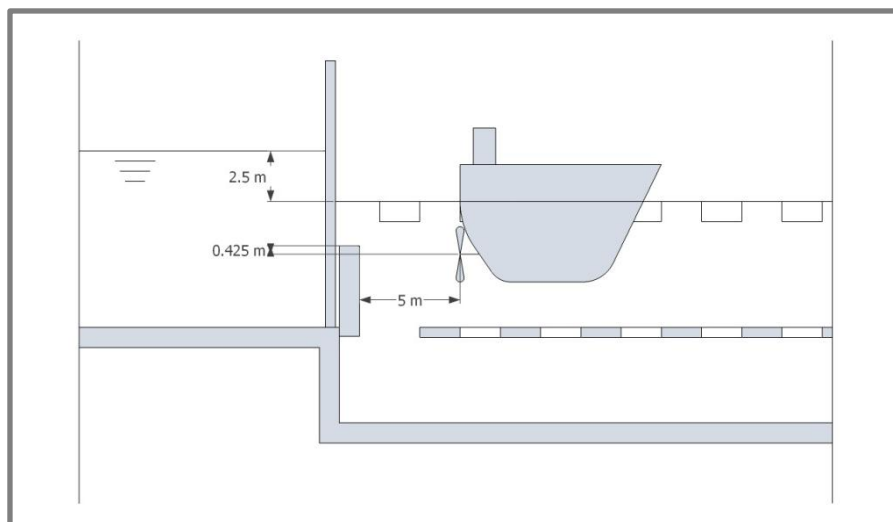


Figure 78: Situation 2 – Location of propeller in respect to sill.

For situation 2, the influence area over which the force spreads out is approximated by a circle with a 4 m diameter. 90% of the largest velocities are present in that area. The calculated force is obtained by assuming conservatively that the maximum force spreads out within this circle.

The calculation method is inserted in appendix H.4.2.

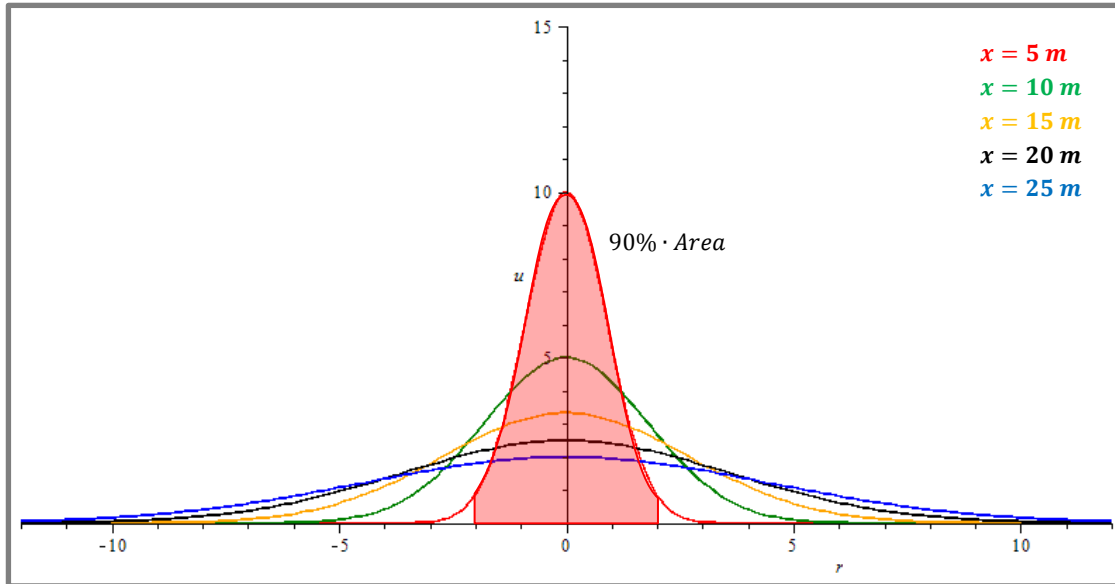


Figure 79: Propeller's velocity distribution along axis perpendicular to propeller jet axis at different distances from the sill.

Again, the lowest part of the propeller is assumed to collide with the level of the bottom of the ship. Figure 80 shows the radius of the propeller and illustrates the reduction of the force on the sill. In the same way as in situation 1, this reduction is calculated in Eq. 0.22 to Eq. 0.24.

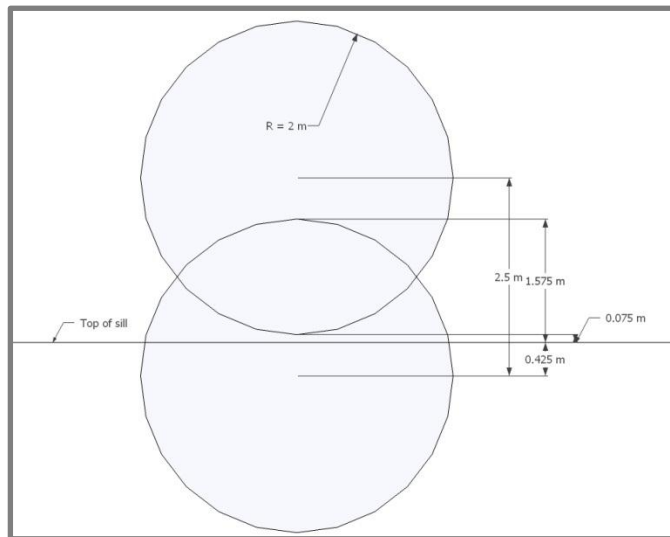


Figure 80: Detailing of influence area of propeller at distance of 5 m after lowering of propeller in respect to sill's level.

$$A_{total} = A_I + A_{II} + A_{III} = \pi \cdot R^2 = 12.566 \text{ m}^2$$

Eq. 0.22

With: $R = 2.0 \text{ m}$

$$A_I = A_{II} = \int_0^p (\sqrt{R^2 - x^2} - d) dx = R^2 \arcsin \frac{k}{D} - \frac{1}{2} \cdot k \cdot d = 2.2980 \text{ m}^2$$

Eq. 0.23

With:

p	$\frac{k}{2}$
k	$2 \cdot \sqrt{2 \cdot R \cdot h - h^2}$
h	$R - d$
d	0.425 m

$$f_{\text{reduction } 2} = \frac{A_{III}}{A_{\text{total}}} = 63.4\%$$

Eq. 0.24

$$F_s \cdot f_{\text{reduction } 2} \cdot f_{\text{turbulence}} \cdot 2 = 989.0 \text{ kN}$$

Eq. 0.25

With: $f_{\text{turbulence}} = 3$

The reduction factor from Eq. 0.24 will theoretically approach a value of 50% when D (and thus x) increases further.

Eq. 0.20 still applies for the force by one thruster. Eq. 0.25 takes two thrusters and the turbulence and reduction factor into account, resulting in a force on the sill of 989.0 kN.

Situation 3

When a ship has sailed over the sill, the propellers induce a force on the sill as a result of caused water flow velocities behind it. Figure 81 shows the situation when a ship is located 5 metres past the sill. The corresponding force is always smaller than the force directly acting on the sill, but a difference is that this force can act in both directions. The other forces are always directed from the lock chamber towards the ES gate.

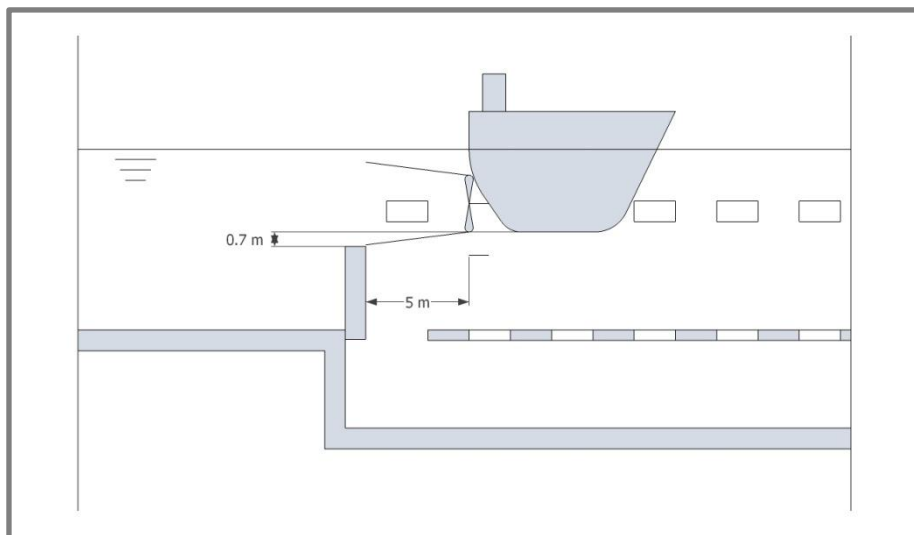


Figure 81: Situation 3 – Location of propeller in respect to sill.

The induced force always occurs in the same direction as the force induced by the return current. The return force is always larger than the propeller force which is reduced by turbulence. They never occur at the exact same moment, which is why it is never a governing force.

Output

The propeller jet as calculated in situation 2 is used in further evaluations. It is from now on assumed to be acting like a concentrated force in the middle of the sill with a value of $F_{\text{propeller}} = 989.0 \text{ kN}$.

The presented values are conservative values, since no losses of energy are assumed when the force spreads through the water.

H.3. Ship collision force

In this paragraph an insight in the order of magnitude is gained by making reference to a calculation of ship impact force on a bridge pier.

(Chen & Duan, 2000, p. 60.6) and (AASHTO, 1991) use Eq. 0.26 to estimate the static ship collision force on a rigid bridge pier. It depends on the weight of the vessel and its speed only. The value of the maximum actual limit speed in the lock chamber is used as vessel impact velocity; this is the same value as the maximum actual limit speed when approaching the lock from outside the lock chamber. (See description of limit speeds and locations in appendix H) With a height of 8.75 m calculations in the appendix lead to an actual limit speed of 1.750 m/s. The impact velocity becomes 1.750 m/s = 3.40 knots.⁵¹

$$F_{\text{collision}} \approx 27.4 \text{ MN} = 27,400 \text{ kN}$$

In this estimation a few things should be noted. This calculated force is in reality spread over a longer time span than just one moment. It's also depending on the type, size, and construction of the vessel.

$$P_s = 0.98 \cdot (DWT)^{0.5} \cdot (V/16) = 27.4 \text{ MN}$$

Eq. 0.26

With:	P_s	Equivalent static vessel impact force [MN]
	DWT	Ship deadweight tonnage [tonnes]
	V	Vessel impact velocity [knots]
	DWT	< 12,000 tonnes (Class VIb)
	V	4.08 knots

Other sources (Svensson, 2009) use Figure 82 for the determination of impact forces on rigid structures in water. When using the same impact speed – expressed in km/h – a comparable impact force is obtained.

$$\text{Impact speed} = 6.3 \text{ km/h}, \quad \text{Ship size} = 12,000 \text{ DWT}, \quad F_{\text{collision}} \approx 30 \text{ MN} = 30,000 \text{ kN}$$

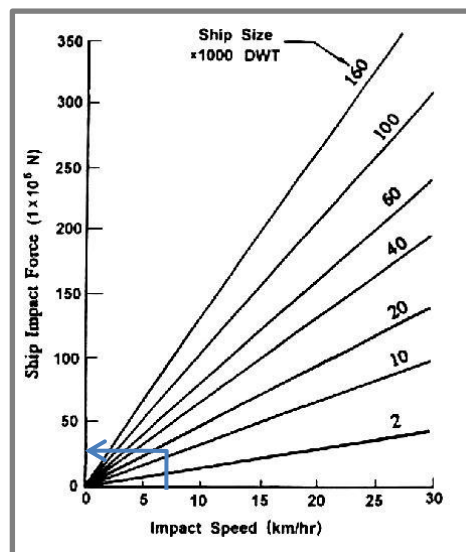


Figure 82: Ship impact force for 6.3 km/h and 12k DWT-line. Adapted from (Svensson, 2009, p. 23).

⁵¹ 1 knot = 1 nautical mile/h = 1.852 km/h = 0.514444 m/s

H.4. Maple calculations

In this section, Maple calculations are presented used in the main report.

H.4.1. Force by return current

First, the return currents are calculated for situation I (at sill, $h = 4.75 \text{ m}$) and situation II (not at sill, $h = 8.75 \text{ m}$). Then, the corresponding force on the sill is calculated.

> restart; $h_I := 4.7;$

$C_m := 1.0 : B_s := 22.8 : T_s := 4 : L_s := 195 : g := 9.81 : b_w := 24 : b_b$
 $:= 24 : a := 90 : y := 0 :$

$A_c := b_w \cdot h_I : A_m := C_m \cdot B_s \cdot T_s ;$

$F_{L_1} := 1 : F_L := \left(\frac{2}{3} \left(1 - \frac{A_m}{A_c} + 0.5 F_{L_1}^2 \right) \right)^{\frac{3}{2}} ;$

$F_{L_2} := F_L : F_L := \left(\frac{2}{3} \left(1 - \frac{A_m}{A_c} + 0.5 F_{L_2}^2 \right) \right)^{\frac{3}{2}} ;$

$F_{L_3} := F_L : F_L := \left(\frac{2}{3} \left(1 - \frac{A_m}{A_c} + 0.5 F_{L_3}^2 \right) \right)^{\frac{3}{2}} ;$

$F_{L_4} := F_L : F_L := \left(\frac{2}{3} \left(1 - \frac{A_m}{A_c} + 0.5 F_{L_4}^2 \right) \right)^{\frac{3}{2}} ;$

$F_{L_5} := F_L : F_L := \left(\frac{2}{3} \left(1 - \frac{A_m}{A_c} + 0.5 F_{L_5}^2 \right) \right)^{\frac{3}{2}} ;$

$V_L := \min \left(F_L \cdot \sqrt{\frac{g \cdot A_c}{b_w}}, \left(\frac{g \cdot L_s}{2 \pi} \right)^{\frac{1}{2}}, g \cdot h_I^{\frac{1}{2}} \right) ;$

$f_v := 0.9 :$

$V_{S_{rough}} := f_v \cdot V_L : V_S := V_{S_{rough}} ;$

$V_{S_{detailed}} := 2.4 \cdot \sqrt{\frac{A_c}{b_w}} \cdot \exp \left(-2.9 \cdot \frac{A_m}{A_c} \right) ;$

$$\begin{aligned}
\alpha_s &:= 1.4 - 0.4 \cdot \frac{V_S^{rough}}{V_L}; A_c := b_b \cdot h_I + h_I^2 \cdot \cot\left(a \cdot \frac{\text{Pi}}{180}\right) : \\
&\quad evalf(A_c); \\
h_{delta0} &:= 2; A_c^* := b_b \cdot (h_I - h_{delta0}) + \cot\left(a \cdot \frac{\text{Pi}}{180}\right) \cdot (h_I - h_{delta0})^2 \\
&\quad - A_m; h_{delta0} := \frac{V_S^2}{2 \cdot g} \cdot \left(\alpha_s \cdot \left(\frac{A_c}{A_c^*} \right)^2 - 1 \right) : \\
h_{delta1} &:= h_{delta0}; A_c^* := b_b \cdot (h_I - h_{delta1}) + \cot\left(a \cdot \frac{\text{Pi}}{180}\right) \cdot (h_I \\
&\quad - h_{delta1})^2 - A_m; h_{delta0} := \frac{V_S^2}{2 \cdot g} \cdot \left(\alpha_s \cdot \left(\frac{A_c}{A_c^*} \right)^2 - 1 \right) : \\
h_{delta2} &:= h_{delta0}; A_c^* := b_b \cdot (h_I - h_{delta2}) + \cot\left(a \cdot \frac{\text{Pi}}{180}\right) \cdot (h_I \\
&\quad - h_{delta2})^2 - A_m; h_{delta0} := \frac{V_S^2}{2 \cdot g} \cdot \left(\alpha_s \cdot \left(\frac{A_c}{A_c^*} \right)^2 - 1 \right) : \\
h_{delta3} &:= h_{delta0}; A_c^* := b_b \cdot (h_I - h_{delta3}) + \cot\left(a \cdot \frac{\text{Pi}}{180}\right) \cdot (h_I \\
&\quad - h_{delta3})^2 - A_m; h_{delta0} := \frac{V_S^2}{2 \cdot g} \cdot \left(\alpha_s \cdot \left(\frac{A_c}{A_c^*} \right)^2 - 1 \right) : \\
h_{delta4} &:= h_{delta0}; A_c^* := b_b \cdot (h_I - h_{delta4}) + \cot\left(a \cdot \frac{\text{Pi}}{180}\right) \cdot (h_I \\
&\quad - h_{delta4})^2 - A_m; h_{delta0} := \frac{V_S^2}{2 \cdot g} \cdot \left(\alpha_s \cdot \left(\frac{A_c}{A_c^*} \right)^2 - 1 \right) : \\
h_{delta5} &:= h_{delta0}; A_c^* := b_b \cdot (h_I - h_{delta5}) + \cot\left(a \cdot \frac{\text{Pi}}{180}\right) \cdot (h_I \\
&\quad - h_{delta5})^2 - A_m; h_{delta0} := \frac{V_S^2}{2 \cdot g} \cdot \left(\alpha_s \cdot \left(\frac{A_c}{A_c^*} \right)^2 - 1 \right) : \\
h_{delta6} &:= h_{delta0}; A_c^* := b_b \cdot (h_I - h_{delta6}) + \cot\left(a \cdot \frac{\text{Pi}}{180}\right) \cdot (h_I \\
&\quad - h_{delta6})^2 - A_m; h_{delta0} := \frac{V_S^2}{2 \cdot g} \cdot \left(\alpha_s \cdot \left(\frac{A_c}{A_c^*} \right)^2 - 1 \right) : \\
h_{delta7} &:= h_{delta0}; A_c^* := b_b \cdot (h_I - h_{delta7}) + \cot\left(a \cdot \frac{\text{Pi}}{180}\right) \cdot (h_I \\
&\quad - h_{delta7})^2 - A_m; h_{delta0} := \frac{V_S^2}{2 \cdot g} \cdot \left(\alpha_s \cdot \left(\frac{A_c}{A_c^*} \right)^2 - 1 \right) : \\
h_{delta8} &:= h_{delta0}; A_c^* := b_b \cdot (h_I - h_{delta8}) + \cot\left(a \cdot \frac{\text{Pi}}{180}\right) \cdot (h_I \\
&\quad - h_{delta8})^2 - A_m; h_{delta0} := \frac{V_S^2}{2 \cdot g} \cdot \left(\alpha_s \cdot \left(\frac{A_c}{A_c^*} \right)^2 - 1 \right) : \\
h_{delta9} &:= h_{delta0}; A_c^* := b_b \cdot (h_I - h_{delta9}) + \cot\left(a \cdot \frac{\text{Pi}}{180}\right) \cdot (h_I \\
&\quad - h_{delta9})^2 - A_m; h_{delta0} := \frac{V_S^2}{2 \cdot g} \cdot \left(\alpha_s \cdot \left(\frac{A_c}{A_c^*} \right)^2 - 1 \right);
\end{aligned}$$

$$U_r := V_S \cdot \left(\frac{A_c}{A_c^*} - 1 \right);$$

$$A_w^* := \frac{y \cdot h_I}{A_c} : U_{r, \max} := U_r \cdot (1 + A_w^*);$$

$$V_L : V_S : U_r : 2 \cdot U_r;$$

0.3122858799

0.2810572919

1.525898675

3.051797350

> restart; $h_I := 8.75;$

$$C_m := 1.0 : B_s := 22.8 : T_s := 4 : L_s := 195 : g := 9.81 : b_w := 24 : b_b := 24 : a := 90 : y := 0 :$$

$$A_c := b_w \cdot h_I : A_m := C_m \cdot B_s \cdot T_s;$$

$$F_{L_1} := 1 : F_L := \left(\frac{2}{3} \left(1 - \frac{A_m}{A_c} + 0.5 F_{L_1}^2 \right) \right)^{\frac{3}{2}};$$

$$F_{L_2} := F_L : F_L := \left(\frac{2}{3} \left(1 - \frac{A_m}{A_c} + 0.5 F_{L_2}^2 \right) \right)^{\frac{3}{2}};$$

$$F_{L_3} := F_L : F_L := \left(\frac{2}{3} \left(1 - \frac{A_m}{A_c} + 0.5 F_{L_3}^2 \right) \right)^{\frac{3}{2}};$$

$$F_{L_4} := F_L : F_L := \left(\frac{2}{3} \left(1 - \frac{A_m}{A_c} + 0.5 F_{L_4}^2 \right) \right)^{\frac{3}{2}};$$

$$F_{L_5} := F_L : F_L := \left(\frac{2}{3} \left(1 - \frac{A_m}{A_c} + 0.5 F_{L_5}^2 \right) \right)^{\frac{3}{2}};$$

$$V_L := \min \left(F_L \cdot \sqrt{\frac{g \cdot A_c}{b_w}}, \left(\frac{g \cdot L_s}{2\pi} \right)^{\frac{1}{2}}, g \cdot h_I^{\frac{1}{2}} \right);$$

$$f_v := 0.9 :$$

$$V_{S_{rough}} := f_v \cdot V_L : V_S := V_{S_{rough}} ;$$

$$V_{S_{detailed}} := 2.4 \cdot \sqrt{\frac{A_c}{b_w}} \cdot \exp \left(-2.9 \cdot \frac{A_m}{A_c} \right);$$

$$\begin{aligned}
\alpha_s &:= 1.4 - 0.4 \cdot \frac{V_S^{rough}}{V_L}; A_c := b_b \cdot h_I + h_I^2 \cdot \cot\left(a \cdot \frac{\text{Pi}}{180}\right) : \\
&\quad evalf(A_c); \\
h_{delta0} &:= 2; A_c^* := b_b \cdot (h_I - h_{delta0}) + \cot\left(a \cdot \frac{\text{Pi}}{180}\right) \cdot (h_I - h_{delta0})^2 \\
&\quad - A_m; h_{delta0} := \frac{V_S^2}{2 \cdot g} \cdot \left(\alpha_s \cdot \left(\frac{A_c}{A_c^*} \right)^2 - 1 \right) : \\
h_{delta1} &:= h_{delta0}; A_c^* := b_b \cdot (h_I - h_{delta1}) + \cot\left(a \cdot \frac{\text{Pi}}{180}\right) \cdot (h_I \\
&\quad - h_{delta1})^2 - A_m; h_{delta0} := \frac{V_S^2}{2 \cdot g} \cdot \left(\alpha_s \cdot \left(\frac{A_c}{A_c^*} \right)^2 - 1 \right) : \\
h_{delta2} &:= h_{delta0}; A_c^* := b_b \cdot (h_I - h_{delta2}) + \cot\left(a \cdot \frac{\text{Pi}}{180}\right) \cdot (h_I \\
&\quad - h_{delta2})^2 - A_m; h_{delta0} := \frac{V_S^2}{2 \cdot g} \cdot \left(\alpha_s \cdot \left(\frac{A_c}{A_c^*} \right)^2 - 1 \right) : \\
h_{delta3} &:= h_{delta0}; A_c^* := b_b \cdot (h_I - h_{delta3}) + \cot\left(a \cdot \frac{\text{Pi}}{180}\right) \cdot (h_I \\
&\quad - h_{delta3})^2 - A_m; h_{delta0} := \frac{V_S^2}{2 \cdot g} \cdot \left(\alpha_s \cdot \left(\frac{A_c}{A_c^*} \right)^2 - 1 \right) : \\
h_{delta4} &:= h_{delta0}; A_c^* := b_b \cdot (h_I - h_{delta4}) + \cot\left(a \cdot \frac{\text{Pi}}{180}\right) \cdot (h_I \\
&\quad - h_{delta4})^2 - A_m; h_{delta0} := \frac{V_S^2}{2 \cdot g} \cdot \left(\alpha_s \cdot \left(\frac{A_c}{A_c^*} \right)^2 - 1 \right) : \\
h_{delta5} &:= h_{delta0}; A_c^* := b_b \cdot (h_I - h_{delta5}) + \cot\left(a \cdot \frac{\text{Pi}}{180}\right) \cdot (h_I \\
&\quad - h_{delta5})^2 - A_m; h_{delta0} := \frac{V_S^2}{2 \cdot g} \cdot \left(\alpha_s \cdot \left(\frac{A_c}{A_c^*} \right)^2 - 1 \right) : \\
h_{delta6} &:= h_{delta0}; A_c^* := b_b \cdot (h_I - h_{delta6}) + \cot\left(a \cdot \frac{\text{Pi}}{180}\right) \cdot (h_I \\
&\quad - h_{delta6})^2 - A_m; h_{delta0} := \frac{V_S^2}{2 \cdot g} \cdot \left(\alpha_s \cdot \left(\frac{A_c}{A_c^*} \right)^2 - 1 \right) : \\
h_{delta7} &:= h_{delta0}; A_c^* := b_b \cdot (h_I - h_{delta7}) + \cot\left(a \cdot \frac{\text{Pi}}{180}\right) \cdot (h_I \\
&\quad - h_{delta7})^2 - A_m; h_{delta0} := \frac{V_S^2}{2 \cdot g} \cdot \left(\alpha_s \cdot \left(\frac{A_c}{A_c^*} \right)^2 - 1 \right) : \\
h_{delta8} &:= h_{delta0}; A_c^* := b_b \cdot (h_I - h_{delta8}) + \cot\left(a \cdot \frac{\text{Pi}}{180}\right) \cdot (h_I \\
&\quad - h_{delta8})^2 - A_m; h_{delta0} := \frac{V_S^2}{2 \cdot g} \cdot \left(\alpha_s \cdot \left(\frac{A_c}{A_c^*} \right)^2 - 1 \right) : \\
h_{delta9} &:= h_{delta0}; A_c^* := b_b \cdot (h_I - h_{delta9}) + \cot\left(a \cdot \frac{\text{Pi}}{180}\right) \cdot (h_I \\
&\quad - h_{delta9})^2 - A_m; h_{delta0} := \frac{V_S^2}{2 \cdot g} \cdot \left(\alpha_s \cdot \left(\frac{A_c}{A_c^*} \right)^2 - 1 \right);
\end{aligned}$$

$$U_r := V_S \cdot \left(\frac{A_c}{A_c^*} - 1 \right);$$

$$A_w^* := \frac{y \cdot h_I}{A_c} : U_{r, \max} := U_r \cdot (1 + A_w^*);$$

$$V_L : V_S : U_r : 2 \cdot U_r;$$

2.332555395

2.099299856

2.374785478

4.749570956

> 1: ES side

2: Above sill

3: Just behind sill

4: In middle of lock chamber

restart;

$$\rho_{fresh} := 1000 : \rho_{salt} := 1030 : g := 9.81 : d_{ship} := 4 : h_{sill} := 4.05 : q := 3.868 :$$

$$h_1 := 8.75 : u_1 := \frac{q}{h_1} : F_1 := \frac{1}{2} \cdot \rho_{salt} \cdot g \cdot h_1^2;$$

$$h_2 : u_2 : F_2 : F_{sill} :$$

$$h_{3 \text{ temp}} := h_1 - d_{ship} - h_{sill} : u_3 : F_3 := \frac{1}{2} \cdot \rho_{salt} \cdot g \cdot h_3^2;$$

$$h_4 : u_4 : F_4 := \frac{1}{2} \cdot \rho_{fresh} \cdot g \cdot h_4^2;$$

0.4420571429

$$u_3 := \frac{h_1 \cdot u_1}{h_{3 \text{ temp}}} : h_3 := \text{sqrt} \left(\frac{\left(\frac{1}{2} \cdot g \cdot h_1^2 + h_1 \cdot u_1^2 - h_{3 \text{ temp}} \cdot u_3^2 \right)}{\frac{1}{2} \cdot g} \right);$$

5.525714286

8.517840922

$$h_4 := \frac{h_{3 \text{ temp}} \cdot u_3}{u_4};$$

$$h_4 := \left(h_3 + \frac{u_3^2}{2 \cdot g} \right) - \frac{u_4^2}{2 \cdot g};$$

$$w := \text{solve}(h_4, u_4);$$

$$u_4 := 0.3842424668;$$

$$h_4;$$

0.3842424668

10.06656040

$$F_{s\ per\ meter} := F_4 + \rho_{fresh} \cdot h_4 \cdot u_4^2 - F_3 - \rho_{salt} \cdot h_3 \cdot u_3^2;$$

$$F_s := F_{s\ per\ meter} \cdot 24;$$

-1.358962268 10⁵

-3.261509443 10⁶

H.4.2. Force by propellers

The flow velocities induced by the propellers are calculated. They are expressed in formulas close to the propeller, at several distances from the propeller and along the lock bottom. Also the force caused by these velocities is given.

restart; with(Student[CalculusI]) :

$$P := 2000000 : \rho_{salt} := 1030 : \rho_{fresh} := 1000 : d_p := 2.75 : h := 0.7 :$$

$$a := 2.8 : b := 15.4 : c := 0.3 : m := 1 : n := 1 :$$

$$d_0 := 0.7 \cdot d_p : z_p := h + \frac{1}{2} \cdot d_p ;$$

1.925

2.075000000

$$u_{p,0} := 1.15 \cdot \left(\frac{P}{\rho_{salt} \cdot d_0^2} \right)^{\frac{1}{3}} ;$$

9.271320792

$$u_{p,axis} := a \cdot u_{p,0} \cdot \left(\frac{d_0}{x} \right)^m : u_p := u_{p,axis} \cdot \exp \left(-\frac{b \cdot r^2}{x^2} \right) ;$$

$$u_{p,maxbed} := c \cdot u_{p,0} \cdot \left(\frac{d_0}{z_p} \right)^n ;$$

$$F_{s,maxorthogonal} := \rho_{salt} \cdot \frac{\text{Pi} \cdot d_0^2}{4} \cdot u_{p,0}^2 : evalf(\%);$$

2.580331450

2.576747065 10⁵

with(plots) :

$$x := 5 : u_{p5} := u_p :$$

$$x := 10 : u_{p10} := u_p :$$

$$x := 15 : u_{p15} := u_p :$$

$$x := 20 : u_{p20} := u_p :$$

$$x := 25 : u_{p25} := u_p :$$

$$\text{plot}([u_{p5}, u_{p10}, u_{p15}, u_{p20}, u_{p25}], r = -12 .. 12, u = 0 .. 15, color = ["Red", "Green", "Orange", "Black", "Blue"]);$$

➔ For plot, see Figure 79.

Appendix

I. Load combinations

To regard the governing load combinations, all possible combinations are described first. After a complete overview, a reasoning follows why some of the combinations are not elaborated. For the remaining combinations, it's pointed out which ones are governing by use of numbers.

The load combinations are based on 4 main features. Their occurrences are described, leading to the complete set of load combinations.

3 life cycle stages:

A difference is made between loads during operation, and loads during maintenance or construction. When the lock is in operation, the lock chamber is filled with water and ships sail through the lock. When maintenance actions are carried out, the lock is dry or the structure is lifted out of the water.

- Loads by structure in operation
- Loads during construction
- Loads during maintenance

3 limit states:

For every load case, different limit states are evaluated.

ALS is sometimes used to separate the accidental loads from the ULS. In this case that is also favoured because of the fact that accidental loads aren't taken into account.

ALS is used, to be able to separate the collision force of a ship. This would be filed under ULS, but since the structure will not be designed to a collision, ULS mustn't include accidental loads.

- ALS includes accidental loads and regular parameters
 $\gamma = 1$
- ULS includes extreme events and higher parameters
 $\gamma_v = 1.5$, $\gamma_p = 1.2$ (or 0.9 when in opposite direction) and $\gamma_g = 1$
- SLS includes the stability of the structure and limitations to deformations or displacements with regular parameters
 $\gamma = 1$

2 sailing directions of ships:

When the gates at the ES are open, ships are able to sail in or out of the lock chamber. When the gates are closed at the ES side, a ship can sail out of the lock chamber at the other side.

To prevent ambiguities and long descriptions of the sailing directions, the directions are pointed out as East (in the line ES – lock chamber - VZM) or West (in the line VZM - lock chamber - ES).

- East

- West

4 extreme water levels:

Each of the situations has its own possible water levels. The ES varies from $+2.5 \text{ m NAP}$ to -2.35 m NAP , while the VZM has a fixed water level of 0 m NAP . A situation without water in the lock chamber is also an extreme water level.

- $+2.5 \text{ m NAP}$
- -2.35 m NAP
- 0 m NAP
- No water in lock chamber

This complete analysis leads to $3 \cdot 3 \cdot 2 \cdot 4 = 72$ load cases.

Some combinations fall out of the total amount of load cases. A short analysis per life cycle stage reduces the amount of load cases considerably. Ship collision isn't taken into account, so all ALS limit states disappear. For the remaining load cases a ULS and SLS limit state is regarded.

During construction, no water is present in the lock. No shipping is possible. $2 \cdot 1 \cdot 1 = 2$
 During maintenance, shipping is not possible. Four different water levels are possible. $2 \cdot 1 \cdot 4 = 8$
 During operation, ships can sail in two directions with three extreme water levels possible. $2 \cdot 2 \cdot 3 = 12$

Now $8 + 12 + 2 = 22$ load combinations remain. All 22 load cases are described in Table 36. It is reasoned why they will or will not be governing. The red combinations are not governing, which results in 10 remaining load cases.

- M3, M4, M5 and M6 are always smaller than M1 and M2. In maintenance the highest water level is governing since this induces the largest loads on the sill when lifted out of the water.
- M7 and M8 are equal to C1 and C2. They are therefore cancelled out.
- O5, O6, O7 and O8 are always smaller than O1, O2, O3 and O4 since higher water levels induce higher maximum forces.
- O9 and O10 will be governing when compared with O11 and O12, because sailing to the east induces propeller jet on the sill. Sailing to the west induces a front wave on the sill, but this is smaller than propeller jet. See appendix H.

Table 36: Overview of load cases.

Load combination	Life cycle stage	Limit state	Sailing direction	Water level
C1	Construction	ULS	No sailing	No water
C2	Construction	SLS	No sailing	No water
M1	Maintenance	ULS	No sailing	$+2.5 \text{ m NAP}$
M2	Maintenance	SLS	No sailing	$+2.5 \text{ m NAP}$
M3	Maintenance	ULS	No sailing	-2.35 m NAP
M4	Maintenance	SLS	No sailing	-2.35 m NAP
M5	Maintenance	ULS	No sailing	0 m NAP
M6	Maintenance	SLS	No sailing	0 m NAP
M7	Maintenance	ULS	No sailing	No water
M8	Maintenance	SLS	No sailing	No water
O1	Operation	ULS	East	$+2.5 \text{ m NAP}$
O2	Operation	SLS	East	$+2.5 \text{ m NAP}$
O3	Operation	ULS	West	$+2.5 \text{ m NAP}$
O4	Operation	SLS	West	$+2.5 \text{ m NAP}$
O5	Operation	ULS	East	-2.35 m NAP
O6	Operation	SLS	East	-2.35 m NAP
O7	Operation	ULS	West	-2.35 m NAP

O8	Operation	SLS	West	−2.35 m NAP
O9	Operation	ULS	East	0 m NAP
O10	Operation	SLS	East	0 m NAP
O11	Operation	ULS	West	0 m NAP
O12	Operation	SLS	West	0 m NAP

The remaining load cases are filled in with the following corresponding loads.

Return flow force	$q_{return} = 35 \text{ kN/m}$, $F_{return} = 840 \text{ kN}$
Propeller jet	$F_{propeller} = 989.0 \text{ kN}$
Dead weight	$q_{weight} = 22.1 \text{ kN/m}$, $F_{weight} = 531 \text{ kN}$
Hydrostatic water pressure	$F_{density \max} = 195 \text{ kN}$
Wind	$q_{wind} = 2.56 \text{ kN/m}$, $F_{wind} = 61.5 \text{ kN}$

Table 37 presents the governing load combinations. The load combinations which are not governing are printed red and not filled in for their total load. Finally, 4 governing load combinations are remaining.

- M1 is governing in vertical direction.
- O3 is larger than C1, but C1 is governing when the structure is in its construction phase or lifted out of water.
- O9 is larger than O1.

Table 37: Governing load combinations.

Load combination	Permanent load(s)	Safety factor	Variable load	Safety factor	Total loads
C1	q_{weight}	1.2	F_{wind}	1.5	636.5 kN ↓ 92.25 kN →
C2	q_{weight}	1	F_{wind}	1	
M1	q_{weight}	1.2			636.5 kN ↓
	$F_{density \max}$	1.2			234 kN →
M2	q_{weight}	1			
	$F_{density \max}$				
O1	q_{weight}	1.2	q_{return}	1.5	
O2	q_{weight}	1	q_{return}	1	
	q_{weight}	1.2			636.5 kN ↓
O3	$F_{density \max}$	1.2	q_{return}	1.5	234 kN → 1,260 kN →
O4	q_{weight}	1	q_{return}	1	
	$F_{density \max}$				
O9	q_{weight}	1.2	$F_{propeller}$	1.5	636.5 kN ↓ 1,485.5 kN ←
O10	q_{weight}	1	$F_{propeller}$	1	

Appendix

J. Dimensioning of sill

The dimensioning of the structure is an iterative process of which only the results are presented in the report's main text. This appendix shows the complete elaboration from loads to dimensions of the main elements of the design.

J.1. Plates

Plates around the structure form the reservoirs. They are assumed to be water- and airtight. To calculate the required plate thickness, the maximum pressure on the plates is determined. This maximum pressure may occur in different situations. The air in the air reservoir in operation is under compression and exerts a force directed outwards. The water in the water reservoir is not under compression which results in an inward directed water pressure on the plates. When the reservoirs are emptied (for maintenance operations for instance) a water pressure is exerted on the plates inward.

Water pressure on air reservoir in operation

The highest water pressure at the middle of the height of the air reservoir occurs at a water level of 0 m NAP. The sill is in its lowest position, which results in a water head of $(6.25 + \frac{1}{2} \cdot h_{\text{reservoir}}) = 6.75$. $P_{\text{inside}} = \rho \cdot g \cdot h = 68.2 \text{ kN/m}^2$. The air reservoir operates at an air pressure of 1.3 bar, which equals $P_{\text{outside}} = 130 \text{ kN/m}^2$. In combination with the maximum load combination exerted on the sill, a pressure of $P = P_{\text{outside}} - P_{\text{inside}} - P_{\text{LC O3}} = -0.45 \text{ kN/m}^2$. (Minus sign indicates the pressure being directed outwards.)

Water pressure on water reservoir in operation

The maximum pressure during operation is according to LC O3 62.25 kN/m^2 . It is assumed that the water at the inner and the outer side is in balance and does not exert an extra force on the plates.

Water pressure on empty reservoirs

The maximum pressure during maintenance occurs when the reservoirs are both set dry. Atmospheric air pressure is present in both reservoirs and the water level is +0 m NAP.⁵² At the bottom of the lock the water pressure is in this case 111 kN/m^2 .

The governing maximum water pressure of 111 kN/m^2 is distributed to the main beams with an internal distance of 0.9 m. Studs are installed with an internal distance of 1 m. See Figure 83. Since the studs are present every metre width and the sill is a metre thick, no studs are present in the sides orthogonal to the figure.

⁵² By choosing this water level, the plate thickness is reduced. Atmospheric pressure in the water reservoir is only needed with big maintenance operations. A water level of 0 m NAP can always be obtained; either by levelling under free decay to the VZM or by filling under free decay from the VZM. For that reason it's also possible to perform big maintenance operations in emergency situations.

The load on the plates is conservatively assumed to be acting as a discontinuous plate on two supporting beams at the ends. Figure 84 shows the difference between a continuous and discontinuous beam over supports. The deflection and acting bending moments are smaller at the right.

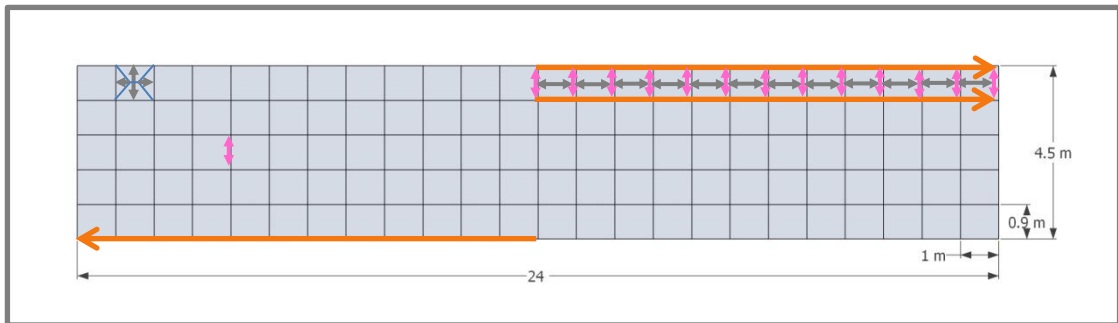


Figure 83: Schematic layout of force distribution of plates (grey) via studs (pink) and main beams (orange) in movable sill.

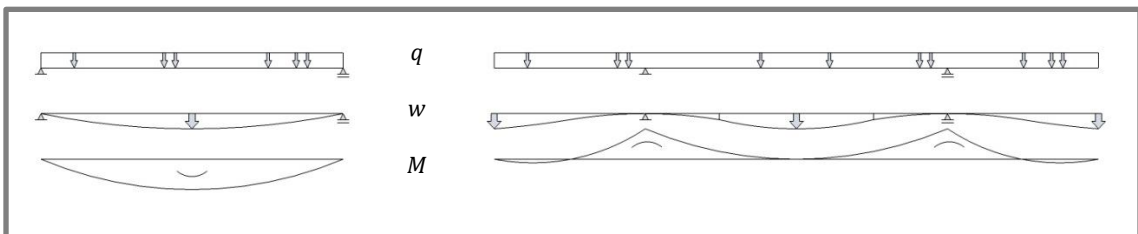


Figure 84: Comparison of deflection and bending moment of discontinuous and continuous beam.

Eq. 0.28 shows the required moment of resistance to cope with the load as presented in Eq. 0.27. Eq. 0.29 shows what thickness the plate needs at minimum to be able to resist the forces exerted on it.

$$q = P_{max} \cdot l_{orthogonal} = 99.9 \text{ kN/m} \quad \text{Eq. 0.27}$$

With:

P_{max}	111 kN/m ²
$l_{orthogonal}$	0.9 m

$$W_d = \frac{M}{f} = 5.31 \cdot 10^4 \text{ mm}^3 \quad \text{Eq. 0.28}$$

With:

M_{Ed}	$\frac{1}{8} \cdot q \cdot l_{parallel}^2 = 12.49 \text{ kNm}$
$l_{parallel}$	1.0 m
f	235 N/mm ²

$$W_d = \frac{1}{6} \cdot b \cdot d^2, \quad d_{plate} = 17.9 \text{ mm} \quad \text{Eq. 0.29}$$

With:

b	1,000 mm
W_d	$5.31 \cdot 10^4 \text{ mm}^3$

A large difference in water pressure is present between the top and the bottom of the sill. The sill is 4.5 m high namely. The same calculation of the plate thickness at the top of the sill leads to a reduction of approximately 4 mm according to Eq. 0.30. This means that the top half of the sill can be configured with plates of 2 mm less thick.

Nevertheless a thickness of 20 mm is chosen for all plating, since it's beneficial to use plates as large as possible. No extra water tight connections are needed at the connection of the plates. The weight of the plates is shown in Eq. 0.31.

$$W_d = \frac{1}{6} \cdot b \cdot d^2, \quad d_{plate} = 13.7 \text{ mm}$$

Eq. 0.30

With:

h	6.5 m
P_{max}	65.7 kN/m ²
q	59.1 kN/m
M_{Ed}	7.39 kNm
W_d	$3.15 \cdot 10^4 \text{ mm}^3$

$$L_{plates} = (4.5 \cdot 24 + 4.5 \cdot 1 + 24 \cdot 1) \cdot 2 \cdot d_{plate} \cdot \rho_{steel} \cdot g = 4.26 \cdot 10^2 \text{ kN}$$

Eq. 0.31

With:

d_{plate}	20 mm
ρ_{steel}	7,800 kg/m ³

Symbol L is used for weight since the symbol W is already in use for moment of resistance.

J.2. Studs

The studs must be able to cope with the moment of resistance as obtained in Eq. 0.32 and Eq. 0.33. Since corrosion must be counteracted as much as possible, areas of steel in connection with water must be reduced maximum. For that reason, a tube is best as stud. When a U-profile is welded to the plates of the reservoirs, less steel is exposed to corrosive conditions than when an H-profile is used for instance. A UPE – 120 profile is chosen to meet the requirements. Figure 85 shows its dimensions.

The used load to determine the dimensions is actually much smaller. In the calculation it is assumed that the water pressure on an area of $1 \cdot 0.9 \text{ m}^2$ is exerted on the stud, but in reality approximately half of that force is directed to the main beam at directly. This is visible in the trapezoid in Figure 83.

$$q = P_{max} \cdot l_{orthogonal} = 111 \text{ kN/m}$$

Eq. 0.32

With:

P_{max}	111 kN/m ²
$l_{orthogonal}$	1.0 m

$$W_d = \frac{M}{f} = 4.78 \cdot 10^4 \text{ mm}^3$$

Eq. 0.33

With:

M_{Ed}	$\frac{1}{8} \cdot q \cdot l_{parallel}^2 = 11.24 \text{ kNm}$
$l_{parallel}$	0.9 m
f	235 N/mm ²

UPE 120

I	$3.92 \cdot 10^6 \text{ mm}^4$
$W_{y,el}$	$6.54 \cdot 10^4 \text{ mm}^3$
$W_{z,el}$	$1.53 \cdot 10^4 \text{ mm}^3$

$$G = 13.2 \text{ kg/m}$$

$$A = 1.68 \cdot 10^3 \text{ mm}^2$$

$$h = 120.0 \text{ mm}, \quad b = 60.0 \text{ mm}, \quad t_w = 5.5 \text{ mm}, \quad t_f = 9.0 \text{ mm}$$

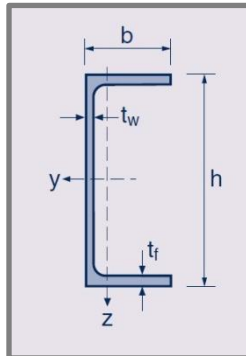


Figure 85: Dimensions of UPE-profile.

This profile does not meet the requirement, since the z -direction must be used for the moment of resistance capacity. When this profile is welded to the side plates, a shape like a hot rolled rectangular tube is formed with the features below. Now, the profile is expected to cope with the loads. The resulting weight is shown in Eq. 0.34.

The assumption of the welded UPE-profile acting like the tubular profile must be checked in a further design stage.

Tube 120 · 60

$$W_{y,el} = 8.14 \cdot 10^4 \text{ mm}^3$$

$$W_{z,el} = 5.05 \cdot 10^4 \text{ mm}^3$$

$$A = 3.09 \cdot 10^3 \text{ mm}^2$$

$$h = 120.0 \text{ mm}, \quad b = 60.0 \text{ mm}, \quad t = 10.0 \text{ mm}$$

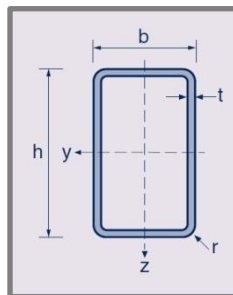


Figure 86: Dimensions of rectangular profile.

$$L_{studs} = G_{stud} \cdot (25 \cdot 4.5 \cdot 2) \cdot g = 2.91 \cdot 10^1 \text{ kN}$$

Eq. 0.34

With: $G_{stud} \quad 13.2 \text{ kg/m}$

J.3. Main beams

The main beams are calculated after assuming a centre to centre distance of 0.9 m. In this way, the total load is distributed over 6 main beams since the structure is 4.5 m high.

Figure 87 shows and Eq. 0.35 calculates the loads and the bending moment on a main beam. Eq. 0.36 shows the required moment of resistance to resist the loads. The fraction $\frac{0.9}{4.5}$ calculates the part of the load which is distributed by one main beam. This is allowed for the assumed even spread load q , not for F actually. That force is actually a load exerted on a circle with a diameter of 4 m. The load on the top of the sill is slightly higher than on the lower part of the sill. Differences are neglected in this design phase, though.

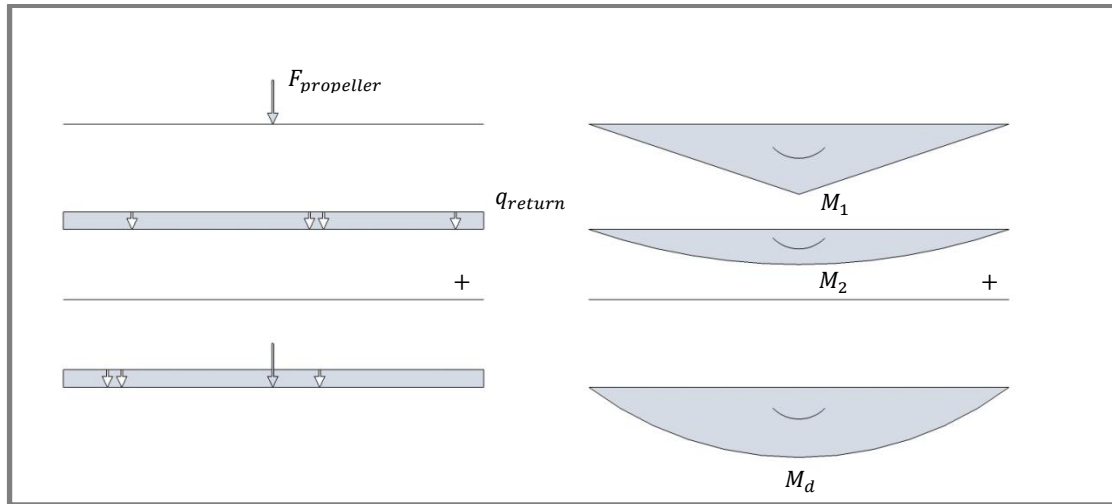


Figure 87: Loads and bending moment on main beam.

$$M_d = M_1 + M_2 = 1,690.8 \text{ kNm}$$

Eq. 0.35

With:

$$M_1 = \frac{1}{4} \cdot \left(F_{propeller} \cdot \frac{0.9}{4.5} \right) \cdot l_{beam} = 1,186.8 \text{ kNm}$$

$$M_2 = \frac{1}{8} \cdot \left(q_{return} \cdot \frac{0.9}{4.5} \right) \cdot l_{beam}^2 = 504 \text{ kNm}$$

$$F_{propeller} = 989.0 \text{ kN}$$

$$q_{return} = 52.5 \text{ kN/m}$$

$$W_{el,min} = \frac{M_d}{f_{y,d}} = 7.195 \cdot 10^6 \text{ mm}^3$$

Eq. 0.36

With:

$$\frac{M_u}{f_{y,d}} = \frac{f_{y,d} \cdot W_{el}}{f_{y,d}} = 235 \text{ N/mm}^2$$

A HEA – 800 profile meets the requirements for the moment of resistance and is chosen as main beam. Figure 88 shows the orientation of the dimensions and Eq. 0.37 shows its weight.

HEA – 800:

$$I = 3.03 \cdot 10^9 \text{ mm}^4$$

$$W_{el} = 7.68 \cdot 10^6 \text{ mm}^3$$

$$G = 224 \text{ kg/m}$$

$$A = 2.86 \cdot 10^4 \text{ mm}^2$$

$$h = 790 \text{ mm}, \quad b = 300 \text{ mm}, \quad t_w = 15.0 \text{ mm}, \quad t_f = 28.0 \text{ mm}$$

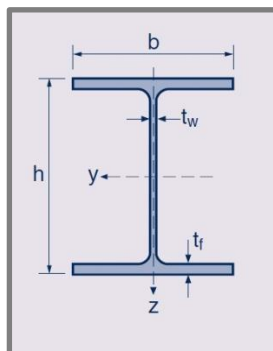


Figure 88: Dimensions of HE-profile.

$$L_{main\ beams} = G_{main\ beam} \cdot (24 \cdot 6) \cdot g = 3.16 \cdot 10^2\ kN$$

Eq. 0.37

With: $G_{main\ beam} \quad 224\ kg/m$

In this design phase it's assumed that the main beams are located inside the reservoirs. This will not change the outer dimensions of the sill. When the screens are operationally affected negatively, it may be better to alter the design.

The deflection of the main beams is calculated in Eq. 0.38. It is rather large, but the beams are relatively long. It's acceptable since the connections to the water and air supply pipes are flexible and there is no space restriction in the direction of the deflection of the main beams.

$$w = \frac{5}{384} \cdot \frac{q \cdot l^4}{EI} = 422.6\ mm$$

Eq. 0.38

With: $q_{max} \quad 62.25\ kN/m$
 $l \quad 24\ m$
 $I \quad 3.03 \cdot 10^9\ mm^4$

J.4. Vertical connection

The vertical connection of the sill to the driving mechanism above water must be able to hold the total weight of the structure. The weight of the entire sill-structure is calculated in Eq. 0.39. In this calculation, the volumes of water and compressed air inside the reservoirs are taken into account, along with the weight of the structural elements. The weight of the individual structural elements follows from the elaborated features per element.

$$L_{total} = L_{plates} + L_{studs} + L_{main\ beams} + L_{water} + L_{air} - L_{displaced\ water}$$

$$= 5.31 \cdot 10^2\ kN$$

Eq. 0.39

With: $L_{water} \quad (3.5 \cdot 1 \cdot 24) \cdot \rho \cdot g = 840\ kN$
 $L_{air} \quad (0.5 \cdot 1 \cdot 24) \cdot \rho_{air} \cdot p \cdot g = 0.197\ kN$
 $p \quad 1.3\ bar$
 $\rho_{air} \quad 1.29\ kg/m^3$
 $L_{displaced\ water} \quad (4.5 \cdot 1 \cdot 24) \cdot \rho \cdot g = 1080\ kN$

$$f_{y,d} = \frac{N}{A}, \quad A = \frac{N}{f_{y,d}} = 2,260\ mm^2, \quad A_{one\ side} \approx 1200\ mm^2$$

Eq. 0.40

With: $f_{y,d} \quad 235\ N/mm^2$
 $N \quad 5.31 \cdot 10^2\ kN$

In Eq. 0.40 a yield stress of $235\ N/mm^2$ is used. It may seem more logical to apply tensile steel stress of $360\ N/mm^2$. By using the yield stress, a conservative value is calculated.

To meet the requirement of the calculated minimum steel cross sectional area, a *CHS*-profile is chosen. Its dimensions can be seen in Figure 89. Eq. 0.41 shows the weight of the used piles.

In this calculation, no extra loads are taken into account. In reality it's possible that slab will settle on the sill. In this design phase that's not taken into account. Since the piles are only subject to tensile forces because of the weight of the structure, the piles are not checked on resistance against buckling.

CHS 114.3/4 $I = 2.11 \cdot 10^6 \text{ mm}^4$
 $G = 10.9 \text{ kg/m}$
 $A = 1.386 \cdot 10^3 \text{ mm}^2$
 $d = 114.3 \text{ mm}, \quad t = 4.0 \text{ mm}$

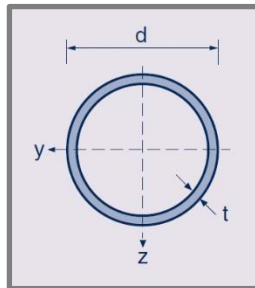


Figure 89: Dimensions of CHS-profile.

$$L_{piles} = G_{piles} \cdot 15 \cdot 2 \cdot g = 3.21 \text{ kN}$$

Eq. 0.41

With: $G_{piles} \quad 10.9 \text{ kg/m}$

J.5. Guiding rail

To detail the force distribution of the structure to its surrounding, different situations have to be regarded. The force distribution to the lock is regarded first. Afterwards, the friction inside the rail is quantified to check, whether adaptations to the design are needed.

J.5.1. Force distribution

When the sill is in operation, it exerts forces on another part of the lock than when it has been lifted out of the water. The different situations are described from top to bottom. Figure 90 helps in understanding the descriptions of where forces are exerted on the lock chamber.

Three different ranges in Figure 90 indicate the possible location of the sill during different situations. The ranges are mentioned first, followed by an analysis of the force distribution within that range.

- Range 1: $> +7.0 \text{ m NAP}$ Sill has been lifted out of the water
- Range 2: $-2.2 \text{ to } +7.0 \text{ m NAP}$ Sill is being lifted out of the water
- Range 3: $-11.0 \text{ to } -2.2 \text{ m NAP}$ Sill is in operation

The yellow area indicates the available space for the force distribution from the movable sill to the lock. As described in section 5.1, some bottom slabs are to be removed. The small yellow space left above the slabs is restricted at its sides by the lock wall and the navigational area; this space is 750 mm wide. In the current situation of the lock, wooden grating is present there. The grates prevented large objects to get stuck in the wall valves when water flowed through. The valves and grating has become obsolete in the new design, since the wall valves are dysfunctional and closed off.

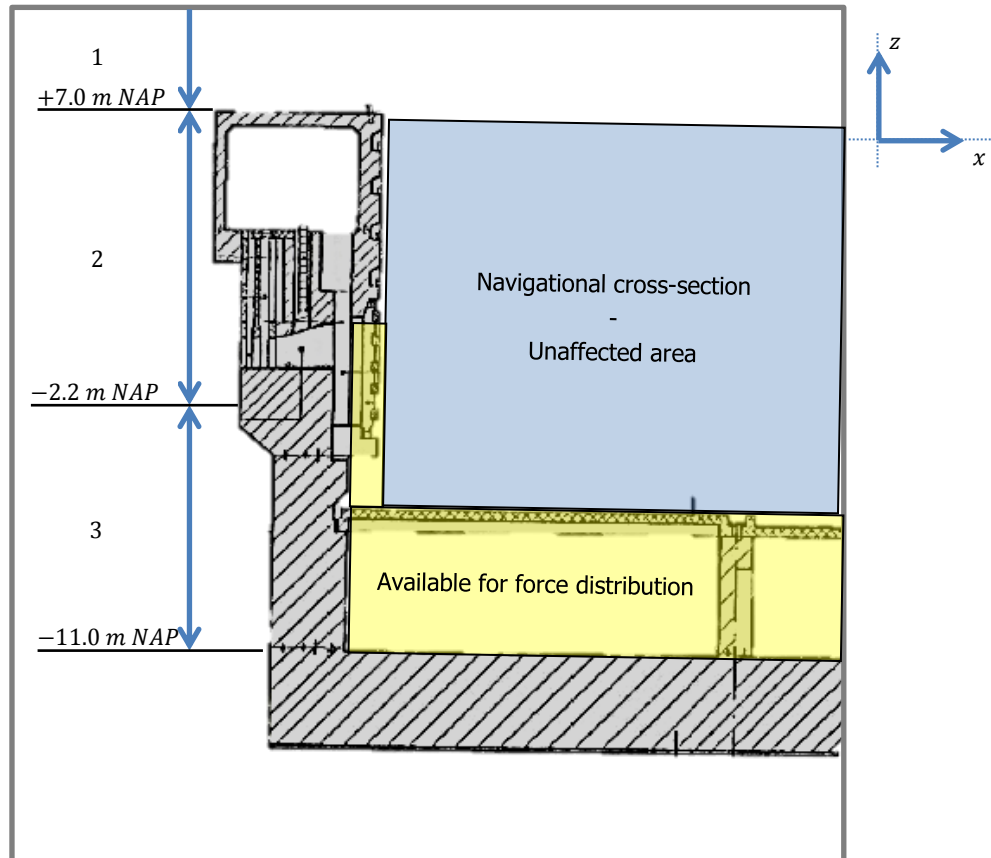


Figure 90: Cross-section of lock chamber. Blue area must remain unharmed for navigational purposes. Yellow area is available for the movable sill. Ranges on the left side indicate different locations of the sill. Adapted from (Rijkswaterstaat Bouwdienst, 2000b).

1. Sill has been lifted out of the water.

When the sill has been lifted out of the water, the bottom level of the sill is above the top level of the lock. The entire movable sill has no connection with the lock chamber. Not even the driving mechanism is in connection with the sill, since the structure is uncoupled from the lock.

This only happens when maintenance actions are required in dry conditions and the lock's operation cannot be affected by a dry or blocked lock chamber. Also when the entire structure is replaced, a situation like this occurs.

2. Sill is being lifted out of the water.

Above the narrow yellow bar in Figure 90, solid concrete is present. Recesses are present in the wall to assemble ladders. Figure 91 shows a top view of this recess with its dimensions. When forces are exerted on the structure, it's pressed against a side of the recess as indicated by the blue arrow.

Load combination C1 applies. The only force on the structure in this case is the horizontal wind load. The vertical load by its weight is directed to the connection of the driving mechanism with the lock chamber. Since the lock is not operational and the sill is located higher than the water level in the closed lock chamber, no ship loads nor hydrostatic pressures are present.

The force is distributed over 4.5 m along both sides of the lock chamber.

$$F_{LC\ C1} = 92.25\text{ kN}, \quad q_{on\ recess} = \frac{\frac{1}{2} \cdot F_{LC\ C1}}{4.5\text{ m}} = 10.25\text{ kN/m}$$

Depending on the concrete compressive stress, the support requires a certain width. Eq. 0.42 shows that a minor support width is enough when the concrete class is B35.

A support of 10 mm is chosen, connected as a strip along the height of the sill. The force distribution to the concrete occurs 250 mm from the side. The recess is 305 mm deep, so a 55 mm tolerance is present along the sides. Figure 92 and Eq. 0.44 show that the resultant force is exerted with an eccentricity of 93.75 mm.

$$w_{\text{support}} = \frac{q}{f_b} = 0.49 \text{ mm}$$

Eq. 0.42

With:

q	10.25 N/mm
f_b	21 N/mm ²

A strut and tie model shows whether the recess is able to withstand the force exerted on it. The influence area of the concrete is equal to thickness in which the force is distributed: 750 mm. The force distribution is calculated in Eq. 0.43.

$$\sigma = \frac{F}{A} \pm \frac{M}{W} = \frac{F}{0.75} \pm \frac{0.125 \cdot F}{\frac{1}{6} \cdot 0.75 \cdot 1^2} = 1 \frac{1}{3} \cdot F \pm F$$

Eq. 0.43

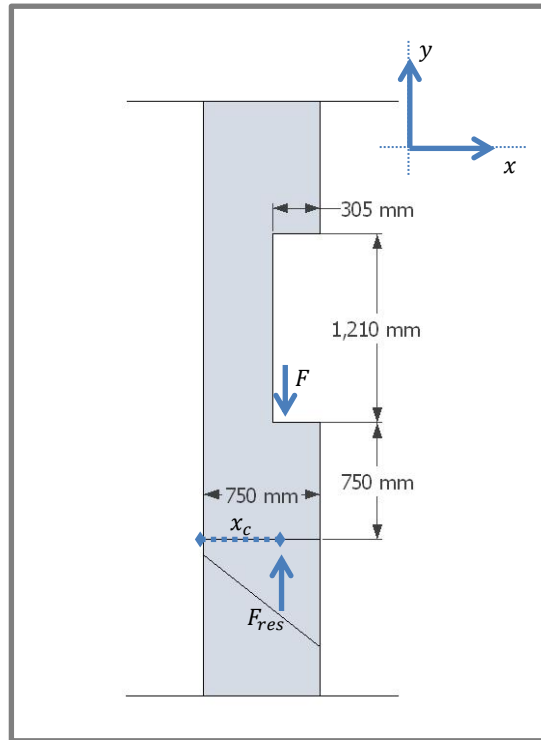


Figure 91: Top view of the recess. F indicates location of exerted force from sill on concrete.

$$\text{eccentricity}_F = x_c - \frac{1}{2} \cdot w_{\text{wall}} = 93.75 \text{ mm}$$

Eq. 0.44

With:

x_c	$\frac{(A_I \frac{1}{2} + A_{II} \frac{2}{3}) \cdot 750}{A_I + A_{II}} = 468.75 \text{ mm}$
w_{wall}	750 mm

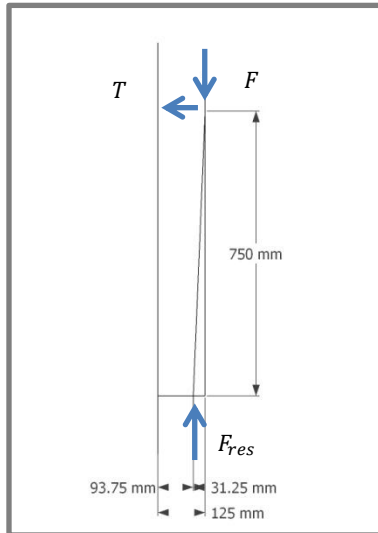


Figure 92: Ratio between compressive force F and tensile force T in the concrete.

$$T = F \cdot \frac{31.25}{750} = 0.042 \cdot F$$

Eq. 0.45

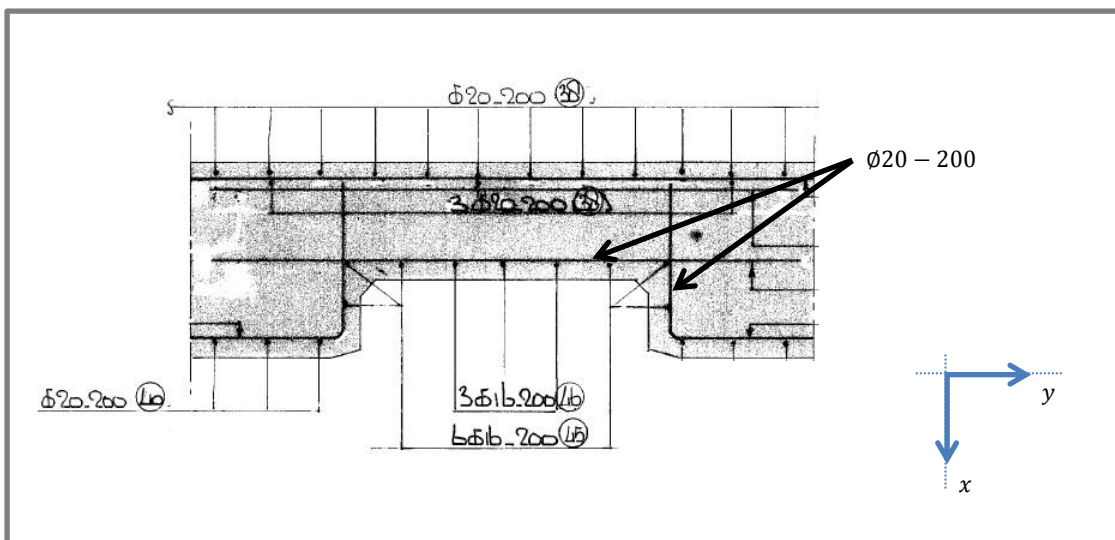


Figure 93: Cross section of recess in top view with reinforcing steel indicated. Adapted from unpublished technical drawings of the lock complex.

Figure 93 shows that in the direction of the tensile force T , a reinforcement of $\text{Ø}20 - 200$ is present. This means that the force exerted on every 200 mm equals $q_{on\ recess} \cdot 0.2 = 33.2 \text{ kN}$. This leads according to Eq. 0.45 to a tensile force of only 1.39 kN . When $FeB - 400$ reinforcing steel is used, Eq. 0.46 shows that the required amount of reinforcing steel is $\text{Ø}2.5 \text{ mm}$. Since $\text{Ø}20 \text{ mm}$ is present, the recess can easily overcome this failure mechanism.

$$A_s = \frac{T}{f_y} = 4.0 \text{ mm}^2 \rightarrow \text{Ø}2.5 \text{ mm}$$

Eq. 0.46

With: T 1.39 kN
 f_y 350 N/mm²

It's assumed that this is the main failure mechanism. A shear analysis is not carried out.

For the vertical load to the driving mechanism, the same weight as in section 5.3.4 can be used. The connection to the concrete is not elaborated in this design stage, but it's not assumed to be problematic. Enough space is available above the top level of the lock to connect the driving mechanism to the concrete.

3. Sill is in operation.

In operation, much larger loads are exerted on the sill. The governing load case is O3. When the force is distributed over 4.5 m along both sides of the lock chamber, the following load applies.

$$F_{LC\ O3} = 1,494\text{ kN}, \quad q_{on\ recess} = \frac{\frac{1}{2} \cdot F_{LC\ O3}}{4.5\text{ m}} = 166\text{ kN/m}$$

An effective way to distribute the forces is possible by installing a steel structure at the walls of the lock. A vertical rail guides the sill in its vertical movement. A steel cantilever of $100 \cdot 250\text{ mm}^2$ slides through a rail of $150 \cdot 250\text{ mm}^2$. The rail is in the horizontal plane supported by steel bars, connected to a plate which is connected to the concrete of the lock chamber walls. Some sketches, along with calculations show that this is possible.

It must be noted that other configurations are possible as well, but one is chosen to demonstrate a possible layout.

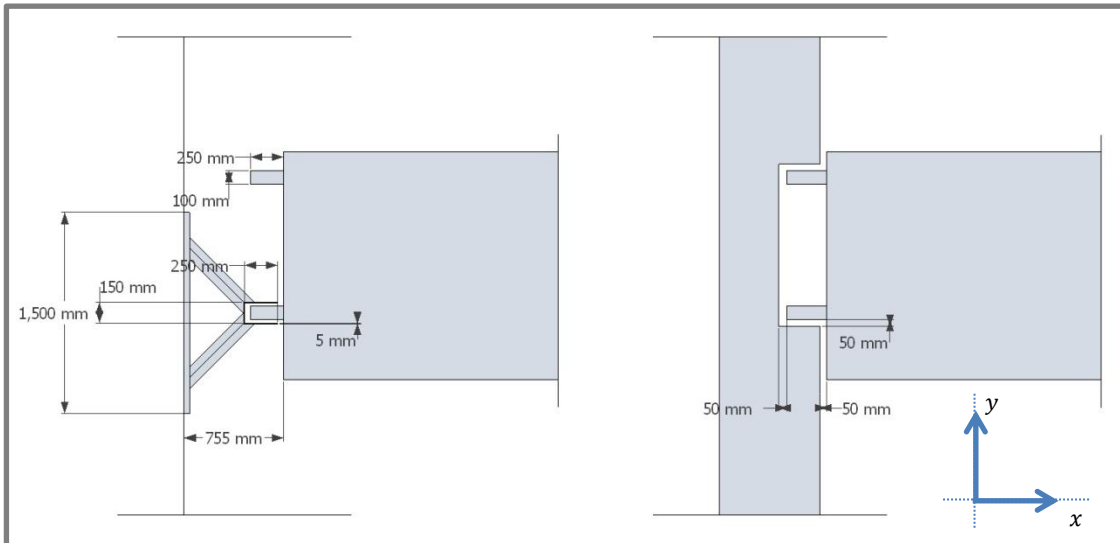


Figure 94: Dimensions of sill in respect to the rail are presented left (range 3 in Figure 90) and in respect to the recess on the right (range 2 in Figure 90).

The rail is present from -11 m NAP to -2.2 m NAP and is therefore 8.8 m high. The supports of the rail are installed at an angle of 45° . The sill is able to induce forces in both directions, so the supports must be able to cope with tensile and compressive stresses of $F \cdot \sqrt{2}$. Eq. 0.47 shows the required amount of steel when supports are present every half metre at both sides.

$$A_s = \frac{F_{max} \cdot \sqrt{2}}{f_y} = 4.50 \cdot 10^2\text{ mm}^2 \quad \text{Eq. 0.47}$$

With: $F_{max} = 74.7\text{ kN}$

The required amount of steel is searched for in a circular cross section, since buckling may occur in different directions. A solid 25 mm tube ($A = 4.91 \cdot 10^2\text{ mm}^2$) suffices, but is not preferred because of complex connections. An open tubular profile is better, so a *CHS*-profile is chosen (just as in Figure 89). The smallest option is a factor 4 too large in terms of its area, but is nevertheless used in further calculation. A check in Eq. 0.34 shows the profile to be resistant to buckling.

CHS – 114.3/5: $I = 2.57 \cdot 10^6 \text{ mm}^4$
 $W_{el} = 4.50 \cdot 10^4 \text{ mm}^3$
 $G = 13.5 \text{ kg/m}$
 $A = 1.717 \cdot 10^3 \text{ mm}^2$
 $d = 114.3 \text{ mm}, \quad t = 5.0 \text{ mm}$

$$N_R \leq \omega_{\text{buckling}} \cdot f_y \cdot A = 4.04 \cdot 10^2 \text{ kN}$$

Eq. 0.48

With:

$$\lambda_{\text{rel}} = \sqrt{\frac{N_E}{F_{\text{Euler}}}} = 0.09, \quad \omega_{\text{buckling}} = 1.0$$

$$N_E = F_{\text{max}} \cdot \sqrt{2} = 1.06 \cdot 10^2 \text{ kN}$$

$$F_{\text{Euler}} = \frac{\pi^2 \cdot EI}{l_{\text{buckling}}^2} = 1.32 \cdot 10^4 \text{ kN}$$

$$l_{\text{buckling}} = 450 \cdot \sqrt{2} \text{ mm}$$

A disadvantage of steel in this case is the occurrence of deflections. This may be problematic when lifting the sill out of the water, but since at that time no large loads are present no critic situation is assumed to occur.

The two steel structures have a total weight of 113 kN. Each one consists of the following elements.

1 vertical rail $150 \cdot 250 \text{ mm}^2$, $t = 5 \text{ mm}$ of 8.8 m long	$G = 2.19 \text{ kN}$
38 diagonal CHS 114.3/5 of 0.71 m long	$G = 3.57 \text{ kN}$
1 plate with dimensions $1.5 \cdot 8.8 \cdot 0.05 \text{ m}^3$	$G = 50.5 \text{ kN}$

J.5.2. Friction in rail

The highest possible additional friction in the guiding rail is calculated to check whether the structure is able to withstand this load. It occurs when the water reservoir as presented in Figure 46 is entirely filled with water, while the rest of the structure is filled with air. The eccentricity of the weight of the water induces a tilting movement of the structure.

The weight of the water (W_{water}) is obtained by the maximum area of $A_{\text{water}} = 3.5 \text{ m}^2$. The moment which the water volume exerts per metre wide (M_{water}) is conservatively calculated by using an eccentricity of $e_{\text{water}} = 0.5 \text{ m}$.

$$W_{\text{water}} = A_{\text{water}} \cdot \gamma_{\text{water}} = 35 \text{ kN/m}$$

$$M_{\text{water}} = W_{\text{water}} \cdot e_{\text{water}} = 17.5 \text{ kNm/m}$$

The moment of forces results in a pair of forces (T) with eccentricity equal to the height of the structure of $h_{\text{sill}} = 4.5 \text{ m}$. This causes a resulting horizontal force $F_{\text{horizontal}}$ on the rail at each side.

$$T = M_{\text{water}} / h_{\text{sill}} = 3.9 \text{ kN}$$

$$F_{\text{horizontal}} = T \cdot \frac{1}{2} l_{\text{sill}} = 46.8 \text{ kN}$$

Assume conservatively that the friction coefficient is 0.5.⁵³ This leads to a required maximum horizontal force to the driving mechanism F_{vertical} per side.

$$F_{\text{vertical}} = 2 \cdot (0.5 \cdot F_{\text{horizontal}}) = 46.8 \text{ kN}$$

The driving mechanism is able to cope with the weight of the structure of 351 kN. Approximately an additional 50 kN per side is assumed to be well possible to insert in the design of the driving mechanism. Another option is to decrease friction by the insertion of wheels for instance, but this is expected to be a more expensive option than increasing the capacity of the driving mechanism slightly.

⁵³ Materials should be used which allow sliding while being strong at the same time. The value of the friction coefficient for dry steel on dry steel is approximately 0.7.

Appendix

K. Details of driving mechanism alternatives

To be able to quantify and compare aspects of the several driving mechanisms, a few general dimensions and properties are assumed. These are kept the same for the different calculations to be able to compare them with each other, even though the actual configuration may look different.

The dimensions are used to calculate energy consumption of the different systems.

Assumed dimensions:

$$b_{Box} = 24 \text{ m}$$

$$d_{Box} = 1 \text{ m}$$

$$h_{Box} = 5 \text{ m}$$

$$d_{Steel} = 0.04 \text{ m}$$

$$\rho_{Steel} = 8,000 \text{ kg/m}^3$$

$$h_{Water} = 4.70 \text{ m}$$

Water column above the sill in ideal situation (sill should be at its maximum height at all times, taking navigation depth in account, being 4.7 metres)

$$\rho_{Water} = 1,000 \text{ kg/m}^3$$

Assumed for this calculation; in reality somewhat higher

$$g = 9.8 \text{ m/s}^2$$

$$u = 0.01 \text{ m/s}$$

Object's velocity. Sill moves one time up and down in 12 hours, so a slow height altering is no problem.

$$C_D = 1.05 [-]$$

Drag coefficient. Value depends on the shape of the object, subjected to drag. 1.05 is the value for a cube and is adopted because the sill is not assumed to be adapted to lower drag forces. (By rounded edges or a wedge on top for instance)

$$\Delta h = 4 \text{ m}$$

$$t_{operation} = \frac{\Delta h}{u} = 400 \text{ s}$$

Time for sill to change from lowered to heightened position, or other way around

Calculated values:

$$V_{Box} = b_{Box}d_{Box}h_{Box} = 120 \text{ m}^3$$

$$V_{Box,Steel} \approx b_{Box}h_{Box}(2d_{Steel}) = 9.6 \text{ m}^3$$

$$W_{Box} = V_{Box,Steel}\rho_{Steel} = 76,800 \text{ kg} \approx 77 \text{ tons}$$

$$W_{Water,Low} = (h_{Water}b_{Box}d_{Box})\rho_{Water} = 112,800 \text{ kg} \approx 113 \text{ tons}$$

$$F_{Box} = W_{Box}g \approx 755 \text{ kN}$$

$$F_{Water} = W_{Water}g = 1,107,400 \text{ N} \approx 1,100 \text{ kN}$$

$$F_{Drag} = \frac{1}{2} \rho_{Water} u^2 C_D (b_{Box} d_{Box}) = 126 \text{ N}$$

$$F_{Total} = 1,855.126 \text{ kN} \approx 1,900 \text{ kN}$$

It is assumed that the sill has to be heightened and lowered two times every day. In this way it adapts its height to the tide. The velocity of this adaption is not very important, it's assumed that a velocity of 1 cm/s is sufficient. Further, it's assumed that heightening and lowering requires the same amount of power.

Winch-cable system

$$P_{Winch} = F_{Total} u = 19 \text{ kW}$$

$$P_{kWh} = \frac{2 \cdot 2 \cdot P_{Winch} t_{operation}}{3600} = 8.44 \text{ kWh/day} \text{ (400s * 2 operations * 2 per day)}$$

To check whether this is a realistic option, cable dimensions are calculated for the assumed dimensions of the sill.

$$f_{steel} = 235 \text{ N/mm}^2 \quad \text{Assumed tensile force of steel cable}$$

$$A_{Steel \text{ cable}} = \frac{\frac{1}{2} F_{Total}}{f_{Steel}} = 4,050 \text{ mm}^2$$

When 1 cables are used per side:

$$A_{Steel \text{ cable}} = \frac{1}{4} \pi \cdot d_{1 \text{ cable}}^2, \quad d_{1 \text{ cable}} = 71.8 \text{ mm}$$

When 6 cables are used per side:

$$\frac{A_{Steel \text{ cable}}}{6} = \frac{1}{4} \pi \cdot d_{6 \text{ cables}}^2, \quad d_{6 \text{ cables}} = 29.3 \text{ mm}$$

This will result in a system with 6 cables at each side in the order of 3 cm thickness. Large wheels will have to be connected to the winch, to guide the thick steel cables.

Hydraulic jacks

$$\eta_{Mechanical} = 0.9 [-]$$

Mechanical efficiency

$$p_{Work} = 200 \text{ bar} = 200 \cdot 10^5 \text{ N/m}^2$$

Installed working pressure

$$p_{Over} = 250 \text{ bar} = 250 \cdot 10^5 \text{ N/m}^2$$

Installed overpressure valve

$$F_{3Jacks} = \frac{F_{Total}}{\eta} = 2,111.11 \text{ kN}$$

$$F_{Per \text{ jack}} = \frac{F}{3} = 703.7 \text{ kN}$$

$$A_{piston} = \frac{F}{p_{work}} = 0.03519 \text{ m}^2$$

$$d_{Jack} = \sqrt{\frac{A_{piston}}{\pi/4}} = 0.212 \text{ m}$$

$$q_{V, Eff} = \frac{V}{t_{operation}} = \frac{\pi d_{Jack}^2 \Delta h}{4 t_{operation}} = 0.0003519 \text{ m}^3/\text{s} \text{ (op of neer beweging)}$$

$$P_{Eff} = q_{Eff} p_{Over} = 8,797.5 \text{ W}$$

$$P = \frac{P_{Eff}}{\eta_{Mechanical} + \eta_{Volumetric}} = 11,500 \text{ W} \text{ (per jack en per sill movement up or down (400s))}$$

$$P_{kWh} = P \frac{t_{operation}}{3600} = 1.2778 \text{ kWh} \text{ (400s)}$$

$$P_{3Jacks, kWh} = 2 \cdot 2 \cdot 3 P_{kWh} = 15.33 \text{ kWh/day} \text{ (400s * 2per day * 2 operations)}$$

Mechanical (cogwheels)

$$P_{Mechanical} = F_{total} u = 19 \text{ kW}$$

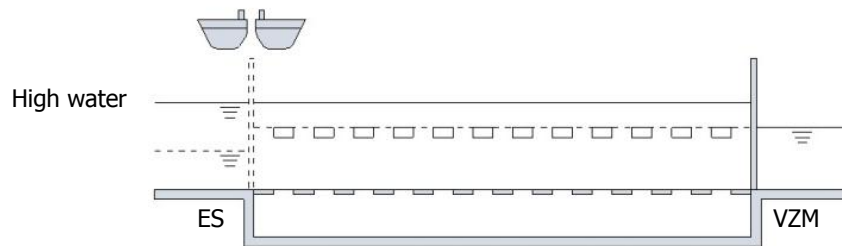
$$P_{kWh} = \frac{2 \cdot 2 \cdot P_{Lyre} t_{operation}}{3600} = 8.44 \text{ kWh/day} \text{ (400s * 2 operations * 2 per day)}$$

Appendix

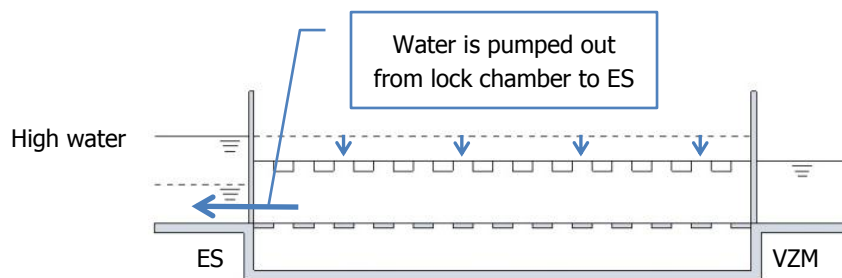
L. New water levelling process in commercial lock

This appendix shows the new water levelling process in the Krammer commercial lock. This new process is required, because the *Duinkerken system* had become dysfunctional and included water levelling. Without levelling water, a lock cannot fulfil its function.

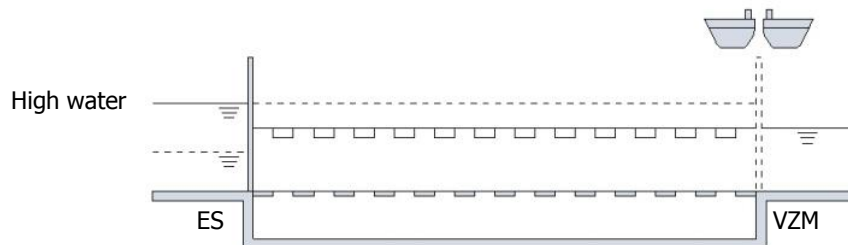
The steps in the locking cycle are described and numbered. A letter indicates whether it's about high or low water at ES. Blue arrows indicate how water flows through the system for water levelling.



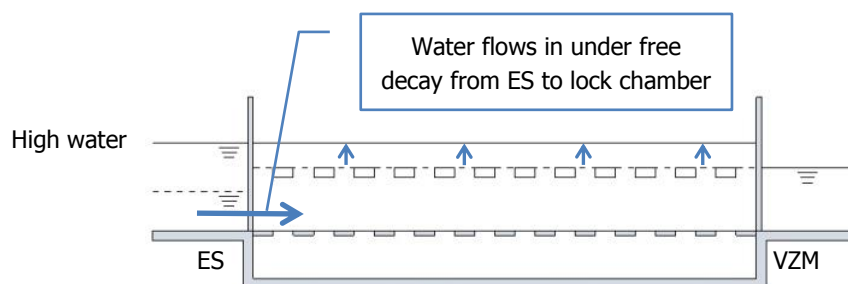
1H. Ships sail in and out of the lock chamber. (ES)



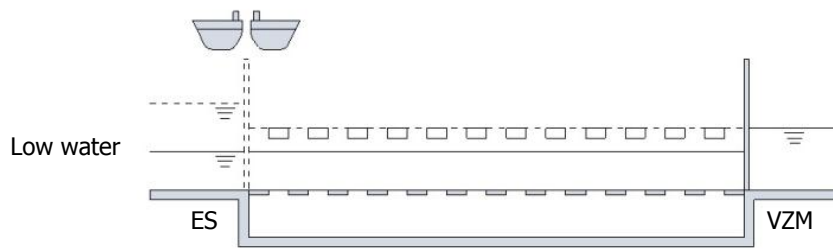
2H. Salt water is pumped back to ES to equalise inside the lock chamber with VZM level.



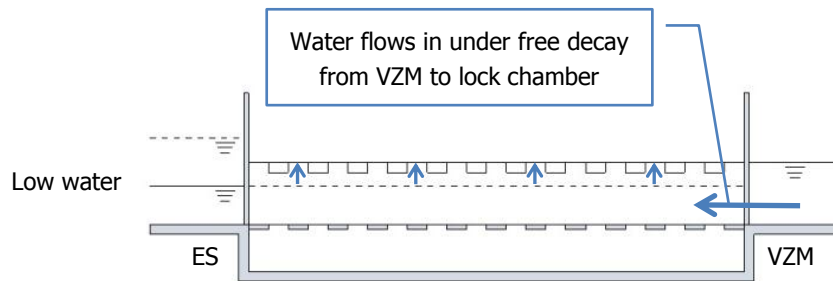
3H. Ships sail in and out of the lock chamber. (VZM)



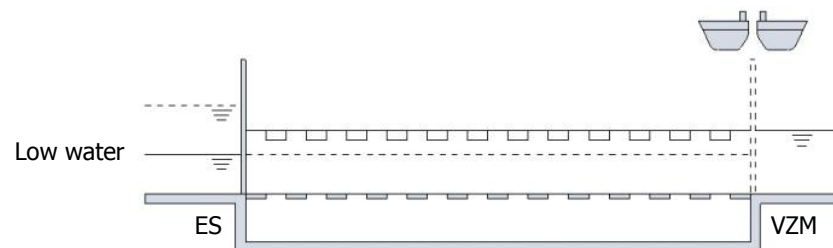
4H. Salt water from the ES flows into the lock chamber under free decay.



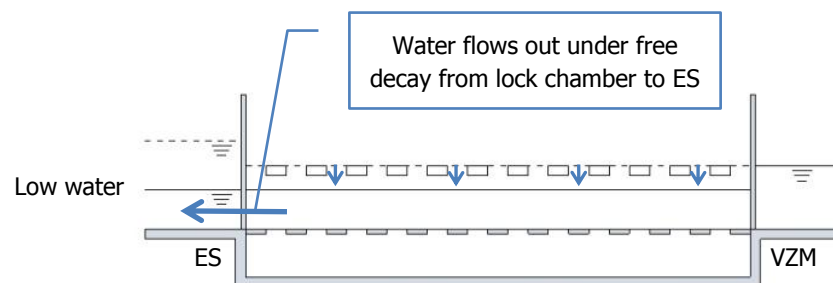
1L. Ships sail in and out of the lock chamber. (ES)



2L. Fresh water from the VZM flows into the lock chamber under free decay.



3L. Ships sail in and out of the lock chamber. (VZM)



4L. Fresh water from the lock chamber flows to the ES under free decay.
(= Fresh water loss)

Appendix

M. Effectiveness calculation

Basic information, salt intrusion reduction and fresh water loss are described in more detail. The exact calculation method is described, leading to the conclusions as described in section 6.2.

M.1. Basic information

The Krammer lock complex consists of 4 lock chambers. The way in which salt intrusion or fresh water loss is divided over the different locks depends on the volume of the lock chambers. In this way, both recreational locks have 3.5% of the salt leakage and fresh water loss, both commercial locks 46.5%.

This means that if a commercial lock has a salt leakage of 1 kg/s, the complex leaks 2.15 kg/s.

Salt leakage and fresh water loss depend on the exchange flow of the regarded lock chamber. Without countermeasures, and with lock gates opened for a long time, experiments show that only 90% of the lock chamber volume exchanges (Deltares, 2011b, p. 24). Salt intrusion reduction is expressed as a percentage of the maximum possible salt leakage.

The time during which the gates are open is not used in the calculation of salt leakage through the Krammer locks, because the gates are open for minimum 28 minutes at each side. Section 2.1 shows that the exchange flow is in the order of 0.7 m/s, which means that the salt water wedge will travel more than 4 times the lock chamber length. It's assumed that the maximum water exchange (90% of lock volume) occurs in that time.

The maximum allowed salt leakage through the entire Krammer lock complex is 60 kg/s. The design of the pilot in the recreational lock is made within that boundary. It has an efficiency of 85%. Thus, the allowed 60 kg/s equals 15% of the initial salt leakage of 400 kg/s.

To estimate the maximum allowable salt leakage, Eq. 0.49 uses the dimensions of the lock and the maximum initial water density difference⁵⁴. This is just an estimate because it's assumed that tide doesn't affect the leakage. The value is recalculated in section 6.2.2. Since 196 kg/s salt leakage is only 46.5% of the total salt leakage through the lock complex, the total value for the Krammer lock complex becomes 422 kg/s.

$$h_{VZM} \cdot (A_{lock} \cdot 90\%) \cdot \Delta\rho_{max} / (t_{locking\ cycle}) = 196\ kg/s$$

Eq. 0.49

With:

h_{VZM}	6.25 m
A_{lock}	$280 \cdot 24\ m^2$
$\Delta\rho_{max}$	$29\ kg/m^3$
$t_{locking\ cycle}$	$93 \cdot 60\ s$

⁵⁴ A maximum water density difference $\Delta\rho_{max}$ of $29\ kg/m^3$ is used in this chapter. Earlier chapters used values for fresh and salt water of respectively $1,000\ kg/m^3$ and $1,030\ kg/m^3$.

In the design of a salt intrusion prevention at the Volkerak locks⁵⁵ it was determined that a salt leakage of 480 kg/s would pass the lock without any preventive measures. The calculated maximum salt leakage of 422 kg/s is in the same order of magnitude as salt leakage at the Volkerak locks and approximately equal to the first estimate of 400 kg/s. For that reason, the calculated value for the maximum salt leakage through one commercial lock of 196 kg/s, as well as the calculation method are assumed to be right.

The *Duinkerken system* has an effectiveness in the order of 90 – 98%. When the system works perfect, salt leakage is reduced by 100%; no water exchanges between ES and VZM.

It's unrealistic to believe that the system works perfect, though. Different studies – supported by several extensive field measurements – concluded that the system has a salt leakage of 3 to 15 kg/s. 15 kg/s for the entire lock complex equals approximately 7.0 kg/s for one commercial lock, and results in an effectiveness of $(196 - 7)/196 = 96\%$. Since this value fits with the known effectiveness of the system, the calculated value for the maximum salt leakage through one commercial lock of 196 kg/s, as well as the calculation method are – again – assumed to be right.

M.2. Salt intrusion

The total salt intrusion is calculated by multiplying the average exchanging water volumes at HW and at LW with the density difference and dividing it with the duration of a locking cycle.

Table 38: Calculated salt intrusion through one Krammer commercial lock.

Config- uration	Water level	Exchange volume I EV I [m ³]	Exchange volume II EV II [m ³]	Total salt intrusion [kg/s]
0	HW	0	0	7.0
	LW	0	0	
1.0	HW	$7.35 \cdot (90\% \cdot A_{lock}) = 44,500$	$6.25/7.35 \cdot (EV I) = 37,800$	182
	LW	$5.35 \cdot (90\% \cdot A_{lock}) = 32,400$	$(EV I) = 32,400$	
1.1	HW	$0.15 \cdot 7.35 \cdot (90\% \cdot A_{lock}) = 6,700$	$0.3 \cdot 6.25/7.35 \cdot (EV I) = 1,700$	11.05
	LW	$0.15 \cdot 5.35 \cdot (90\% \cdot A_{lock}) = 4,900$	$0.3 \cdot (EV I) = 1,500$	
1.2	HW	$0.15 \cdot 4.7 \cdot (90\% \cdot A_{lock}) = 4,300$	$0.3 \cdot (EV I) = 1,300$	8.8
	LW	$0.15 \cdot 4.7 \cdot (90\% \cdot A_{lock}) = 4,300$	$0.3 \cdot (EV I) = 1,300$	

Table 38 shows the calculated salt leakage through one commercial lock for the situations with and without installed movable sill. The *Duinkerken system* ideally does not have exchanging volumes of water with a density difference; hence this calculation method can't be used for that system. The value for salt intrusion is obtained by studies as explained in section 6.2.1.

In Table 39 the effectiveness is expressed as a percentage. The percentages are the calculated reduction compared to the newly calculated maximum possible salt leakage of 182 kg/s.

The benefits compared with doing nothing are enormous. The additional benefit of installing a sill is approximately $((6.1 - 4.8)/6.1) = 21\%$ when compared to a configuration without sill.

⁵⁵ This design became obsolete by postponing the decision to turn the VZM into a salt water basin. As consequence of this decision, the system in the Krammer locks needed to be upgraded. See appendices G.1 and A.3.1.

Table 39: Effectiveness of different configurations in Krammer commercial lock.

Configuration	Salt intrusion reduction	Salt intrusion
0 <i>Duinkerken system</i>	$(182 - 7)/182 = 96.2\%$	3.8%
1.0 No system	$(182 - 182)/182 = 0\%$	100%
1.1 Air bubble- & water screen	$(182 - 11.1)/182 = 93.9\%$	6.1%
1.2 Air bubble- & water screen & sill	$(182 - 8.8)/182 = 95.2\%$	4.8%

M.3. Fresh water loss

Table 40 shows the calculated fresh water loss. The last column is obtained by dividing the average of the exchanging water volumes at HW and at LW by the duration of a locking cycle.

Configuration 0 has a fresh water loss equal to the volume of fresh water that's not exchanged with salt water before the gates open to the ES. Since no salt water is wanted at the VZM, returning of salt water is not performed very exact. Operationally, it's tried to get the level of the interface between fresh- and salt water at the level of the bottom of ships inside the lock. For this reason a water volume of the lock's surface times 4 m depth is assumed as fresh water loss.

"Exchange volume II" is always the same since at VZM side the tide and the configuration doesn't affect flow of fresh water into the lock chamber.

Configuration 1.2 with sill has a restricted outflow to the upper 4.7 m.

Table 40: Calculated fresh water loss in one Krammer commercial lock.

Config- uration	Water level	Exchange volume II EV II [m ³]	Exchange volume I EV I [m ³]	Water levelling [m ³]	Total fresh water loss [m ³ /s]
0	HW	$A_{lock} \cdot 4 = 27,000$		<i>Integrated</i>	4.8
	LW	$A_{lock} \cdot 4 = 27,000$		<i>Integrated</i>	
1.0	HW	$6.25 \cdot (90\% \cdot A_{lock}) = 37,800$	(EV II) = 37,800	-	9.1
	LW	$6.25 \cdot (90\% \cdot A_{lock}) = 37,800$	$5.35/6.25 \cdot (EV II) = 32,400$	$A_{lock} \cdot (6.25 - 5.35) = 6,000$	
1.1	HW	$0.3 \cdot 6.25 \cdot (90\% \cdot A_{lock}) = 11,300$	$0.15 \cdot (EV II) = 1,700$	-	1.10
	LW	$0.3 \cdot 6.25 \cdot (90\% \cdot A_{lock}) = 11,300$	$0.15 \cdot 5.35/6.25 \cdot (EV II) = 1,500$	$A_{lock} \cdot (6.25 - 5.35) = 6,000$	
1.2	HW	$0.3 \cdot 6.25 \cdot (90\% \cdot A_{lock}) = 11,300$	$0.15 \cdot 4.7/6.25 \cdot (EV II) = 1,300$	-	1.02
	LW	$0.3 \cdot 6.25 \cdot (90\% \cdot A_{lock}) = 11,300$	$0.15 \cdot 4.7/6.25 \cdot (EV II) = 1,300$	$A_{lock} \cdot (6.25 - 5.35) = 6,000$	

The benefits of the new configurations are significant. *Configuration 1.2* scores $((4.8 - 1.02)/4.8 =)$ 78.8% higher than the current system. The additional benefit of *1.2* in respect to *1.1* is $((1.10 - 1.02)/1.10 =)$ 7.6%.

Appendix

N. Energy consumption calculation

This appendix elaborates on the energy consumptions by air bubble- and water screens in configurations with and without a movable sill in the Krammer commercial lock.

Also the energy costs of the different configurations in the locks are presented.

Chapter 6.3 holds as base for this appendix.

N.1. Water levelling

Energy consumption by levelling of water is determined by the available pumps in the Krammer recreational lock. In that system, water levelling takes place by pumps when the water level at the ES is higher than at the VZM.

The energy consumption of the installed pumps is 31.5 kW for every discharged m^3/s . This ratio between power and discharge is assumed linearly dependant, and is obtained from (Rijkswaterstaat, 1989).

The *Duinkerken system* is entirely based on water flows through an ingenious culvert system. Section 2.2 elaborates its design. A water depth of 1 m in the lock chamber is displaced for levelling. For exchange of water a depth of 3.7 m (recreational) or 6.25 m (commercial) is displaced. In Table 41 the consumed energy is calculated by the average displaced amount of water.

The total energy consumption is found to be $4.8 \cdot 10^6 \text{ kWh/year}$. In unpublished documents it's stated that the locks consume $5.3 \cdot 10^6 \text{ kWh/year}$ ($0.3 \cdot 10^6$ by the recreational and $5 \cdot 10^6$ by the commercial lock). As the calculated value equals the known value approximately, a calculation by use of the pump capacity of $31.5 \text{ kWh}/(\text{m}^3/\text{s})$ is assumed right.

Table 41: Calculation of consumed energy per year.

Lock	Volume [m^3]	Time [min]	Discharge [m^3/s]	Power [kWh/cycle]	Consumption [$10^6 \text{ kWh}/\text{year}$]
Recreational lock	$90 \cdot 9 \cdot (3.7 + 1)$	19	3.34	33.3	0.4
Commercial lock	$280 \cdot 24 \cdot (6.25 + 1)$	34	23.88	426.3	4.4

Table 42 shows the consumed energy for water levelling in the Krammer locks. These values are used in the comparison of the new configurations with and without sill.

Table 42: Calculation of consumed energy for water levelling per locking cycle.

Lock	Volume [m ³]	Time [min]	Discharge [m ³ /s]	Power [kW/cycle]	Consumption [kWh/cycle]
Recreational lock	90 · 9 · 1	4	3.38	106.3	7.09
Commercial lock	280 · 24 · 1	5	22.4	705.6	58.8

N.2. Air bubble screen

To determine the amount of power required for the different configurations, reference is made to available figures in reports and earlier designs of comparable systems. The relationship is determined between the lock configuration and the required air flow. Knowing this number, estimations can be made of the required air flow in locks with other dimensions.

The energy consumption of the compressors is 250 kW for every discharged m³/s (Rijkswaterstaat Zeeland, 2012, p. 35). Table 43 shows this to be true for the known air flows required in the Volkerak locks.

At the Krammer recreational lock 120 kW is installed. Eq. 0.50 calculates the required air flow by using the same compressor capacity.

Table 43: Check on installed power at Volkerak locks.

	Air flow [Nm ³ /s]	Compressor capacity [kW/(Nm ³ /s)]	Required power [kW]	Installed power per lock chamber [kW]
Volkerak commercial lock	1.77	250	442.5	450
Volkerak recreational lock	1.18	250	295	320

$$\text{Air flow} = \frac{P_{\text{installed}}}{C_{\text{compressor}}} = \frac{120}{250} = 0.48 \text{ Nm}^3/\text{s}$$

Eq. 0.50

The required air flow for bubble screens in other configurations depends on the dimensions of the screen (height and width) and on the water pressure at the origin of the air bubbles. All these dependencies are assumed to be linear. An extensive analysis is needed to determine this air flow exactly, but that's not within the scope of this thesis. In Table 44 calculations are given of the air flow in the Volkerak locks of 1.64 Nm³/s, which is close (7.9%) to the actual value of 1.77 Nm³/s. It makes clear that the assumed linear dependency is acceptable for a first design phase.

The linear dependency is used in further calculations to estimate power consumption of air bubble screens in other configurations.

Table 44: Calculated required air flow in Volkerak commercial lock.

Type	Width [m]	Max. height [m]	Pressure [bar]	Air flow [Nm ³ /s]	Δ [%]
Volkerak commercial	24	7.5	2.25	1.64	1.77 7.9

Table 45 calculates capacities of the pumps by use of different known configurations. Both capacities are used and compared in further calculations. Differences between the two capacities result in Table 46 in differences of required air flow discharges within a 10% margin. This is assumed to be in the right order of magnitude.

Table 46 determines the required air flows for the Krammer lock complex. The maximum height in the configurations with movable sill is 4.7 metres, because the sill operates in such a way that a stable water depth is being maintained. The pressures at the configurations with sill are significantly lower than at configurations without sill. A pressure difference of 1 *bar* is required in the current design of the pilot, where in the new design (configuration with sill) 0.3 *bar* is assumed to be enough. (see section 0.)

Table 47 shows the required power in the Krammer commercial lock with and without movable sill. The consumed power in the last column is calculated based on the fact that the screen is active 28 minutes during a locking cycle. (See Table 13 on page 19.)

The used water pressures are explained in Table 48. The last column represents the difference between the two calculations in a percentage.

Table 45: Calculated capacity.

	Width [m]	Max. height [m]	Pressure [bar]	Air flow [Nm ³ /s]	Capacity [(Nm ³ /s)/(m ² · bar)]
Krammer recreational	9	6.2	2.12	0.48	$4.06 \cdot 10^{-3}$
Volkerak commercial	24	7.5	2.25	1.77	$4.37 \cdot 10^{-3}$

Table 46: Determined air flow rates for air bubble screens in various lock configurations.

Type	Width [m]	Max. height [m]	Pressure [bar]	Air flow		Δ [%]
				[Nm ³ /s]		
				(4.06 · 10 ⁻³)	(4.37 · 10 ⁻³)	
Krammer commercial	24	8.75	2.375	2.02	2.18	7.9
Krammer recreational with sill	9	4.7	1.27	0.22	0.24	9.1
Krammer commercial with sill	24	4.7	1.27	0.60	0.64	6.7

Table 47: Consumed power per locking cycle of Krammer commercial lock.

	Required air flow [Nm ³ /s]	Compressor capacity [kW/(Nm ³ /s)]	Required power [kW]	Consumed power [kWh/cycle]
Krammer commercial	2.02	250	506	236
Krammer commercial with sill	0.60	250	148	69.1

Table 48: Origin of working pressures for different configurations.

	Pressure by water depth [h/10 or bar]	Pressure loss [bar]	Regulator [bar]	Total pressure [bar]
Volkerak commercial	0.75	0.5	1.0	2.25
Krammer recreational	0.62	0.5	1.0	2.12
Krammer commercial	0.875	0.5	1.0	2.375
Krammer recreational with sill	0.47	0.5	0.3	1.27
Krammer commercial with sill	0.47	0.5	0.3	1.27

N.3. Water screen

The power needed for an effective water screen in different configurations of locks is determined in a comparable way as with the air bubble screens. The required discharge is calculated after a dependency is made clear between lock configuration and discharges of known designs. Finally, the calculated discharge is translated to a power demand.

Table 49 shows the capacity of the water pumps. Conservatively, a value of 78 is used in further calculation.

Table 49: Determined pump capacity of installed pumps.

	Max. required discharge [m ³ /s]	Installed power [kW]	Pump capacity [kW/(m ³ /s)]
Volkerak commercial lock	4.4	300	68
Krammer recreational lock	1.4	110	78

Table 50 shows that the water discharge is approximately linearly dependent to the width and height of the screen. Water pressure does not play a role in these calculations as it did for calculations for the air bubble screens.

Table 50: Determined capacity of pumps.

	Width [m]	Max. height [m]	Max. required discharge [m ³ /s]	Capacity [(m ³ /s)/m ²]
Volkerak commercial lock	24	7.5	4.4	$\frac{4.4}{24 \cdot 7.5} = 2.44 \cdot 10^{-2}$
Krammer recreational lock	9	6.2	1.4	$\frac{1.4}{9 \cdot 6.2} = 2.51 \cdot 10^{-2}$

Table 51 shows that all deviations are within a 3% range, so linearly dependency is assumed to be right. Choose for commercial lock without and with sill respectively 5.3 and 2.8 m³/s. Table 52 shows calculated consumed power per locking cycle. In this calculation it's used that the screens are active for a period of 28 minutes per cycle.

Table 51: Determined discharge in Krammer commercial lock. Bold values are calculated.

	Width [m]	Max. height [m]	Max. required discharge [m ³ /s] (2.44 · 10 ⁻²)	Δ [%] (2.51 · 10 ⁻²)
Krammer commercial	24	8.75	5.13	5.27 2.7
Recreational with sill	9	4.7	1.03	1.06 2.8
Commercial with sill	24	4.7	2.76	2.83 2.5

Table 52: Consumed power per locking cycle.

	Max. required discharge [m^3/s]	Pump capacity [$kW/(m^3/s)$]	Required power [kW]	Consumed power [$kWh/cycle$]
Krammer commercial lock	5.3	78	351	164
Krammer commercial lock with sill	2.8	78	218	102

N.4. Costs

The next page gives an overview of the calculation of energy costs for the same configurations in the Krammer commercial locks as used in chapter 6.

General	Energy unit price	0.15 €/kWh
	Number of lockings per day	57 -
	Number of locking cycles per day	28.5 -
	Duration of active screens per locking cycle	28 min
	Duration of levelling per locking cycle	5 min

0	Commercial lock	Water levelling	Energy consumption per locking cycle	426.3 kWh
			Energy consumption per year	4,437,623 kWh/year
			Energy costs per year	665,643 €/year

Totals configuration 0: 4,437,623 kWh/year
665,643 €/year

1.0	Commercial lock	Water levelling	Energy consumption per locking cycle	58.8 kWh
			Energy consumption per year	306,043 kWh/year
			Energy costs per year	45,906 €/year

Totals configuration 1.0: 306,043 kWh/year
45,906 €/year

1.1	Commercial lock	Air bubble screen	Required power	506.0 kW
			Energy consumption per locking cycle	236 kWh
			Energy consumption per year	2,458,059 kWh/year
			Energy costs per year	368,709 €/year
		Water screen	Required power	351.0 kW
			Energy consumption per locking cycle	164 kWh
			Energy consumption per year	1,705,097 kWh/year
			Energy costs per year	255,764 €/year
		Water levelling	Energy consumption per locking cycle	58.8 kWh
			Energy consumption per year	306,043 kWh/year
			Energy costs per year	45,906 €/year

Totals configuration 1.1: 4,469,199 kWh/year
670,380 €/year

1.2	Commercial lock	Air bubble screen	Required power	148.0 kW
			Energy consumption per locking cycle	69 kWh
			Energy consumption per year	718,958 kWh/year
			Energy costs per year	107,844 €/year
		Water screen	Required power	218.0 kW
			Energy consumption per locking cycle	102 kWh
			Energy consumption per year	1,059,006 kWh/year
			Energy costs per year	158,851 €/year
		Water levelling	Energy consumption per locking cycle	58.8 kWh
			Energy consumption per year	306,043 kWh/year
			Energy costs per year	45,906 €/year
		Sill movement	Energy consumption per day	15.3 kWh
			Energy consumption per year	5,599 kWh/year
			Energy costs per year	840 €/year

Totals configuration 1.2: 2,089,606 kWh/year
313,441 €/year

Colophon

Title	:	Salt intrusion prevention in locks; designing a movable sill in the existing Krammer commercial navigation locks.
University	:	Delft, university of technology
Company	:	Royal HaskoningDHV
Date of publication	:	22-4-2013
Location of publication	:	Amersfoort, the Netherlands
Number of pages	:	212
Author	:	B. van Tongeren, BSc
Esam committee	:	Prof. <i>dr. ir.</i> S.N. Jonkman <i>ir.</i> A.J. van de Kerk <i>ir.</i> W.F. Molenaar Prof. <i>dr. ir.</i> W.S.J. Uijtewaal
Version	:	Final
